Characterization and quantification of deposits build up and removal in straw suspension fired boilers

Jensen, Peter Arendt; Shafique Bashir, Muhammad; Wedel, Stig; Jappe Frandsen, Flemming; Wadenbäck, Johan; Pedersen, Søren Thaaning; Dam-Johansen, Kim

Publication date:
2013

Document Version
Publisher's PDF, also known as Version of record

July 2013, DTU no. 50530

Energinet.dk project no. 7217

Final report: Characterization and quantification of deposits build up and removal in straw suspension fired boilers

Peter Arendt Jensen[1], Muhammad Shafique Bashir[1], Stig Wedel[1], Flemming Frandsen[1], Johan Wadenbäck[2], Søren Thaaning Pedersen[2], Kim Dam-Johansen[1].

1. Department of Chemical and Biochemical Engineering
Technical University of Denmark
Søltofts Plads, Building 229, DK-2800, Kgs. Lyngby, Denmark
2. Vattenfall A/S, Amager Power Plant,
Kraftværksvej 37, DK-2300, Copenhagen S, Denmark

CHEC no. R1301

Abstract

This project deals with ash deposit formation in suspension fired biomass power plant boilers. The project has been conducted in a tight collaboration between Vattenfall and the CHEC Research Centre at DTU Department of Chemical Engineering. A large part of the project has been performed by conducting advanced probe measurements at the Amagerværkets Vattenfall owed boilers. It was the objective of the project to provide an improved understanding of ash deposit formation and removal in biomass suspension fired boilers. The project have provided a large amount of knowledge on the following issues: 1) The influence of local boiler conditions on deposit formation in suspension fired boilers using wood or co-firing straw and wood, 2) quantification of deposit removal in biomass suspension firing boilers with regards both to natural shedding and soot blower induced shedding, 3) established relations of the properties of fuel ash, fly ash and deposits, 4) use of coal ash to remedy biomass ash induced boiler deposit problems.

Table of contents

Appendices

A1. Literature review. Characterization and quantification of deposits build up and removal in straw suspension fired boilers. Muhammad Shafique Bashir, Flemming Frandsen, Peter Arendt Jensen.

A2. Design and Development of Probes for Online Monitoring of Deposit Build-up and Removal. Muhammad Shafique Bashir, Peter Arendt Jensen, Stig Wedel, Flemming Frandsen, Johan Wadenbäck, Søren Thaaning Pedersen, Kim Dam-Johansen.

A3. Journal paper: Ash Transformation and deposit build-up during biomass suspension and grate firing: Full-scale experimental studies. Fuel processing Technology 97 (2012) 93-106. Muhammad Shafique Bashir, Peter Arendt Jensen, Flemming Frandsen, Stig Wedel, Kim Dam-Johansen, Johan Wadenbäck, Søren Thaaning Pedersen.

A4. Journal paper: Suspension-Firing of Biomass. Part 1: Full-scale Measurements of Ash Deposit Build-up. Energy & Fuels 2012, 26, 2317-2330. Muhammad Shafique Bashir, Peter Arendt Jensen, Flemming Frandsen, Stig Wedel, Kim Dam-Johansen, Johan Wadenbäck, Søren Thaaning Pedersen.

A5. Journal paper: Suspension-Firing of Biomass. Part 2: Boiler Measurements of Ash Deposit shedding. Energy & Fuels 2012, 26, 5241-5255. Muhammad Shafique Bashir, Peter Arendt Jensen, Flemming Frandsen, Stig Wedel, Kim Dam-Johansen, Johan Wadenbäck.

A6. Suspension-firing of wood with coal ash addition: Probe measurements of ash deposit build-up at Avedøre Power Plant (AVV2). Muhammad Shafique Bashir, Peter Arendt Jensen, Flemming Frandsen, Stig Wedel, Kim Dam-Johansen.

A7. Mechanistic modeling of deposit formation. Muhammad Shafique Bashir, Peter Arendt Jensen, Flemming Frandsen, Stig Wedel, Kim Dam-Johansen.

A8. Innovative ideas for deposit shedding. Muhammad Shafique Bashir, Peter Arendt Jensen, Flemming Frandsen, Stig Wedel, Johan Wadenbäck, Søren Thaaning Pedersen, Kim Dam-Johansen.

1.0 Introduction

The project deals with deposit problems related to suspension firing of biomass in power plant boilers. The use of biomass for power production has until recently mainly been done at grate fired boiler units. When this project was initiated the suspension co-firing of straw with wood was started at the Amagerværket boiler plant. Detailed knowledge on deposit formation and shedding in suspension fired boilers has therefore been limited. Especially the removal of biomass ash deposits (shedding) naturally or by sootblowing is an area where relatively limited accurate knowledge is available. By conducting the proposed project more accurate scientifically based knowledge are provided on subjects as: 1) deposit formation in suspension fired boilers using wood or co-firing straw and wood, 2) quantification of deposit removal in biomass suspension firing with regards both to natural shedding and soot blower induced shedding, 3) use of coal ash to remedy biomass ash induced boiler deposit problems.

The project has been conducted in a tight collaboration between Vattenfall and the CHEC Research Centre at DTU Department of Chemical Engineering. A large part of the project has been performed by conducting advanced probe measurements at the Amagerværkets Vattenfall owed boilers. The project was funded by Energinet.dk and Vattenfall. The plan of project activities have been somewhat changed along the time. The probe measurements in the boilers had to be adjusted to the actual operation of the boilers, and development of a vertical deposit probe demanded more resources than originally anticipated. The project has provided a very large amount of valuable new knowledge on biomass ash deposition that is described in this report.

2.0 Literature review

As part of the project a literature review was conducted and can be seen in Appendix 1. A short resume of the review is provided here. Traditionally solid fuel power plant boilers have been developed to use coal as fuel. Since around 1990 combined heat and power grate boilers firing straw have been developed in Denmark and in later year's pulverized fuel boilers have been designed to use biomass as fuel. The applied fuels have included co-firing of straw and coal, firing of wood and co-firing of wood and straw. Straw and wood causes increased problems with deposit formation in power plant boilers, and have compared to coal high contents of Cl and potassium in the ash. Straw typically have a fuel ash content of 5 wt% that have high concentrations of K and Si, and wood fuels often have an ash content of 1 wt% that have high concentrations of K and Ca.

The ash deposit formation is caused by the fly ash present in the boiler chamber. The biomass fly ash formation process is quite different in grate fired and suspension fired boilers. The fly ash in grate fired boilers is mainly caused by volatilization of alkali rich ash species and typically only around 20 wt% of the fuel ash is transferred to the fly ash, while the residual 80 wt% is removed from the boiler chamber as bottom ash. In suspension fired boilers most of the fuel ash is entrained into the flue gas and the fly ash and the fuel ash have nearly similar chemical compositions.

Ash deposit formation in boilers reduce heat transfer to boiler walls and may in severe cases block flue gas channels, and make it necessary to stop boiler operation and clean the boiler manually. Initially conducted Danish experiments with 100% straw suspension combustion led to several unscheduled boiler short downs.

The ash deposit formation on boiler surfaces are coursed be several processes such as, diffusion and condensation on heat transfer surfaces of volatile inorganic species (often dominated by alkali salts), thermophoresis and diffusion of aerosol particles and impaction of larger particles on boiler walls. Generally

more particles stick to boiler surfaces when a higher fraction of the deposit or the incoming particles are melted.

Most studies in deposit formation and deposit properties have been conducted in grate biomass fired boilers. Typically the deposits have an inner layer rich in KCl and K_2SO_4 formed by condensation and diffusion and outer deposit layers rich in K, Ca and Si that is mostly formed by particle impaction. Studies on deposit formation in grate fired boilers have been conducted in several cases, often using deposits probe to investigate the deposit formation rate and the chemistry of biomass deposits. It has been seen that straw fuels cause more severe deposit formation than wood fuels, and that an increased fuel alkali content cause an increased deposit formation rate.

Shedding of deposits can happen naturally or induced by deposit removal technologies such as soot blowing. In grate straw fired boilers the removal of deposits in the superheater area is mainly caused by melting of the outer most deposit layer, and in areas of the boiler with lower temperatures both natural shedding and soot blower induced shedding takes place.

Before this project was started deposit formation processes and removal were mainly investigated in biomass grate boilers. Because of the different fly ash formation process in the two boiler types detailed knowledge on deposit formation and shedding in biomass suspension fired boilers are wanted.

3.0 Design, construction and commissioning of deposit probes

Deposit probes are extensively used to understand ash deposit formation and shedding processes in solid fuel boilers. In most previously conducted ash deposition measurements in biomass grate boilers reasonably simple horizontal water and air cooled tube probes have been used. The quantification of the deposit rate is then done by taking out the probe from the boiler chamber, remove and weighting the collected deposits, and then calculate the deposit formation rate based on the collected weight divided by the probe surface and the probe residence time in the boiler.

The advanced horizontal deposit tube probe used during the measurements in the present study was developed in previous DTU projects, and was only modified with respect to boiler port mounting, and a video camera recording system. The probe shown in Figure 1 can make online data collections of deposit mass and heat uptake. The probe is cooled by water and air, whereby it is possible to determine the heat uptake by the probe and keep a stable surface temperature. The probe was approximately inserted 1.8 meters into the boiler chamber and had a diameter of 40.5 mm. A load cell is used to detect the force caused by the mass of the ash deposit on the probe, and thereby an online signal of the deposit mass is provided. A video camera is used to make video recordings of the deposit formation process, and local registration of flue gas temperature is done by a thermo element or a suction pyrometer. A soot blower probe could be inserted into the boiler chamber along the deposit probe. The sootblower probe can remove deposits on the deposit probe by use of a high pressure air jet. By changing the soot blower probe position and the pressure of air delivered to the probe the peak impact pressure (PIP) of the air jet hitting the deposits could be changed.

It was one of the original objectives of the project to investigate ash deposit build-up on tube walls in the furnace region of a boiler, and a vertical ash deposit probe was therefore designed and constructed to simulate the conditions of the boiler furnace wall. The probe was made as a 130 mm diameter plate facing into the boiler chamber, and could be mounted on a boiler port. The probe was cooled by water and air, whereby it was possible to determine heat uptake by the probe and keep a stable surface temperature. The probe hung on a hinge connected to a flange and a load cell was used to detect the force caused by the mass

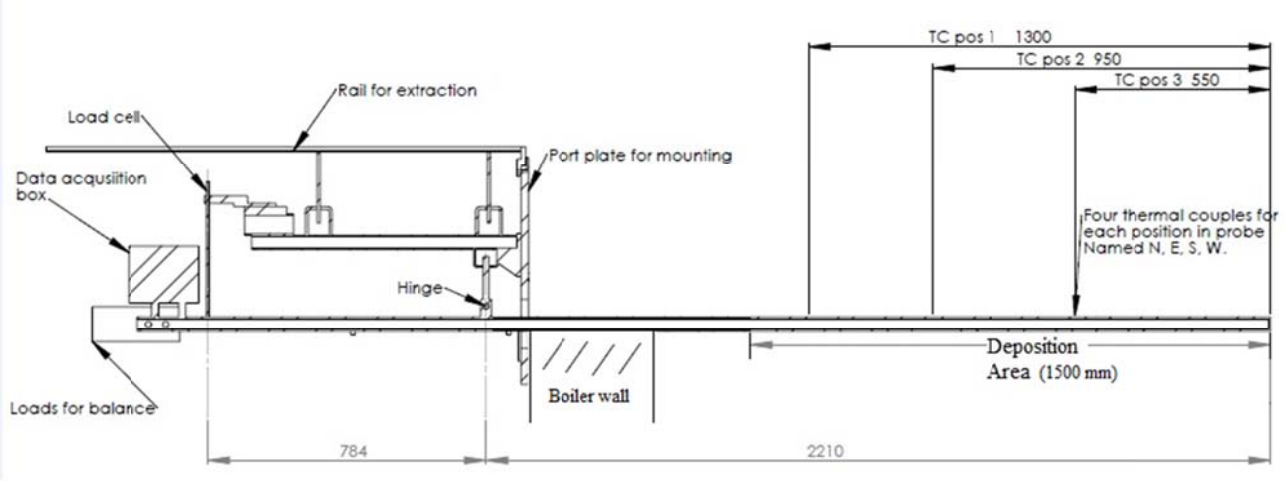

Figure 1. Schematic of the advanced horizontal deposit tube probe

of the ash deposit on the probe. The vertical probe was tested at the Amager Unit 1 (AMV1) biomass boiler. The experiments were done by inserting the probe, so that the probe plate was at level with the boiler wall. The results were satisfactory with respect to controlling the probe surface temperature at the required levels. A main problem however, proved to be the collection of the ash deposits. The boiler was operated at a sub pressure, and to keep the weighting capability of the probe system a free space between the probe and the port is needed, this caused a high inflow of air, that prevented the deposit formation process. It was tried to seal the space between the probe and the port, and then simply remove the probe after some time, and then collect the accumulated deposits. However, the deposit was removed from the probe surface during the extraction of the probe, because of the high air inlet flow. A possible solution could be covering of the complete set-up with a box, and this may have eliminated the problem with the air flow. However, it was decided that resources and time had to be spend on other parts of the project work. Further details regarding the deposit probes can be found in Appendix 2.

4.0 Probe measurements in biomass fired boilers

4.1 Probe measurements in the Amager plants suspension fired boiler unit AMV2 using wood and straw, and comparison with grate boiler probe measurements

A series of full-scale and long duration deposit probe measurements were conducted in the AMV2 biomass suspension boiler to investigate the deposit formation rate, probe heat uptake and ash transformation. Probe measurements were conducted in the 250 MWth boiler, firing straw and wood in suspension, and the results were compared with measurements conducted in straw-fired grate boilers. The probe surface temperature used for all the measurements was kept constant at a value of 500°C. It was identified that the deposit formation rate increases moderately with straw share increase, when straw is co-fired with wood in a suspension boiler. It was found that during 35% straw fuel share on mass basis, a deposit formation rate of 33 g/m2/h (initial 12 h) was observed, while the corresponding deposit formation rate increased to 41 g/m2/h when 100% straw was fired. Straw grate firing probe measurements (conducted at the Avedøreværket unit 2), the measured deposit formation rate was nearly similar at a level of approximately 38 g/m2/h.

(a)

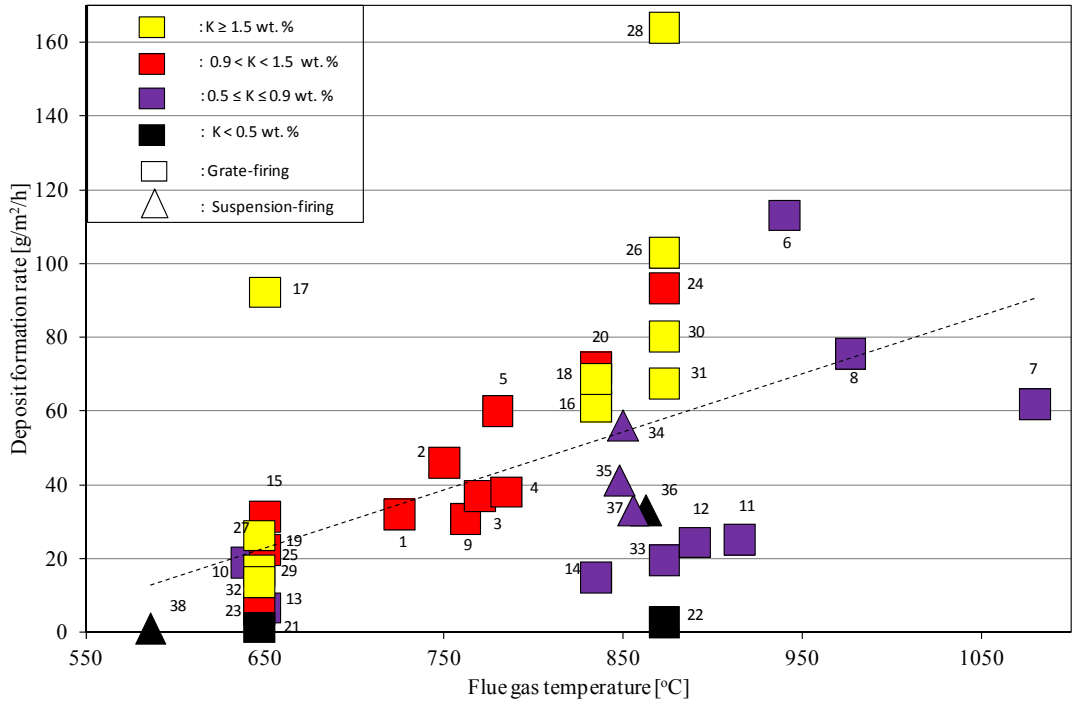

(b)

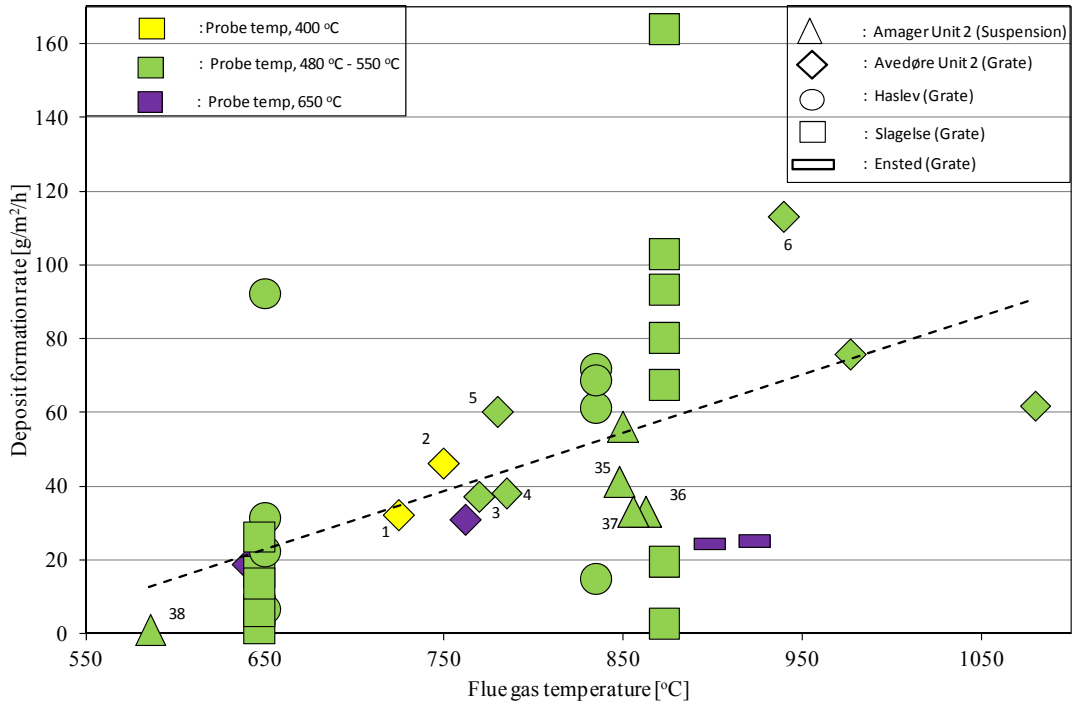

Figure 2. Impact of flue gas temperature on deposit formation rates, a) four different sets of fuel alkali contents and two types of straw firing technologies, b) different sets of probe surface temperatures and 5 different boilers. Amager Unit 2 is a straw and wood-fired suspension boiler. Avedøre Unit 2 is a straw-fired grate boiler. Haslev is a cigar type boiler where big bales of straw are fired directly. Slagelse and Ensted are both straw-fired grate boilers. Graph details: a) the color represents the range of fuel alkali in wt.%, while the point shape represents the straw firing technology, b) the color represents the probe surface temperature, while the point shape represents the boiler type.

The suspension boiler probe data were compared with data from previously conducted grate boiler deposit probe measurements, and in Figure 1 is shown the influence of flue gas temperature, fuel alkali content and boiler type on measured deposit formation rates. The comparison shows an increasing trend in deposit formation rate with increase in flue gas temperature. At a flue gas temperature of 650 °C, the deposit formation rate is typically from 5 to 30 g/m2/h and at 900 °C, the deposit formation rate is typically 20 to 110 g/m2/h. At higher fuel alkali contents (K > 1.5 wt.%), the increase in deposit formation rate with flue gas temperature was more significant, compared to the increase in the deposit formation rate at lower fuel alkali contents (K $\leqslant$ 0.5 wt.%). An increased flue gas temperature probably increases the fraction of molten ash as well as provides an increased content of gas phase alkali species, and both will lead to an increased deposit formation rate. It was also observed that the deposit formation rates measured in suspension and grate boilers are on similar levels. This was observed even though the concentration of fly ash in the flue gas was significantly higher in the straw suspension-fired boiler.

Shedding events registered by a CCD camera showed that the predominant phenomenon of deposit removal during 80% straw firing in suspension with wood was debonding.

The elemental composition of fly ash generated during straw suspension firing shows higher contents of Si and Ca, compared to grate firing fly ash that is rich in the volatile elements K, Cl and S. SEM-EDX analysis indicated that the fly ash generated during straw firing in suspension consists of three kinds of particles: 1) flake type Si rich particles, 2) molten or partially molten particles (> 20 μm) rich in Si, K and Ca with small amounts of Mg, P and potassium salts on the outer surface, and 3) small particles rich in K, Cl and S (between 0.1 and 5 μm). Chemical analysis of the outer layer of upstream deposits during 35% straw-firing and 100% straw-firing indicated that by increasing the straw share in the fuel, the K, Cl and Si contents were increased, while the Ca and Mg contents were reduced.

It was also found that 35% straw firing with wood does not create severe fouling and slagging on the heat exchanger tubes at the AMV2. The experiences of the operational staff indicates that the boiler operation period may exceed more than one month without deposit related operational problems when firing maximum 50% straw with wood on mass basis. The findings related to deposit management during straw suspension firing are:

- At higher flue gas temperatures (750-950°C, in the AMV2 boiler), efficient soot blowing is needed to manage the boiler tube deposits with small superheater tube spacing (113 mm, current case). An increase in superheater tube spacing probably will lead to the absence of tube clogging by ash deposits.
- At flue gas temperatures below 650°C, deposit formation rate is small and deposits can be easily removed by sootblowers.

Further documentation of the probe measurements and the obtained results of the study can be seen in appendix 3.

4.2 Probe investigation in the Amager plant suspension fired boiler unit AMV1 measuring deposit formation rates and shedding

Probe measurements of deposit build-up and removal (shedding) in the 350 MWth AMW1 suspension boiler, firing straw and wood were conducted. The influence of fuel type (straw share in wood), probe exposure time, probe surface temperature (500, 550, and 600 °C), and flue gas temperature (600−1050 °C) on ash deposit formation rate has been investigated. A systematic procedure to determine deposit formation rate

from in situ probe measuring deposit data was developed and termed the derivative-based deposit formation rate (DDF-rate). This is the directly measured deposit formation rate between mayor shedding events. A comparison with previously conducted probe measurements at different straw-fired boilers was made based on another measure of deposit formation rate – the integral deposit formation rate (IDF-rate). The IDF rate is determined by weighting the collected deposits from the probe after it has been removed from the boiler, and then calculates the deposit formation rate based on the collected weight divided by the probe surface and the probe residence time in the boiler. Most previously conducted probe measurements (Including the measurements presented in section 4.1) have provided IDF rates that do includes the shedding events in the deposit formation rate.

Ash transformation was investigated by bulk ash analysis of the fuel ash, fly ash and deposit layers. Quantification of naturally occurring deposit shedding, as well as sootblower induced shedding were done. The Peak Impact Pressure (PIP) (Local sootblower pressure) needed to remove the deposits by sootblowing was determined. The data treatment of the deposit formation (DDF rate) and shedding rates were done by dividing all the measurements into 6 hour intervals. Thereby the influence of fuel, probe temperature and flue gas temperature could be investigated. An example of a result is seen in Figure 3 where the measured net deposition accumulation rate is shown as a function of flue gas temperature. The net deposition accumulation rate is equal to the DDF rate minus the total deposit shedding rate. The net deposit accumulation rate increases with increasing flue gas temperature. It can be seen, as an example, that the net deposit accumulation rate is generally low (mean value of 452 g/m^2/h) at lower deposit probe mass loads (< 5,000 g/m^2), compared to a mean value of 1155 g/m^2/h for deposit mass loads greater than 5,000 g/m^2. (At the conditions: probe temperature 500°C, flue gas temperature about 900-910°C and a straw share of more than 20 wt.%).

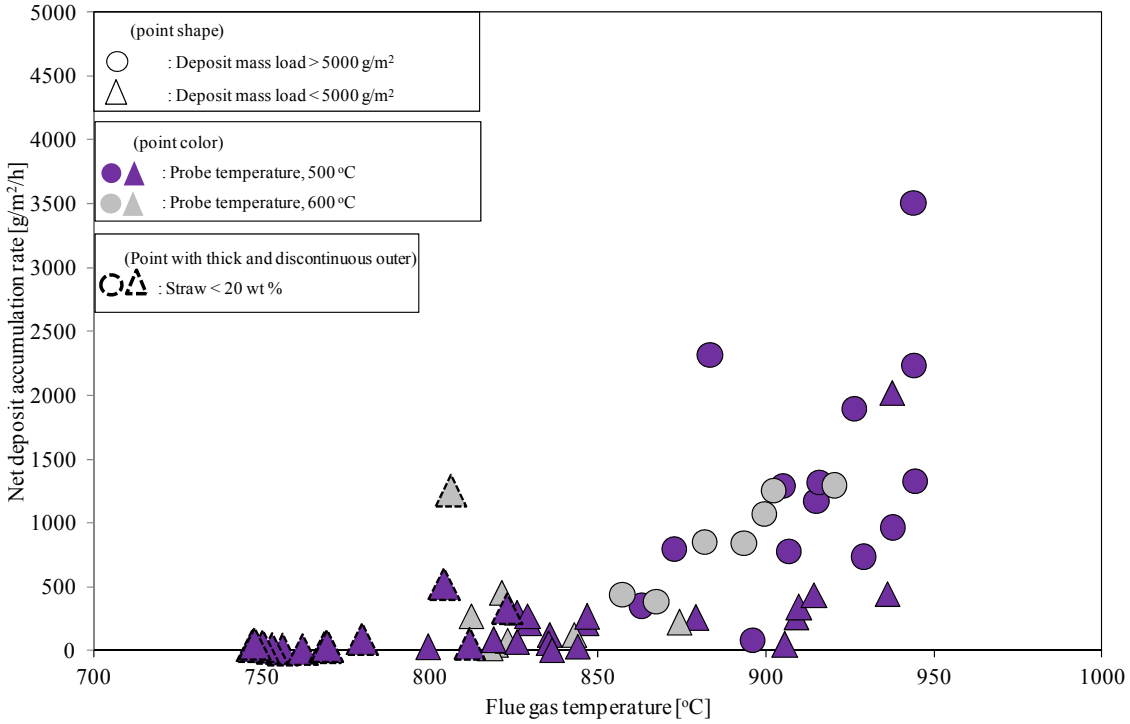

Figure 3. Impact of flue gas temperature on the net deposit accumulation rate. The particular point shape represents the deposit mass load; the color represents the probe surface temperature, while point (larger in size) with thick and discontinuous outer is representative for straw share in wood.

The overall conclusions of the probe measuring campaign conducted in the AMV1 boiler are the following:

- The bulk chemical composition of straw and wood suspension-fired fly ash shows relatively higher contents of Si, Ca, and lower contents of volatile elements (K, Cl and S), compared to grate firing conditions.
- The upstream side deposit outer layers on the probe contain high concentration of Si, K and Ca, indicating that larger particles impact on and stick to the probe on the upstream side. K, S and Cl were found in higher proportions on the downstream side deposit layers indicating that the downstream deposits to a greater extent are formed by thermophoresis and/or condensation of KCl and K_2SO_4. The innermost layers were rich in K, Cl and S.
- The DDF-rate increases with increased straw share in wood and with increase in flue gas temperature, but probe surface temperatures have no significant influence on the measured DDF-rates. DDF rates were typically bellow 1000 g/m^2/h when the flue gas temperature was bellow 870°C, while DDF rates up to 4000 g/m^2/h were observed at flue gas temperatures above 900°C.
- Video recordings revealed that deposit shedding was primarily through debonding, where a deposit layer is being removed due to a break off of the deposit from the tube surface.
- It was observed that the shedding process is a stochastic process, where the shed amounts are highly variable even at constant conditions. We believe the amount of deposit shed is strongly related to the strength of the inner most salt rich deposit layer.
- The deposit shedding process was characterized by calculation of the average amount of deposit removed at a shedding event [g/m^2] and the frequency of the shedding events [h^{-1}] in 6 h periods. The average shedding event magnitude was 716 g/m^2 during natural deposit shedding and 805 g/m2 during plant sootblower induced shedding. The shedding frequencies were 0.81 h^{-1} and 0.89 h^{-1} during natural deposit shedding and plant sootblower shedding events, respectively. Based on the shedding magnitude and frequency it was possible to calculate a shedding rate [g/m^2/h].
- The deposit shedding rates increased at high flue gas temperatures (> 850°C) and high probe deposit mass loads (> 5,000 g/m^2) where also high deposit formation rates are observed (DDF-rate).
- The shedding rate is in most cases higher at a probe temperature of 500°C than at a probe temperature of 600°C.
- The net deposit accumulation rate increases with an increase in flue gas temperature, and the net deposit accumulation rate is low (mean value 452 g/m^2/h) at lower deposit mass load (< 5,000 g/m^2) on the probe, compared to a mean value of 1155 g/m^2/h for deposit mass load greater than 5,000 g/m^2 (at the conditions: probe temperature 500°C, flue gas temperature about 900-910°C and a straw share of more than 20 wt.%).
- Generally no clear tendency for the impact of probe surface temperature on net deposit accumulation rate was seen.
- A sootblower probe was used to investigate the needed PIP to remove the deposits. At lower temperatures (500°C), the deposits formed at an exposure time of less than 91 h could be removed with a PIP of less than 55 kPa. At higher probe surface temperature (600°C), the PIP needed to remove the probe deposits significantly increase.

Detailed description of this study was provided by two journal papers that can be seen in appendix 4 and 5.

4.3 Deposit probe investigation in the Avedøre wood suspension fired boiler

A series of deposit probe boiler measurements were conducted at the Avedøre Unit 2 wood and natural gas suspension-fired boiler, to investigate ash deposition with coal ash addition. The probe was placed just below

the radiation shield in the top of the boiler chamber. The measurements included deposit mass, heat uptake, flue gas temperature and video registration. The overall conclusions are summarized in the following points:

- Changes in biomass boiler load lead to some degree to changes in boiler flue gas temperature and the used coal ash to wood ash ratio in the conducted experiments. It is therefore difficult to determine which changes that causes the observed large changes in the deposit formation rate. However, a high increase in local flue gas temperature seemed to increase the deposit formation rate.
- Video monitoring revealed that the deposits formed were not sticky and could be easily removed by gravity shedding even at very high flue gas temperatures (> 1350°C). Deposit removal through surface melting was not observed. This indicates that potassium (K) has been captured by coal ash to form deposits with high melting temperatures.
- SEM-EDX analysis of deposits showed high contents of Ca, Al and Si, indicating that K has been captured by the coal ash to form deposits rich in calcium-aluminum-silicates. Cl was not found either on the upstream side or on the downstream side of the probe deposits, and Cl has probably been released to the gas phase as HCl(g).

Further description of the Avedøre Unit 2 probe measurements can be found in appendix 6.

5.0 Modeling

Modeling of the ash deposition process and heat uptake in a suspension fired biomass boiler was done to get better understandings of the key processes responsible for ash deposition. Due to project resources constrains it was decided to limit the modeling to the deposit formation process and leaves out the shedding process. The model used is a modified version of the model developed by Zhou et al. [1]. The model describes the deposit related processes as a function of the local parameters as flue gas velocity, flue gas temperature, probe surface temperature and fly ash properties. Deposit formation processes as condensation of ash species, thermophoresis coursed deposition formation by small particles and impactions of larger particles are included in the model. Simulation results showed that for straw and wood co-combustion when the straws share was high, there is an increase in the deposit mass uptake and DDF-rate with an increase in flue gas temperature. Increased flue gas temperatures increase the fraction of molten ash and that will lead to higher amount of the fly ash being deposited. The results of changed probe surface temperature showed that the changed probe surface temperatures in the range from 500 to 600°C do not seem to significantly influence the deposit formation rate. The model over predicts the ash deposition rate quantitatively but the qualitative behavior was in accordance with the experimental findings. The heat uptake model predictions were comparable with experimental findings both quantitatively and qualitatively. From a practical point of view, it was seen that the flue gas temperature and share of straw in wood are the two main parameters responsible for an increased deposit formation on superheater tubes. Further description of the modeling work can be found in appendix 7.

6.0 Ideas for obtaining improved deposit shedding

At some brainstorming meetings during the project novel ideas for deposit removal were discussed. The following methods for improving deposit removal were considered:

- Using of mechanically methods in the form of scraping metal rings on superheater tubes or rapping gear equipment as originally used on waste incineration plants. In boiler areas with flue gas temperatures bellow 800°C such mechanically equipment may be used.

- It may be possible to perform more detailed optimization of the sootblower control systems based on the detailed knowledge about the deposit removal properties obtained in the present project
- Use of adequate additives in the production of biomass fuel pellets to minimize deposits formation. This could be done by adding Si and Al rich species to straw pellets.

Further description on the deposit reduction methods can be found in appendix 8.

7.0 Resume and Conclusions

It was the objective of this project to provide an improved understanding of ash deposit formation and removal in biomass suspension fired boilers, also called pulverized fired biomass boilers. A large part of the work was conducted as a PhD project by Muhammad Shafique Bashir that obtained his PhD degree based on the project. The results of this project is documented in this final report, in the PhD thesis by Muhammad Shafique Bashir and in three published peer reviewed journal papers that appear as appendix 3, 4 and 5 in this report. The following main activities were conducted in the project:

- A literature study mainly summarizing the results obtained in previous investigations conducted on biomass fired combined heat and power grate boilers
- Development and test of a vertical deposit probe that could be used in the boiler chamber area, and further development of the advanced horizontal deposit formation probe that is mainly used in the superheater area. The vertical probe development was stopped because too large resources were needed to finish a well functioning probe system.
- Horizontal probe deposit measurements were conducted on the Vattenfall AMV2 suspension boiler firing wood and straw, and the results was compared with previously tests conducted on grate fired boilers
- Horizontal probe deposit measurements were conducted on the Vattenfall AMV1 suspension boiler. There was developed a method for Derivative Deposition Formation rate (DDF rate) determination (The deposit formation rate excluding shedding events) and also detailed studies of shedding were conducted
- Deposit probe measurements at the Avedøre suspension fired wood boiler unit was conducted investigating the influence of coal ash addition
- A modeling study on deposit formation in suspension fired biomass boilers was conducted.

The following main results were obtained:

- The measured deposit formation rates (IDF) from grate firing and suspension firing of biomass have been compared and the levels were reasonably similar. The influences of fuel composition, flue gas temperature and metal surface temperature on deposit formation rates (on both IDF and DDF rates) have been established.
- The chemical composition characteristics of fly ash and deposits in biomass suspension fired boilers are described based on chemical analysis of fly ash and deposit samples.
- Video recordings revealed that deposit shedding was primarily through de-bonding where a large fraction of the deposits breaks of near the tube metal surface. It was observed that the natural shedding process is a stochastic process, where the shed amounts are highly variable even at constant conditions. Also the shedding data were analyzed with respect to the influences of fuel composition, flue gas temperature and metal surface temperature, and it was found that especially a metal surface temperature increase made the deposit more difficult to remove.

- A soot blower probe was used to investigate the needed PIP to remove deposits. It was observed that both an increased metal surface temperature and an increased deposit age increased the PIP needed to remove the deposit.
- Wood suspension combustion with coal ash reduces the content of Cl in deposits. Relatively high flue gas temperatures appeared in the top of the wood fired boiler chamber, and even then was seen deposit that was removed by natural shedding.
- Modeling of deposit formation rates showed generally the same trends as observed in the measurements, but the model do not give quantitatively accurate predictions.

Some proposals for further work that could improve the power plant owner's capacity to deal with biomass ash deposit induced boiler operation problems are:

- More detail modeling of the deposit and shedding process (work on this issue is initiated in the strategic research centre financed GREEN project).
- Provision of more fundamental biomass ash related data important when modeling biomass ash deposition processes. Such fundamental data includes fly ash melting properties, deposit adherence strength and biomass deposit heat transfer conductivity.
- The fly ash formation process in biomass suspension fired boilers is not well know and should be further studied (work on this issue is initiated in the strategic research centre financed GREEN project)
- The Vertical probe could be an important tool for investigating deposit formation in the boiler chamber area, however further development of the system is needed.
- Some practical methods to efficiently reduce deposit formation have been proposed. Large scale tests will be needed to make a further development of these methods.

Danish Resumé

En øget anvendelse af biomasse i store suspensionsfyrede kraftværker er en relativt økonomisk og effektiv måde, at anvende biomasse til kraft-varme produktion. Sammenlignet med kulfyring giver anvendelsen af biomasse anledning til dannelse af relativt store mængder af askebelægninger i fyrrummet og på overhederne. Disse belægninger kan i nogle tilfælde forøge korrosions problemer, og ved kraftig belægningsdannelse kan det være nødvendigt at stoppe og rense kedlen manuelt. For at begrænse problemerne kan overhedertemperaturen sænkes, men det formindsker el virkningsgraden. Dette projekt har sigtet mod tilvejebringelse af eksperimentelle data der forøger forståelsen af askebelægnings-dannelse og -afkast i biomasse suspensionsfyrede kedler. Der er i projektet udført belægningsondemålinger på forskellige biomassefyrede suspensions kedler. Der er anvendt to typer af belægningssonder i projektet. Der er anvendt en horisontal sonde der er blevet videreudviklet, og som kan registrerer temperaturer, belægningsvægt og energioptag; og hvor belægningsprocessen kan videofilmes. Der er desuden taget de første skridt til udvikling af en vertikal sonde, der vil kunne anvendes til målinger af belægningsdannelse på kedelvægge i fyrrummet.

Den første fuldskala målekampagne blev udført på Amagerværkets unit 2, som er en 250 MWth suspensions fyret kedel der anvender halm og træ. De opnåede sonde måle resultater blev sammenlignet med målinger udført på en 105 MWth halmfyret ristekedel. Elementaranalyse af flyveasker viste, at flyveaske fra suspensionsfyring af halm har et højt indhold af Si, K og Ca, mens flyveaske fra halmfyring på rist havde højt indhold af K, Cl og S. Der blev fundet belægningsdannelses rater som var nogenlunde ens for det suspensionsfyrede og det ristefyrede anlæg.

Den anden probe målekampagne blev udført på Amagerværkets 350 MWth suspensionsfyrede blok et kedel, der forbrænder halm og træ. Målet med dette studie var at undersøge effekten af; brændselstype (andel af halm i træ), sondeeksponeringstid, sondeoverfladetemperatur (500°C, 550°C og 600°C) samt røggastemperatur (600-1050°C) på transient belægningsopbygning og afkast. To forskellige mål for belægningsopbygningshastigheden blev anvendt til dataanalysen, IDF (Integrated Deposit Formation) raten og DDF (Differential Deposit Formation) raten. IDF raten angiver belægningsopbygningsraten inkluderende både opbygning og afkast i et givet tidsinterval. DDF raten angiver den øjeblikkelige belægningsopbygningsrate i en periode hvor der ikke sker belægningsafkast. Generel ses betydeligt højere DDF rater end de bestemte IDF rater.

Belægningsopbygningsraten blev influeret af røggastemperatur og halm fraktion, mens ændringer i sondens overfladetemperatur ikke havde væsentlig indflydelse. Kvantificering af naturligt forekommende belægningsafkastning samt belægningsfjernelse forårsaget af værkets sodblæsning blev foretaget via masseoptags signaler fra belægningssonderne. Resultaterne viste at afkastningsprocessen er stokastisk, og at mængden af afkastet belægning varierer selv ved konstante lokale betingelser. I de fleste tilfælde var afkastningshastigheden højere ved en sonde temperatur på 500°C end 600°C.

Belægninger i kedler fjernes ofte ved sodblæsning, hvor en stråle af højtryksdamp rettes mod kedeloverflader belagt med askebelægninger. En sodblæserprobe med trykluft blev anvendt til at undersøge det nødvendige sodblæser stråle stagnationstryk (PIP) som krævedes for at fjerne belægningerne. Forsøgene viste at de dannede belægninger ved en sonde temperatur på 500°C og en eksponeringstid kortere end 91 timer kan fjernes med et PIP på under 55 kPa. Øget sonde eksponeringstid og/eller sonde overfladetemperatur (600°C) øgede det nødvendige PIP for fjernelse af belægningerne.

En tredje målekampagne med den horisontale sonde blev udført på Avedøreværkets 800 MW_{th} suspensionsfyret kedel, der anvender træ og naturgas med tilsætning af kulflyveaske. Resultaterne viste at tilsætningen af kulflyveaske kan påvirke akseaflejringsprofilen samt aflejringernes egenskaber. På trods af at tilsætningen af kulflyveaske øger belægningsdannelseshastigheden, lader belægningerne dannet ved røggastemperaturer på 1250-1300°C og under kulaske tilsætning, til at blive afkastet med en højere frekvens, hvilket indikerer at de er lettere at fjerne.

En tidligere udviklet mekanistisk model for askeopbygning og varmeoptag er anvendt til simuleringer, og resultaterne er sammenlignet med en del af de tilvejebragte sondemåledata. Modellen beskriver de belægningsdannende processer som funktion af lokale parametre, som røggastemperatur, sonde overfladetemperatur og ændringer i flyveaske sammensætning. Simuleringerne viste at modellen giver kvalitativt overensstemmende resultater med sonde måledata, mens den kvantitative bestemmelse af belægnings rater ikke er bestemt præcist.

Acknowledgment

The financial support by Energinet.DK and the financial support by Vattenfall A/S is gratefully acknowledged. We would like to thank Vattenfall A/S and DONG Energy A/S for access to their boilers. We are thankful to the operational staff at the Amager Power Station (Vattenfall) and Avedøre Power Station (DONG) for their technical support during the full-scale measurements. Special thanks go to DTU CEN for help in SEM-EDS analysis.

References

1. H. Zhou, P. A. Jensen, F. J. Frandsen, Fuel, 86 (2007), 1519-1533.

September. 2012, DTU no. 50530

Appendix A1

Literature review

Energinet.dk project no. 7217

Characterization and quantification of deposits build up and removal in straw suspension fired boilers

Muhammad Shafique Bashir, Flemming Frandsen, Peter Arendt Jensen

Department of Chemical and Biochemical Engineering

Technical University of Denmark

Søltofts Plads, Building 229, DK-2800 Lyngby, Denmark

CHEC no. R1301

Literature Review

1.1 Introduction

The utilization of renewable energy sources seems to be essential because of the increase in CO_2-emissions, increase in world energy demands and depletion of fossil fuels. Biomass is considered to be one of the most widely accepted environmental friendly renewable energy sources. The most commonly used biomass fuels include wood, short-rotation woody crops and agricultural wastes [51]. In the last two decades, much attention has been paid in the world for biomass (co)-combustion for heat and power production. Traditional biomass contributes significantly to the world's energy supply, accounting for about 10% of the world's energy supply [1]. A significant share of biomass in simple stoves accounts for the global biomass consumption and an increased application of modern biomass boilers in developing and in developed countries can result in improved energy efficiency and reduction in harmful emissions [2]. In the regions with larger forests like Northern and Central Europe, wood can be the predominant biomass type used for energy production while in agriculture areas, agricultural waste (straw) can be used.

Biomass - straw and wood - has had increasing use in Denmark since 1990 and by the end of 2009, there were 8 biomass-fired and 5 biomass co-fired plants in Denmark [4]. The power plants in Denmark have been obliged to use 1.0 Mt of straw and 0.2 Mt of wood chips annually [5]. In the recent debates, new initiatives are being discussed, aiming for complete substitution of coal with biomass in the largest cities and industrial districts in Denmark [7, 8]. The complete substitution of coal with biomass would be possible either by commissioning of new biomass-fired boilers and/or retrofitting of existing coal-fired boilers. This process could be extremely challenging because biomass fuels differ in many ways from coal, having higher moisture contents, lower heating values and a variety of impurities, chlorine (Cl), alkali metals (K and Na), sulfur (S) and nitrogen (N) etc. [9]. Biomass fuel ashes are compared to fossil fuel ashes often rich in elements such as chlorine (Cl), alkali metals (K and Na), silicon (Si) and calcium (Ca), and the release of some of these elements to gas phase during combustion may form alkali chlorides and ash with lower melting temperature, leading to severe ash deposition and corrosion of boiler coils [2, 5, 10-22]. Large deposit formation problems may limit the electrical efficiency by limiting the maximum applicable superheater temperatures, and the deposits may also cause many boiler stops where different parts of the boiler have to be cleaned. The heat transfer through the heat exchanger can be consequently reduced, thereby reducing the

efficiency of the boiler. As the growing interest in utilizing biomass in heat and power production increases, the understanding of the fundamentals of biomass combustion has considerably increased in the recent years through extensive research. However, the available full-scale experimental studies on ash deposition in biomass-fired boilers have been reported based on measurements in grate boilers. Only limited data is available from biomass suspension firing where improved knowledge on ash transformation, and transient deposit formation and shedding is wanted to optimize design and operation. In addition, predictive modeling of ash deposition and shedding in biomass suspension-fired boilers is an area demanding significant research.

An overview of the current knowledge about biomass as a fuel, biomass combustion technologies, release of inorganic elements from biomass, ash deposition, properties of deposits, deposit shedding mechanisms and techniques, and ash deposition modeling is presented in this chapter.

1.2 Biomass Fuel and Ash Formation

Biomass is typically composed of three main components (cellulose, hemi-cellulose and lignin) and a number of minor components (lipids, proteins, water and ash). The fraction of each class of component varies depending on species, type of plant tissue, stage of growth and growing conditions [17, 53].

1.2.1 Biomass as a CO_2-neutral Fuel

The use of biomass as a fuel for heat and power production is an obvious solution to the societal energy demands because of the uncertainty and depletion of fossil sources. The issues related to global warming caused by CO_2-emissions has put an additional focus on the so called CO_2-neutral fuels - biomass. The legal binding of green house gases was established for the first time in 1997, named as the Kyoto Agreement, aiming to reduce the total emissions by 5.2% by the year 2012 [2]. Biomass was then considered all over the world a potential source to reduce the net CO_2-emissions from fossil fuels. In addition to the use of biomass only for energy production, co-firing options with coal have also been practiced in the last two decades [2]. As shown in Figure 2. 1 a significant reduction in CO_2-emissions is possible by increasing the boiler efficiency and utilizing larger share of biomass in coal-fired power plants.

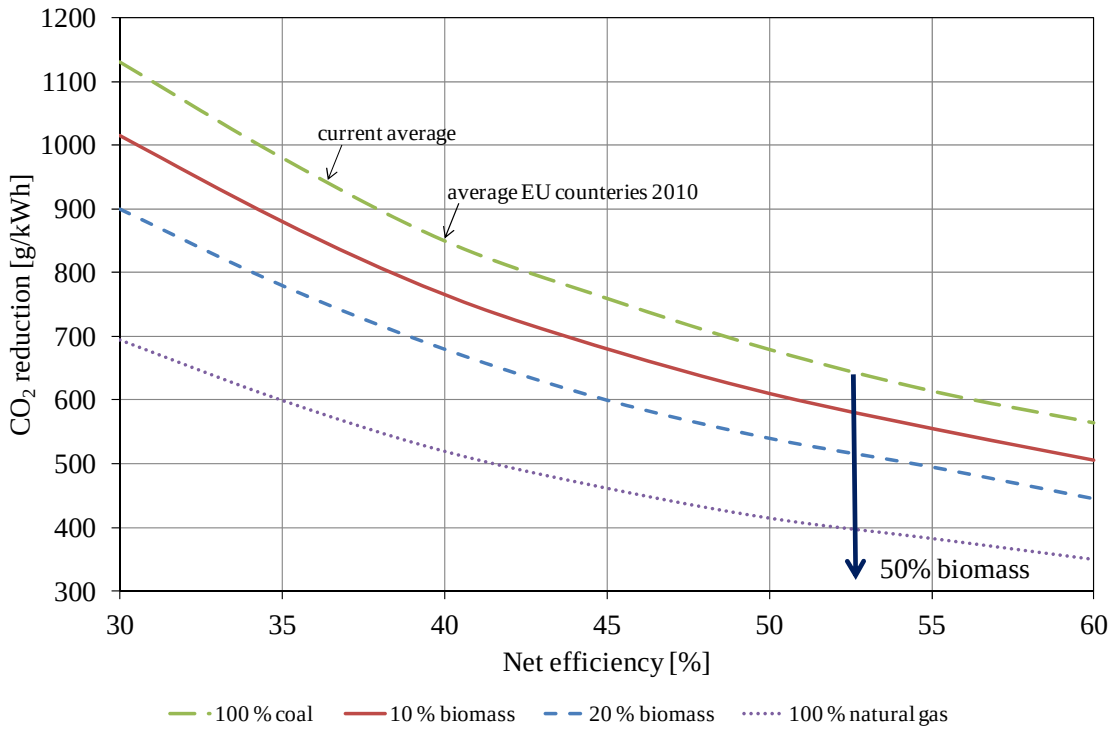

Figure 2. 1: Possible reduction in CO_2-emissions by increasing boiler efficiency and introduction of biomass to co-fired power plants [23].

Despite the introduction of biomass, the Danish electricity production has been, and still is characterized by the utilization of coal and oil. Electricity production in Denmark in terms of percentage of fuels other than coal is shown in Figure 2. 2. Significant drop in the coal share is evident from the last two decades [54]. Until the early 1990s, coal was the dominant fuel used in the production of electricity. In 2009, oil, natural gas and renewable energy together accounted for 46.3% of fuel consumption for electricity production. The share of renewable energy was the largest among the fuels other than coal. Biomass contributes about 36.1% to the renewable energy [54].

Based on the Danish energy policy in the last couple of decades, several full-scale measuring campaigns have been conducted in order to investigate the thermal conversion and utilization of biomass for heat and power production [2]. The ambitious targets for Danish energy for year 2050, demands further research on thermal conversation of biomass. To achieve a goal of fossil-fuel-free Denmark, the Danish government is ambitious to include biomass as the second largest source of energy supply in 2050, accounting for more than 27% (Figure 2. 3) [8].

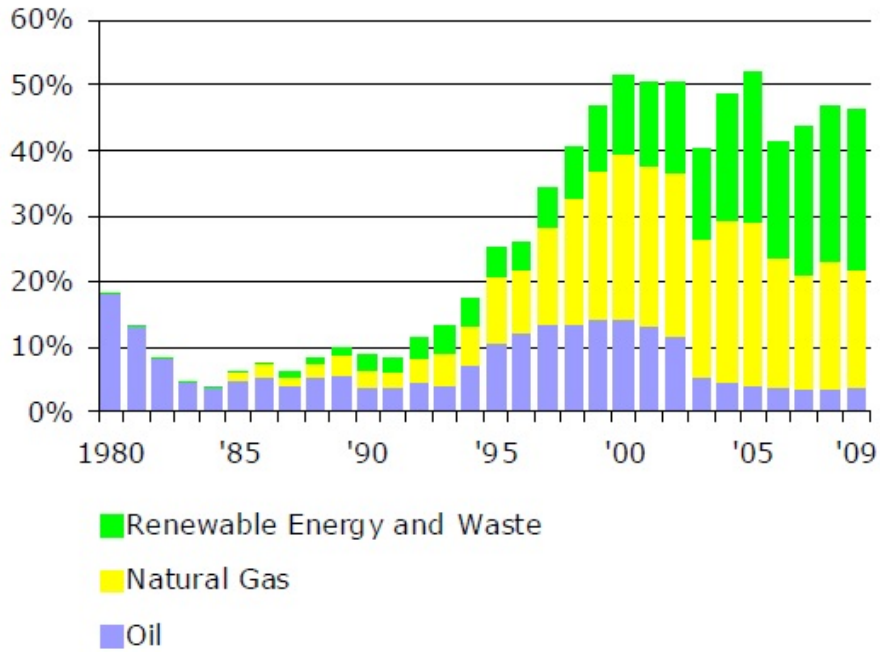

Figure 2. 2: Share of fuels other than coal for electricity production in Denmark (in percentage contribution of each fuel) [54].

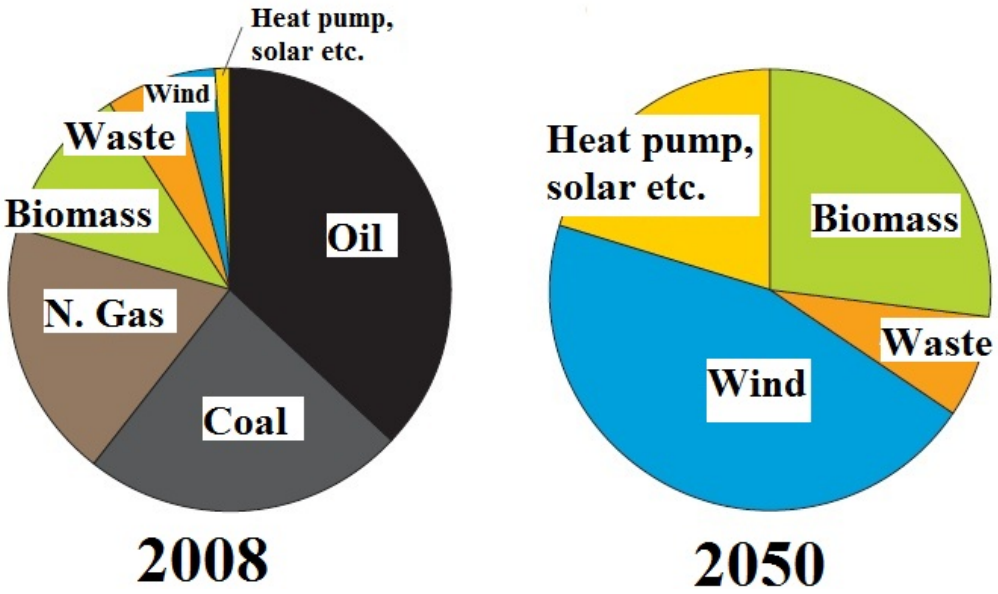

Figure 2. 3: Danish energy target for 2050 [8].

1.2.2 Characterization of Biomass Fuels

Biomass fuels are different from coal in various ways. Biomass fuels are characterized by energy density and thereby create serious issues in handling and transportation of the fuel. Coal is a sedimentary organic substance originating from vegetation and formed during millions of years in the earth's crust. Coal is normally ranked based on the degree of coalification that increases

with increasing maturity. High rank fuels are characterized by lower H:C and O:C ratios as shown in Figure 2. 4 (Van Krevlen Diagram). Biomass fuels are characterized by higher H:C and O:C ratios, and find the least place in the upper right section of Figure 2. 4. Atomic O:C ratio has significant impact on the heating values of the solid fuels. The heating values of the solid fuels normally decreases with increase in atomic O:C ratios.

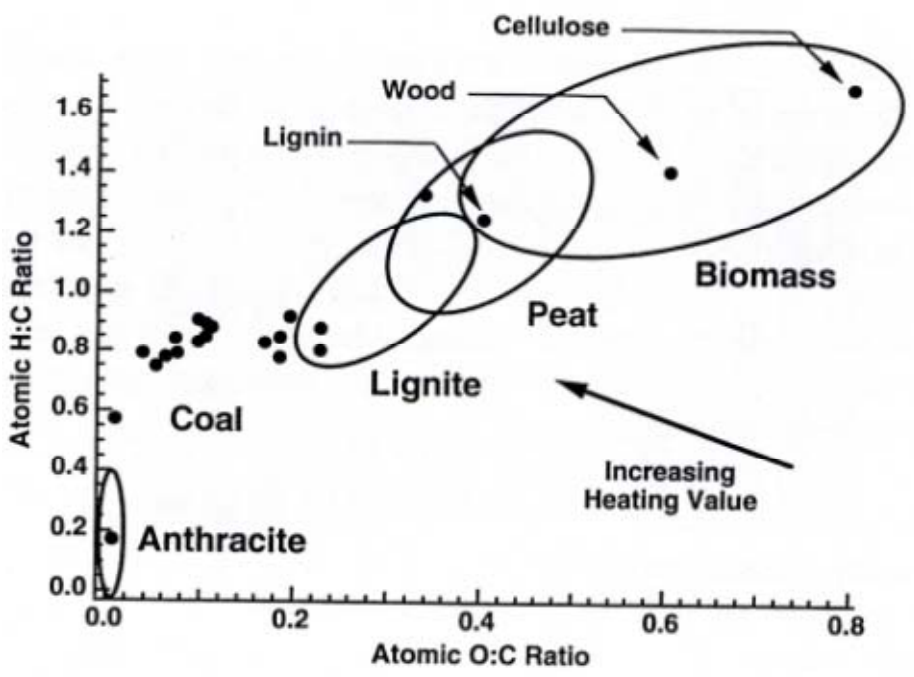

Figure 2. 4: A Van Krevlen diagram, showing atomic O:C and H:C ratios as a function of fuel ranks [14].

Nutrients needed for plant growth are the majority of the ash forming elements found in annual biomass. Furthermore, inorganic impurities can also occur as a result of contamination of the biomass with soil during harvest transport or handling. The most abundant ash forming elements in annual biomass are K, Cl, S, Ca, Mg, P, and Si [53]. In annual biomass, K and Cl are normally present in high concentrations and these will remain in ionic form and are not metabolized by the plant [53]. In wood, the presence of K and Cl is comparatively lower compared to the annual biomass fuels. S is present in biomass as inorganic sulfate and organically associated S of aliphatic nature such as in proteins, sulfate esters, and sulfur lipids [53]. As annual crops are characterized by high growth rates compared to wood tree, and thereby high production rates of proteins which require a rich S supply [53].

The inorganic material can occur as discrete minerals (soil contamination), amorphous phases, and organically associated present in the plant itself where it is embedded in the carbon matrix or simply salts dissolved in pore water [15]. In the organic phase, the inorganic material is often

present as cations associated with oxygen-associated functional groups. According to Jenkins [44], in many biofuels the dominant fraction of the inorganic material is probably associated to oxygen containing functional groups, and more than 90% of K in clean biomass fuels appears as either water-soluble, or ion-exchangeable in ammonium acetate.

The composition of wood chips, Danish straw, and coal is shown in Figure 2. 5 based on lower heating values of the fuels. It can be seen that straw contains significant amounts of Cl, K, while coal is characterized by higher S contents. A more detailed composition of Danish straw, wood chips and coal (fired in Denmark) with possible variations is shown Table 2. 1. Na is found in high contents in wood, while the elements such as Al and Fe which play a significant role for ash deposition in coal-fired boilers are only present in small concentrations in straw and wood.

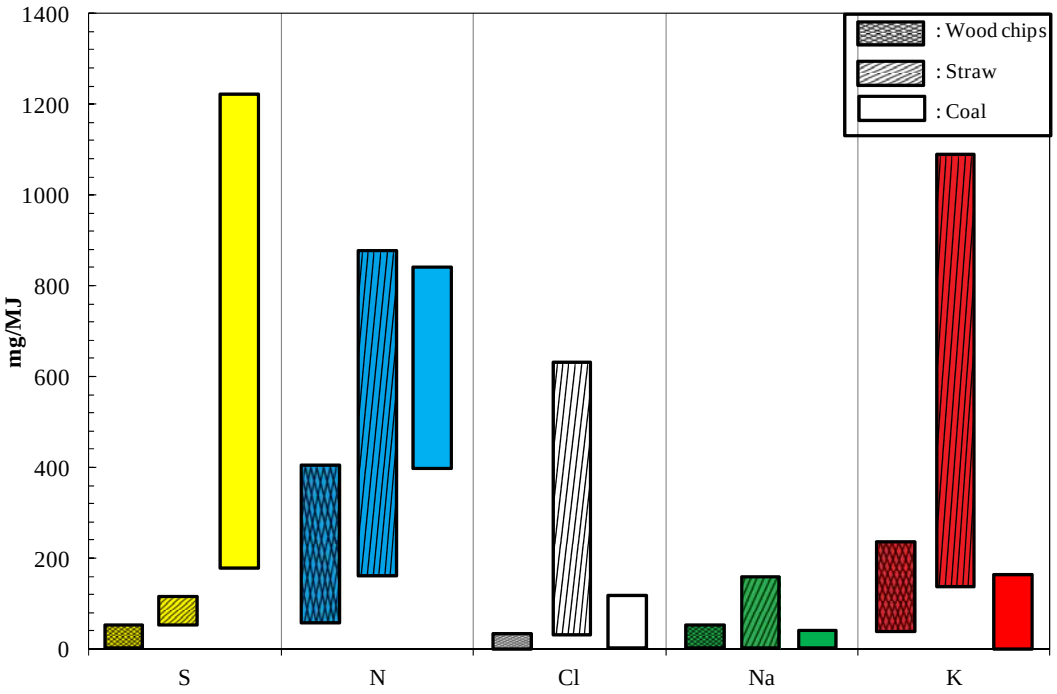

Figure 2. 5: S, N, Cl, Na and K contents in wood chips, Danish straw and coal (fired in Denmark) based on heating value of the fuel. Modified from Sander [59].

Differences between coal and straw are observed when comparing the chemical composition of the inorganic matter in coal and biomass as shown in Table 2. 2. The elemental composition of the ash-forming matter after ashing the fuel samples according to a standard ashing procedure are provided. It is common practice to give the percentage of each of the elements analyzed as if they were present as their most common oxides [2, 9]. It is important to note that the elements very seldom are present in the ash as the oxides indicated, but normally as some more complex compounds [9]. Remarkable difference in the composition of biomass-derived ashes and coal ashes is evident in terms of K, Ca and Si.

Table 2. 1: Difference in properties of Danish straw, wood chips and coal. Adopted from Flemming [2] Sander [59], Telfer et al. [61] and Glarborg et al. [62].

		Coal		Wheat straw		Wood chips	
Specie	Unit	Typical	Variation	Typical	Variation	Typical	Variation
Moisture	wt.%	3.0	2.1-14.0	14.0	8.0-23.0	45	20.0-60.0
LHV	MJ/kg	30.0	29.0-32.0	18.6	18.0-19.0	19.5	18.5-20.5
Ash	wt.% dry	10.0	4.0-11.0	4.5	2.0-7.0	1.0	0.3-6.0
Volatiles	wt.% dry	30.0	5.0-35.0	78.0	75.0-81.0	81.0	70.0-85.0
H	wt.% dry	5.0	3.0-6.0	5.9	5.4-6.4	5.8	5.2-6.1
C		88.0	69.0-93.0	47.5	47.0-48.0	50.0	49.0-52.0
N		1.5	1.0-1.8	0.7	0.3-1.5	0.3	0.1-0.7
S		1.0	0.9-5.0	0.15	0.1-0.2	0.05	<0.1
Cl		--	0.04-0.17	0.4	0.1-1.1	0.02	<0.1
Si		2.1	--	0.8	0.1-1.5	0.1	<1.0
Al		0.28	--	0.005	<0.03	0.015	<0.1
Fe		--	0.08-0.74	0.01	<0.03	0.015	<0.1
Ca		--	0.62-0.95	0.4	0.2-0.5	0.2	0.1-0.9
Mg		--	0.57-0.78	0.07	0.04-0.13	0.04	<0.1
Na		--	1.52-1.86	0.05	<0.3	0.015	<0.1
K		--	0.02-0.03	1	0.2-1.9	0.1	0.05-0.40
P		--	--	0.08	0.03-0.20	0.02	<0.1

The different fuel and ash properties of biomass in comparison with solid fossil fuels result in different combustion and deposition behavior. K rich vapors, salts and silicates with relatively low melting temperature ranges are formed during straw combustion [17]. These potassium components play a significant role in the deposit formation because they act as glue bonding the individual fly ash particles together [22]. The differences are summarized based on the combustion and deposition behavior by Yin et al. [60] as,

- Biomass fuels generally have higher volatile contents and lower heating values than coal
- Pyrolysis starts at a lower temperature for biomass fuels
- The fractional heat contribution by volatiles in biomass is of order of approx. 70% compared to approx. 36% for coal

- ❖ Biomass chars have higher oxidation reactivity, probably as a result of presence of alkalies in the char matrix
- ❖ Straw has more free alkali in ash and can aggravate fouling and slagging problems

Table 2. 2: Fuel analysis of biomass and coal fuels. Adopted from Frandsen [2]. [a] wt.%, [b] % d.f. [c] % d.a.f.

Fuel	Alfalfa	Straw (Rape)	Spruce	Bark	Illinois (6)	Upper (F)	Wyodak (A)	Beulah (Z)
Moisture[a]	6.9	6.4	6.1	5.4	7.97	1.13	28.09	32.24
Ash[b]	10.9	9.7	0.5	4	14.25	13.03	6.31	6.59
C[c]	44.6	44.7	50.9	51.6	70.46	84.39	52.52	47.77
O[c]	47.4	47.5	43.3	42.9	18.57	6.86	42.47	47.74
H[c]	5	5.1	5.6	5.1	4.54	4.64	3.75	3.16
S[c]	0.23	0.3	0.01	0.05	5.18	2.64	0.48	0.58
Na[c]	2.34	1.4	0.11	0.42	1.25	1.54	0.78	0.75
Cl[c]	0.46	0.98	0.01	0.02	0.05	0	0.02	0.04
Ash[c]								
SiO_2	11.5	7.8	21.2	25.5	42.63	44.39	36.6	18.89
Al_2O_3	1.1	1.6	1.3	2.8	14.95	22.38	17.71	9.83
Fe_2O_3	0.5	0.8	1.1	2.0	25.34	22.25	6.61	7.31
CaO	16.9	22.9	32.7	36.5	8.27	4.34	21.67	24.67
MgO	2.5	2.5	3.2	2.7	0.95	1.06	5.79	7.97
Na_2O	0.6	6.8	0.2	0.3	1.17	0.32	1.89	7.75
K_2O	34.8	21.6	9.4	4.7	1.59	2.54	0.47	0.44
TiO_2	5.5	5.1	3.3	1.8	0.74	1.06	1.18	0.33
P_2O_5	16	3.9	21.6	13.7	0.11	0.11	0.83	0.44
SO_3	5.1	12.7	1.1	1.2	4.24	1.06	7.56	22.28

1.2.3 Biomass Combustion Technologies

A correct evaluation of available combustion technology options for biomass conversion is important to ensure a successful and optimal biomass utilization [60]. Based on the certain type of biomass fuels, transportation cost and combustion behavior, different combustion technologies can be employed. The most commonly used systems for biomass combustion are grate-fired boilers, fluidized bed boilers and suspension-fired boilers. The choice of combustion technology is depended upon the nature and severity of the operational problems and fuel handling problems.

In grate boilers, the fuel is combusted in the bottom part of the furnace chamber on a moving bed. In biomass grate-fired boilers, two mechanisms generally generate fly ash, volatilization of inorganic elements and particle entrainment. As shown in Figure 2. 6, the alkali metals, S and Cl are released from the fuels, and the formation of these flame-volatile elements resulted in the formation of aerosols when the flue gas is cooled down in the convective pass region.

Different types of grate configurations are employed based on the specific combustion requirements of a solid fuel. In a stationary slopping grate boiler, the grate does not move but the fuel burns as it slides down the slope. In a traveling grate boiler, fuel is fed in at the one side of the grate and has to be burnt before it reaches the ash dumping site of the furnace. With a vibrating grate boiler, the fuel is fed evenly over the whole grate. Suspension firing of biomass is a fairly recent development and is practiced in relatively few installations.

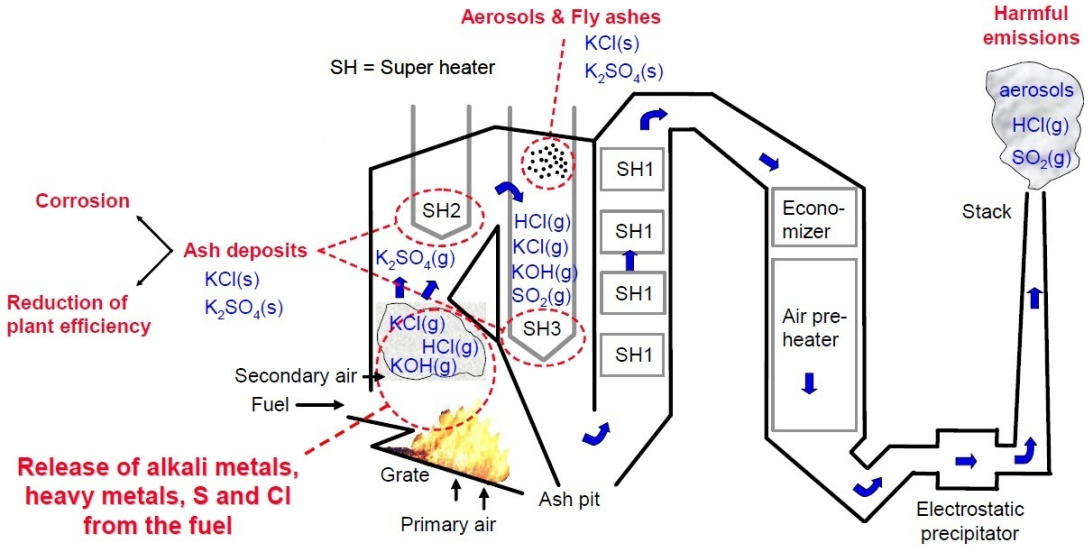

Figure 2. 6: Schematic drawing of a grate-fired boiler used for biomass firing [63].

Table 2. 3: Operating comparison of solid fuel firing technologies. Adopted from Glarbog et al. [62].

Technology	Combustion temp.	Gas velocity	Residence time (gas)	Residence time (solid)	Air to fuel	Ash split (fly ash /bottom ash)
	^{o}C	m/s	s	s	ratio	%
Grate	1100-1300	4-9	1.0-3.0	1000-10000	1.3-2.5	5-30/70-95
Fluidized bed	850-900	5-8	0.5-6.0	500-1000	500-1000	--
Suspension	1100-1500	5-10	1-3	1-3	1.1-1.3	80-90/10-20

In biomass suspension firing, pulverized biomass typically from pellets crushed in the roller (coal) mills is blown into the burners, where the fuel particles are burned in suspension. Combustion of straw and/or wood in suspension-fired units is an attractive option because of the often high electrical efficiency of these plants (46-48%), compared to the traditional grate-fired systems (25-30%) [2]. A disadvantage of this technology is that fuel requires a comparable large amount of pre-treatment. In suspension firing, offsetting the higher efficiency results in the cost associated with drying and meeting the required fuel particle size for combustion [37]. For proper combustion in suspension fired boilers, biomass fuels are required to have a

moisture content less than 15% and a fuel particle size of less than 6 mm, but this is not universal [64]. Thus, for suspension burning of fuel, the fuel handling systems require more careful design than conventional biomass firing systems [66]. The schematic drawing of a typical biomass suspension-fired boiler is shown in Figure 2. 7. Suspension-fired combustion systems are generally associated with very large solid fuel boilers for power generation, and are not fueled with biomass alone, although there are a small number of biomass fired boilers in operation in Denmark and Sweden [5, 24, 37, 38]. Literature reports of detailed test work on pulverized fuel fired systems firing 100% biomass are relatively rare [5, 37, 38, 51]. During suspension firing, fuel particle residence time is of the order of a few seconds and peak flame temperatures are higher compared to grate firing conditions [37]. Furnace design and combustion conditions differ and the resulting fly ash and ash deposits can have different characteristics and physical appearances. A brief comparison of combustion technologies based on the common combustion variables is shown in Table 2. 3.

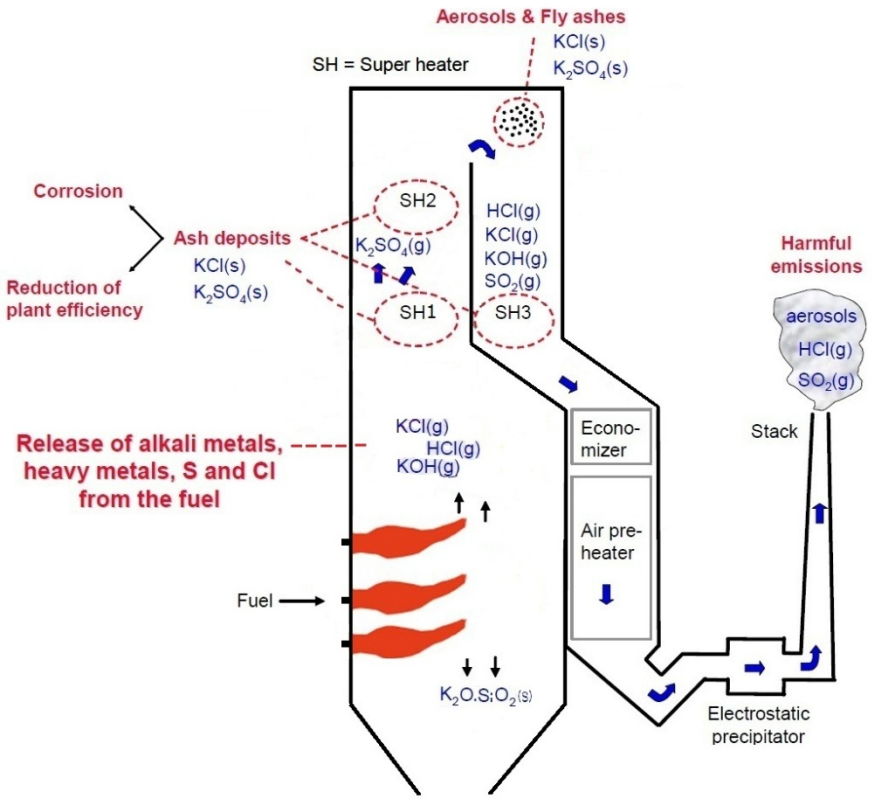

Figure 2. 7: Schematic drawing of a suspension-fired boiler used for biomass firing. Modified from Tobiasen et al. [5] and van Lith [63].

In fluidized bed combustors, the fuel particles are suspended in a fluidizing air stream in the presence of coarse-grained bed material [65]. For fluidized bed combustors, their average combustion temperature is about 850 ^{o}C, significantly lower than suspension firing systems as

shown in Table 2. 3. However, apart from fouling and slagging, the main issue while firing herbaceous based biofuels in fluidized bed combustors is the agglomeration of the bed material due to the presence of alkali metals in fuel ashes [65].

1.2.4 Release of K, S and Cl during Biomass Combustion

The principal release of alkali metals, Cl and S for biomass combustion in a grate-fired boiler is shown in Figure 2. 8. In the combustion zone, the inorganic matter, principally K, Cl and, in less amount, S, are volatilized as KCl, KOH, SO_2 and HCl. The nucleation begins when these volatilized elements become super saturated over solid particles containing Si and Na. K_2SO_4(s) is the first to become saturated (1000 ^oC) followed by KCl(s,l) (700 ^oC) [29, 60]. Submicron particles are mainly composed of K^+, Na^+, Cl^- and SO_4^{-2}, which together accounts for 80% of the submicron particles mass [10, 29]. Dayton and Milne [67], states that KCl was the primary gaseous alkali species released from combustion of straws and grasses with higher Cl and K contents, whereas KOH(g) was the most abundant alkali vapors released from feedstock with high alkali metal and low Cl contents. The release of Cl fits well for its presence in the fuel but combustion of a feedstock with higher K contents does not necessarily mean the high level of potassium (K) gases [53].

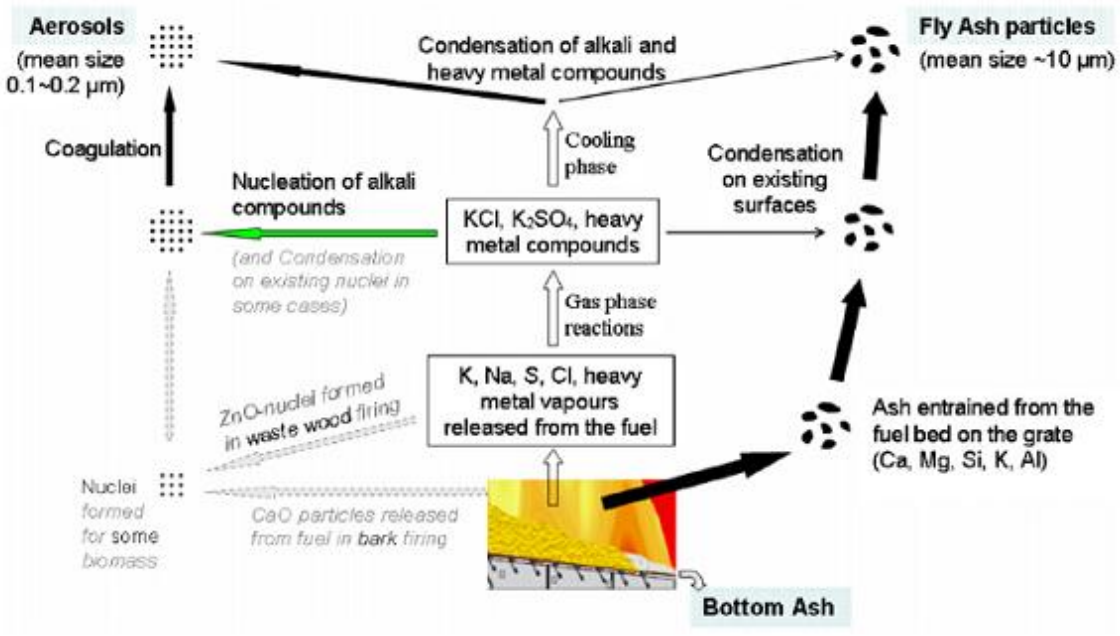

Figure 2. 8: Schematic illustration of biomass combustion and ash transformation on a grate [60].

A laboratory scale reactor, meeting requirements of grate firing, was applied by Knudsen [29] to investigate the release behavior of Cl, K and S from four different types of biofuels. The results showed that between 20 and 60% of the total K is released at 900 ^oC depending upon

the fuel type. At temperatures above 900 °C, the relative K-release increased almost linearly as a function of temperature until 60-90% is released at 1150 °C [29]. Based on this experimental work, the conclusion was that the K-release in grate-fired boilers is significant for fuels containing high amounts of Cl and/or high amounts of K relative to Si [29]. Whereas, the K release is expected to be low for high Si fuels and low Cl-content [29]. Results showed that Cl is released in two steps, between 30-60% was released below 500 °C, while the remaining Cl was released in a second step between 650 and 800 °C. In the fuel samples with relatively low Cl-content, more than 80% of the fuel Cl was released in a single step below 650 °C [29]. Nevertheless, at combustion above 800 °C, Cl was exclusively released to the gas phase [29]. It was also concluded that, if the biofuel contains relative high amounts of Ca compared to Si, the S release was relatively low and independent of combustion temperature. In general, the occurrence of other ash forming elements such as Cl, K and P are indirectly coupled to the S release. For instance, a higher Cl-content result in a higher K-release due to formation of KCl, which will leave more Si to react with Ca and thus more S is released. The S-release was more than 30% in the temperature range investigated for all fuels. This is probably related to the occurrence of substantial amounts of volatile organic S in the biofuels. The experimental work showed that the S-release in grate-fired boilers is controlled by the availability of K and Ca to capture S in the bottom ash. The availability of K and Ca is largely determined by the relative concentration of Si [29].

Pilot-scale biomass suspension firing results of Nordgren et al. [27] showed that more than two third of K in the fly ash from straw was water soluble, out of which the contribution of KCl was more than 40%. In addition, higher level of HCl emissions were observed when pure straw was fired, compared to the HCl emissions resulted from wood and bark combustion [27]. According to Nordgren et al. [27] much higher K released to the gas phase was observed during suspension firing compared to grate firing, possibly due to high heating rates, high fuel particle temperature and limited mixing between the different fuel particles in the flame/furnace. Recent results of straw dust firing in an entrained flow reactor has showed that the aerosol rich particles were formed from the nucleation, condensation, and coagulation of the vaporized flame-volatile elements K, Cl, S, and P species [39]. The particle formation mechanism of these species during straw grate and suspension firing was believed to be similar due to similar kind of aerosols formed. Fly ash particles resulted from straw dust firing were primarily molten or partially molten spherical particles rich in K, Ca, and Si, and to some extent Si rich flakes.

1.3 Biomass Ash Deposit Formation

1.3.1 Deposit Formation Processes

When solid fuel is burned, inorganic material is being released to the flue gas in the form of gases, liquids and solid particles and the fate of the inorganics depend upon the mode of occurrence, local conditions inside the boiler, and boiler design [42]. Dry ash particles, sticky particles and gaseous ash species form deposits on the boiler surfaces. Deposits are formed due to accumulation of fly ash particles and aerosols starting by the condensation of inorganic vapors on exposed surfaces cooler than the flue gas in the boiler. Subsequent chemical reactions within the deposit and sintering will further contribute to the build-up of the deposits layers and strength [53]. Composition of the deposits can vary depending upon the position in the boiler, boiler type and fuel composition. Ash deposit formation is believed to be controlled by; diffusion followed by condensation, thermophoresis, inertial impaction and eddy impaction [28].

1.3.1.1 Diffusion followed by Condensation

In this process vapors are liquefied on surfaces colder than the surrounding gas. The difference in equilibrium partial pressure of the gaseous compounds caused by the temperature difference between the tube surface and the surrounding gas results in the duffusion of gas molecules toward the superheater tube. The amount of condensate in a deposit depends on the mode of occurrence of the inorganic material [10, 14]. Significant amount of K, Cl, and S is released in the gas phase during straw combustion and the condensable salts may considerably alter the deposit properties [17]. Condensed material can lower the porosity with a granular deposit, and when in contact with heat transfer surface, increase the bonding strength of the deposit leading to difficult removal of the deposits [20].

Diffusion of submicron species following the Brownian movement takes place for submicron-particles with diameters below 0.1 μm. Normally, the amount of material deposited by small particle diffusion is less significant than that by vapor phase diffusion. Another way of ensuring a concentration gradient for Fick's diffusion is by chemical reaction around the rim of the deposit.

1.3.1.2 Thermophoresis

Thermophoresis is related to the movement of particles in a thermal gradient from a high temperature toward a low temperature. This phenomenon is caused by the surrounding gas molecules which continuously collide with the particles from all directions. The gas molecules on the hot fluid side of the particle contains a higher average kinetic energy because of the

higher velocity than those on cold fluid side, and this results in a net force on the particle causing them to move opposite to the temperature gradient [17]. Vapors may homogeneously nucleate to form a fume and subsequently deposit by thermophoresis on the surface and vapors may heterogeneously condense on other particles in the boundary layer and arrive at the surface through thermophoresis [10]. Deposits formed through condensation and thermophoresis covers the entire circumference of the tube (see Figure 2. 9). Significant experimental work on particle deposition by thermophoresis has been carried out by Baxter and Sinquifield [55].

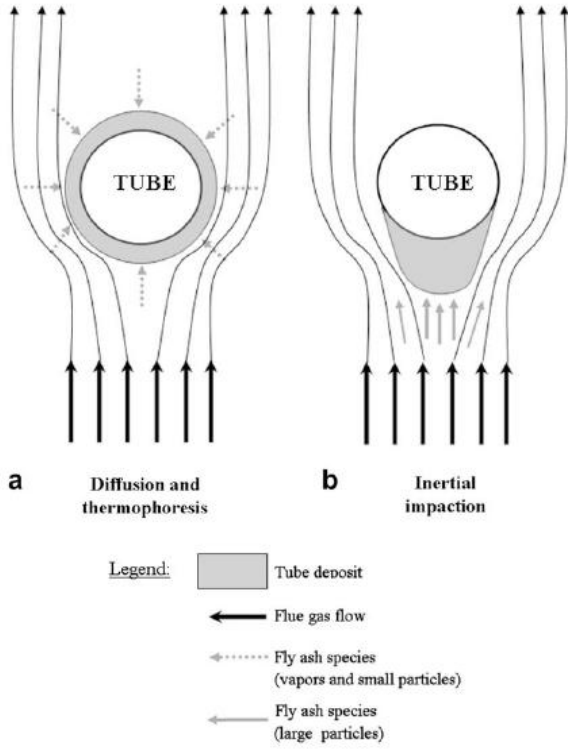

Figure 2. 9: Deposit formation on a tube, a) diffusion and thermophoresis, b) inertial impaction [42].

1.3.1.3 Inertial Impaction

Inertial impaction takes place when large particles (> 10 µm) with a large inertia do not follow the gas streamlines approaching heat transfer surface, e.g. a cylindrical tube but instead impacts on the surface. Nielsen [17] states that the capture efficiency of the particles depends upon the composition and viscosity of the melt fraction, angle of impaction, and the thermal and chemical compatibility between the particle and the deposit surface [20]. Ash particles that impact on a molten or liquid coated surface will to a higher degree stick to the surface. If the particle has too much kinetic energy in excess, it may bounce off the surface and become re-entrained in the flue gas steam [20]. The rate of inertial impaction depends upon geometry of

the target, particle size, ash melting and density, and the gas flow properties [10, 14]. Deposits formed by the inertial impaction are coarse-grained and typically form an elliptically shaped deposit in the direction of the flue gases [17] (Figure 2. 9). Significant experimental work has been conducted by Barnocky and Davis on deposition by inertial impaction [56].

1.3.2 Development of Ash Deposits

1.3.2.1 Slagging

Slagging is dominant in the area of radiant heat transfer and the initial layers of slagging comprises of primarily small, lightly sintered particles, and few larger particles that have impacted, and deformed upon impact. The composition of the initial layers for coal combustion is mostly simple metal oxides together with glassy silicate phases, but this depends a lot on the feedstock composition [20].

As the deposit grows the temperature on the outside surface increases and eventually pass the melting temperature of the deposited low melting material, at least in the outer layers (Figure 2. 10 and Figure 2. 11). As the deposit surface becomes molten, most of the reaching particles tend to stick and thus the outer layer composition of slagging deposit becomes similar to the bulk fly ash chemical composition. Low excess air and inappropriate air/fuel ratio can lead to increasing slagging deposits, and reducing conditions, and excessive slagging may lead to extension of the flame into the convective section of the boiler, and possibly causing slagging there also [17, 20].

1.3.2.2 Fouling

Fouling deposits form in the convective sections of the boiler and consist of fly ash particles and condensed volatile species that are more loosely bonded than the slags. Initially the outer layer of the fouling deposit is porous but later on sintering strength builds up in the deposit as a function of time and temperature [17]. In coal-fired systems, high-temperature fouling occurs in the regions where temperature exceeds the stability of the sulfate phases and consists of fly ash particles which are primarily bonded together with silicate liquids [17]. Low-temperature fouling occurs in the colder parts of the convective pass where the gas temperature is in the range of 650-975 ^{o}C and the sulfate phase dominates the bonding mechanism between the particles [17, 57]. There are a number of common knock-on problems associated with the formation of excessive levels of ash fouling deposits in the convective sections of the boilers. These apply to all boilers fired with biomass fuels: Firstly, the generation of higher flue gas velocities in the open gas pass channels through the bank, result in increased gas-side erosion wear of the tube surfaces. Secondly, when there is excessive convective pass fouling, with

blockage of a significant number of flue gas passes in the tube banks, there is tendency for the generation of high metal temperatures in tubes in the flue gas passes that remain open [17, 57]. This can result in accelerated metal wastage due to gas side corrosion.

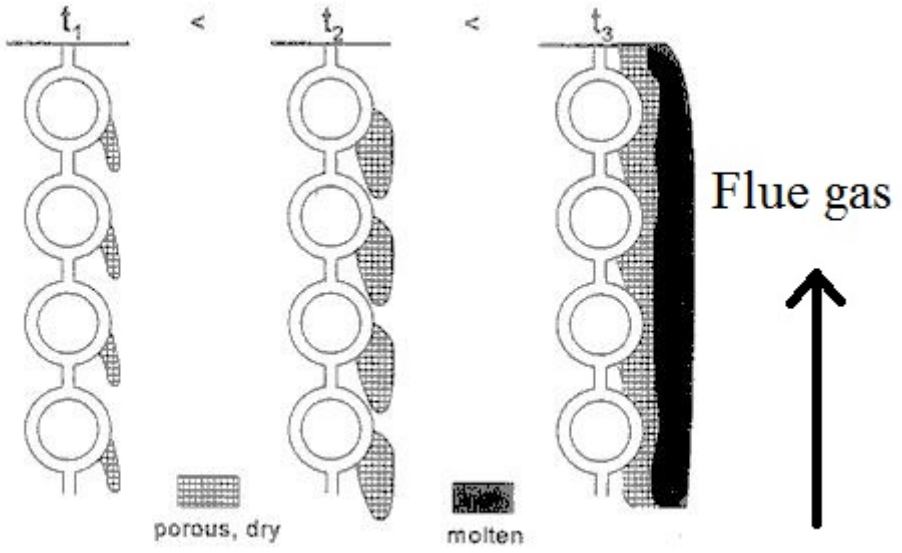

Figure 2. 10: Slagging in the high temperature region [15].

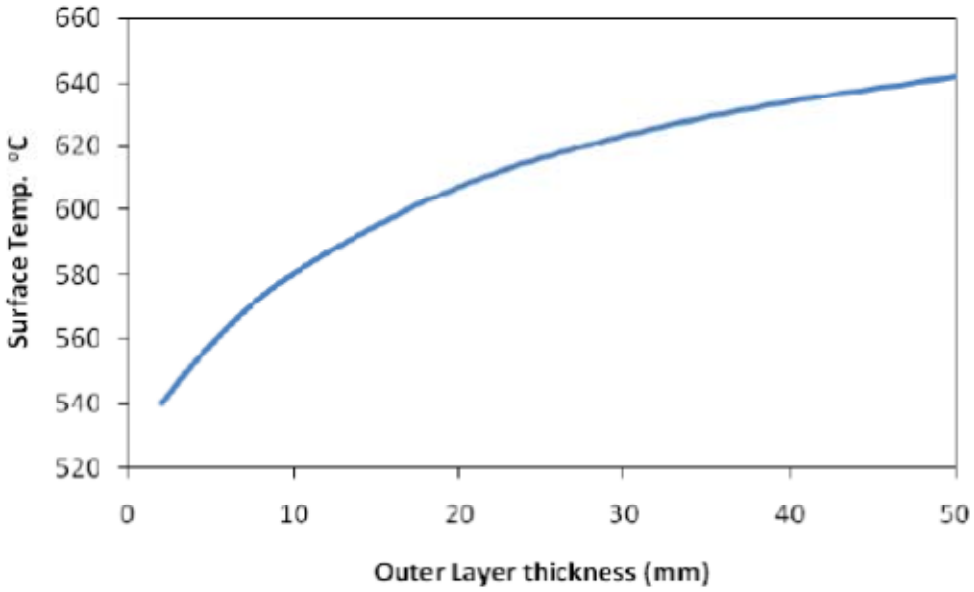

Figure 2. 11: Graphical representation of deposit outer layer thickness impact on deposit outer surface temperature. Simulation results using a standard coal ash.

1.3.2.3 Deposit Strength and Maturation

According to Nowok [58], from an engineering standpoint, a key role in achieving the performance goals in ceramics and glass ceramics is to enhance the strength of the these materials. However, high deposit strengths create the basic problem of deposit removal from heat exchange surfaces. Baxter [10] states that the primary reason for strength build-up in deposits is the increase in the area of contact between particles within the deposit, which is primarily due to sintering or chemical reaction.

In addition to other reasons, with the passage of time the deposits become hard and difficult to remove as according to Jensen [46], the total deposition flux was reasonably independent of time in a straw-fired grate boiler, while the fraction of hard deposits increased with time. In addition, the fraction of hard deposit was found to be correlated with the S content in the deposits, the gas temperature and the amount of K in straw.

Severe deposits formed on the superheater tubes during straw and coal co-firing are shown in Figure 2. 12, whereas mature deposits formed on the screen tubes during 100% straw firing in suspension can be seen in Figure 2. 13. Ash deposits on the heat transfer surfaces cause severe problems for effective heat transfer and severe ash deposition may even cause plugging of flue gas channels as shown in Figure 2. 13.

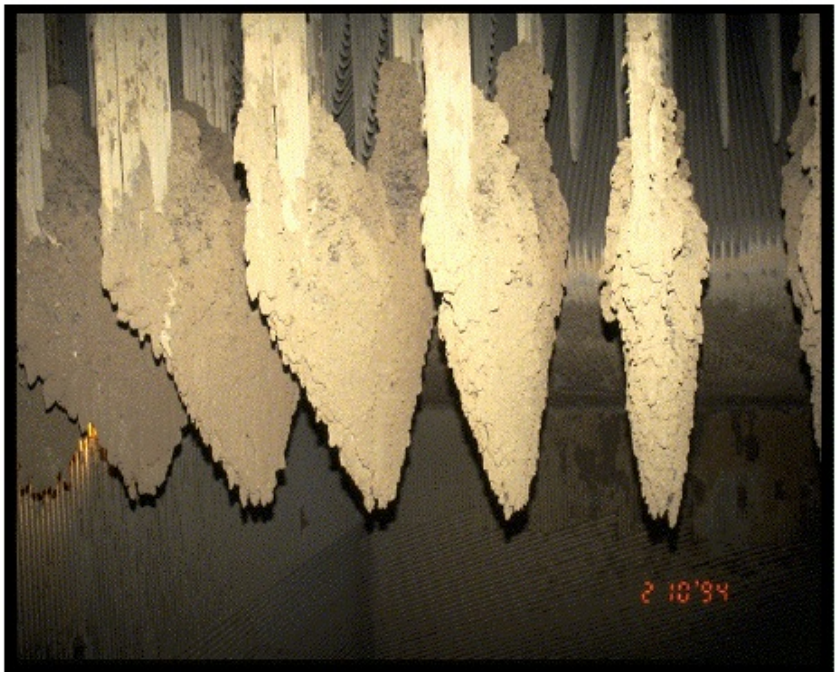

Figure 2. 12: Ash deposition on the superheaters during straw and coal co-firing [2].

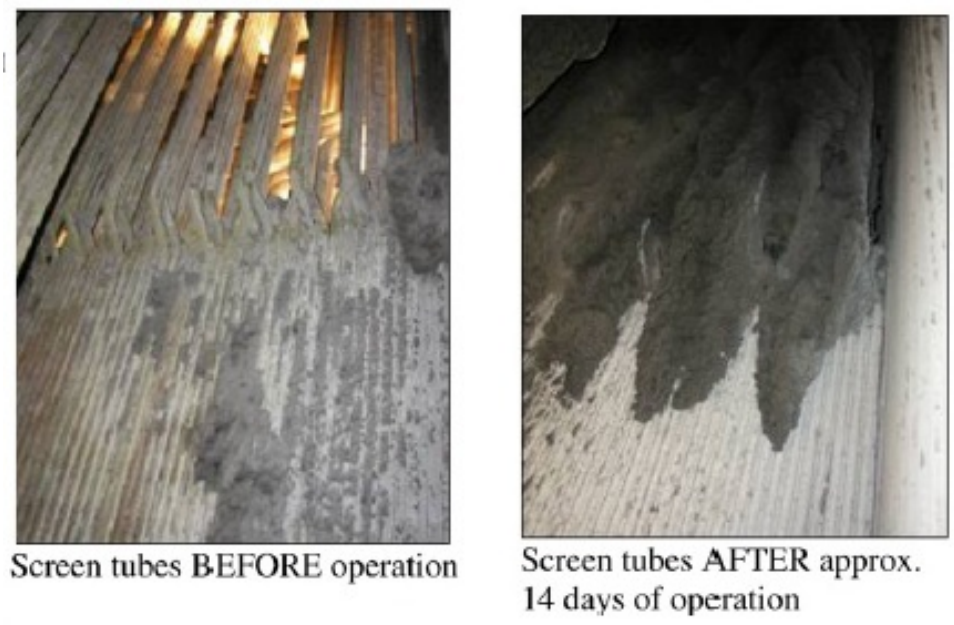

Figure 2. 13: Ash deposition on the screen tubes during 100% straw firing in suspension [5].

1.3.2.4 Deposit Sintering

The driving force for the sintering is the surface energy of the particles. The energy change caused by densification is connected with a decrease in surface area and a lowering of the surface energy by elimination of solid-vapor interfaces and formation of new lower energy solid-solid interfaces. Sintering may occur by several mechanisms as shown in Figure 2. 14. Liquid state sintering involving a viscous liquid is typically referred to as viscous flow sintering. The rate of neck growth as a result of viscous flow sintering has been shown to be time dependent and controlled by the viscosity of the silicate liquid [20]. Chemical reaction sintering occurs when a reaction between particles leads to the formation of a third component, which forms the necks between the particles [20]. The reaction may also take place between the particles and the surrounding gas phase. Chemical reaction sintering can be important for fouling especially in the low temperature section of the flue gas channel. Solid state sintering is caused by diffusion along the particle surface, through the interior of the particles, and through the surrounding gas by vaporization and subsequent condensation. Solid state sintering is a slower sintering mechanism than the ones involving melt, but nevertheless plays an important role in the densification of low temperature fouling deposits [42]. Liquid phase or viscous phase sintering appears mainly to be the dominant mechanism.

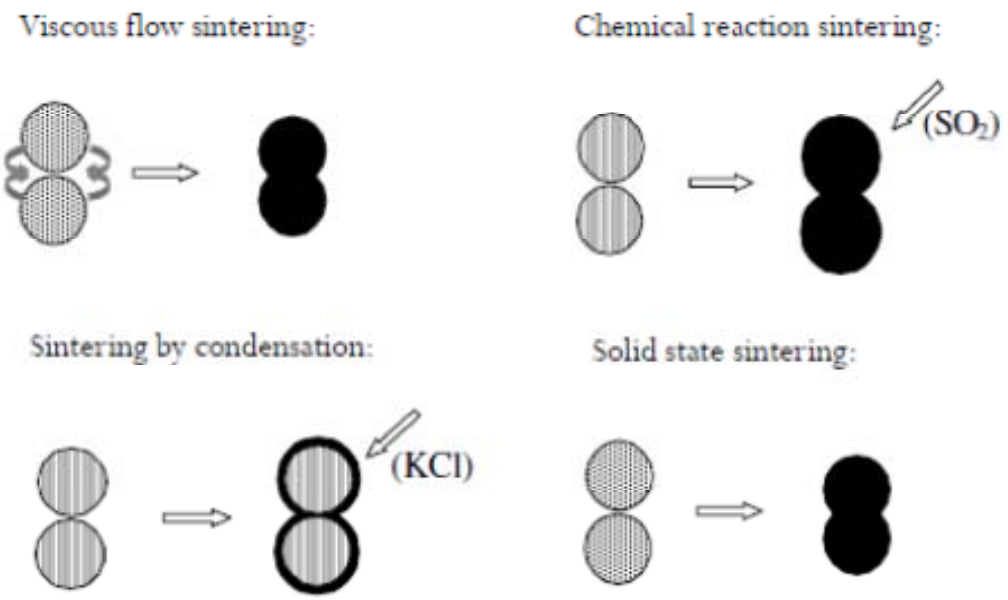

Figure 2. 14: Graphical representation of different types of deposit sintering [2].

1.3.2.5 Deposit Structure in Straw-fired Boilers

Principal sketch of the wheat straw-derived deposits formed on a deposition probe during tests at Sandia Multi Fuel Combustor (MFC) is shown in Figure 2. 15. The deposits consist of two parts, 1) an inner layer, uniform, smooth and covering most of the surface area of the probe, and 2) the main part of the deposit located on the upstream side of the probe and consisting of individual particles. The inner layer, rich in flame-volatilized species (often alkali salts), provide a sticky surface for trapping inertial impacted particles which are non-sticky [17]. Nielsen [17] states that the deposit on the upstream side of the probe consists of impacted fly ash particles and large amounts of condensable salts, forming a matrix that glues the fly ash particles together. The fly ash particles were dominated by K and K-Ca silicates.

The structure of the mature deposits formed during straw grate firing at the Ensted boiler at a flue gas temperature just below 900 ^{o}C is shown in Figure 2. 16. It can be seen that the inner deposit layer is salt rich (KCl, K_2SO_4), intermediate deposit layer dominated Si, Ca rich particles embedded in KCl, while the outer layer of deposits is dominated by KCl, S, and, Si and Ca rich particles [21].

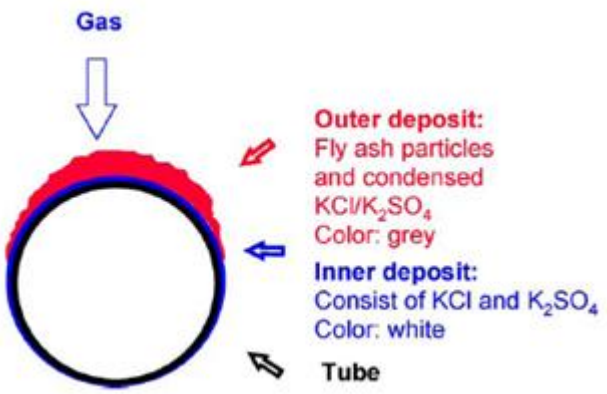

Figure 2. 15: Principal sketch of the wheat straw-derived deposits during pilot-scale experiments at Sandia MFC [17].

1.3.3 Deposit Physical and Chemical Properties

The important properties of a deposit regarding successful operation in a biofuel-fired boiler are; feasibility of removal from heat transfer areas, effective thermal conductivity and emissivity, physical strength of the deposit, elemental and chemical composition of the deposit, and morphology and melting behavior of the deposit [42], outlined below.

1.3.3.1 Melting Behavior

The concept of T_{15} and T_{70} is often used by researchers representing the temperatures where the deposit has 15% and 70% molten phase respectively. It is believed that significant deposit formation takes place when the melt fraction percentage is between T_{15} and T_{70} [9, 17]. This concept is normally applied for ashes containing a significant fraction of salts [9, 17]. At temperature lower than T_{15}, the deposit is almost solid, rigid and non-sticky, and in principle easy to remove, whereas for temperature above than T_{70} the deposit becomes fluid like a slag [17]. The broader the temperatures gap between these two temperatures for a particular deposit material, the wider the critical area where severe thick deposits are expected to grow [17].

Deposition rate as a function of melt fraction for two different types of salt mixtures is shown in Figure 2. 17. A significant difference in terms of ash deposition can be seen when the salts tested have liquid content less than 20% compared to when the liquid content is > 20%. One of the conditions for the formation of a physically strong deposit is the formation of a liquid phase, which can bind solid ash particles [42]. The influence from K-contents in the deposit is critical based on its ability to drastically lower the first melting temperature of ash particles, so that deposits will contain liquid phase at lower temperatures [47].

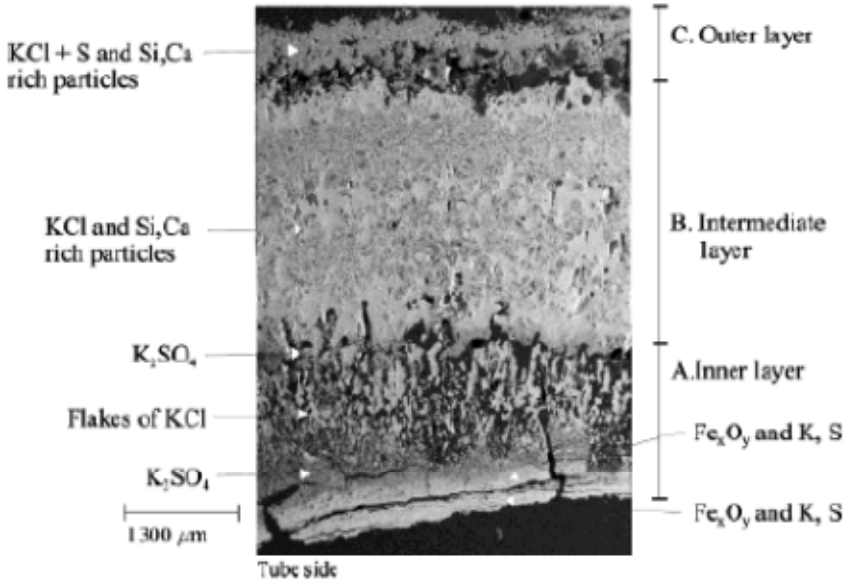

Figure 2. 16: Structure of mature deposits from Ensted boiler (straw grate fired boiler). The superheater steam temperature was from 389 to 470 °C and the flue gas temperature was just below 900 °C [21].

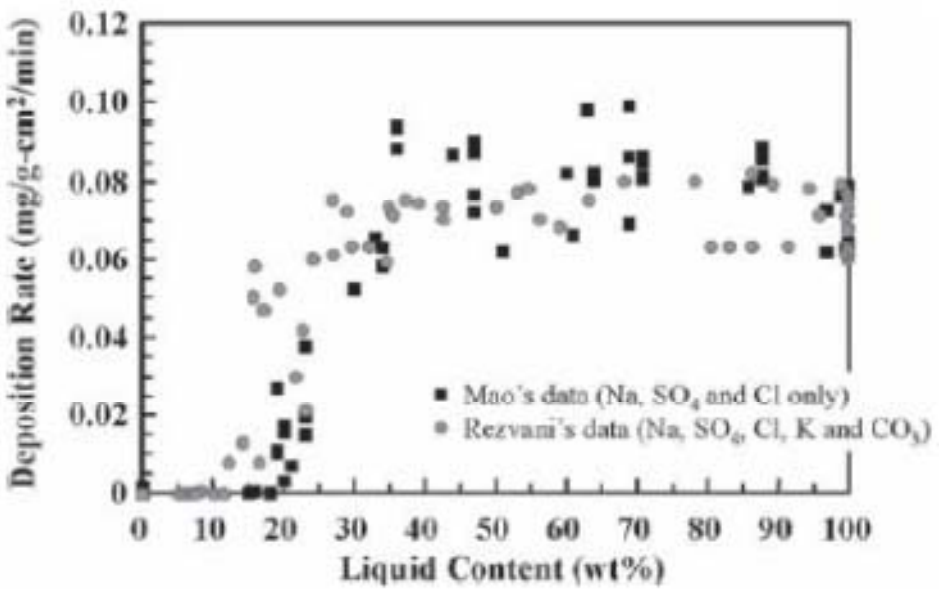

Figure 2. 17: Deposition rate as a function of melt fraction for two different types of salt mixtures [68].

Hansen [15] studied the melting behavior of the deposits as a function of temperature. The fly ash and deposits were found to consist of large fraction of KCl and a smaller fraction of K, Ca, Al-silicates and quartz. The salt part melted in the range from 650 and 750 °C, whereas the silicate phase melted in the range of 1000 and 1200 °C.

1.3.3.2 Thermal Properties

Thermal properties (thermal conductivity and emissivity) are influenced by the deposit physical structure. According to Zbogar et al. [42], the effective thermal conductivity of deposits depends upon the solid phase and gas phase thermal conductivity, the porosity, the size distribution of the pores or particles, and the degree of deposit sintering. Porous deposits have lower thermal conductivity compared to less hard deposits.

1.4 Shedding of Deposits

To minimize deposition problems, different strategies can be employed, e.g. use of additives that can convert the vaporized inorganic species to less harmful forms [5, 26, 39], pre-treatment of fuels by leaching out alkali [40], co-firing with clean fuels [41], inhibition of sintering [2], and use of effective deposit shedding techniques [42]. Use of additives and pre-treatment of fuels by leaching are less cost effective compared to the use of effective deposit shedding [5, 40].

1.4.1 Mechanisms of Deposit Shedding

Shedding may be initiated at the surface of the deposit, along the deposit tube interface and inside the deposit depending on the local boiler conditions and the deposit properties [42]. Deposit shedding can be caused artificially as a part of the boiler operation, e.g. by sootblowing, or naturally, without any operational or mechanical influence [2, 42]. The important mechanisms of ash shedding are (Table 2. 4) [42]:

- Erosion, when non-sticky, relatively large and sharp edged often SiO_2-rich fly ash particles collide with non-sticky areas on a deposit surface causing deformation (ductile deposits) and a cutting action (brittle deposits) [2, 43] (Figure 2. 18).
- Gravity shedding when the gravity force exceeds the tube adhesion strength. Gravity shedding also includes deposit shedding through surface melting. Gravity shedding by surface melting is explained in Figure 2. 19 and section 2.4.3.
- Through temperature changes and differences in the thermal expansion coefficients of the tube and deposit. Local temperature changes may be caused by sootblowing or by load variations/fluctuations.
- Mechanically induced tension in the deposit typically caused by vibrations or momentum transfer from sootblowing.

Table 2. 4: Deposit shedding mechanisms [42].

Shedding mechanism	Debonding	Within deposit	Deposit removal
Erosion			√
Gravimetric	√	√	
Melting			√
Thermal induced tension a) Combustion fluctuations b) Load changes c) Sootblowing	√	√	
Mechanical induced tension a) Mechanical fluctuations b) Sootblowing	√	√	

The erosion mechanism (gravity shedding) for ash deposit on a tube is shown in Figure 2. 18. According to Raask [43], the erosion rate is influenced by the shape of the incoming particles. Highly abrasive, hard and angular quartz grains cause erosion by cutting, whereas glass spheres first produce a surface deformation. Erosion wear is also influenced by the particle size of the impacting material. Smaller particles (smaller than 5 μm) have a small inertial momentum and they are carried around the object with the gas flow [42, 43]. The erosion rate increases as the particle size increases but obtain a constant value for larger particle (45 μm [42, 43]).

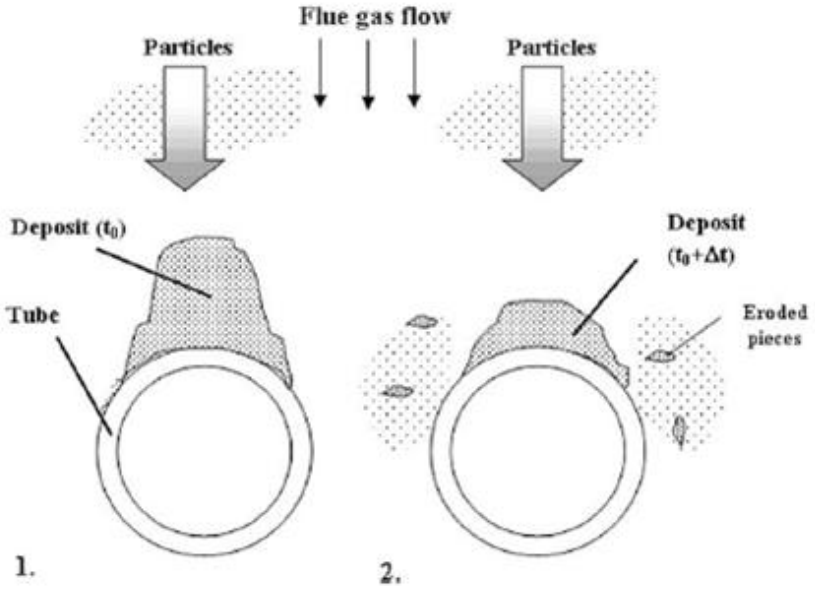

Figure 2. 18: Deposit erosion mechanism, 1) initial deposits on the tube, 2) deposits after shedding though erosion [42].

Gravitational shedding is possible when the effect of gravity upon the deposit becomes larger than the attachment strength of the deposit on the tube or the internal strength of the deposit. Debonding occurs when the stresses initiated by the sootblower are greater than the tube-deposit adhesive bond at some point on the tube deposit interface.

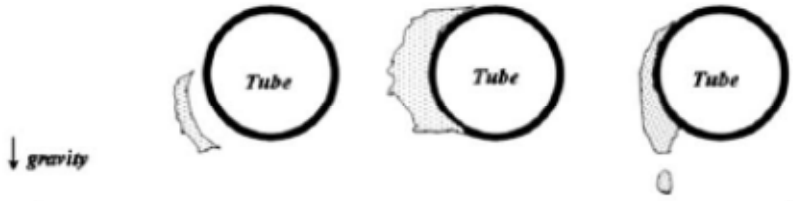

Deposit characteristic	Weak deposit (low strength value)	Strong deposit (high strength value)	Low-melting-point deposit
Shedding characteristic	Debonding	No debonding	Melting and flow

Figure 2. 19: Relationship between the deposit viscosity and the deposit strength. Cases are ordered in the sequence of decreasing viscosity [42].

Gravity shedding is also possible by melting of the deposits especially in the furnace region. If the combustion conditions are suitable for the development of a low viscosity slag deposits, molten deposits may flow down the boiler walls. The temperature gradient through such a deposit will cause the slag layers close to the wall surface to be solid, while the outer deposit layer will be molten. A relationship between the deposit viscosity and the deposit strength is shown in Figure 2. 19. It can be seen that for deposit with the high liquid phase viscosity, the adhesive strength is not sufficient enough to hold the deposit in place, resulting in shedding by its own weight. Whereas, the temperature of the deposit on the right side is high enough to cause melting of the deposit, and shedding through surface melting.

Thermal shock induced shedding is caused by temperature changes, due to the difference in the thermal expansion coefficients of the tubes and deposits. A sudden temperature gradient may cause an uneven expansion of the deposit and the tube, or, distinct, adjacent, deposit layers, leading to deposit fractures. The sudden temperature gradients can be caused by fluctuations of the flue gas or steam temperature. Artificially, ash deposits can be removed from the heat transfer surfaces by inducing mechanical or thermal stresses inside them. This can be done using the impact of the high pressure steam, air and water, or by changing the thermal load etc. [36, 44].

1.4.2 Industrial Deposit Shedding Techniques

1.4.2.1 Sootblowing

Sootblowing is currently the most common deposit shedding system used in coal, biomass and Kraft recovery boilers. Water, high pressure air or steam may be used in sootblowing systems [70]. Deposit removal occurs indirectly, due to mechanical and thermal stresses, induced in the deposit. The cleaning fluid is forced through nozzles that remove deposits from the heat transfer surfaces. The Peak Impaction Pressure (PIP) is an important parameter in sootblower design defined as the stagnation pressure (one half the fluid density times fluid velocity squared) measured along the centerline of the nozzle downstream of the nozzle outlet. PIP drops off at increasing distances from the nozzle outlet because of the fluid deceleration associated with the dispersion of the flow downstream of the nozzle exit. The peak impact pressure (PIP) is used to measure the effectiveness of a soot blower nozzle. In order to remove the deposit, jet must have a PIP value that induces tensions in the deposit is greater than the deposit mechanical strength, or the adhesion strength at the deposit-tube interface [70]. Longitudinal and lateral component of a force, caused by the interaction between a sootblower jet and a deposit are shown in Figure 2. 20. Conventional sootblower nozzles produce an under-expanded jet, which causes a dissipative shock wave to occur outside the nozzle exit. This shock wave irreversibly converts a substantial portion of the kinetic energy of the jet into internal energy, thereby reducing the PIP available for deposit removal. If the nozzle is designed so that the jet achieves full expansion before it exits the nozzle, shock waves will be eliminated. This will increase the energy available for deposit removal [71].

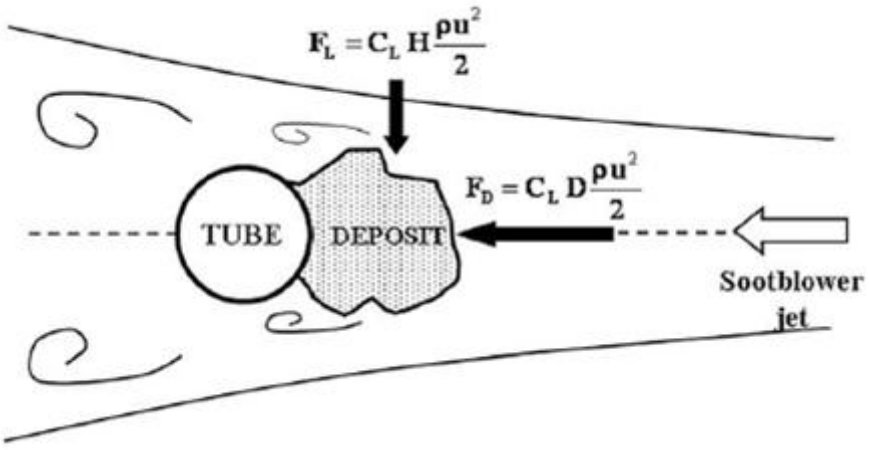

Figure 2. 20: Longitudinal and lateral component of a force, caused by the interaction between a sootblower jet and a deposit [36].

Different types of sootblowers commonly employed in the boilers are shown in Figure 2. 21. Rotary sootblowers consist of a long tube with nozzles that remains inside the system and normally placed in cool flue gas zone to avoid from corrosion problems [72]. The nozzles are distributed along the tube surface and also around its circumference. The retractable sootblowers consist of a long lance with two or four nozzles in it. The nozzles are normally at the end of the lance. The retractable lance moves alongside its length and also rotates. The wall sootblowers are designed to clean the slag deposits on furnace walls. They are used in coal-fired boilers for this purpose. A nozzle in a short retractable lance tube is inserted just inside the face of the wall and rotates once to blow the fluid across the surface wall. The jet is slightly angled back toward the furnace wall. Rake blowers are designed for cleaning plane heat transfer surfaces. There are several tubes that allow the cleaning between the closely spaced fins. These blowers are usually found in the cooler parts of a boiler like the economizer and the air pre-heater.

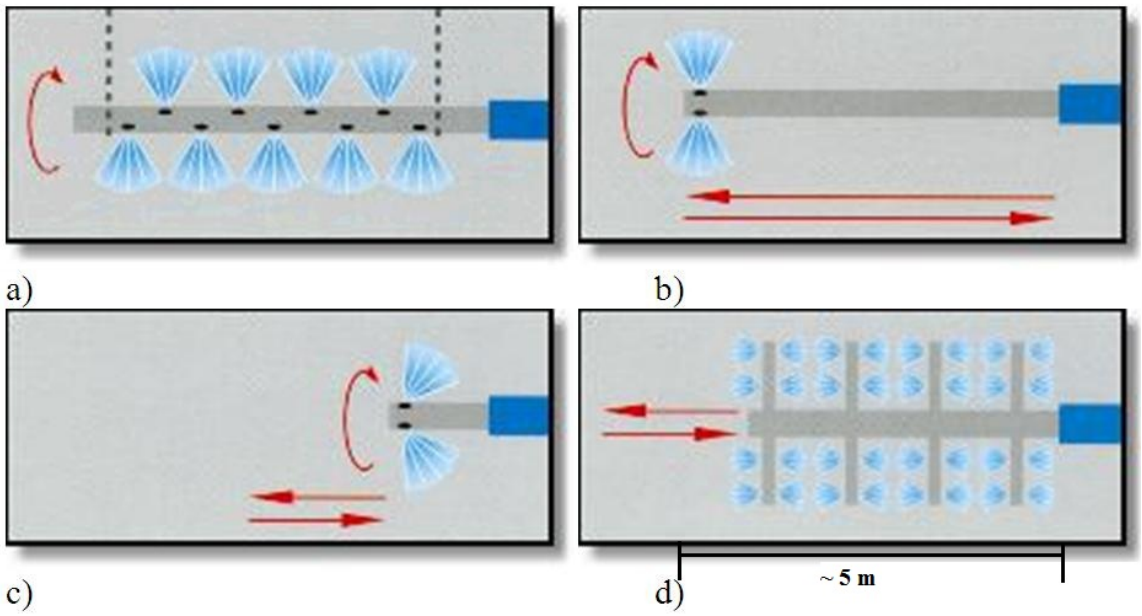

Figure 2. 21: Different sootblowers employed in solid fuel fired boilers, a) rotary, b) retractable, c) wall, d) rake [72].

The chemical composition and the thermal characteristics of the oxide layer, formed on the boiler tubes, influence the strength of the adhesive bond between an oxide surface and an ash deposit [70]. Non-sintered porous deposits do not posses much strength, and are easily blown away from the surface. The tube surface temperature has a significant effect on the process of deposit removal. Increasing the tube surface temperature often makes the deposit more difficult to remove. For a weak brittle deposit a sootblower jet impact can lead to a break-up of

the deposit as shown in Figure 2. 22. Dense, hard deposit on the other hand, can be removed by debonding from the tube surfaces (Figure 2. 22).

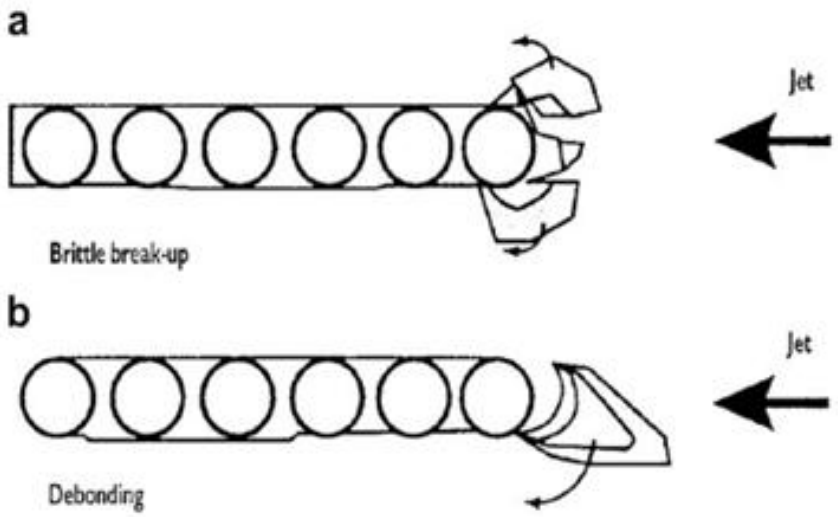

Figure 2. 22: Mechanisms of deposit removal: brittle break-up (a) and debonding (b) [36].

Sootblowing frequency must be balanced with the negative results of erosion because the condensate in the soot blowing can result in unnecessary corrosion [70].

1.4.2.2 Use of Additives

In order to avoid deposition problems in biomass fired boilers, the use of different additives can be useful. The additives change the fly ash composition produced by favoring the formation of Cl in the gas phase (HCl), and the formation of ashes with melting temperatures greater than the sticking temperatures. Many additives have been tested both in pilot-scale and full-scale measurements in biomass-fired boilers [5, 26, 73]. The commonly used additives include Ca, S and P rich materials. Sørensen et al. [74] proposed that the addition of additives rich in Ca and P form phases rich in K-Ca-P that have higher melting temperatures. ChlorOut, a concept developed and patented by Vattenfall AB, consists of an aqueous solution of $(NH_4)_2SO_4$ that is sprayed into the combustion zone at temperatures around 800-900 ^oC, upstream of the superheaters [75]. It effectively converts alkali chlorides (e.g., KCl) into alkali sulphates (e.g., K_2SO_4). This concept has been successfully tested in a number of biomass-fired fluidized bed boilers [76]. Significant reduction in the deposition rate and Cl contents in the deposits has been reported [76]. However, the amount of $(NH_4)_2SO_4$ and/or Ca, S and P rich additives needed to cope with K in a straw suspension-fired boiler can be beyond economical constraints.

Addition of additives in the fuel for K capture or leaching out of K from fuel is also employed to reduce the potential ash deposit formation on the superheater tubes. Other additives may also be used to inhibit sintering of ash deposits [2, 40].

1.4.2.3 Addition of Coal Fly Ash

The presence of Al and Si in coal fly ash can make it good candidate to capture K from biomass-fired boilers. Addition of coal fly ash can be economically feasible for wood-fired boilers where the amount of coal ash needed to capture K will be smaller compared to the amount of coal ash needed in straw suspension-fired boilers.

1.4.2.4 Shot Cleaning

In shot cleaning, small balls are used to clean the heat transfer surfaces in a boiler. The balls are available in different geometries and materials. They are pneumatically transported to the upper section of the boiler, and then fall by gravity and impact the heat transfer surfaces. Deposits are removed and fall in the dust outlet, while the balls are collected and recycled to the next cleaning cycle [70].

1.4.2.5 Sound Waves

Sound waves are used to clean the heat transfer surfaces by creating pressure fluctuations in a flowing gas stream. Normal frequencies are of 125 Hz to 250 Hz in the 140 to 150 dB range but infrasonic horns with frequencies between 15 to 20 Hz also exist [70].

1.4.2.6 Rapping Gears/Mechanical Fluctuations

Rapping gears are hammers beaten on reinforced heat surface headers either mechanically or pneumatically. Because of the vibrations created by the hammers, the deposit can fall from the heat transfer surfaces [70]. Deposits that are not strongly bonded with tube can be removed using mechanical hitting (vibrations), as is done in some waste incinerators.

1.4.2.7 Detonation Wave Techniques

Detonation wave technique is also used to shed ash deposits. The detonation occurs when a fuel-oxidant mixture is combusted in an ignition chamber connected to a pipe with the same or smaller diameter. Thus, the pipe has the function of transforming the flame front into a detonation wave, and bringing the wave to the desired location. A normal detonation wave has a velocity of 2200 m/s and a pressure up to 20 times the original pressure of the reactants [70]. The main mechanisms for deposit removal are pressure forces and thermal shock [70, 77].

1.4.3 Review of Deposit Shedding Investigations

Most deposit shedding studies have been based on measurements in lab-scale equipment, grate-fired boilers and Kraft recovery boilers, while only limited data are available from biomass suspension firing. A review of shedding investigations in different solid-fuel fired boilers and lab-scale facilities is shown in Table 2.5. Ash deposit shedding through surface melting in the high temperature superheater region at the Avedøre straw grate-fired boiler was investigated by Zbogar et al. [35]. The results showed that deposit surface melting was the main mechanism of ash deposit shedding at flue gas temperatures greater than 1000 ^{o}C. The ash deposit shedding through surface melting at three different flue gas temperatures can be seen in Figure 2.23. The results showed that deposit shedding through surface melting was significant when flue gas temperature was higher than 1100 ^{o}C, the deposit surface layer was partially melted at 1000 ^{o}C, and at a temperature of 900 ^{o}C, the deposits contain mainly porous solid phase [35]. It was also found that the initial deposit formation mechanism was by condensation of salts, and then followed by upstream inertial impaction of the fly ash particles. The deposit build-up and shedding reached a steady state level after 7 days.

Deposit shedding at the Avedøre straw grate-fired boiler was investigated by Zhou et al. [33] by using an artificial sootblowing probe in a lower temperature superheater region nearer to the convective pass at flue gas temperatures between 700 and 800 ^{o}C. Investigations of Zhou et al. [33] showed that the probe surface temperature can have an influence on the Peak Impact Pressure (PIP) needed to remove the deposit. The measured PIP values were significantly lower at a probe surface temperature of 400 ^{o}C compared to a probe surface temperature of 550 ^{o}C.

Lab-scale investigations by Kaliazine et al. [36] and Sabet [78] also indicate an increase in adhesion strength of the deposit and the metal surface at higher probe surface temperatures (> 500 ^{o}C). However, after reaching a temperature value where the deposit inner layer changed to complete liquid phase, the adhesion strength was significantly reduced. Andersen [20] used temperature controlled probe for sampling of deposits during full-scale measurements in a straw and coal fired boiler. Natural deposit shedding was observed when ash deposits fall off from the probe. Shedding was believed to occur when sudden changes were seen in the probe surface temperature on the upstream side of the probe. Natural deposit shedding was observed by Madhiyanon et al. [79] during pilot-scale combustion studies of oil-palm empty-fruit-bunch (K-rich fuel). Visual observations of deposit formation and shedding on the probe showed that the deposits fall off in the form of pieces from the upstream side of the probe.

Table 2. 5: Review of shedding investigations in different solid-fuel fired boilers and lab-scale facilities.

Location	System	Size	Flue gas temp. (^{o}C)	Fuels	Shedding mechanism	Ref
Avedøreværket Bio Boiler, Unit 2	Dedicated straw-fired boiler. Big bales of straw are fired on a grate.	105 MW_{th}	900-1200	Danish straw	Shedding through surface melting	[35]
Avedøreværket Bio Boiler, Unit 2	Dedicated straw-fired boiler. Big bales of straw are fired on a grate.	105 MW_{th}	700-900	Danish straw	Shedding through artificial sootblowing.	[33]
Studstrup Power Station, Unit 1	Back wall fired boiler with 12 burners.	380 MW_{th} /150 MW_{e}	950-1150	Straw with Bituminous Columbian coal and American coal. Separate injection of straw up to 20% on thermal basis.	Natural shedding was observed as part of investigating ash deposition in a 2 years demonstration program.	[20]
University of Toronto	Lab-scale facility	--	--	Wood material was considered as deposit and gypsum was used as the bonding material.	Deposit removal by debonding. Lab-scale deposit removal experiments were performed for application in Kraft recovery boilers.	[36, 78]
University of Technology Thonburi, Thailand	Grate-fired furnace	150 kW_{th}	790-810	Oil-palm empty-fruit-bunch	Natural shedding was observed as part of investigation of ash deposition.	[79]

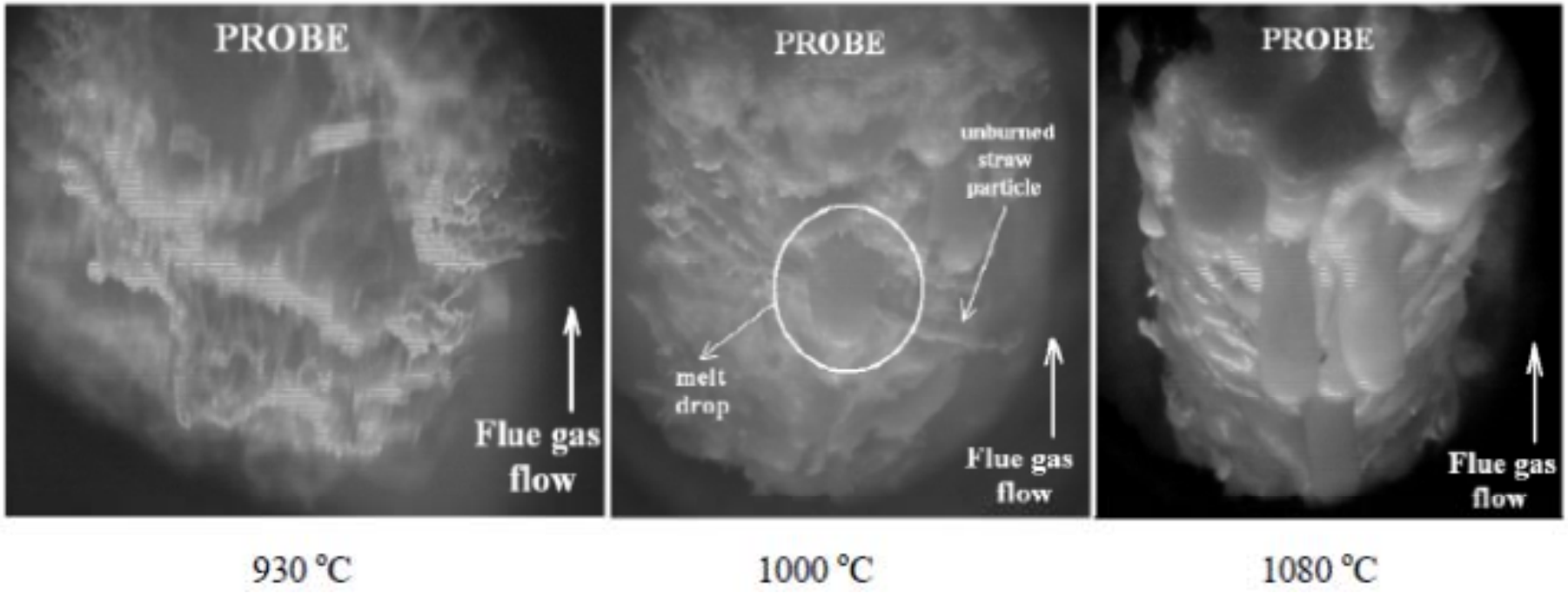

Figure 2. 23: Pictures of the deposit probe during full-scale measurements at a straw grate-fired boiler at three different flue gas temperatures [35].

1.5 Practial Experiences of Biomass Suspension Firing

1.5.1 Review of Ash Deposition during Pilot-scale Biomass Suspension Firing

Some pilot-scale biomass suspension-fired investigations on ash transformation and deposition can be found in the literature and are reviewed in Table 2. 6. Lokare et al. [28] investigated the ash deposition rate for a suite of biomass fuels and biomass fuel blends (50-50 wt.%) in a 10 kW down-fired, multi-fuel flow reactor. In addition to the increase in deposition rate with fuel ash contents, higher ash deposition rates were observed for fuels with higher Cl-content. Robinson et al. [80] investigated American wheat straw, Danish wheat straw, red oak wood and switchgrass in a 30 kW Multi-fuel Combustor (MFC) at Sandia National Laboratories. Results of the ash deposition were similar to the investigations made by Lokare et al. [28] in such a fashion that the deposition rate increased linearly as a function of Cl-content in the fuel. The results showed significantly higher ash deposition rate for Danish straw, compared to switchgrass even though the ash contents of the Danish straw were lower than for switchgrass. In the same MFC reactor, the results of Nielsen [17] showed a deposit collection efficiency of 0.05-0.25 during Danish straw combustion. The deposit collection efficiency reduced to 0.01-0.04 when straw was co-fired with coal, possibly due to chemical interactions. Theis et al. [41] investigated specified mixtures of peat with bark, and peat with straw in an entrained flow reactor. Results showed a cleansing effect of peat in all mixtures with straw by reducing the ash deposition rate. The conclusion was that up to 30 wt.% bark and up to 70 wt.% straw in a mixture with peat can be burned without encountering increased deposition rates. In addition to fuel ash contents, the impact of fuel ash chemistry on ash deposit formation rates was evident. Nordgren et al. [27] investigated ash deposition behavior of straw and different woody biomasses in a 150 kW swirl powder burner. A deposition rate of 90 $g/m^2/h$ for pure straw reduced to 50 $g/m^2/h$ when straw was fired with wood at 50 wt.% share. Experimental investigations by Shenassa [81] in an entrained flow reactor also revealed increased deposit formation rates with increase in Cl contents of the feedstock.

Wu et al. [73] investigated deposition behavior of Danish straw with and without the addition of spent bleaching earth and kaolinite as additives in an entrained flow reactor. Reduced ash deposition propensity was resulted when spent bleaching earth and kaolinite were added to straw. In addition, the contents of Cl in the deposits were reduced in the presence of additives both due to dilution effects and chemical interactions. Investigation of ash deposition behavior

during combustion of straw and biomass fuels was made by Jensen et al. [82] in the same reactor, with and without the addition of Ca and P rich additives. Ash deposition rate was found to be linked with total fuel ash contents, and to some extent K contents in the fuel ash. Capablo et al. [83] investigated ash deposition and ash transformation during biomass combustion in an entrained flow reactor and a swirl burner furnace, respectively. More than 10 alternative biomass fuels with and without the addition of kaolin and limestone were investigated. The ash deposition rate was found to be linear function of ash contents of the fuels. Ash transformation results revealed two kinds of fly ash particles when biomass fuels were combusted in the swirl burner furnace. Particles will diameter less than 1 µm were found to be rich in K, Cl, S and P, while the larger particles were rich in Si, K and Ca.

Most of the above mentioned studies revealed that the combustion of individual biomass fuels in different reactors showed a correlation between ash deposition rate and fuel ash contents as shown in Figure 2. 24. However, a mixture of biomass fuels and combustion of biomass fuels in the presence of additives did not follow the similar trend of increase in ash deposition with increase in fuel ash contents as shown in Figure 2. 25, where the data points with a large spread show reduced ash deposition rates compared to individual biomass combustion. The chemical interactions among the ash species could be effective in lowering the ash deposition rates.

In addition to the impact of fuel ash, and, K and Cl-content in the fuel ash, flue gas temperature may also be effective to increase the gas phase concentration of gas phase alkalies and melting behavior of the produced fly ash. K in the fuel ash can increase the fraction of molten ash as well as provide an increased content of gas phase alkali species at higher flue gas temperatures, and both will lead to an increased deposit formation rate. For the pilot-scale studies conducted at a flue gas temperatures close to 1000 ^{o}C, the ash deposition increases linearly with increase in Cl-content in the fuels (see Figure 2. 26). However, the trend cannot be seen when the flue gas temperatures close to 800 ± 50 ^{o}C as shown in Figure 2. 27. The possible explanation could be that the K-release can be significant for fuels containing high amounts of Cl and/or high amounts of K relative to Si, whereas, the K release is expected to low for high Si fuels and low Cl-content [29]. The presence of K and Cl can potentially decrease the melting temperature of the fly ash produced.

The review of above mentioned studies indicate that the true identification of the impact of the flue gas temperature and fuel ash contents on ash deposition propensity is of significant importance to quantify ash deposition in straw and wood suspension-fired power boilers.

Table 2. 6: Review of biomass suspension firing experiments reported in literature at different pilot-scale facilities.

Location	System	Size	Flue gas temp. (^{o}C)	Probe temp. (^{o}C)	Fuels	Issues/Fingings	Ref
Birmingham Young University	Multi-fuel, down-fired reactor with 120 mm inside diameter. Auxiliary methane was used to preheat the reactor.	10 kW	1000	500	Six pure biofuels and eight & biomass fuel mixtures (50 wt.%).	Ash deposition. Ash deposition rate was higher for fuels with higher ash and Cl-content. The deposition rate reduced for biomass mixtures due to dilution effects and chemical interactions.	[28]
Sandia National Laboratories USA	Multi-fuel, down-fired turbulent entrained flow reactor with natural gas burner. Reactor is 4.2 m high with 150 mm inside diameter. Electrical heated to control temperature of the walls.	30 kW	1000	540	Coal, straw and wood fuels. Individual fuels and fuels with different co-firing combinations.	Ash deposition and corrosion. Higher deposition rate for fuels with higher ash and Cl-content. Corrosion was induced by Cl in the deposits (resulted from fuel).	[17, 80]
University of Toronto	Entrained flow reactor with natural gas addition for complete combustion. Combustion temperature adjusted by addition of air. The reactor is 6.5 m high with 180 mm furnace diameter.	□ 5 kW	1000	550	Bark, peat and straw fuels. Individual fuels and fuels with different co-firing combinations.	Ash deposition and deposit characterization. High deposition rate for straw. Up to 30 wt.% bark and up to 70 wt.% straw in a mixture with peat can be burned without significant ash deposition.	[41]
Umeå/Luleå University, Vattenfall Sweden	Swirl powder burner.	150 kW	800 /500	550 /250	Straw, bark and wood samples were fired alone and with different co-firing combinations. Thermodynamic calculations were also performed.	Ash transformation and ash deposit build-up rate (RBU). RBU for straw was higher compared to woody biomasses. Equilibrium was achieved selectively and ash matter was strongly fractioned.	[27]
Pilot-scale plant CHEC, DTU	Electrical heated entrained flow reactor having an internal diameter of 79 mm and length of about 2 m.	5 kW	750	470	100% straw, straw in combination with spent bleaching earth and kaolinite.	Ash chemistry and deposition behavior. Additives were effective in reducing deposition propensity and in reducing Cl and K in the deposits.	[73]
Pilot-scale plant CHEC, DTU	Electrical heated entrained flow reactor having an internal diameter of 79 mm and length of about 2 m.	5 kW	800	400-600	Combustion of biomass fuels with and without the addition of Ca and P rich additives.	Characterization and quantification of deposits. Fuels with high K content bind more Cl in the deposit. Molar ratios, P/(Na+K) (1.9-3.2) and P/Ca (0.8-0.9) resulted in high reduction efficiency of Cl in deposits.	[82]
Pilot-scale plant CHEC, DTU	Electrical heated entrained flow reactor having an internal diameter of 79 mm and length of about 2 m.	5 kW	800	500	12 alternative biomasses including, straw, wood, pectin waste etc. Biomass co-firing in combination with additives.	Ash chemistry and deposition behavior. High fuel ash content resulted in higher deposit formation fluxes.	[83]
Swirl burner furnace CHEC, DTU	Swril burner furnace.	--	800-1200	--	Different alternative biomasses.	Ash transformation. Two distinct kinds of particles were observed. Particles less than 1 µm were rich in K, Cl, S and P, while larger particles were rich in K, Ca and Si.	[83]

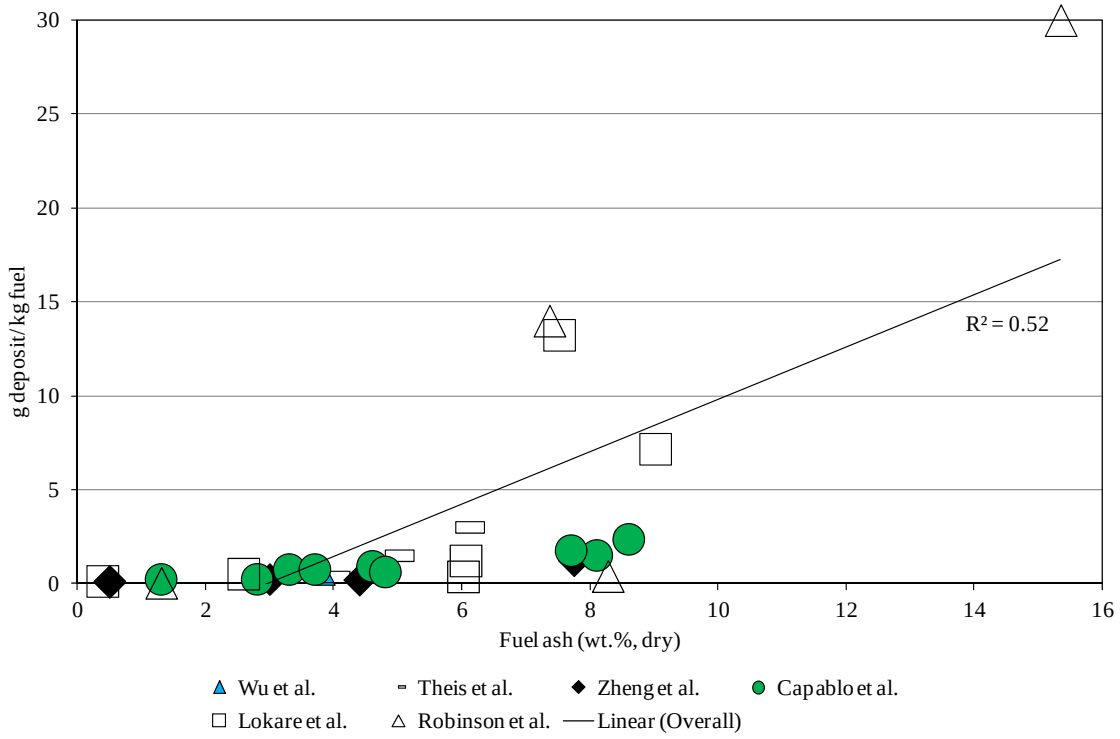

Figure 2. 24: Ash deposition rate reported for individual biomass fuels during pilot-scale suspension firing [28, 41, 73, 80, 82, 83]. Flue gas temperature was between 800 and 1000 °C.

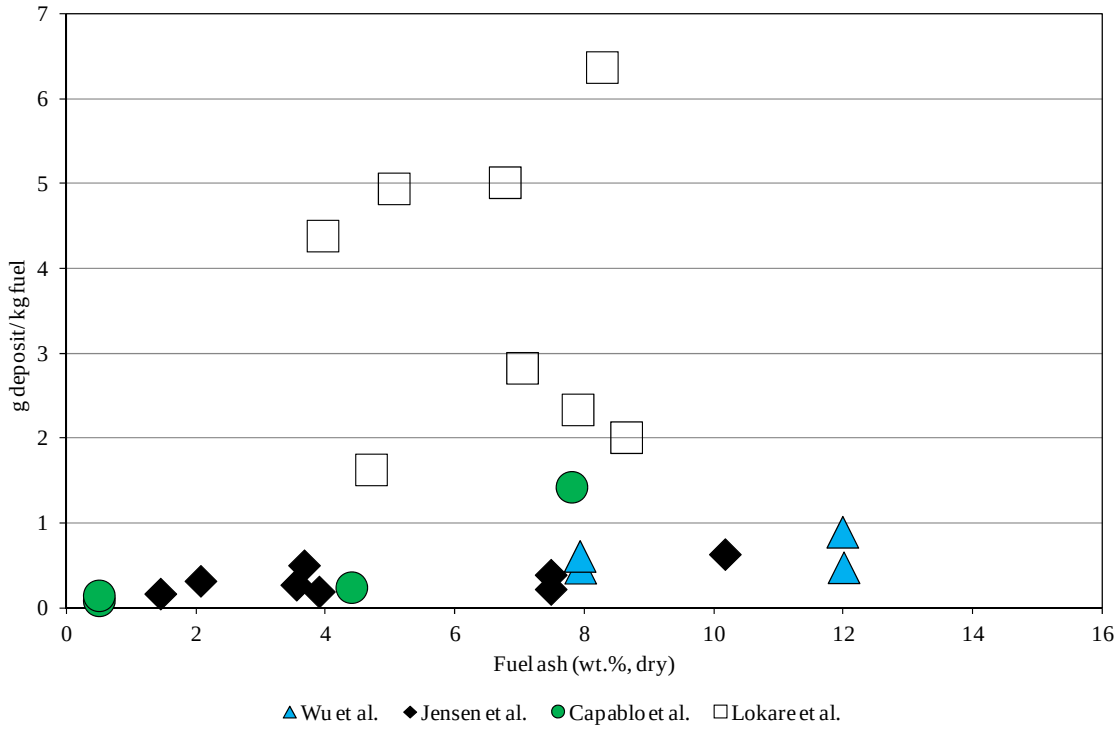

Figure 2. 25: Ash deposition rate reported for pilot-scale suspension firing of biomass mixtures and/or with addition of additives [28, 41, 73, 82, 83]. Flue gas temperature was between 800 and 1000 °C.

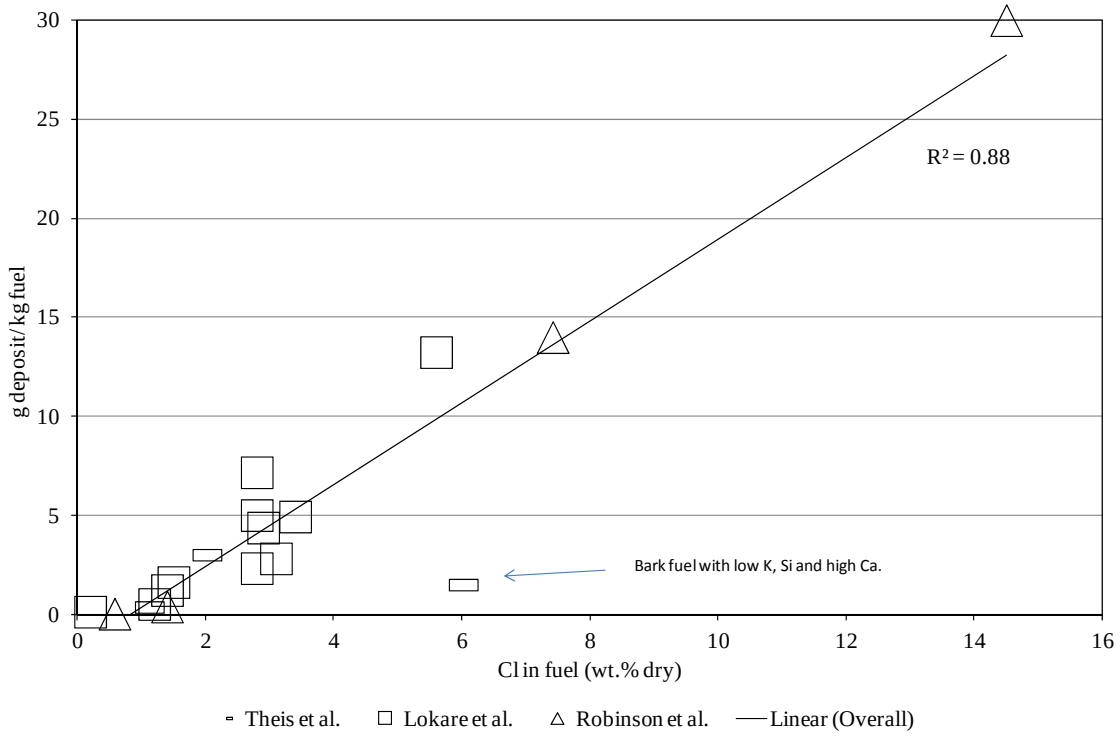

Figure 2. 26: Ash deposition rate as a function of Cl-content in the biomass fuel during pilot-scale suspension firing. Flue gas temperature was around 1000 °C [28, 41, 80].

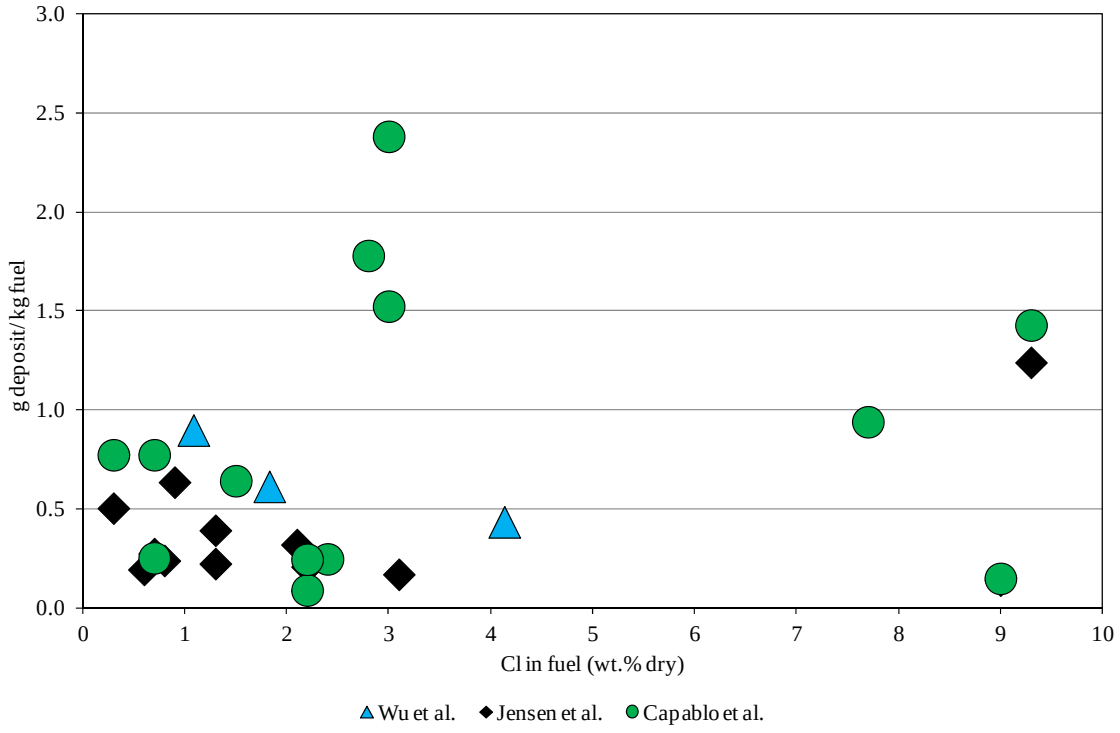

Figure 2. 27: Ash deposition rate as a function of Cl-content in the biomass fuel during pilot-scale suspension firing. Flue gas temperature was around 800 ± 50 °C [73, 82, 83].

1.5.2 Review of Ash Deposition during Full-scale Biomass Suspension Firing

Research on ash deposit formation during full-scale suspension firing of biomass (straw and wood) is scarce. The available full-scale investigations are by Jensen et al. [24] and Skrifvars et al. [38] on ash deposit formation during suspension firing of wood, and by Tobiasen et al. [5] and Jenkins et al. [51] on ash deposit formation during suspension firing of straw. These studies have revealed some important features about ash deposit formation during wood suspension firing. On the other hand, an extensive and detailed study on the transient formation of ash deposit at different locations of the boiler is still not available in literature, and this information is needed to further promote the utilization of straw and wood in suspension firing plants.

A review of the available full-scale studies on ash deposition in biomass suspension-fired boilers is shown in Table 2. 8. Tobiasen et al. [5] investigated the addition of different additives on ash deposition and overall boiler operation at Amagerværket Unit 2 (AMV2). AMV2 is a rebuilt coal boiler and the design of superheater tubes was not made accordingly that it can be used but it was used for straw firing [5]. The factors that affect the appropriate use of additives include additive particle size distribution, reactivity, reaction temperature and time and cost [5]. The overview of results is shown in Table 2. 7. Results of the full-scale measurements demonstrated that despite the use of the additives, more ash deposition resulted in the boiler for some of the additives. With chalk, the deposit flux increased significantly, and also deposits were white whereby back radiations from the slag layer on the superheater tubes were large and heat transfer was reduced. Bentonite, gave no operational problems and deposit flux was also reduced. Sand was not effective in reducing Cl contents in the fly ash and in deposits. DCP ($CaHPO_4.2H_2O$) appears to be effective in reducing Cl contents in the fly ash and the deposits, but caused problems of back radiation. Overall, sand and bentonite appeared to be attractive. Sand appeared to be cheap, but it was less reactive, and bentonite was expensive.

Unit 1 at Amager Power Station (AMV1), commissioned in 2009, is the first dedicated biomass suspension-fired boiler that was designed to fire straw and/or wood. No full-scale results have been reported regarding ash deposition from this boiler except the results presented in the present study. Moderate deposit formation rates in the range of 1 to 12 $g/m^2/h$ were measured during full-scale measuring campaign at Avedøreværket Unit 2 (AVV2), a wood suspension-fired boiler. Regarding ash deposition, no systematic tendency was observed regarding the applied fuel combinations, wood, natural gas and furnace oil. Cl contents in the deposits were low in the high flue gas temperature region, while further downstream in the flue gas channel Cl-rich deposits appeared.

Table 2. 7: Overall comparison of four additives investigated at AMV2, modified from Tobiasen et al. [5].

Evaluation of deposits	Sand	DCP	Chalk	Bentonite
Reduction in the collected amount of deposits	No	Yes	No	Yes
Reduction in Cl in the fly ash	No	Yes	No	Yes
Boiler operation	No back radiation	Back radiation	Back radiation	No back radiation

Investigation by Skrifvars et al. [38] in a down-fired suspension boiler firing wood showed increased deposition rate (12 to 74 g/m^2/h) at higher flue gas temperature (920 ^{o}C), and reduced deposition rates (3 to 13 g/m^2/h) were measured at lower flue gas temperatures (750 ^{o}C). Suspension firing tests of leached straw with rice hulls at a straw suspension-fired boiler showed no significant increase in ash deposition rates, compared to the reference case of rice hulls. The Cl contents in the deposits were found to be unchanged [51].

Compared to the limited number of full-scale measurements for pure biomass suspension firing, a significant number of full-scale measurements for straw and coal co-firing can be found in literature and some of these are reviewed in Table 2. 8. A more detailed investigation by Andersen [20] during co-firing straw at Studstrup Power Plant Unit 1 showed that co-combustion of straw and coal can effective if ash 'synergy' is satisfactory. The products of combustion of biomass materials when co-fired with coal in a large utility boilers tend to have a higher level of sub-micron fume and vapor, and the fly-ash particles tend to be significantly smaller than those formed by the combustion of pulverized coal [20}. Biomass materials tend to have a relatively low ash content compared to most coals; however, the biomass ash materials tend to be relatively rich in alkali and alkaline earth metal, and these are effective fluxes for the alumino-silicate coal ashes. At low co-firing ratios, at about 10% on energy basis, recent plant experience has indicated that slagging and fouling tend to be modest [37]. However, experiences have also shown that coal quality is a very important factor when firing coal with straw due to ash deposition problems [2]. Fly ash from coal firing is often sold as filler for use in concrete mixes (among other uses), but this is not the case for fly ash from biomass firing. The reason is that the required contents of total alkali, Cl and residual carbon for the fly ash to be used in the concrete production are 5 wt.%, 0.1 wt.% and 5 wt.%, respectively. These limits were exceeded if more than 20% biomass is used on energy basis with coal [2, 20], nevertheless, this has been increased now.

Table 2. 8: Review of full-scale suspension firing of biomass.

Location	System	Size	Fuels	Issues/Fingings	Ref
Suspension Firing (Biomass)					
Amagerværket Power Station, Unit 2, Denmark	Drum-type boiler with 12 burners. Retrofitted from oil to coal, and then coal to biomass.	250 MW_{th}	Pulverized straw with and without the addition of additives.	Fouling and slagging. Issues of air pollution control equipments. Sand and bentonite resulted to be good additives.	[5]
Amagerværket Power Station, Unit 1, Denmark	Dedicated straw, wood and coal fired boiler with 12 burners.	350 MW_{th}	Pulverized straw and wood with different co-firing combinations	No measurements except made in the present study.	[84]
Avedøreværket Power Station, Unit 2, Denmark	Pulverized wood-fired boiler.	800 MW_{th}	Pulverized wood, natural gas and furnace oil.	Ash deposition, NOx and SOx emissions.	[24]
Jordbro Boiler, Sweden	Down-fired.	80 MW_{th}	Pulverized wood in combination with different shares of peat and S.	Deposition and corrosion.	[38]
California Energy Boiler	Suspension-fired.	26.5 MW_e	Leached straw (20-25 wt.%) and rice hull.	Fouling and stack sampling.	[51]
Suspension Firing (Straw and Coal)					
Amagerværket Power Station Unit 3, Denmark	Opposed wall fired boiler with 16 burners.	250 MW_{th}	Bituminous coal with high S in combination with different straw fuel fractions, typically 0 to 20 % on thermal basis.	Fouling and slagging, emissions, performance of air pollution control equipments, and flame stability.	[85, 86]
Vestkraft Power Station, Unit 1, Denmark	Front-wall fired with 12 burners in three levels.	330 MW_{th} / 125 MW_e	Bituminous coal from Russia and Columbia in combination with different straw fuel fractions, typically 10 to 25% on thermal basis. Straw was added through straw burners in the middle level.	Ash deposition, corrosion, fly ash, emissions.	[87]
Kynndby Power Plant, Unit 3, Denmark	Down-fired.	180 MW_{th}	Coal-straw.	Ash deposition.	[88]
Studstrup Power Station, Unit 1, Denmark	Back wall fired boiler with 12 burners.	380 MW_{th} / 150 MW_e	Straw with Bituminous Columbian coal and American coal. Separate injection of straw up to 20% on thermal basis.	2 years demonstration program. Fouling/slagging, corrosion, fuel handling and emissions related issues were investigated.	[20]
Studstrup Power Station, Unit 4, Denmark	Opposed wall fired with 24 burners.	900 MW_{th} / 350 MW_e	Straw with Bituminous Columbian and South African coal. Injection of straw using six modified burners. Injection of straw up to 20% on thermal basis.	Performance of air pollution, control equipment (DeNOx catalyst), and ash.	[89]

1.6 Modeling of Ash Deposit Formation

Ash deposition modeling in biomass fired boilers is primarily based on three requirements, a) deposition flux, mass of deposit/area/time ($g/m^2/h$), b) location of the deposits in the boiler, c) physical and chemical properties of the deposits and corresponding heat transfer considerations and materials related aspects [2, 90]. Generally, ash deposition models can be cataloged into three levels, i.e. the empirical indices model, the mechanistic model, and the most complicated CFD (Computational Fluid Dynamics) model.

Wang and Harb [91] summarized several existing models for ash deposition and heat transfer through the deposits and classified the total process into nine issues: (1) ash formation; (2) fluid dynamics and particle transport; (3) particle impaction; (4) particle sticking; (5) deposition growth as a function of location in the combustion chamber; (6) deposition properties and strength development; (7) heat transfer through the deposition layer; (8) the effect of deposition on operating conditions (temperatures and heat fluxes) in the combustor; (9) deposition structure and its effect on flow patterns in the combustion facility.

Traditionally, power generating facilities and some researchers have attempted to predict the severity of coal ash deposition by calculating empirical indices based upon the overall ash composition of the coal. These indices are less accurate predictors when extrapolated to other coals or operating conditions. This can be attributed to their use of overall ash compositions, while in fact deposition is initiated and propagated by individual ash particle with varying compositions and sizes.

The mechanistic models, in which the calculations of the complicated combustion process and the fluid dynamics are simplified, have been used for assessing ash deposition tendency and for predicting ash deposit behavior. Generally, a viscosity model relevant to silicate glass together with measurements of particle size and composition as well as the deposition composition is included. Detailed analysis of coal mineralogy, coal size distribution data, boiler design details, and boiler operating conditions were used as input to predict ash deposition in a pulverized coal-fired boiler and to assess boiler performance associated with the use of specified coal by Erickson et al. [92]. The simulations were in fair agreement with their tests.

The mechanistic models can provide a basement for developing comprehensive mathematical models that can simulate ash deposition and its impact on overall efficiency. A dynamic mechanistic model of ash deposit build-up and shedding through surface melting was established and demonstrated by Zhou et al. [31] in a straw grate-fired boiler. The predicted results were close to the results obtained from full-scale measurements, where a steady state was achieved between deposit build-up and shedding after 7 days.

A CFD-based deposition model was established and demonstrated by Kær [93, 94], in which the ash deposition from fly ash particles (2-250 μm) by inertial impaction, turbulent, and thermophoretic mechanisms, and KCl vapors-formed particles (□ 0.5 μm) by diffusion, turbulent, and themophoretic mechanisms was considered.

1.7 Conclusions on Literature Review

Traditionally solid fuel power plant boilers have been developed to use coal as fuel. Since around 1990 combined heat and power grate boilers firing straw have been developed in Denmark and in later year's pulverized fuel boilers have been designed to use biomass as fuel. The applied fuels have included co-firing of straw and coal, firing of wood and co-firing of wood and straw. Straw and wood causes increased problems with deposit formation in power plant boilers, and have compared to coal high contents of Cl and potassium in the ash. Straw typically have a fuel ash content of 5 wt% that have high concentrations of K and Si, and wood fuels often have an ash content of 1 wt% that have high concentrations of K and Ca.

The ash deposit formation is caused by the fly ash present in the boiler chamber. The biomass fly ash formation process is quite different in grate fired and suspension fired boilers. The fly ash in grate fired boilers is mainly caused by volatilization of alkali rich ash species and typically only around 20 wt% of the fuel ash is transferred to the fly ash, while the residual 80 wt% is removed from the boiler chamber as bottom ash. In suspension fired boilers most of the fuel ash is entrained into the flue gas and the fly ash and the fuel ash have nearly similar chemical compositions.

Ash deposit formation in boilers reduce heat transfer to boiler walls and may in severe cases block flue gas channels, and make it necessary to stop boiler operation and clean the boiler manually. Initially conducted Danish experiments with 100% straw suspension combustion led to several unscheduled boiler short downs.

The ash deposit formation on boiler surfaces are coursed be several processes such as, diffusion and condensation on heat transfer surfaces of volatile inorganic species (often dominated by alkali salts), thermophoresis and diffusion of aerosol particles and impaction of larger particles on boiler walls. Generally more particles stick to boiler surfaces when a higher fraction of the deposit or the incoming particles are melted.

Most studies in deposit formation and deposit properties have been conducted in grate biomass fired boilers. Typically the deposits have an inner layer rich in KCl and K_2SO_4 formed by condensation and diffusion and outer deposit layers rich in K, Ca and Si that is mostly formed by impaction. Studies on deposit formation in grate fired boilers have been conducted in several cases, often using deposits probe to

investigate the deposit formation rate and the chemistry of biomass deposits. It has been seen that straw fuels cause more severe deposit formation than wood fuels, and that an increased fuel alkali content cause an increased deposit formation rate.

Shedding of deposits can happen naturally or induced by deposit removal technologies such as soot blowing. In grate straw fired boilers the removal of deposits in the superheater area is mainly caused by melting of the outer most deposit layer, and in areas of the boiler with lower temperatures both natural shedding and soot blower induced shedding takes place.

Before this project was started deposit formation processes and removal were mainly investigated in biomass grate boilers. Because of the different fly ash formation process in the two boiler types detailed knowledge on deposit formation and shedding in biomass suspension fired boilers are wanted.

References

[1] REN21 (Renewable Energy Policy Network for 21st Century) Global Status Report, 2011. www.ren21.net/Portals/97/documents/GSR/REN21_GSR2011.pdf

[2] F. J. Frandsen, Ash formation, deposition and corrosion when utilizing straw for heat and power production, Doctoral Thesis, 2011, Technical University of Denmark, ISBN 978-87-92481-40-5.

[3] M. P. Glazer, Alkali metals in combustion of biomass with coal, PhD Thesis, 2006, Technical University of Delft. Available online (19-03-2012),

http://repository.tudelft.nl/view/ir/uuid:404df03f-cbaf-49b4-9eee-5661806b8a5e/

[4] M. Montgomery, S. A. Jensen, U. Borg, O. Biede, T. Vilhelmsen, Materials and Corrosion, 62 (2011), 593-605.

[5] L. Tobiasen, R. Skytte, L. S. Pedersen, S. T. Pedersen, M. A. Lindberg, Fuel Processing Technology, 88 (2007), 1108-1117.

[6] H. Egsgaard, U. Hansen, P. A. Jensen, P. Glarborg, Combustion and Gasification Technologies, Risø Energy Report 2, Technical University of Denmark.

http://www.risoe.dk/rispubl/energy_report/ris-r-1430s35_39.pdf

[7] J. M. Johansen, Release of inorganic matter during combustion of biomass, M.Sc. Thesis, 2011, Department of Chemical and Biochemical Engineering, Technical University of Denmark.

[8] Green energy - towards a Danish energy without fossil fuels, Klimakommissionen (Climate Commission), 2010, Denmark. ISBN (www) 978-87-7844-878-1.

[9] M. Hupa, Energy & Fuels, 26 (2012), 4-14.

[10] L. L. Baxter, Biomass and Bioenergy, 4 (1993), 85-102.

[11] M. Leckner, F. Winter, A. K. Agarwal, Handbook of combustion, volume 4: solid fuels, 2010, Wiley-VCH, ISBN 978-3-527-32449-1.

[12] B. Sander, N. Henriksen, O. H. Larsen, A. Skriver, C. Ramsgaard-Nielsen, J. N. Jensen, K. Stærkind, H. Livberg, M. Thellefsen, K.Dam-Johansen, F. J. Frandsen, R. van der Lans, J. Hansen, Emissions, corrosion and

alkali chemistry in straw-fired combined heat and power plants, Proceedings of 1st World Conference on Biomass for Energy and Industry, 05-09 June, Sevilla, 2009.

[13] L. L. Baxter, Ash deposit formation and Deposit properties: A comprehensive summary of research conducted at Sandia's Combustion Research Facility, SAN2000-8253, Sandia National Laboratories, Livermore, CA 94550 USA, 2000.

[14] B. M. Jenkins, L. L. Baxter, T. R. Miles (Jr.), T. R. Miles, Fuel Processing Technology, 54 (1998), 17-46.

[15] L. A. Hansen, Melting and sintering of ashes, PhD Thesis, 1998, Technical University of Denmark, ISBN 87-90142-31-4.

[16] L. L. Baxter, T. R. Miles, T. R. Miles (Jr.), B. M. Jenkins, T. Milne, D. David, R. W. Bryers, L. L. Oden, Fuel Processing Technology, 54 (1998), 47-78.

[17] H. P. Nielsen, Deposition and high temperature corrosion in biomass-fired boilers, PhD Thesis, 1998, Technical University of Denmark, ISBN 87-90142-47-0.

[18] T. R. Miles, T. R. Miles (Jr.), L. L. Baxter, R. W. Bryers, B. M. Jenkins, L. L. Oden, Biomass and Bioenergy, 10 (1996), 125-138.

[19] L. L. Baxter, Fuel Processing Technology, 56 (1998), 81-88.

[20] K. H. Andersen, Deposition formation during coal straw co-combustion in a utility pf-boiler, PhD Thesis, 1998, Technical University of Denmark, ISBN 87-90142-47-0.

[21] P. A. Jensen, F. J. Frandsen, J. Hansen, K. Dam-Johansen, N. Henriksen, S. Hörlyck, Energy & Fuels, 18 (2004), 378-384.

[22] F. J. Frandsen, Fuel, 84 (2005), 1277-1294.

[23] K. Bendixen, USC technology in CCT boilers applying biomass co-firing, Proc. of Power-Gen Europe, 28{30 June, Milano, 2005.

[24] P. A. Jensen, M. Dall'ora, W. Lin, S. Clausen, J. Hansen, P. Simonson, M. Berg, A. D. Jensen Measurements on the 800 MWth Avedøre oil, gas and wood co-fired suspension-boiler-Analysis of emission, burnout, deposit and FTIR measurements from April 2005, PSO Project 6526, Report R0802, CHEC Research Centre, Technical University of Denmark, 2008.

[25] K. A. Christensen, M. Stenholm, H. Livbjerg, J. Aerosol Sci., 29 (1998), 421-444.

[26] J. H. Zeuthen, P. A. Jensen, H. Livbjerg, J. P. Jensen, Energy & Fuels, 21 (2007), 699-709.

[27] D. Nordgren, H. Hedman, N. Padban, D. Boström, M. Öhman, Fuel Processing Technology, (2011), doi:10.1016/j.fuproc.2011.05.027.

[28] S. S. Lokare, J. D. Dunaway, D. Moulten, D. Rogers, D. R. Tree, L. L. Baxter, Energy & Fuels, 20 (2006), 1008-1014.

[29] J. N. Knudsen, Volatilization of inorganic matter during combustion of annual biomass, PhD Thesis, 2004, Technical University of Denmark, ISBN 87-91435-11-0.

[30] P. M. Walsh, A. N. Sayre, D. O. Loehden, L. S. Monroe, J. M. Beer, A. F. Saro_m, Prog Energy Combust Sci, 4 (1990), 327-346.

[31] H. Zhou, P. A. Jensen, F. J. Frandsen, Fuel, 86 (2007), 1519-1533.

[32] M. Hupa, B-J, Skrifvars, A. Moilanen, Fuel Processing Technology, 62 (1989), 131-137.

[33] H. Zhou, F. J. Frandsen, P. A. Jensen, P. Glarborg, Ash deposit forrmation and removal in biomass-fired boilers, PSO Project 4106, Report R0603, CHEC Research Centre, Technical University of Denmark, 2006.

[34] C. L. Senior, Energy & Fuels, 11 (1997), 416-420.

[35] A. Zbogar, F. J. Frandsen, P. A. Jensen P. Glaborg, P. Hansen, Energy & Fuels, 20 (2006), 512-519.

[36] A. L. Kaliazine, F. Piroozmand, D. E. Cormack, H. Tran, TAPPI Journal, 80 (1997), 201-207.

[37] IFRF Combustion Handbook, January 16, 2009.

http://www.handbook.ifrf.net/handbook/index.html

[38] B-J. Skrifvars, T. Lauren, M. Hupa, R. Korbee, P. Ljung, Fuel, 83 (2004), 1371-1379.

[39] H. Wu, Co-combustion of fossil fuels and waste, PhD Thesis, 2011, Technical University of Denmark.

[40] P. A. Jensen, B. Sander, K. Dam-Johansen, Biomass and Bioenergy, 20 (2001), 447-457.

[41] M. Theis, B. J. Skrifvars, M. Hupa, H. Trans, Fuel, 85 (2006), 1125-1130.

[42] A. Zbogar, F. J. Frandsen, P. A. Jensen, P. Glarborg, Prog Energy Combust Sci, 35 (2009), 31-56.

[43] E. Raask, Mineral impurities in coal combustion, Edition 41, Hemisphere Publishing Corporation, 1985.

[44] M. I. Jameel, D. E. Cormack, H. Tran, T. E. Moskal, Tappi Journal, 77 (1994), 135-142.

[45] L. A. Hansen, H. P. Nielsen, F. J. Frandsen, J. Hansen, K. Dam-Johansen, S. Höorlyck, A. Karlsson, Fuel Processing Technology, 64(2000), 189-209.

[46] P. A. Jensen, M. Stenholm, P. Hald, Energy & Fuels, 11 (1997), 1048-1055.

[47] P. Isaak, H. N. Tran, D. Barham, D. W. Reeve, Journal of pulp and paper science, 13(5) (1987), 154-158.

[48] K. Wieck-Hansen, P. Overgaard, O. H. Larsen, Biomass and Bioenergy, 19 (2000), 395-409.

[49] J. Sandberg, U. Sand, R. B. Fedhila, International Journal of Green Energy, 3 (2006), 43-61.

[50] H. M. Brink, J. P. Smart, J. M. Vleeskens, J. Williamson. Fuel, 73 (1994), 1712-1717.

[51] B. M. Jenkins, R. B. Williams, P. R. Bakker, S. Blunk, D. E. Yomogida, W. Carlson, J. Duffy, R. Bates, K. Stuci, V. Tiangco, Combustion of leached straw for power generation, 4th Biomass Conference of the Americas, Pergamon, Elsevier Science, Oxfored, UK, 1999, pp 1357-1363.

[52] Fundamentals in Biotechnology, Volume 7, Chapter: Biomass Feedstocks, pp. 315-324. Editor(s) H. W. Doelle and S. Rokem. ISBN 978-1-84826-258-7 (e-book).

[53] L. Hindiyarti, Gas phase sulfur, chlorine, and alkali metal chemistry in biomass combustion, PhD Thesis, 2007, Technical University of Denmark, ISBN 87-91435-58-7.

[54] Danish Energy Agency, Denmark, www.ens.dk.

[55] L. Baxter, G. Hatch, S. A. Sinqui_eld, W. J. Frederick An experimental study of the mechanisms of fine particle deposition in Kraft recovery boilers, 1998, International Chemical Recovery Conference Proceedings.

[56] G. Barnocky, R. H. Davis, Elastohydrodynamic collision and rebound of spheres: Experimental veri_cation, Phys. Fluid, 31 (1998), 1324-1329.

[57] J. P. Hurley, S. A. Benson, Energy & Fuels, 9 (1995), 775-781.

[58] J. W. Nowok, Journal of Institute of Energy, 69 (1996), 9-11.

[59] B. Sander, Biomass and Bioenergy, 12(3) (1997), 177-183.

[60] C. Yin, L. A. Rosendahl, S. K. K_r, Prog Energy Combust Sci, 35(2008), 725-754.

[61] M. A. Telfer, D. K. Zheng, Energy & Fuels, 12(6) (1998), 1135-1141.

[62] P. Glarborg, A. D. Jensen, Combustion and Harmful Emission Control [28244 E08], Course Notes, Technical University of Denmark, 2002.

[63] S. C. van Lith, Release of inorganic elements during wood-firing on a grate, PhD Thesis, 2005, Technical University of Denmark, ISBN 87-91435-29-3.

[64] Major technologies for the exploitation of renewable energy sources, May 12, 2008.

www.eppo.go.th/encon/encon-DC-Cogen10-Chap5.doc

[65] S. v. Loo, J. Koppejan, The handbook of biomass combustion and co-firing, 2008, Published by Earchscan, ISBN 978-84407-249-1.

[66] M. Berg, S. T. Pedersen, G. Rohde, VGB Powertech, 87 (2007), 93-95.

[67] D. C. Dayton, R. J. French, T. A. Milne, Energy & Fuels, 9 (1995), 855-865.

[68] H. Tran, X. Mao, D. C. S. Kuhn, R. Backman, M. Hupa, Pulp Pap. Can., 130 (2002), 29-33.

[69] P. A. Jensen, H. Zhou, F. Frandsen, J. Hansen, Ash deposits removal in biomass power plant boilers, 15th European Biomass Conference and Exhibition, 7-11 May, Berlin, 2007.

[70] S. Stitt, H. Junker, L. L. Baxter, Optimization of deposit removal in biofueled boilers: review of control systems, technologies and mechanism, Eltra Project no. 3144, TW 13317.00, Report 02-1036, Tech-wise, 2002, 1-27.

[71] M. I. Jameel, D. E. Cormack, H. Tran, T.E. Moskal, TAPPI Journal, 77(5) (1994), 135-142.

[72] Rosnik GmbH + Co, September 15, 2008.

http://www.rosink.com/en/Apparatebau/rb/index_russbl.htm

[73] H. Wu, P. Glarborg, F. J. Frandsen, K. Dam-Johansen, P. A. Jensen, Energy & Fuels, 25 (2011), 2862-2873.

[74] L. Sørensen, J. Fjellerup, U. Henriksen, International Patent Number WO 01/05911 A2, 2001.

[75] ChlorOut, European Patent EP 1354167, International Patent Application: PCT/SE 02/00129, 2002.

[76] H. Kassman, M. Berg, Ash related problems in wood-fired boilers and effect of additives, Workshop on ash deposition and corrosion, Glasgow, 2006.

[77] Z. Huque, Experimental investigation of slag removal using pulse detonation wave technique, NIST, DOE/HBCU/OMI Annual Symposium, Miami, Fl, March 16-18, 1999.

[78] S. A. Ebrahimi-Sabet, A Laboratory study of deposit removal by debonding and its application to fireside deposits in Kraft boilers, PhD Thesis, 2001, Department of Chemical Engineering and Applied Chemistry, University of Toronto, ISBN 0-612-58923-4.

[79] T. Madhiyanon, P. Sathitruangsak, S. Sungworagarn, S. Pipatmanomai, S. Tia, Fuel Processing Technology, 96 (2012), 250-264.

[80] A. L. Robinson, H. Junker, L. L. Baxter, Energy & Fuels, 16 (2002), 343-355.

[81] R. Shenassa, Dynamic carryover deposition in an entrained ow reactor, PhD Thesis, 2000, Department of Chemical Engineering and Applied Chemistry, University of Toronto, ISBN 0-612-49833-6.

[82] P. A. Jensen, L. H. Sørensen, G. Hu, J. K. Holm, F. Frandsen, U. B. Henriksen, Combustion experiments with biomass fuels and additives in a suspension-fired entrained ow reactor - Test of Ca and P rich additives used to minimize deposition and corrosion, Report R0504, CHEC Research Centre, Technical University of Denmark, 2005.

[83] J. Capablo, P. A. Jensen, K. H. Pedersen, K. Hjuler, L. Nikolaisen, R. Backman, F. Frandsen, Energy & Fuels, 23 (2009), 1965-1976.

[84] E. Gjernes, Fuel exibilty at Amager unit 1 using pulverized fuels. Proc. of Power-Gen Europe, Cologne, Germany 2006.

[85] L. S. Pedersen, H. P. Nielsen, S. Kiil, L. A. Hansen, K. Dam-Johansen, F. Kildsig, J. Christensen, P. Jespersen, Fuel, 75 (1996), 1584-1590.

[86] L. S. Pedersen, D. M. Morgan, W. L. van de kamp, J. Christensen, P. Jespersen, K. Dam-Johansen, Energy & Fuels, 11(2) (1997), 439-446.

[87] B. Sander, EU project UCOR, Utilization of residues from biomass co-combustion in pulverized coal boilers, results from full-scale co-firing of coal and straw at the Vest Kraft Power Station Unit 1, Elsam Engineering A/S, Report No. 02-443, 2002.

[88] F. J. Frandsen, H.P. Nielsen, P. A. Jensen, L. A. Hansen, H, Libbjerg, K. Dam-Johansen, P. F. B. Hansen, K. H. Andersen, H. S. S_rensen, O. H. Larsen, B. Sander, N. Henriksen, P. Simonsen, Impact of mineral impurities in solid fuel combustion, edited by Gupta et al. Kluwer Academic, New York, pp 71-78, 1999.

[89] B. Sander, K. Wieck-Hansen, Full-scale investigations on alkali chemistry and ash utilization by co-_ring of straw, 14th European Biomass Conference and Exhibition, October, Paris, 2005.

[90] A. Zbogar, F. J. Frandsen, P. A. Jensen, P. Glarborg, Prog Energy Combust Sci, 31 (2005), 21-56.

[91] H. Wang, J. N. Harb, Prog Energy Combust Sci, 23 (1997), 267-282.

[92] T. A. Erickson, S. E. Allan, D. P. McColler, J. P. Hurley, S. Srinivasachar, S. G. Klang, J. E. Baker, M. E. Morgan, S. A. Johnson, R. Borio, Fuel Processing Technology, 44 (1998), 155-171.

[93] S. K. K_r, Numerical investigation of deposit formation in straw-fired boilers, PhD Thesis, Aalborg University, Denmark, ISBN 87-89179-39-0, 2001.

[94] S. K. Kær, L. Rosendahl, Extending the modeling capacity of CFD codes applied to biomass-fired boilers, Proc. ECOS 2003, June 30 - July 2, 2003, Copenhagen, Denmark, 251-264.

[95] A. Brink, T. Lauren, P. Yrjas, M. Hupa, J. Friesenbichler. Fuel Processing Technology, 88 (2007), 1129-1135.

[96] H. B. Vuthaluru, Fuel, 78 (1999), 1789-1803.

[97] S. Gupta, R. Gupta, G. Bryant, T. Wall, S. Watanabe, T, Kiga, K. Narukawa, Energy & Fuels, 23 (2009), 2570-2575.

[98] T. Heinzel, V. Siegle, H. Spliethoff, K. R. G. Hein, Fuel Processing Technology, 54 (1998), 109-125.

[99] S. P. Hanson, M. F. Abbott, Prog Energy Combust Sci, 24 (1998), 503-511.

[100] IFRF Suction Pyrometer, user information document, 2007, International Flame Research Foundation, Netherlands.

[101] M. S. Bashir, P. A. Jensen, F. J. Frandsen, S. Wedel, K. Dam-Johansen, J. Wadenb ack, S. T. Pedersen, Fuel Processing Technology, 97 (2012), 93-106.

[102] L. A. Hansen, H. P. Mickelsen, F. J. Frandsen, K. Dam-Johansen, O. H. Larsen, Fuel Processing Technology, 54 (1998), 95-108.

[103] K. H. Andersen, F. J. Frandsen, P. F. B. Hansen, K. Wieck-Hansen, I. Rasmussen, P. Overgaard, K. Dam-Johansen, Energy & Fuels, 14(4) (2000), 765-780.

[104] J. Hansen, P. A. Jensen, P. Glarborg, Deposit probe measurements in the Avedøre and Ensted straw-fired grate boilers, PSO Project 4792, Report R0705, CHEC Research Centre, Technical University of Denmark, 2007.

[105] A. A. Masi_a, B. J. P Buhre, R. P. Gupta, T. F. Wall, Fuel Processing Technology, 88 (2007), 1071-1081.

[106] K. salmenoja, Field and laboratory studies on chlorine-induced superheater corrosion in boilers-fired with biofuels, PhD Thesis, 2000, Faculty of Chemical Engineering, Åbo Akademi, Åbo/Turku, Finland.

[107] Y. Zheng, P. A. Jensen, A. D. Jensen, B. Sander, H. Jusker, Fuel, 86 (2007), 1008-1020.

[108] M. S. Bashir, P. A. Jensen, F. J. Frandsen, S. Wedel, K. Dam-Johansen, J. Wadenb ack, S. T. Pedersen, Energy & Fuels, 26 (2012), 2317-2330.

[109] M. S. Bashir, P. A. Jensen, F. J. Frandsen, S. Wedel, K. Dam-Johansen, J. Wadenböack, S. T. Pedersen, Energy & Fuels, (accepted).

[110] J. R. Kittrel Advances in Chemical Engineering, 8 (1970), 97-103.

[111] D. J. Pritchard, D. W. Bacon, Chemical Engineering Science, 33 (1978), 1539-1543.

[112] Matlab, signal processing toolbox, March 31, 2011.

http://www.mathworks.com/help/toolbox/signal/resample.html

[113] Moving slope calculation, December 16, 2010.

http://www.mathworks.com/matlabcentral/fileexchange/16997-movingslope

[114] Online book, December 31, 2010. Chapter 15, pp. 277-284

http://www.dspguide.com/

[115] Matlab, curve fitting toolbox, March 31, 2011.

http://www.mathworks.com/help/toolbox/curvefit/bq_6yqb.html

[116] J. R. Brock, J. Col. Sci., 17 (1962), 768.

[117] R. C. Flagan, J. H. Seinfeld, Fundamentals of air pollution engineering, Prentice-Hall Inc., New Jersey, (1988).

[118] S. Vargas, Straw and coal ash rheology, PhD Thesis, 2001, Technical University of Denmark, ISBN 87-90142-64-0.

September. 2012, DTU no. 50530

Appendix A2

Design and Development of Probes for Online Monitoring of Deposit Build-up and Removal

Energinet.dk project no. 7217

Characterization and quantification of deposits build up and removal in straw suspension fired boilers

Muhammad Shafique Bashir, Peter Arendt Jensen, Stig Wedel, Flemming Frandsen, Johan Wadenbäck, Søren Thaaning Pedersen, Kim Dam-Johansen

Department of Chemical and Biochemical Engineering

Technical University of Denmark

Søltofts Plads, Building 229, DK-2800 Lyngby, Denmark

CHEC no. R1301

1.1 Introduction

A significant amount of ash can be deposited on the boiler furnace walls and on the superheater tubes when firing KCl-containing biomass (straw) and/or co-firing high share of KCl-containing biomass with coal. To obtain accurate information on ash deposition in biomass-fired boilers, or, more precisely, to quantify ash deposition on the boiler furnace chamber and on the superheater tubes, one of the most effective ways is to use deposit probes. The deposit probes find key importance during combustion of solid fuels, and are extensively used to understand ash deposit formation and shedding processes, and to quantify and characterize the deposits. In addition, investigations of deposit pattern, composition and morphology on each side of the probe - the upstream and the downstream side - can further help to understand the mechanisms responsible for ash deposition on each side. Based on the experimental conditions, deposit probes can be air-cooled or water and air-cooled. In addition, deposit probes can be used for short time testing or for extensive full-scale measurements. Deposit probes find use either in the furnace region to investigate slagging propensity by simulating conditions of water walls or in the superheater region to investigate fouling and/or slagging by simulating conditions of typical superheater tubes. In this work, two probes are used; 1) a deposit probe used in the superheater region, termed as the horizontal probe, and 2) a deposit probe used in the boiler furnace region, termed as the vertical probe.

The ash deposition rate during simple probe measurements is normally determined by dividing the collected amount of the deposits with the probe exposure time. However, advanced probes can be more effective to truly identify online deposition and shedding processes, which are difficult to monitor using a simple deposit probe. Another advantage of the advanced on-line probes is that even though some information on the deposit formation process might be obtained using different simple deposit probes for different durations, there can be difficulties in guaranteeing identical boiler conditions for all probes [95]. Advanced online probes can be used to identify deposit mass uptake, deposit shedding, deposit characterization, and probe heat uptake using the temperature rise of the probe cooling fluid(s). This complete set of information finds key role to quantify transient deposit build-up and shedding, and most importantly to model ash deposit build-up and shedding processes based on the applied biomass fuel, local flue gas temperature, applied probe conditions and boiler operational conditions.

In addition to the quantification of deposit build-up, deposit shedding quantification is equally important in order to optimize the sootblowers employed in biomass-fired boilers. Steam, water and air sootblowing are the most commonly applied shedding techniques to shed deposits in the superheater region and in the boiler chamber region. Biomass-fired boilers have several water and steam sootblowers depending on the local flue gas temperature, deposit sintering characteristics and deposit

quantity [2, 35]. The sootblower cleaning effectiveness depends on the sootblower location, cleaning media and Peak Impact Pressure (PIP) [44, 70, 78]. Quantification of PIP needed to remove the deposit by using artificial sootblowing probe can an effective way to optimize the design and operation of sootblowers employed in biomass suspension-fired boilers.

This chapter covers an overview of the deposit probes used for ash deposit build-up and deposit characterization studies. The horizontal ash deposition probe used during the ash deposit build-up measurements and a simple artificial sootblowing probe used to remove the deposits are described in detail. The design, functionality and commissioning of a vertical ash deposition probe simulating the conditions of the boiler furnace wall is also discussed.

1.2 Review of Deposit Probes used for Ash Deposit Build-up Investigations

The deposit probes can find their use based on the experimental requirements i.e. deposition rate, deposit chemistry and morphology etc. Various types of deposit probes used for different experimental investigations can be found in literature.

1.2.1 Types of Deposit Probes Based on Mechanical Design

The deposit probes can be divided based on the mechanical design. The probes can be inserted in the furnace section to quantify and/or characterize slagging on the furnace walls (vertical probe) or can be used in superheater section to quantify and/or characterize deposits by simulating conditions of superheaters (horizontal probe).

1.2.1.1 Horizontal Probes

Horizontal probes are normally a long rod inserted in the superheater region of the boiler to simulate conditions of a typical plant superheater. Horizontal probe can be used for the quantification and characterization of deposits on the upstream and on the downstream side of the probe. This can be useful information to determine the ash deposition mechanisms responsible for the deposition on each side of the probe. Jensen et al. [46] investigated deposition fluxes using an air-cooled probe in the superheater region of straw-fired boilers. Vuthaluru et al. [96] used a deposition probe to study different pretreatments of coal in pulverized fuel boilers regarding deposition rates. In a recent study, Madhiyanon et al. [79] used an advanced online ash deposition probe. The probe was a double annular probe and it was possible to measure the changes in the deposit mass and fouling resistance due to ash deposition. A schematic of the deposit probe is shown in Figure 3.1. Two load cells were used to measure

the amount of ash deposited, while the temperature rise of the cooling fluids was used to determine the fouling resistance caused by ash deposition.

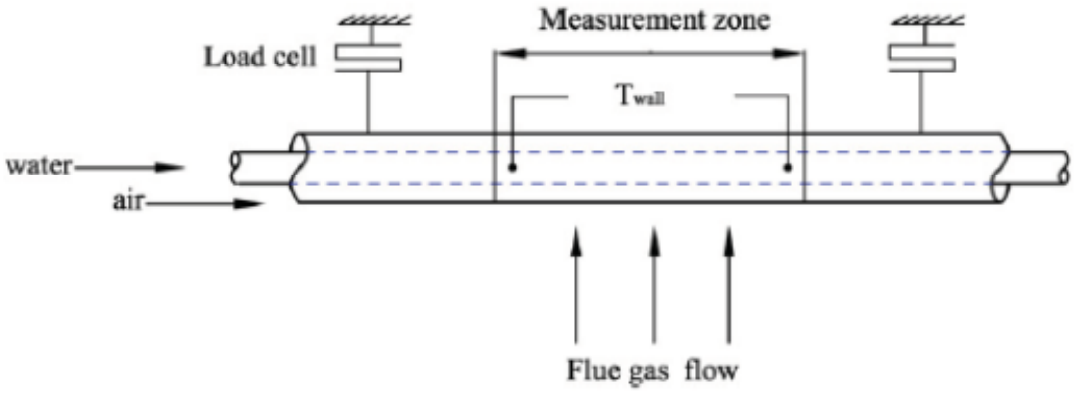

Figure 3. 1: Schematic of the deposit probe used by Madhiyanon et al. [79] to measure mass of and fouling resistance.

1.2.1.2 Vertical Probes

Significant amount of deposits can result on the water walls in the boiler furnace when biomass fuels with higher KCl proportions are fired in suspension-fired boilers. In order to simulate the conditions of water walls, use of a vertical probe is a rather new concept. To investigate deposition and heat uptake in the furnace region, Gupta et al. [97] performed pilot-scale and full-scale experiments in the furnace region by using a deposition probe simulating the slagging conditions in the furnace region of a coal-fired boiler. Heinzel et al. [98] made investigations of slagging in co-combustion of biomass and coal using air-cooled probes. Illustration of a typical vertical probe used by Hasnson et al. [99] for slagging investigations during pilot-scale studies is shown in Figure 3.2. A temperature array is used to measure the probe temperature. The probe is cooled by water to simulate conditions of water walls.

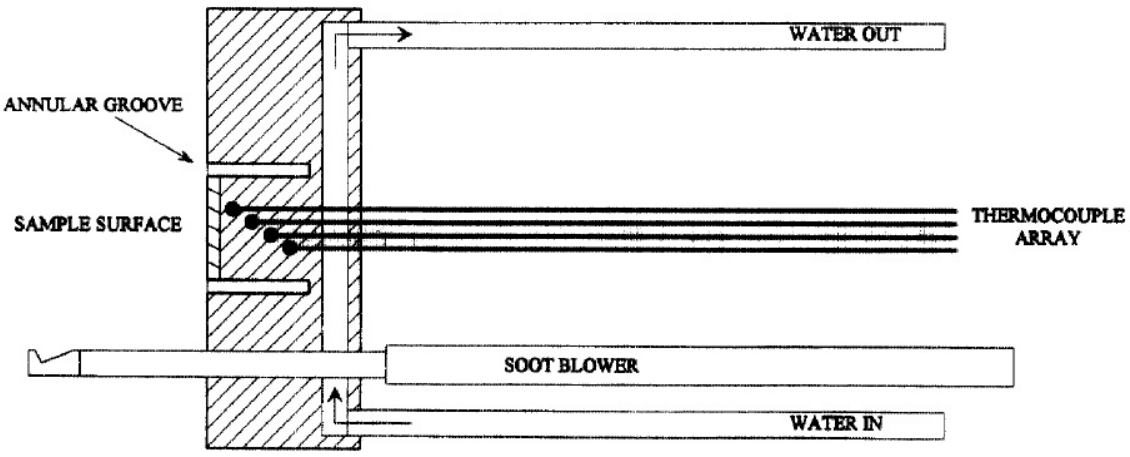

Figure 3. 2: Illustration of a typical vertical probe for slagging investigations [99].

1.2.2 Types of Deposit Probes Based on Cooling Media

The deposit probes can be divided based on the cooling media used to keep a stable probe surface temperature during the measurements. The cooling media can be different based on the flue gas temperature and probe dimensions.

1.2.2.1 Air Cooled Probes

Air cooled probes are used for pilot-scale and/or full-scale investigations, primarily when the heat load to the probe is small. They can be used at higher flue gas temperatures (> 800 ^{o}C) during pilot-scale investigations due to a lower heat load (smaller probe surface area), compared to full-scale measurements, where higher temperature of the air coming out of the probe can be risky.

Nielsen [17] an advanced air-cooled pilot-scale probe for investigation of potassium salts on heat transfer surfaces. The probe consisted of two small (2 x 3 cm) vertical plates which were placed approximately 2 cm apart. A larger horizontal plate (6 x 9 cm^2) that completely covered the underlying plates was placed 0.5 cm above the two vertical plates. This way, the horizontal plate shielded the vertical plates from the particles in the gas that came from above, allowing only vapors and submicron particles to deposit on the vertical plates. The schematic of the probe is shown in Figure 3.3. Brink et al. [95] designed and tested an air-cooled probe for on-line monitoring of deposition growth. The heat flux and corresponding thickness of the deposit was investigated for a couple of measurements in a 440 kW$_{th}$ grate boiler firing wood chips, bark and waste wood-fired. The deposit probe was made of a 38 x 5 mm tube and a thermocouple was mounted at the outer surface to adjust the probe temperature close to the set point. The highest deposition rate was found during waste wood firing, whereas wood chips caused the lowest deposit build-up rate. However, it was found that the calculated thickness of the deposits was larger than the measured one, thereby demanding possible improvements in the probe design.

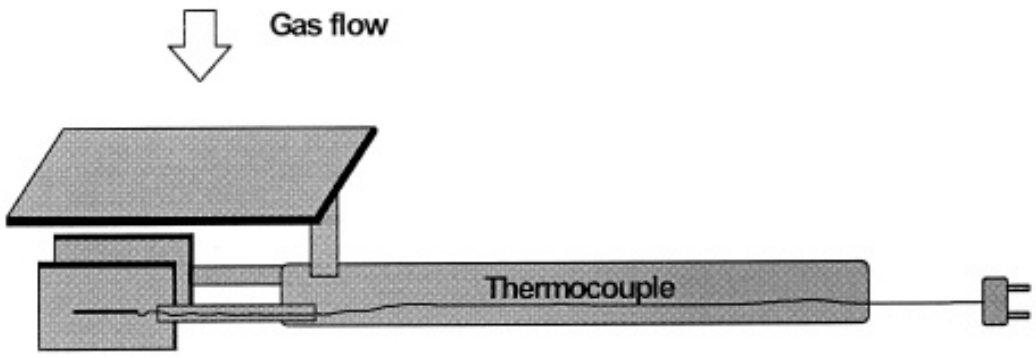

Figure 3. 3: Schematic drawing of the probe used for investigation of potassium salts deposition on heat transfer surfaces [17].

Andersen [20] used a temperature controlled probe for deposit sampling during full-scale measurements in a straw and coal fired boiler. The probe was an advance form of the probe that was used for corrosion investigations. The probe was temperature controlled and it was possible to identify the shedding events of the deposits based on the sudden changes in the probe surface temperature. A schematic of the probe is shown in Figure 3.4 (a).

1.2.2.2 Water and Air Cooled Probes

If the probe heat load is significant, the use of solely air cooled probe is not an appropriate solution due to difficulties in keeping the probe surface temperature at the desired level, and a possible high air outlet temperature. Therefore, water can be used as cooling media along with air. Water and air cooled probes are in most of the cases, used during full-scale measurements when the flue gas temperature is higher (> 800 ^{o}C). These probes are normally designed as double annular tubes and with air flow in the innermost and outermost tube to avoid corrosion problems and to keep the probe surface temperature close to the target temperature. The water flow is normally kept constant, while the air flow is changed based on the target probe surface temperature fluctuations. Andersen [20] used an air and water cooled probe for sampling of deposits during full-scale measurements in a straw and coal fired boiler in the high flue gas temperature region of the boiler. The probe was temperature controlled and it was possible to identify the shedding events of the deposits based on the sudden changes in the probe surface temperature. A schematic of the probe is shown in Figure 3.4 (b).

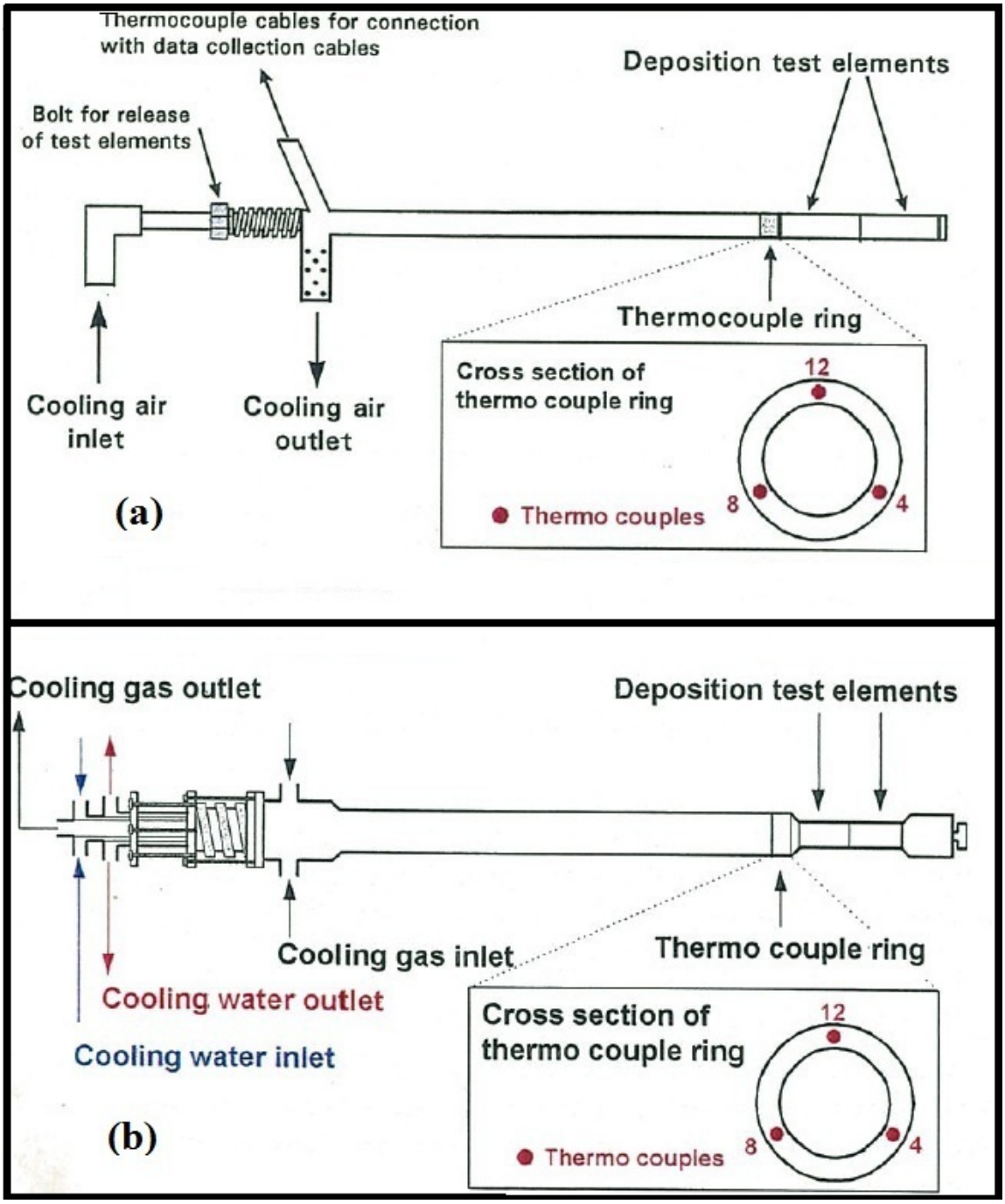

Figure 3. 4: Schematic outline of the air cooled (a) and air-water cooled (b) deposition probe [20].

Ash deposition flux and shedding through surface melting in the high temperature superheater region (near boiler furnace) at a straw grate-fired boiler was investigated by Zbogar et al. [35] using an advanced online ash deposition/shedding probe. It was found that surface melting is the main mechanism of deposit shedding at a flue gas temperatures greater than 1000 ^{o}C. Deposit build-up and shedding at the Avedøre straw grate-fired boiler was investigated by Zhou et al. [33] by using a deposition probe and an artificial sootblowing probe in a lower temperature superheater region nearer to the convective pass at flue gas temperatures between 700 and 800 ^{o}C. The remarkable achievement

of these probes was the simultaneous on-line ash deposition and shedding investigations with video monitoring.

Most of the studies on ash deposition in biomass or in coal-fired power plant are short time probes because of costly extensive measurements.

1.3 Description of the Horizontal Ash Deposition Probe System

1.3.1 Horizontal Ash Deposition Probe

The horizontal deposit probe used during the measurements in the present study was the same as was used by Zhou et al. [33] with minor modifications. Schematic view of the deposition probe system with identified positions of probe temperature measurements, deposition area, port plate for mounting, hinge, load cell and rail for pulling out the probe is shown in Figure 3.5, while a simplified schematic illustration of deposit probe system is shown in Figure 3.6. The probe was made of stainless steel, about 3 m long and having an outer diameter of 40.5 mm. The probe was cooled by water and air, whereby it was possible to determine heat uptake by the probe and keep a stable surface temperature. The probe hung on a hinge connected to a flange. A balance at the rear was used to oppose fluctuations in the boiler and to keep the probe aligned horizontally. A load cell was used to detect the force caused by the mass of the ash deposit on the probe.

A cross-sectional view of the probe perpendicular to the probe axis and cross-sectional view along axis of annuli is shown in Figure 3.7. It can be seen that in each horizontal position of the probe (TC position 1, 2 and 3), four thermocouples provided temperatures at the N, E, S and W positions.

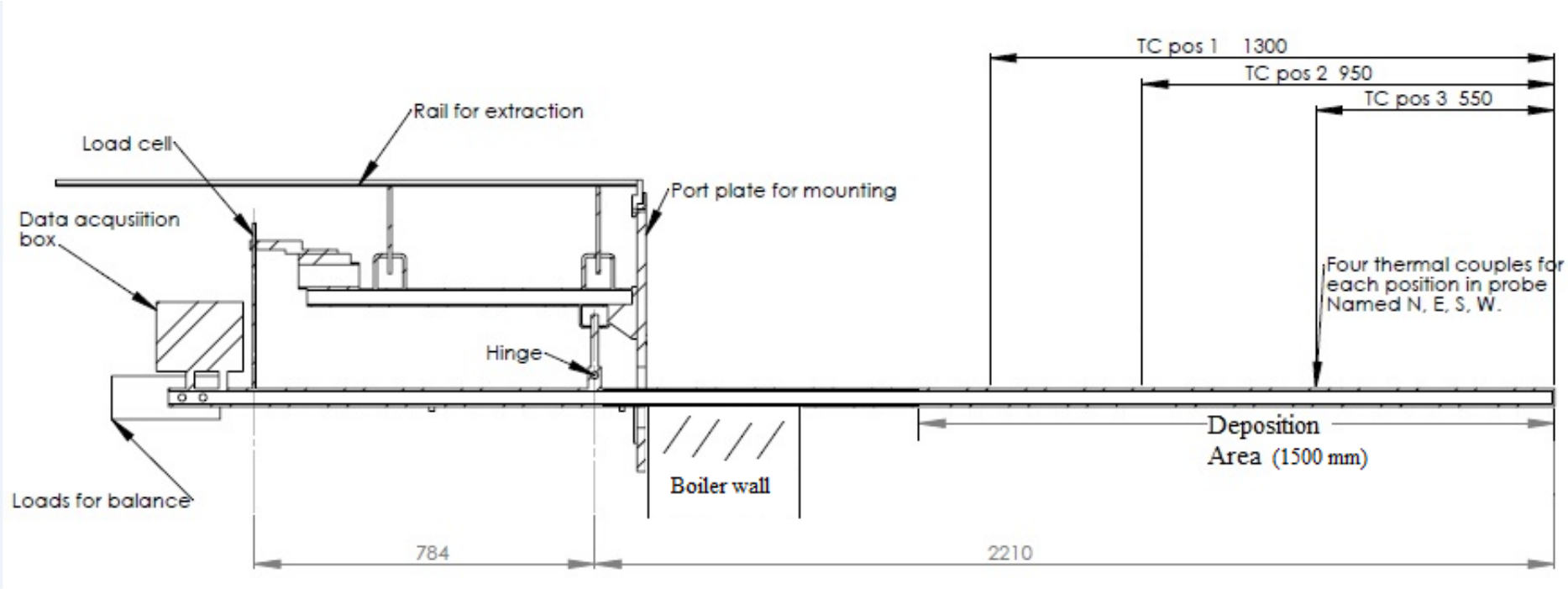

Figure 3. 5: Schematic view of the horizontal probe with identified positions of probe temperature measurements, deposition area, port plate for mounting, hinge, load cell and rail for pulling out the probe.

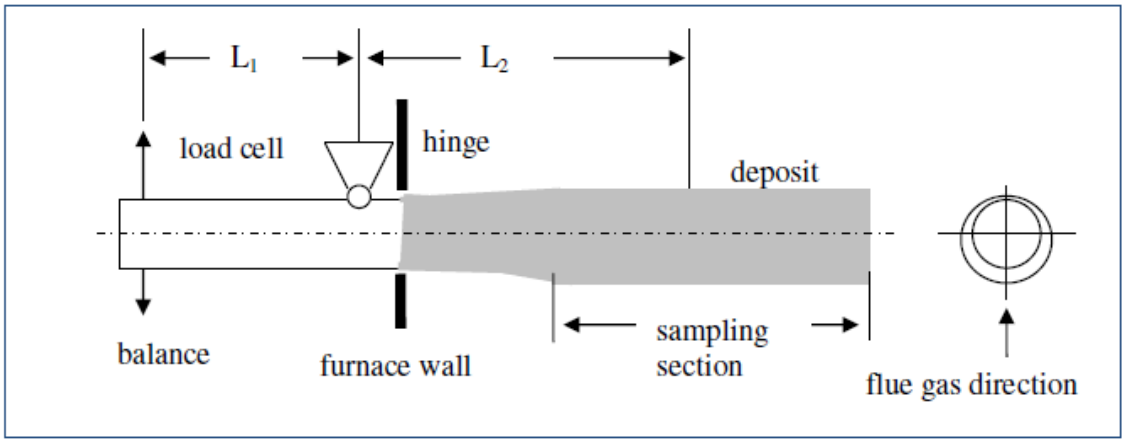

Figure 3. 6: Schematic illustration of the horizontal probe system.

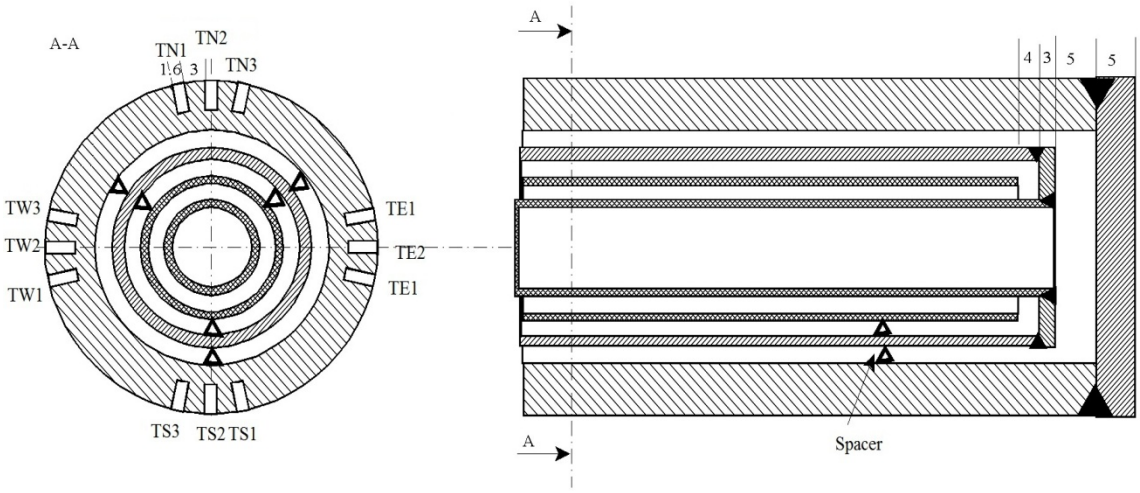

Figure 3. 7: Cross-sectional view perpendicular to probe axis and cross-sectional view along axis of annuli.

1.3.1.1 Quantification of the Deposits Mass Uptake

As shown in Figure 3.5 the length of the effective ash sampling section was approximately 1500 mm, depending on the probe position relative to the boiler inner wall. The ash sampling was determined by the distribution of the deposit thickness along the probe after the probe was removed from the boiler. The thickness of the deposit was quite uniform along the sampling section of the probe. The deposit mass uptake was calculated using the following balance,

$$m_d \cdot g = \left(m_{d,i} - m_{d,f}\right) \cdot g \cdot \frac{L_1}{L_2} \qquad (3.1)$$

where m_d is the deposit mass (g), $m_{d,i}$ is the initial signal of the load cell, $m_{d,f}$ is the final signal of the load cell, g is the gravitational acceleration, and L_1 and L_2 are the distances from

the hinge to the balance and to the mass center of the deposit, respectively. For the used probe: $\frac{L_1}{L_2} = \frac{785}{1460}$, while the definitions of L_1 and L_2 can be seen in Figure 3.6. It is important to mention that the deposit mass is only obtainable if the probe is uniformly caused by the deposit in a reasonable fashion.

1.3.1.2 Quantification of the Probe Heat Uptake

The water and air flow rates are measured by flow meters at the inlets of the probe, and the temperatures of the water and air are measured by 4 thermocouples at the inlets and the outlets. The following heat balance equation was used for heat uptake calculations using steady state assumptions,

$$Q = m_w \cdot C_{p,w} \cdot (T_{w,out} - T_{w,in}) + m_a \cdot C_{p,a} \cdot (T_{a,out} - T_{a,in}) \quad (3.2)$$

where Q is the heat uptake (W), m is the flow rate (kg/s), C_p is the heat capacity (J/Kg.K), T is the temperature (K), and w and a represent water and air, respectively. The corresponding heat flux (W/m^2) would be,

$$q = \frac{Q}{s} \quad (3.3)$$

where s is the effective probe surface area. The selected length for the effective heat transfer surface is 2 m. Here, 2 m is selected because approximately 2 m of the probe was inside the boiler.

1.3.2 Description of the Port Plate

The kind of data needed during the full-scale measurement campaign by using the above mentioned horizontal probe is ash deposit mass uptake, heat uptake by the probe, flue gas temperature measurement by thermocouple and suction pyrometer, and video monitoring. To fulfill these requirements, a special type of port plate was prepared that could be mounted in the inspection whole of the boiler. Schematic drawing of the port plate used during the measurements is shown in Figure 3.8. In the large port, a small port for the deposit probe, a port for the thermo-element, a CCD (charge-coupled device) camera port and a port for the suction pyrometer and artificial sootblowing probe can be seen. A significant effort was made to make each port capable of meeting the experimental results. As an example, a view of the deposition probe system used for the measurements at Amagerværket Unit 1 (AMV1) is shown in Figure 3.9. The angle of the camera was adjusted in a way that maximum area of the deposit

probe could be seen. The CCD camera registered the deposit formation and removal processes on the probe.

The flue gas temperature near the probe was continuously measured, using a simple thermocouple in a protective shell. In addition, a suction pyrometer (International Flame Research Foundation model, IFRF [100]) was also used for some periods during each test.

At the end of each experiment, the probe was carefully taken out of the boiler; the deposits were removed, weighed, and photographed. The pattern and characterization of the deposits were then made based on the deposits visual analysis. The deposits were scratched from the upstream and downstream side of the probe for further detailed analysis. In some of the measurements, on each side of the deposit probe, there were seen more than two deposit layers and the deposits were then characterized based on the structure and thickness of the deposit layers.

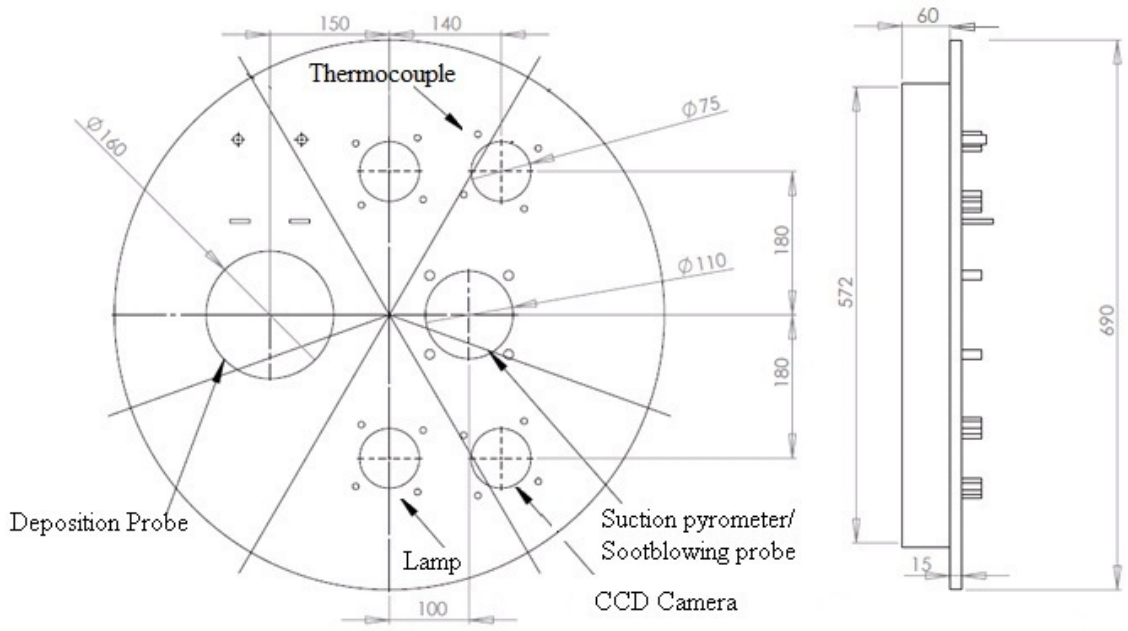

Figure 3. 8: Schematic drawing of the port plate used for measurements conducted using the horizontal probe.

1.3.3 Description of the Artificial Sootblowing Probe

An artificial sootblowing probe with an external diameter of 42.2 mm and a length of 3 m was used for *in situ* removal of deposits. A schematic drawing of the sootblowing probe is shown in Figure 3.10 and the detailed sootblower nozzle drawing can be seen in Figure 3.11. The sootblower probe nozzle was of convergent-divergent shape, and air at a supply pressure of 6.0

bar the jet was fully expanded. The sootblower nozzle was fixed at the end of the probe. The Peak Impact Pressure (PIP) of the nozzle was measured along the axial centerline as a function of the supplying air pressure in the laboratory at room temperature. The PIP of the jet, defined as the centerline stagnation pressure of the jet, was used to characterize the removal of deposits by the sootblowing probe. The measured values of PIP are shown in Figure 3.12 and it is important to notice that these values are measured at room temperature. In the applied range of PIP, there can be a little impact of flue gas temperature on PIP, but the measurement of PIP at temperatures close to the flue gas temperature was not possible. The measured PIP increases with the supplied air pressure, and drops off quickly with the axial distance from the nozzle exit (Figure 3.12).

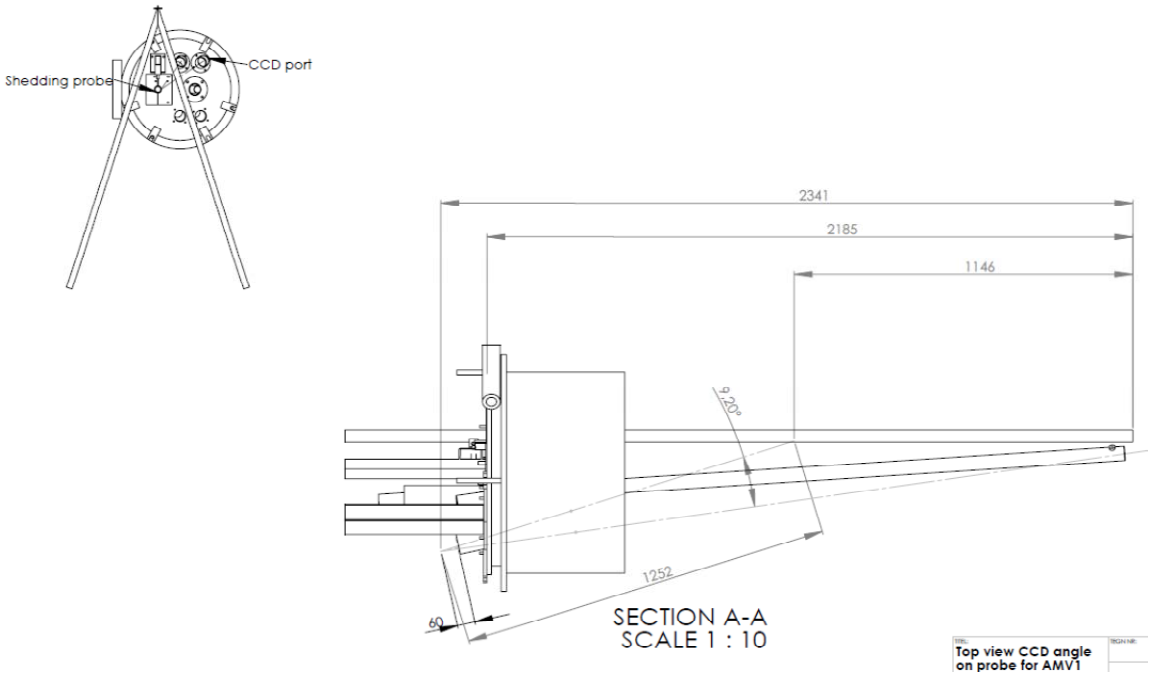

Figure 3. 9: Schematic illustration of the deposition probe system used in the inspection hole at AMV1.

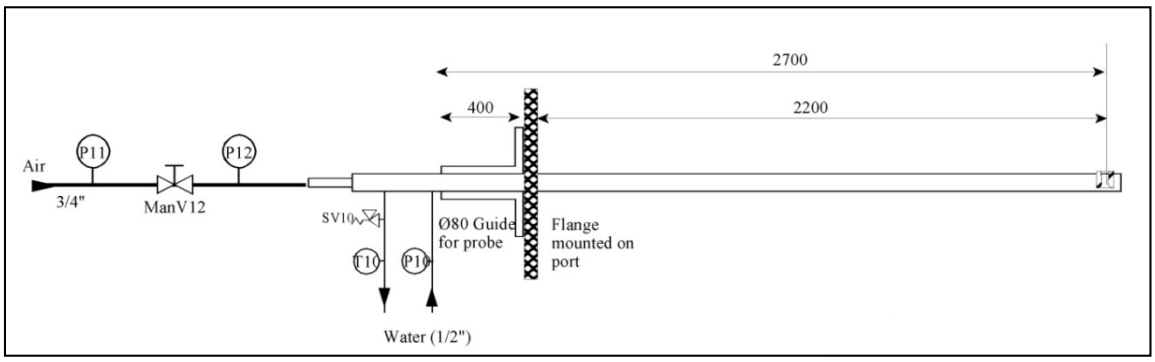

Figure 3. 10: Overall sootblowing probe set up with water and air flow description. (P10, P11 and P12 are pressure gauges for air, P10 is pressure gauge for water (to act a cooling media), while, T10 is temperature indicator.

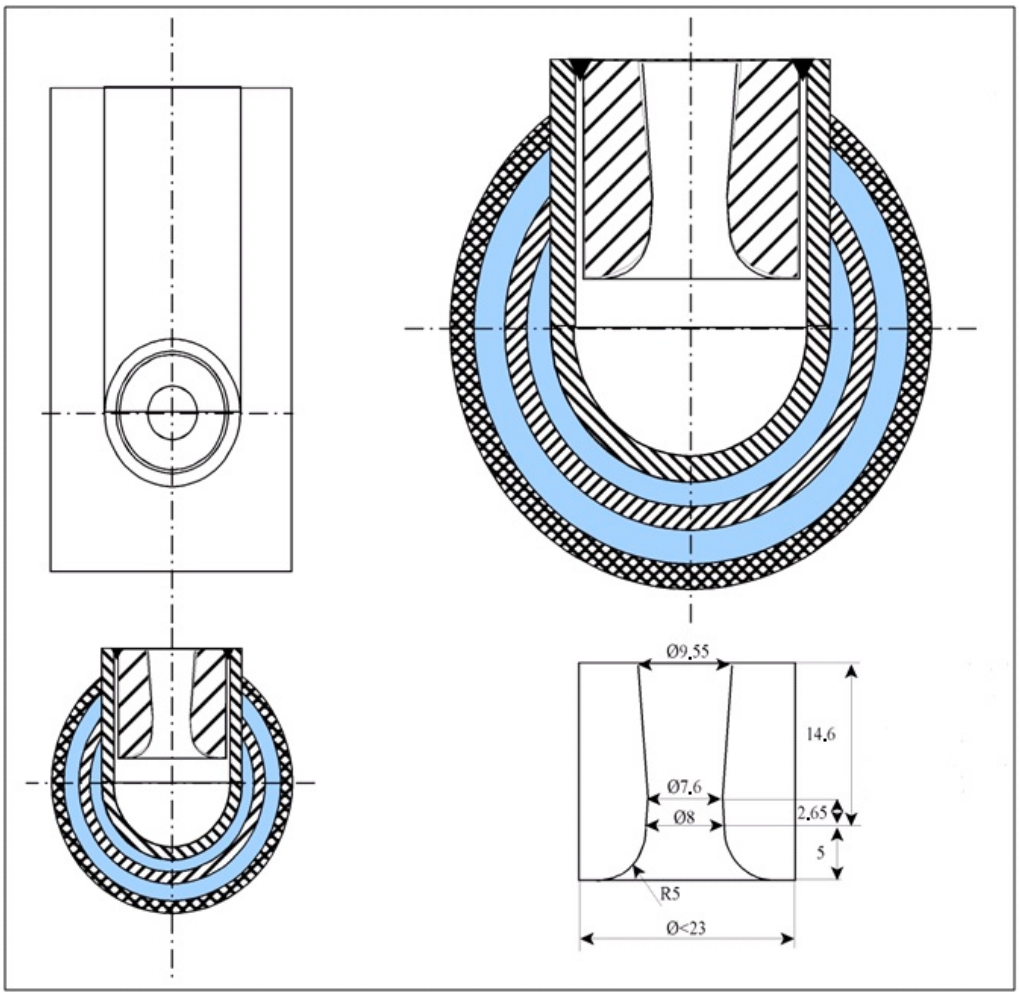

Figure 3. 11: Detailed drawings of the sooblowing nozzle.

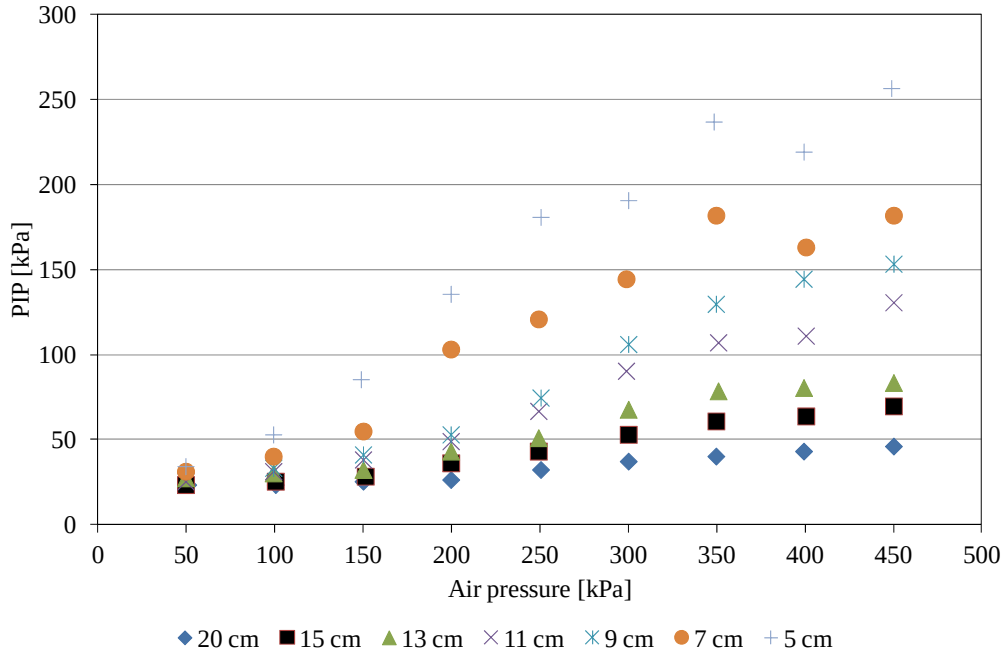

Figure 3. 12: The measured Peak Impact Pressure (PIP) as a function of applied air pressure at varying downstream distance from the nozzle exit at room temperature.

1.4 Design and Development of the Vertical Ash Deposition Probe

It was one of the objectives of the project to investigate ash deposit build-up in the furnace region of the boiler, and a vertical ash deposit probe was therefore designed to simulate the conditions of the boiler furnace wall. Before the start of the design of the probe, heat transfer calculations were performed to calculate the air flow needed to cool the probe, and to identify of the probe dimensions for the only available port at the boiler. The proposed layout of the vertical probe for heat uptake calculations is shown in Figure 3.13.

The overall heat balance equation can be written as,

$$\frac{dQ_{in}}{dL} = \frac{dQ_c}{dL} + \frac{dQ_{rad}}{dL} \tag{3.4}$$

$$dQ_c(r) = h_f (T_{fg} - T_{m,o}) \cdot \pi (r^2 - (r - \Delta r)^2) \tag{3.5}$$

$$\frac{dQ_c}{dr} = h_f (T_{fg} - T_{m,o}) \cdot \pi \cdot 2r \tag{3.6}$$

$$\frac{dQ_c}{dL} = h_f (T_{fg} - T_{m,o}) \cdot \pi \cdot 2(r_o - L) \tag{3.7}$$

$$\frac{dQ_{rad}}{dL} = \varepsilon_{steel} \sigma (T_{fg}{}^4 - T_{m,o}{}^4) \cdot \pi \cdot 2(r_o - L) \tag{3.8}$$

Here ε_{steel} is the emissivity of the metal and σ is the Stephen Boltzmann constant.

$$\frac{dQ_{in}}{dL} = (T_{m,o} - T_{m,i}) \cdot \frac{k_m}{x_1} \cdot \pi \cdot 2(r_o - L) \tag{3.9}$$

Here, x_1 is the metal plate thickness, and k_m is the metal plate thermal conductivity.

$$dT_g \cdot C_{p_{air}} \cdot \dot{m} = dL \cdot \frac{dQ_{in}}{dL} \tag{3.10}$$

$$\int_0^L dT_g = \int_0^L \frac{1}{C_{p_{air}} \cdot \dot{m}} \cdot dQ_{in} \tag{3.11}$$

The boundery conditions are, BC1: at $L = L,\ r = r_o$ and $T_g = T_{g,i}$ (3.12)

BC2: at $L = 0,\ r = r_o - r_1$ (3.13)

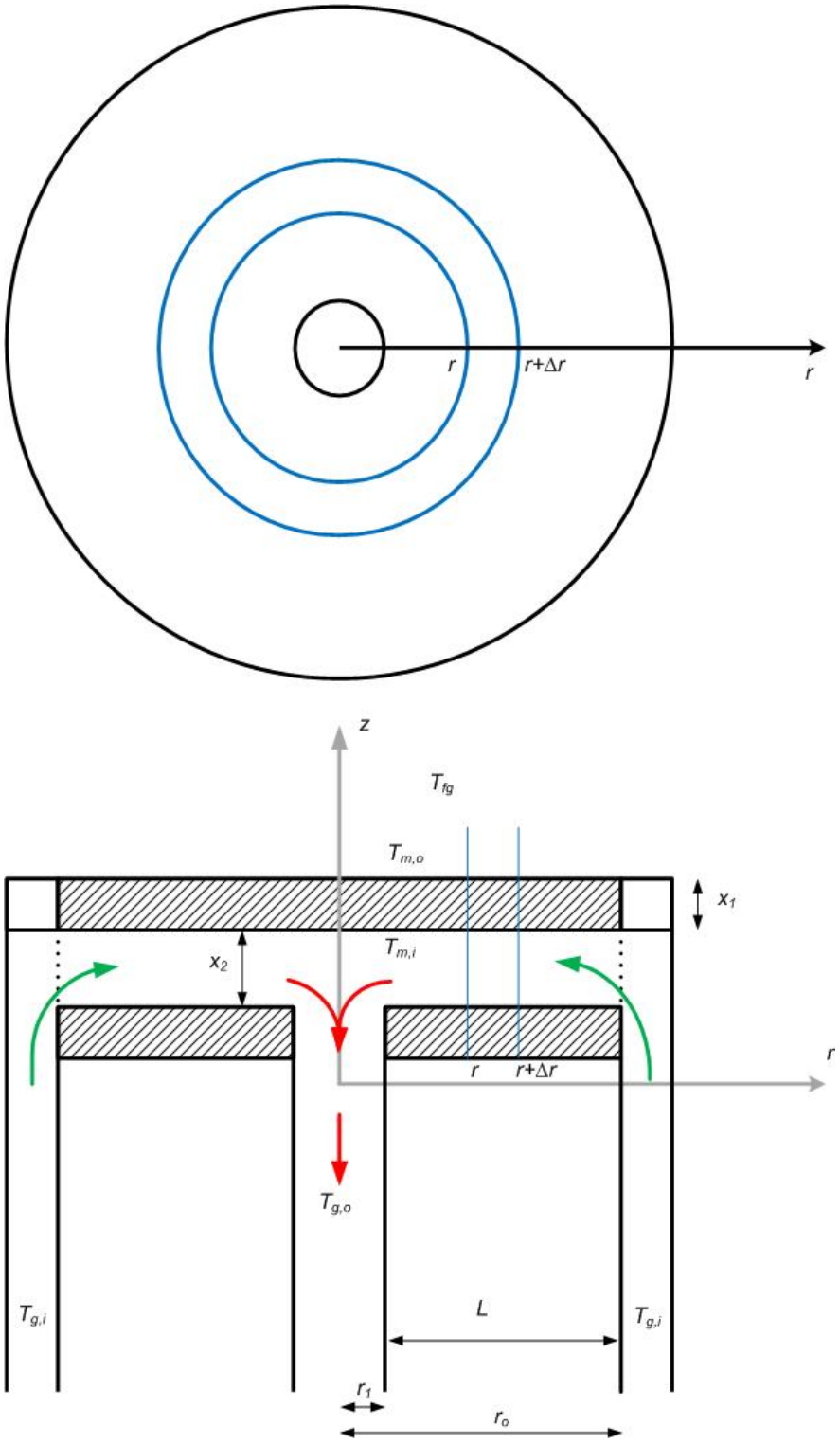

Figure 3. 13: Proposed layout of vertical probe for heat uptake calculations.

The above mentioned set of equations was solved for different sets of inlet air temperature, air velocity and slit thickness. It was found that the deposit temperature and the metal temperature vary insignificantly and even a significant amount of air flow was not able to cool

the probe at the desired temperature range, between 400 and 650 ^{o}C. A typical example of the results of outlet air temperature, deposit temperature and metal temperature is shown in Figure 3.14. The heat transfer calculations revealed that there is need of removable metallic pins to be installed in the metal plate to enhance the heat transfer. In addition, a water chamber was prepared for heat transfer enhancement.

A complete drawing of the vertical probe is shown in Figure 3.15, while the vertical probe with cut and angled view is shown in Figure 3.16. The probe was made of stainless steel, with 130 mm diameter facing the boiler chamber. The probe was cooled by water and air, whereby it was possible to determine heat uptake by the probe and keep a stable surface temperature. The probe hung on a hinge connected to a flange using the same principal of horizontal probe. A load cell was used to detect the force caused by the mass of the ash deposit on the probe. The temperatures measurements were made at 45^{o}, 135^{o}, 225^{o}, 315^{o} position of the probe, while a thermocouple in the middle of the probe was used as the target probe surface temperature as shown in Figure 3.17.

A special type of port plate was prepared that could be mounted at a acoustic pyrometer port at Amager Unit 1 (AMV1). More details of the boiler can be found in Chapter 5. The probe measuring position was about 9 m above the upper row of the burners. In the port plate, a small port for the deposit probe and a port for the thermo-element was made as shown in Figure 3.15. A S-type thermocouple was placed just close to the deposition probe port.

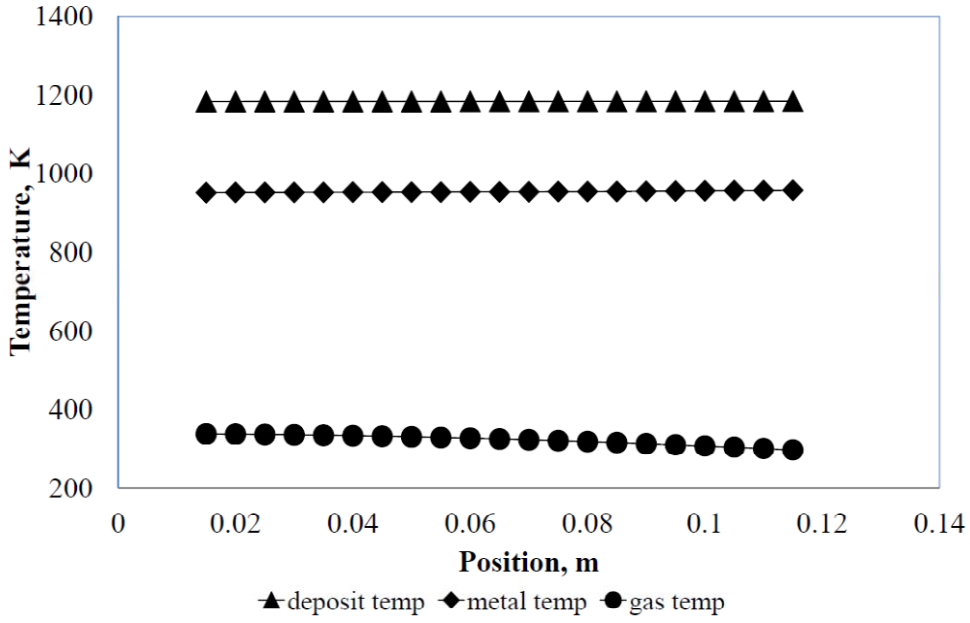

Figure 3. 14: Calculated air and probe metal temperatures.

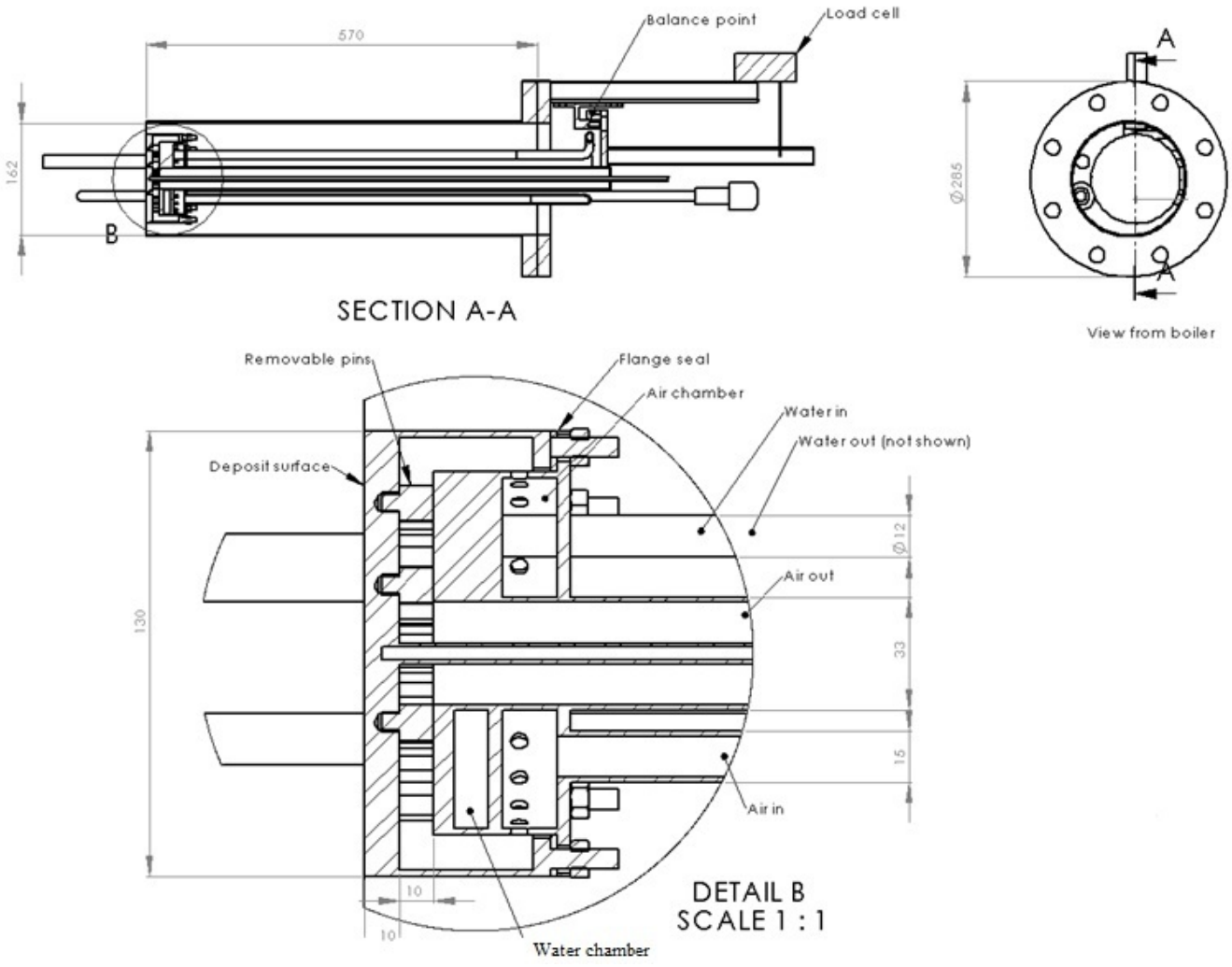

Figure 3. 15: Detailed drawings of the vertical probe system.

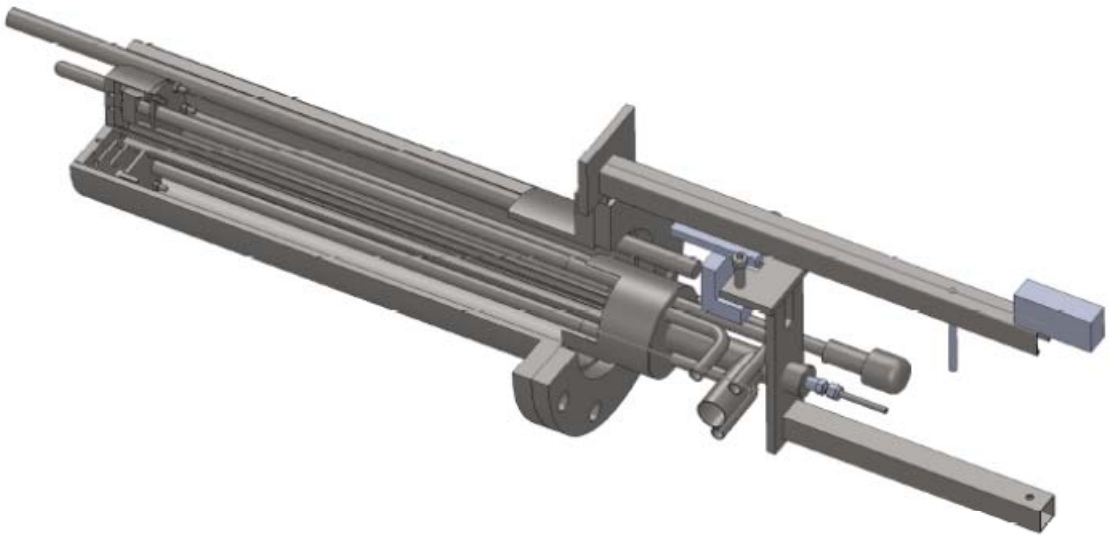

Figure 3. 16: Drawing of the vertical probe with cut and angled view.

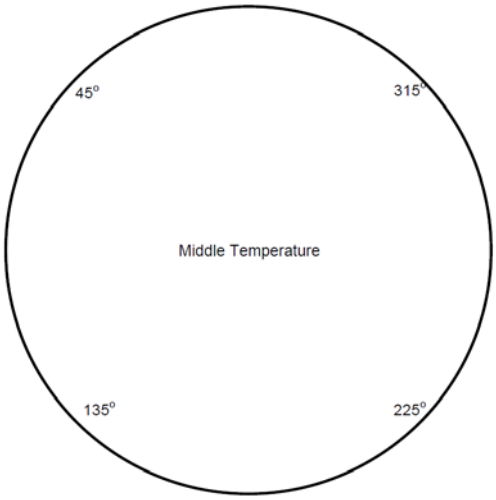

Figure 3. 17: Position of the thermocouples on the vertical probe, seen from boiler to the wall.

The deposit mass uptake and probe heat uptake were calculated by using the same equations used for the horizontal ash deposition probe. An endoscope could potentially be used for video monitory, but a market search revealed that none meeting the current requirements is available. An endoscope that can be used at high flue gas temperatures (1200 ^{o}C) is available, but lacking the ability to look back at the deposition probe.

1.4.1 Commissioning of the Vertical Probe

The vertical probe measurements were conducted at Amager Unit 1 (AMV1). The vertical probe was mounted on the balance point, and goes through a tube into the boiler. The experiments were done by inserting the probe, so that the plate was at level with the boiler wall. The parameters that could be changed were the plate surface temperature and the exposure time. At the end of each experiment,

the probe was carefully taken out of the boiler; the deposits were removed, weighed, and photographed. The pattern and characterization of the deposits was then made based on the deposits visual analysis. A summary of the conducted measurements by using vertical probe is shown in Table 3.1. As the boiler was operating at under-pressure, a pressure difference between the boiler and the outside, forced us to close the gap between the port plate and the deposit probe, in order to stop the air flow. This effectively disabled the mass-uptake measurements by the probe. As explained in the table in most of the measurements conducted the collected amount of the deposits is very small and even an increase in probe surface temperature is not effective in enhancing the deposit mass uptake. However, the set point temperature was held nicely through the commissioning period, which is satisfying, but because of the limitations that only one probe measuring position has to be used, the commissioning phase was ended with partial success. As an example, the results of probe surface temperature measured during test 3 (see Table 3.1) are shown in Figure 3.18. The results seems to be satisfactory in controlling the probe surface temperature at the required levels. The main problem however proved to be the collection of the ash deposits, which, if present, were removed because of the air inlet flow, when the probe was extracted. Covering of the complete set-up with a box could have eliminated the problem of air flow, but that was beyond the time schedule of the Ph.D. project.

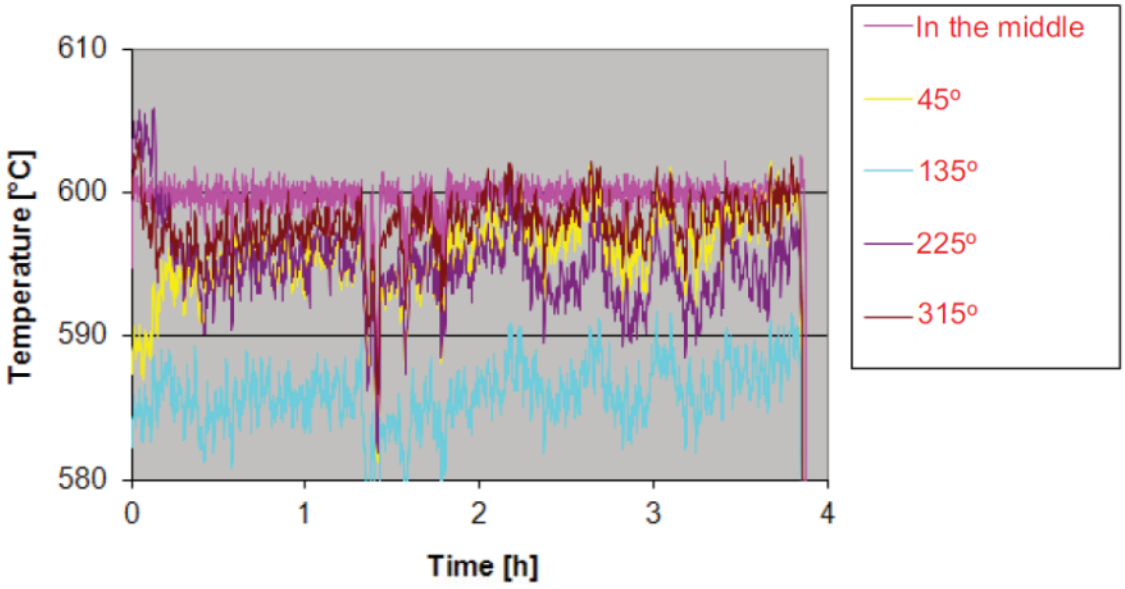

Figure 3. 18: Temperature measurements of thermo-elements attached on the vertical probe. The values shown are for test number 3.

Table 3. 1: Summary of the conducted measurements using vertical probe.

Experiment number	Probe surface tempeature	Exposure time	Results and comments
	^{o}C	H	
1	450	168	Very few deposits on the probe were seen. The probe seems to be corroded. In addition, sealing tape that was used to stop air flow was broken, thereby the experiment was not successful.
2	550	48	Very few deposits on the probe were seen, even though the air inlet was completely sealed. The probe was corroded.
3	600	4	Small layer of deposits was seen on the probe. The probe seems to be corroded.
4	650	24	Some deposits were seen on the probe from the side boiler wall. However these deposits were blown away while taking the probe out of the boiler.

The picture of the probe taken just after an experiment is shown in Figure 3.19. It can be seen that the amount of deposits collected is extremely low.

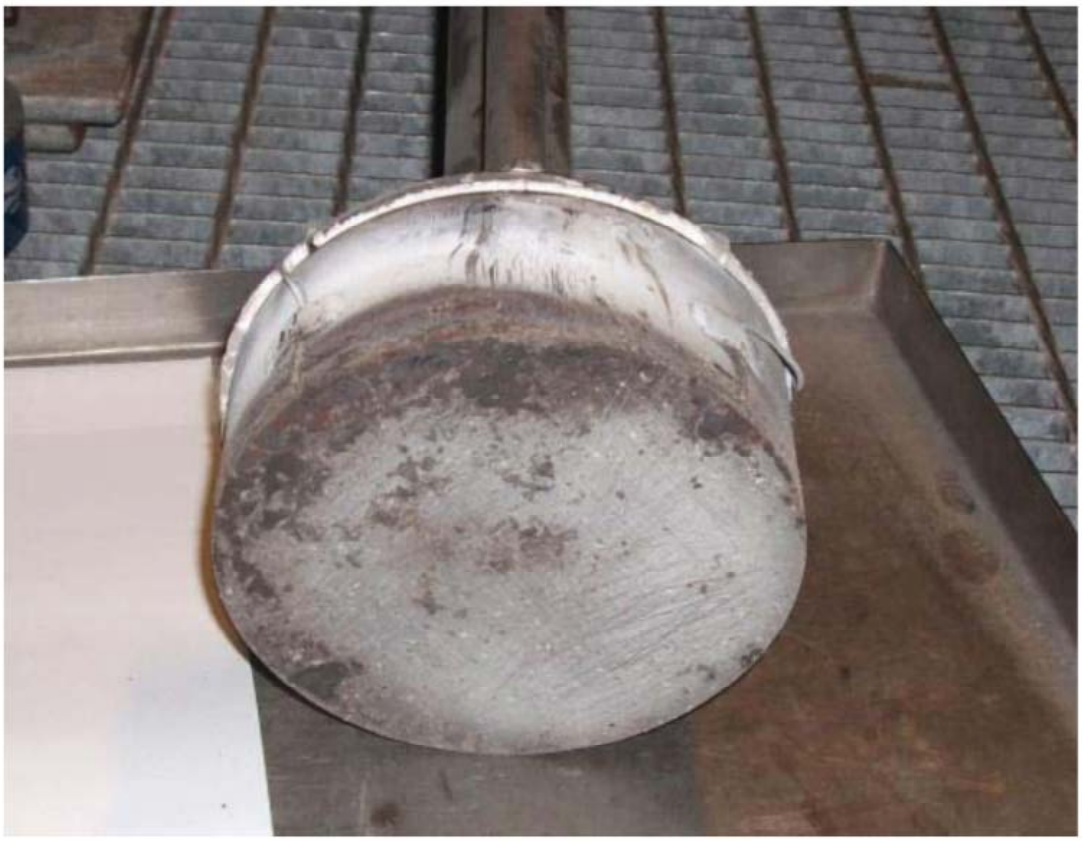

Figure 3. 19: Picture of the vertical probe taken just after finishing an experiment.

1.5 Conclusions

Deposit probes are extensively used to understand ash deposit formation and shedding processes in solid fuel boilers. In most previously conducted ash deposition measurements in biomass grate boilers reasonably simple horizontal water and air cooled tube probes have been used. The quantification of the deposit rate is then done by taking out the probe from the boiler chamber, remove and weighting the collected deposits, and then calculate the deposit formation rate based on the collected weight divided by the probe surface and the probe residence time in the boiler.

The advanced horizontal deposit tube probe used during the measurements in the present study was developed in previous DTU projects, and was only modified with respect to boiler port mounting, and a video camera recording system. The probe can make online data collections of deposit mass and heat uptake. The probe is cooled by water and air, whereby it is possible to determine the heat uptake by the probe and keep a stable surface temperature. The probe was approximately inserted 1.8 meters into the boiler chamber and had a diameter of 40.5 mm. A load cell is used to detect the force caused by the mass of the ash deposit on the probe, and thereby an online signal of the deposit mass is provided. A video camera is used to make video recordings of the deposit formation process, and local registration of flue gas temperature is done by a thermo element or a suction pyrometer. A soot blower probe could be inserted into the boiler chamber along the deposit probe. The sootblower probe can remove deposits on the deposit probe by use of a high pressure air jet. By changing the soot blower probe position and the pressure of air delivered to the probe the peak impact pressure (PIP) of the air jet hitting the deposits could be changed.

It was one of the original objectives of the project to investigate ash deposit build-up on tube walls in the furnace region of a boiler, and a vertical ash deposit probe was therefore designed and constructed to simulate the conditions of the boiler furnace wall. The probe was made as a 130 mm diameter plate facing into the boiler chamber, and could be mounted on a boiler port. The probe was cooled by water and air, whereby it was possible to determine heat uptake by the probe and keep a stable surface temperature. The probe hung on a hinge connected to a flange and a load cell was used to detect the force caused by the mass of the ash deposit on the probe. The vertical probe was tested at the Amager Unit 1 (AMV1) biomass boiler. The experiments were done by inserting the probe, so that the probe plate was at level with the boiler wall. The results were satisfactory with respect to controlling the probe surface temperature at the required levels. A main problem however, proved to be the collection of the ash deposits. The boiler was operated at a sub pressure, and to keep the weighting capability of the probe system a free space between the probe and the port is needed, this caused a high inflow of air, that prevented the deposit formation process. It was tried to seal the space between the probe and the port, and then simply remove the probe after some time, and then collect the accumulated deposits. However, the deposit was removed from the probe surface during the extraction of the probe, because of the high air inlet flow. As a possible solution; covering of the complete set-up with a box could have eliminated the problem with the air flow, but it was decided that resources and time had to be spend on other parts of the project work.

September. 2012, DTU no. 50530

Appendix A3

Journal paper: Ash Transformation and deposit build-up during biomass suspension and grate firing: Full-scale experimental studies. Fuel processing Technology 97 (2012) 93-106.

Energinet.dk project no. 7217

Characterization and quantification of deposits build up and removal in straw suspension fired boilers

Muhammad Shafique Bashir, Peter Arendt Jensen, Flemming Frandsen, Stig Wedel, Kim Dam-Johansen, Johan Wadenbäck, Søren Thaaning Pedersen

Department of Chemical and Biochemical Engineering

Technical University of Denmark

Søltofts Plads, Building 229, DK-2800 Lyngby, Denmark

CHEC no. R1301

Fuel Processing Technology 97 (2012) 93–106

Contents lists available at SciVerse ScienceDirect

Fuel Processing Technology

journal homepage: www.elsevier.com/locate/fuproc

Ash transformation and deposit build-up during biomass suspension and grate firing: Full-scale experimental studies

Muhammad Shafique Bashir [a], Peter Arendt Jensen [a,*], Flemming Frandsen [a], Stig Wedel [a], Kim Dam-Johansen [a], Johan Wadenbäck [b], Søren Thaaning Pedersen [b]

[a] Department of Chemical and Biochemical Engineering, Technical University of Denmark, Building 229, DK-2800, Lyngby, Denmark
[b] Vattenfall A/S, Amager Power Plant, Kraftværksvej 37, DK-2300, Copenhagen S, Denmark

ARTICLE INFO

Article history:
Received 13 September 2011
Received in revised form 17 January 2012
Accepted 18 January 2012
Available online 14 February 2012

Keywords:
Wood
Straw
Fly ash
Deposit formation rate
Grate-fired boiler
Suspension-fired boiler

ABSTRACT

An attractive option for reducing the net CO_2 emissions is to substitute coal with biomass in large power plant boilers. However, the presence of chlorine (Cl) and alkali metals (K, Na) in biomass may induce large operational problems due to ash deposit formation on the superheater tubes. The aim of this study was to investigate ash transformation and deposition behavior in two biomass-fired boilers, firing wheat straw and/or wood. The influence of straw firing technology (grate and suspension) on the ash transformation, deposit formation rate and deposit characteristics has been investigated. Bulk elemental analysis of fly ashes revealed that fly ash from suspension firing of straw has high contents of Si, K and Ca, while fly ash from straw firing on grate was rich in the volatile elements K, Cl and S. Investigations of deposit formation rates were made in the superheater and convective pass regions of the boilers by use of an advanced online deposit probe. During straw firing on grate, the measured deposit formation rate was close to 38 g/m^2/h. Data from straw suspension firing showed a deposit formation rate of 41 g/m^2/h. The deposit formation rates during straw suspension firing and straw grate firing were on similar levels. This was observed even though the concentration of fly ash in the flue gas was significantly higher during straw suspension firing. The influence of co-combustion of wood with straw on deposit formation rate, probe heat uptake and deposit characteristics was also investigated during suspension firing conditions. Data from 35% straw suspension firing with wood showed a deposit formation rate of 33 g/m^2/h for the first 12 h. The deposit formation rate increased to 41 g/m^2/h with 100% straw firing. The probe heat uptake reduction up to 40 h of exposure time was 3.0, 7.3, 8.4 and 16.5 kW/m^2 during 35, 65, 80 and 100% straw firing, respectively.

1. Introduction

Utilization of biomass in large power plant boilers is an efficient method to reduce CO_2 emissions from fossil sources. However, biomass-derived ashes contain substantial amounts of K and Cl, and the use of biomass, especially straw, therefore constitutes a serious technical challenge [1–8]. Combustion of straw induces large operational problems due to ash deposit formation on the superheater tubes [9–13]. Ash deposition may subsequently induce corrosion problems [11–13]. The deposit formation during biomass combustion is a dynamic process, consisting of both deposit build-up [14] and removal (shedding) processes [15,16]. Shedding may be initiated at the surface of the deposit, along the deposit tube interface and inside the deposit depending on fuel and operating conditions and corresponding deposit properties [16].

In Denmark, straw has usually been combusted in grate-fired combined heat and power (CHP) plants. In grate-fired boilers, the fuel is combusted in the bottom part of the furnace chamber on a moving bed. Suspension-fired systems, originally used for coal combustion, have also been considered for biomass combustion. Combustion of straw and/or wood in suspension-fired units is an attractive option because of the often high electrical efficiency of these plants (46–48%), compared to traditional grate-fired systems (25–30%) [13]. However, when biomass is used in suspension-fired boilers, the deposit flux on the superheater tubes is expected to increase. When straw is burned in stoker and grate-fired boilers, the percentage of fly ash entrained is typically 10–30%, while 80–90% is entrained during suspension firing [5]. Vattenfall A/S in Copenhagen retrofitted a suspension-fired boiler at the Amager Power Station (Amagerværket, Unit 2), from coal to straw, but experienced some fouling and slagging problems in the superheater regions and furnace walls.

Some full-scale experimental studies on ash deposition in biomass-fired boilers have been reported based on measurements in grate boilers [13,15,18–20]. Only limited data is available from biomass suspension firing where improved knowledge on ash transformation and transient deposit formation is needed to optimize design and operation [13,14,17,21]. Pilot-scale suspension-fired investigations by Nordgren et al. [17] and Theis et al. [22] indicate reduced deposit formation rate by co-firing straw with woody biomass and co-firing straw with peat,

* Corresponding author. Tel.: +45 45252849; fax: +45 45882258.
E-mail address: paj@kt.dtu.dk (P.A. Jensen).

0378-3820/$ – see front matter
doi:10.1016/j.fuproc.2012.01.018

respectively. However, full-scale studies on 100% straw and wood suspension firing are rare to find except the investigations made by Tobiasen et al. [23] and Skrifvars et al. [24]. Therefore, further full-scale boiler deposit studies of straw suspension firing with wood will be useful to optimize the boiler operation and to improve our understanding of the ash deposit formation process.

The aim of this study was to investigate ash transformation and deposition behavior in two biomass-fired boilers, firing wheat straw and/or wood. The influence of straw firing technology (grate and suspension) on the ash transformation, deposit formation rate and deposit characteristics has been investigated. Full-scale measurements of ash deposition were made in the superheater and convective pass regions of Unit 2 at the Amager Power Station (straw and/or wood suspension-fired, AMV2) and Unit 2 at the Avedøre Power Station (straw grate-fired, AVV2). The measurements were conducted by use of an advanced online ash deposition probe. The composition of fuel and fly ash was analyzed, and straw ash transformation in suspension and grate firing conditions was investigated. The influence of co-combustion of wood with straw on deposit formation rate, probe heat uptake and deposit characteristics was also investigated during suspension firing conditions.

2. Equipments, materials and methods

2.1. Boilers

The probe measurements were conducted at Amager Power Station, Unit 2 (AMV2), firing biomass (wheat straw and/or wood) in suspension. A brief comparison has been made between the AMV2 data and data obtained from probe measurements conducted at the Avedøre Power Station, Unit 2 (AVV2), firing straw on a grate.

AMV2 was previously a coal-fired suspension drum-type boiler. It was retrofitted in 2003 to use pure pulverized biomass fuel with different shares of straw and wood. AMV2 is a 250 MW_{th} front wall-fired boiler with 12 burners at three levels with a maximum overall capacity of 57 t/h biomass. The boiler capacity was reduced to ~70% when it was retrofitted from pulverized coal to straw [25]. Tobiasen et al. [23] and Berg et al. [25] mentioned that certain changes in the boiler systems were made in order to make the boiler capable of firing biomass. The solid fuel grinding mills (old coal mills, roller mills) were re-used with modifications, and also the fuel pipes and the low-NO_x coal/oil-burners were re-used [25]. In the burners, the outer part of the primary air tube with flame holder was shortened in order to obtain an earlier mixing of inert primary air/fuel and secondary combustion air in the burner opening [25].

Measurements at AMV2 were conducted from February to April during the district heating season. A schematic drawing of the boiler is shown in Fig. 1(a). Probe measurements were conducted at position 1 in the superheater region (SH, 1st Pass) and position 2 in the tube bank region (TB, 2nd Pass). Previous experiences at AMV2 have shown that when straw is fired, significant ash deposition occurred on the superheater tubes and furnace walls, which made it necessary to manually clean the boiler at regular intervals. The maximum operation period on 100% straw was limited to approximately two weeks due to severe ash deposition on the superheaters that have insufficient distance between them (113 mm) [23,25]. Cleaning of the boiler was only possible during complete shutdown, leading to long periods without heat/power production and significant cleaning costs [23,25]. The probe measurement positions used are shown in Fig. 2 before and after manual cleaning, showing significant ash deposition in the superheater region and possible obstruction of the flue gas flow. A more elaborative drawing of the boiler including the probe measuring positions is shown in Fig. 3.

The composition of the fuels fired at the boiler is shown in Table 1, while some of the combustion variables, boiler load, excess air ratio, flue gas flow and calculated gas velocity for the tests at AMV2 are shown in Table 2.

AVV2 is a dedicated straw-fired vibrating grate boiler with a thermal capacity of 105 MW_{th}, corresponding to 26 t/h of straw. A schematic drawing of the boiler and probe measuring position is shown in Fig. 1(b). More details about the boiler can be found in previously published papers [13,15,19].

Table 1
Composition of fuels fired during the measurements.

Analysis	Straw (AVV2)	Straw (AMV2)	Wood (AMV2)
Proximate analysis			
Moisture (wt.%, a.r.)	10.20	7.40	9.45
Ash (wt.%, d.b.)	4.70	5.90	3.30
Volatiles (wt.%, d.b.)	76.60	75.50	79.50
MJ/kg: a.r.	–	16.00	16.65
Ultimate analysis (wt.%, d.b.)			
C	47.23	45.00	49.10
H	6.34	5.90	6.20
N	0.406	0.630	0.130
S	0.090	0.088	0.018
Si	1.100	1.357	0.750
Al	0.0084	0.0277	0.0510
Ca	0.34	0.43	0.20
Fe	0.0077	0.0460	0.0340
K	0.920	0.826	0.087
Na	0.024	0.0944	0.029
Cl	0.358	0.398	0.010
Mg	0.065	0.065	0.031

2.2. Ash deposition probe

A schematic of the applied deposit probe is shown in Fig. 4. The probe was made of stainless steel, about 3 m long and having an outer diameter of 40.5 mm. The probe was cooled by water and air, whereby it was possible to determine heat uptake by the probe and keep a stable surface temperature. The probe hung on a hinge connected to a flange. A balance at the rear was used to oppose fluctuations in the boiler and to keep the probe aligned horizontally. A load cell was used to detect variations of the force caused by the mass of the ash deposit on the probe. In total, 12 thermocouples were placed inside the outer probe metal tube; four thermoelements at three different horizontal positions. In each horizontal position (1, 2 and 3), the four thermocouples provided temperatures at the N, E, S and W positions (Fig. 4(b)). In some of the measurements, a CCD (charge-coupled device) camera registered the deposit formation and removal processes on the probe. The flue gas temperature near the probe was continuously measured, using a simple thermocouple in a protective shell. Additionally, a suction pyrometer (International Flame Research Foundation model, IFRF [26]) was also used for some periods in order to confirm the accuracy of the thermocouple flue gas temperature measurements.

2.3. Fuels

The analysis of the fuels fired during the measurements is shown in Table 1. It is seen that straw fuels contain a higher amount of ash than wood. Fuel analysis also shows that the straw fuel is rich in Si, K and Cl, compared to the wood fuel. The slight difference in the fuel analysis of straw from AVV2 and straw from AMV2 is possibly due to seasonal variations (rain and time of harvesting).

2.4. Procedure of experiments

A series of probe measurements were conducted at AMV2 in the superheater region with 35, 65, 80 and 100% straw shares mixed with wood. Each measurement lasted 3–5 days. The probe surface temperature was fixed to 500 °C in all the measurements in order to simulate typical superheater tubes in a biomass-fired boiler [19,23]. A single test was conducted in the tube bank region when firing Wood pellets (Fig. 1(a)). Both tests at AVV2 were conducted in the convective pass

Table 2
Overall comparison of conducted measurements at AMV2 and AVV2 in terms of deposit formation rate, probe heat uptake and deposit characteristics. The flue gas temperature for the first four tests at AMV2 is the thermocouple temperature plus 160 °C. SH: superheater, TB: tube bank.

Boiler	AMV2 (suspension)					AVV2 (grate)	
Location (test no.)	SH (1)	SH (3)	SH (2)	SH (4)	TB (5)	SH (1)	SH (2)
Exposure time (h)	90	72	124	76	24	743	72
Probe metal temperature (°C)	500	500	500	500	500	500	500
Straw (% mass basis)	35	65	80	100	0	100	100
Wood (% mass basis)	65	35	20	0	100	0	0
Mean boiler load (%)	46.1	62.9	50.4	53.4	51.8	85–95	90–95
Mean flue gas temperature (°C)	848	820	849	837	581	770	785
Excess air ratio (λ)	2.20	2.19	2.19	2.26	2.20	–	–
Flue gas flow (N m^3/s)	309.8	395.4	319.2	336.5	275.6	–	–
Bulk gas velocity (m/s), calculated	4.30	5.49	4.43	4.67	3.83	7.05[a]	–
Net plant sootblowing frequency (1/h)	0.85	–	0.92	1.10	–	–	–
Deposit formation rate, (g/m^2/h), 12 h	33.0	–	33.0	41.0	~1.0	36.8[b]	38.0[c]
(Mean flue gas temperature, 12 h)	(856)		(863)	(848)	(586)	(760–800)	(775–809)
Deposit mass uptake (g/m^2)							
Initial (2 h)	105	150[d]	198	707	3	810[b]	80[e]
After 40 h	516	1274[f]	280	2610	–	~3390[g]	1860[h]
Final (2 h)	1041	1475	1520	1670	–	~4050	~2440
Heat uptake (kW/m^2)							
Initial (2 h)	32.2	29.4[d]	32.9	37.1	12.4	40.3[b]	40.6[e]
After 40 h	29.2	22.1[f]	24.5	20.6	–	30.0[g]	27.0[h]
(Heat uptake reduction)	(3.0)	(7.3)	(8.4)	(16.5)		(10.3)	(13.6)
Final (2 h)	23.3	23.1	21.3	28.3	10.2	19.0	28.7
Number of deposit layers							
Upstream side	2	3	3	3	2	3	2
Downstream side	1	2	2	2	1	2	2
Mean deposit thickness (mm)							
Upstream side	~5	~20	~25	~25	~3	10–30	~6
Downstream side	~2	~3	~5	~5	~1	~6	~2

[a] Measured.
[b] 22 h.
[c] 27 h.
[d] 1.2 h.
[e] 2.1 h.
[f] 45 h.
[g] 47.3 h.
[h] 49 h.

region nearer to the first superheater (Fig. 1(b)). The influence of straw-firing technology (grate and suspension) on the ash transformation, deposit formation rate and deposit characteristics has been investigated by comparison of results from the two boilers. A summary of the main experimental conditions is shown in Table 2. At AMV2, in the areas where the probe was mounted the mean flue gas temperature was in the range of 580–850 °C and the mean calculated flue gas velocity was in the range of 3.83–5.49 m/s. At AVV2, the mean flue gas temperature was in the range of 770–785 °C and the measured flue gas velocity was 7.05 m/s during test 1.

The overall boiler load during the measuring campaigns at AMV2 is shown in Fig. 5. Full load at AMV2 corresponds to 57 t/h of straw. It can be seen that AMV2 was shut down after some days. The overall boiler load was between 85 and 95% during the measurements at AVV2. Full load at AVV2 corresponds to 26 t/h of straw.

3. Results and discussion

Main combustion variables during the probe tests such as fuel mixture, flue gas temperature, and excess air ratio are shown in Table 2. The flue gas temperature near the probe was continuously measured, using a simple thermocouple in a protective shell. In the superheater area of AMV2, the suction pyrometer typically registered a 150–160 °C higher flue gas temperature than the thermocouple. This temperature difference was probably due to strong radiation effects in the boiler.

Retractable steam sootblowers were used for 2–5 min during boiler operation; typically after regular intervals (40–45 min) during measurements at AMV2 (tests 1–4). Sometimes the sootblowers were completely stopped for a couple of hours. The sootblower located nearest to the probe measuring position was shut down during the measurements, while sootblowers located about 4 m below the measurement position, and in the front wall of the measurement position were still in operation. The mean sootblowing frequency during the tests at AMV2 is shown in Table 2. Sootblower operation caused significant fluctuations in the air flow used to keep the probe temperature constant at 500 °C and corresponding changes in the probe heat uptake signal. When plant sootblowers were in operation, some fluctuations in the deposit mass uptake signal were also prominent.

3.1. 100% straw and wood firing in suspension at AMV2

Examples of probe measuring results of 100% straw and wood firing at AMV2 are shown in Fig. 6. The local flue gas temperature, deposit mass uptake and probe heat uptake measured during 100% straw firing are shown in Fig. 6(a). Some fluctuations in the deposit mass uptake and probe heat uptake signals were induced by a poor control of the probe air supply particularly when plant sootblowers were in operation. However, by showing average values over 1000 s, those short time fluctuations are leveled out. The boiler was running at a load of 53.4% during the test. The flue gas temperature shown in Fig. 6(a) is the thermocouple temperature plus 160 °C (the typical difference in temperature readings during the measurements with suction pyrometer and thermocouple). The registration of the deposit mass uptake signals showed an average amount of 707 g/m^2 of deposits that were collected on the probe in the initial 2 h. The deposit mass increases gradually through the first 40 h and during the 40–43-hour period, the deposit mass increased to more

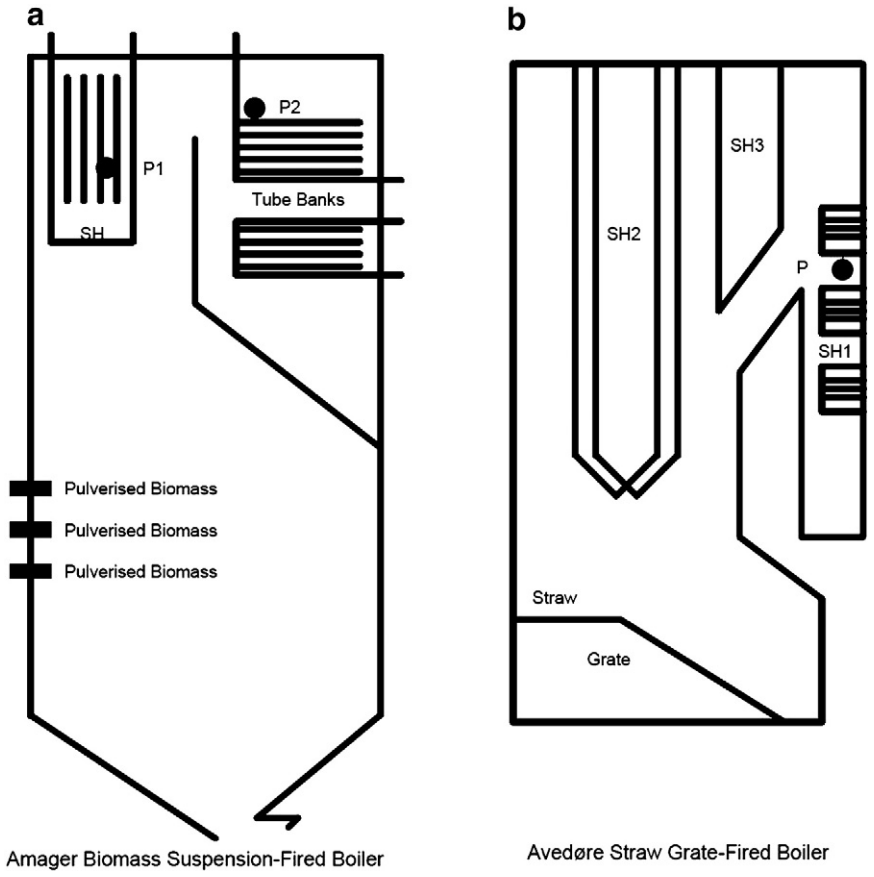

Fig. 1. Schematic view of boilers. The locations of the probe measuring positions (P1, P2) at AMV2 (a) and probe position (P) at AVV2 (b) are identified. SH stands for superheater.

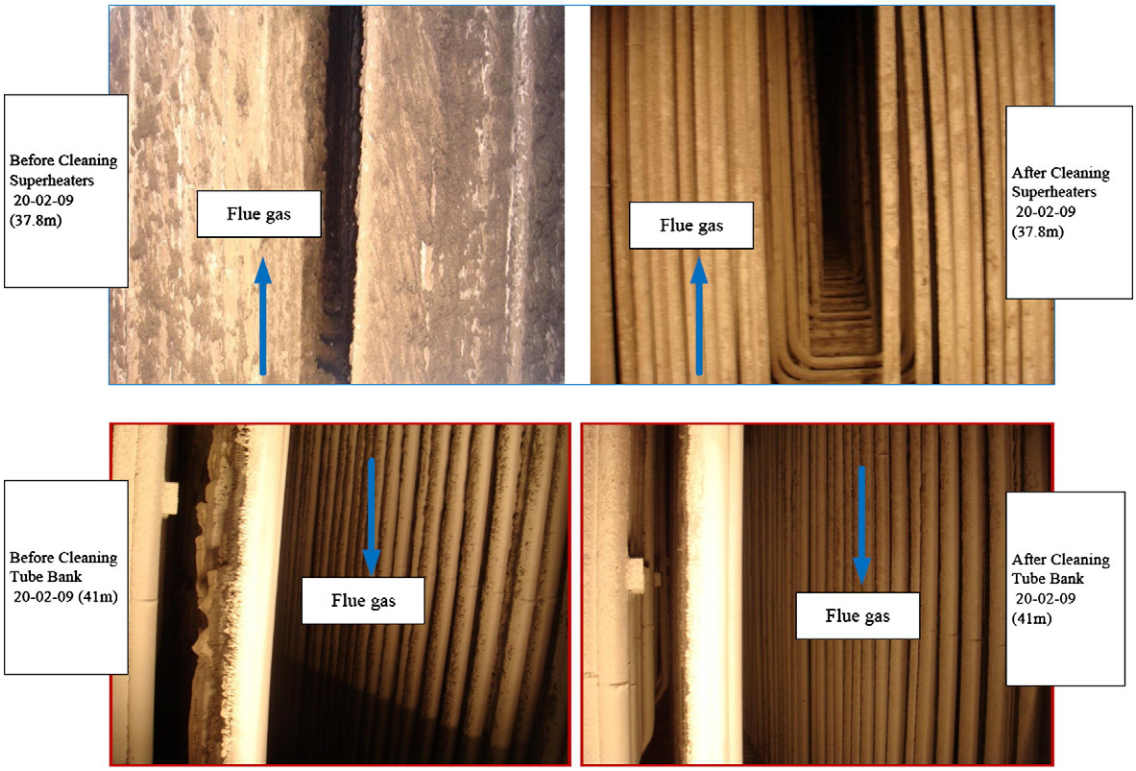

Fig. 2. Images of the probe measurement positions before and after manual cleaning during 100% straw firing at AMV2. The upper image is from the superheater region (SH, 37.8 m stands for probe measuring position) and the bottom image is from the tube bank region (TB, 41 m stands for probe measuring position). It can be seen that severe ash deposition has clogged the superheater tubes.

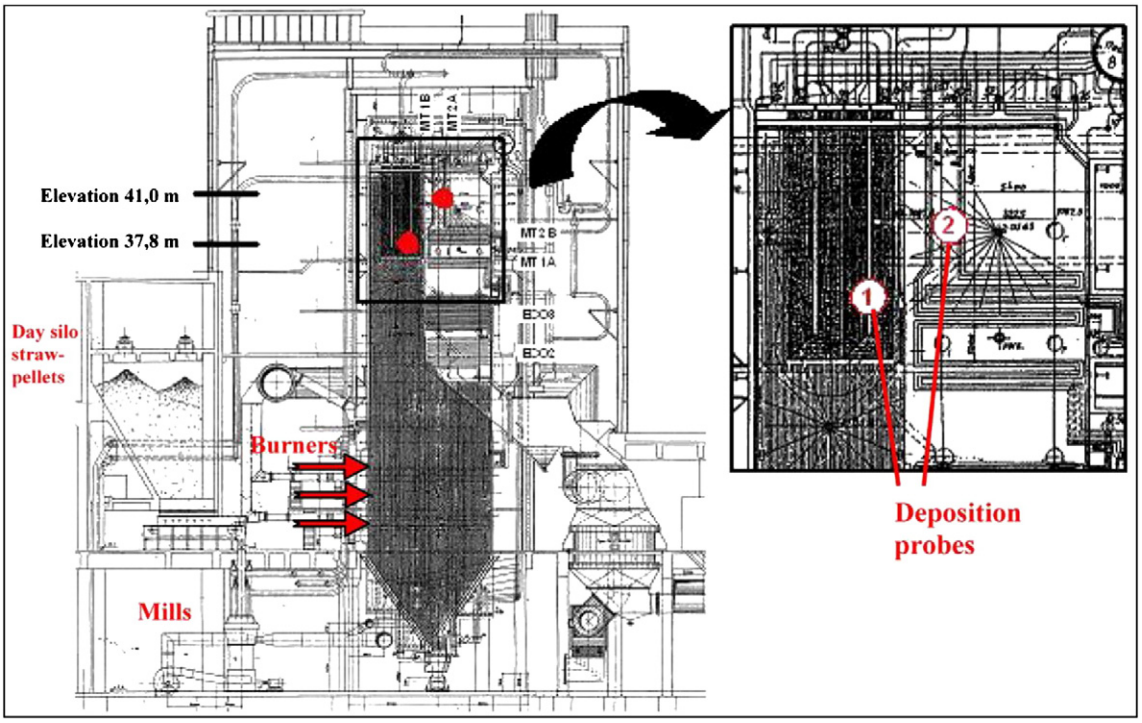

Fig. 3. Schematic view of AMV2 boiler with identification of silos, mills, burners and deposition probe measuring positions. Modified from Ref. [23].

than 3200 g/m^2. After a peak in the flue gas temperature, there was a steep reduction in the deposit mass due to removal of a complete layer of deposits. For the rest of the measurement, the deposit mass uptake signal remained between 1500 and 2000 g/m^2. The probe heat uptake decreases continuously to a level of 20 kW/m^2 during the first 28 h. The probe heat uptake stays at that level for the next 20 h, whereafter it fluctuates around that level possibly due to flue gas temperature fluctuations. After the test was finished, the probe was removed from the boiler chamber and deposit samples from the probe surface were collected. Deposits obtained after the 100% straw firing test were sintered and adhered strongly to the probe.

A single measurement in the tube bank region (Position 2, Fig. 1(a)) was conducted with 100% wood firing. Measurement results are shown in Fig. 6(b). The mean flue gas temperature was 581 °C during this test. The deposit mass uptake signal fluctuates around zero, indicating only intermittent adhesion of a powdery ash deposit to the probe. The probe heat uptake during this measurement is nearly constant for long periods, where it stays just below10 kW/m^2.

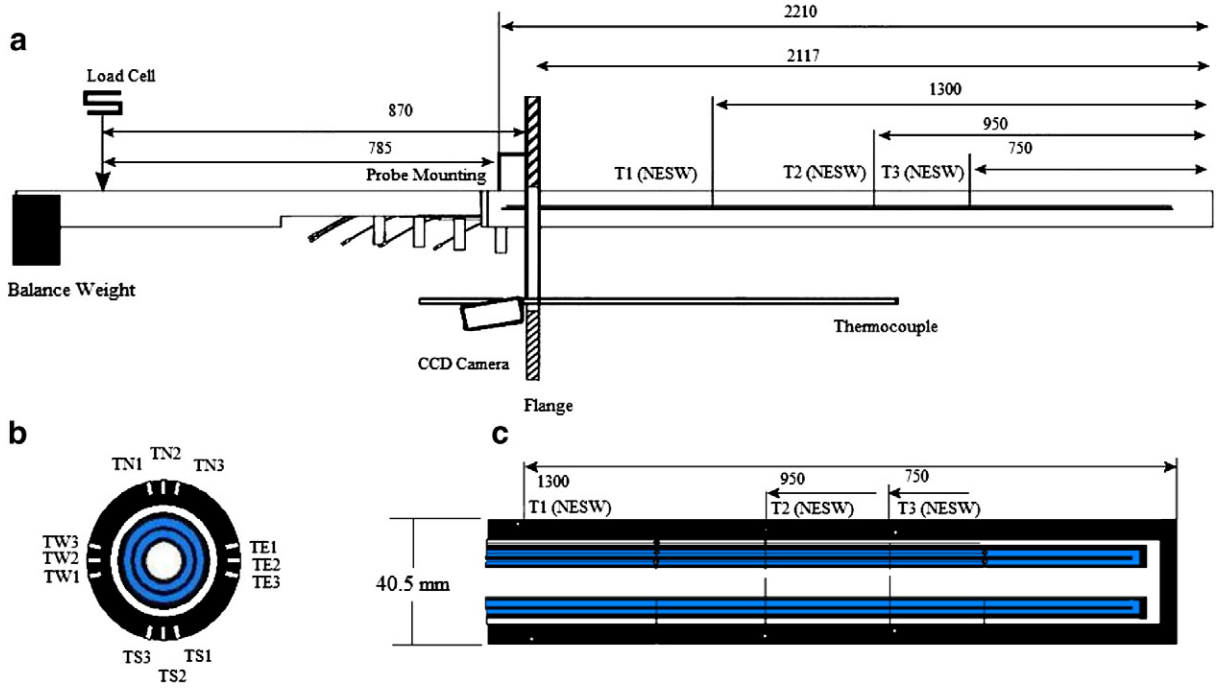

Fig. 4. Schematic presentation of the ash deposition probe, a) overall schematic view of the probe, b) cross-sectional view perpendicular to probe axis, c) cross-sectional view along axis of annuli.

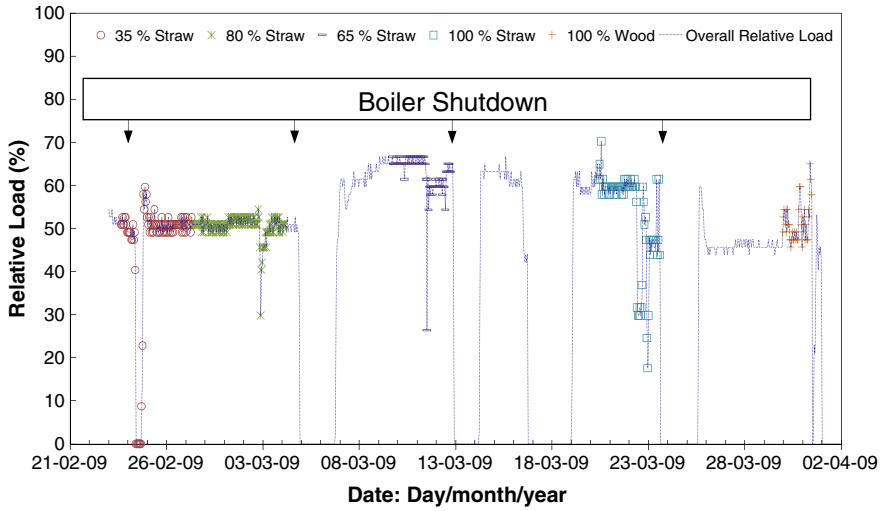

Fig. 5. Percentage of applied boiler load during each measurement at AMV2 and boiler shutdown incidents.

3.2. Comparison of full-scale measurements

Comparison of the results regarding the probe exposure time, mean boiler load, flue gas temperature, bulk gas velocity, deposit mass uptake, probe heat uptake, and deposit characteristics is shown in Table 2. The first four out of five measurements at AMV2 were made in the superheater (SH) region, while the last measurement was conducted in the tube bank (TB) region. Both measurements at AVV2 were conducted in the convective pass region nearer the first superheater. During test 1 (35% straw firing) at AMV2, the deposit formation rate was 33 g/m^2/h for the first 12 h. The deposit formation rate increased to 41 g/m^2/h when 100% straw was fired. The deposit formation rate in the tube bank region (test 5) during 100% wood suspension firing was extremely small (~1 g/m^2/h). It can also be seen that the deposit formation rate and primarily the initial deposit mass uptake (average for 2 h) increase when 100% straw was fired (Table 2). Decreased deposit formation rates have been observed by Nordgren et al. [17] and Lokare et al. [28] by introducing different biomass fuels with decreasing straw contents during pilot-scale suspension-fired investigations. This is possibly due to ash dilution effects and/or chemical interactions [17,28]. Another possible reason could be that a larger amount of condensed KCl (from straw) can possibly increase the contact area between particles, and when in contact with the probe surface, strengthen the bonding of the deposit on the superheater tube. During both tests at AVV2, the deposit formation rate was similar and close to 38 g/m^2/h in the initial 22–27 h.

The reduction in the probe heat uptake up to 40 h of exposure time at AMV2 increases with increasing straw share (see Table 2). The probe heat uptake reduction up to 40 h of exposure time was 3.0, 7.3, 8.4 and 16.5 kW/m^2 during 35, 65, 80 and 100% straw firing, respectively. The probe heat uptake reduction during straw-grate firing was 10.3 and 13.6 kW/m^2 for test 1 and test 2 at AVV2, respectively. The data shown in Table 2 indicate generally a moderate increase in deposit formation rate and heat uptake reduction (up to 40 h) with increased straw share. However, the data show also some fluctuations that are possible during full-scale measurements because of the associated difficulties to keep all parameters reasonably constant.

A comparison of previous full-scale deposit probe measurements made at different straw-fired boilers and the current measurements is shown in Table 3 and Fig. 7. The boiler types, combustion variables such as fuel type and local flue gas temperature, probe surface temperature, and the measured deposit formation rates are shown in Table 3. The data points in Fig. 7, even those at approximately the same conditions, have a large spread, which is a result of the difficulties of keeping all operational parameters constant during full-scale measurements. However, within the range of deposit formation rates from 1 to 160 g/m^2/h, the following reasonably systematic tendencies can be observed.

- A tendency to increased deposit formation rate with an increase in flue gas temperature is observed. At a flue gas temperature of 650 °C, the deposit formation rate is typically from 5 to 30 g/m^2/h and at 900 °C, the deposit formation rate is typically 20 to 110 g/m^2/h. At higher fuel alkali contents (K > 0.9 wt.%, yellow and red points), the increase in deposit formation rate with flue gas temperature is steeper compared to the increase in the deposit formation rate at lower fuel alkali contents (K ≤ 0.9 wt.%, violet and black points). Increased flue gas temperatures probably increase the fraction of molten ash as well as provide an increased content of gas phase alkali species, and both will lead to an increased deposit formation rate.
- Most of the deposit measurements were conducted with probe surface temperature in the range from 480 to 550 °C (all marked green in Fig. 7(b)) and a few were conducted with lower (400 °C) or higher temperatures (650 °C). It can be seen that changed probe surface temperatures in the range from 400 to 650 °C do not seem to significantly influence the deposit formation rate.
- The deposit formation rates during straw firing in suspension and grate boilers are on similar levels as indicated by points 1–33 (grate, square symbols) and 34–38 (suspension, triangular symbols) in Fig. 7(a). This is observed even though the concentration of fly ash in flue gas was significantly higher during suspension firing.
- The deposit formation rate measured by the advanced in situ deposit probe (points 1–6 and 35–38 in Fig. 7(b)) and measurements obtained with the more simple deposit probes show reasonably similar results indicating that both methods can be used to determine initial deposit formation rates.

At the end of each experiment at the AMV2 boiler, the probe was carefully taken out of the boiler; the deposits were removed, weighed, and photographed. The deposit's pattern and characterization are summarized in Table 2. Images of the probe after each experiment are shown in Fig. 8. The deposits obtained after 35% straw firing at AMV2, were brownish and with an approximate thickness of 5 mm on the upstream, and 2 mm on the downstream side of the probe. The deposits were evenly distributed on the deposition sampling area of the probe (up to 1500 mm starting from the tip of the probe). During 65% straw firing, the deposits were evenly distributed with an approximate thickness of 20 mm on the upstream side and 3 mm on the downstream side. During 100% straw firing at AMV2, the deposits were sintered and formed three layers on the upstream side and two layers on the downstream side of the probe. The white layer of deposits on the downstream side of the probe indicates that potassium salts have been deposited via

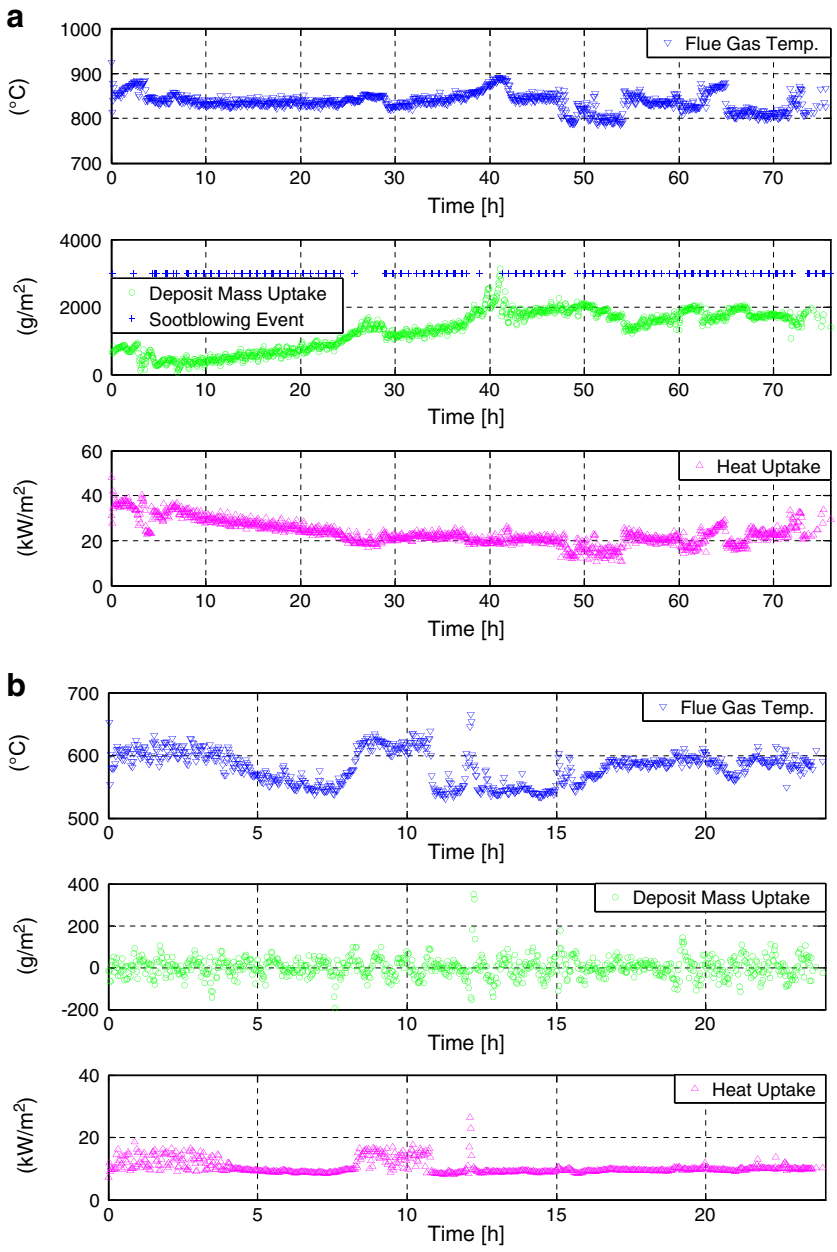

Fig. 6. Flue gas temperature, deposit mass uptake and probe heat uptake during measurements at AMV2, a) 100% straw firing, superheater region measurements (test 4, signals averaged to 1000 s), b) 100% wood firing, tube bank region measurements (test 5, signals averaged to 100 s).

condensation and thermophoresis (Fig. 8(d)). During 100% wood firing at AMV2 in the tube bank region, the deposits were powder-like and evenly distributed along the entire circumference of the probe and could be easily removed by sootblowing. Deposits during test 1 at AVV2 were somewhat unevenly distributed when the deposit probe was removed from the boiler, while during test 2 at AVV2, the deposits were rough and evenly distributed.

3.3. Video observations

The amount of deposit on a probe is a function of deposit build-up and shedding events. The deposit mass uptake signals were continuously monitored and deposit removal events were confirmed by video recordings. The larger shedding events appear as sudden downward changes in the deposit mass uptake signal with concurrent sudden increases in the probe heat uptake signal (Fig. 9(a)). For the shedding event at 113.3 h, Fig. 9(b) and (c) show images of the probe before and after shedding during 80% straw firing at AMV2. For most of the shedding events during 80% straw firing at AMV2, it was found that the predominant deposit removal mechanism was debonding i.e. the phenomenon when a complete layer of deposit detaches from the superheater tube. The gravitational force exerted by the increasing amount of deposit exceeded the available adhesion strength.

3.4. Chemical compositions of fly ashes and deposits

Fly ash samples were collected from the electrostatic precipitator (ESP) during measurements at AMV2 and finally an overall

Table 3
Deposit formation rates measured during the previous and current full-scale measurements. Avedøre Unit 2 is a straw-fired grate boiler. Ensted is also a straw-fired grate boiler. Haslev is a cigar type boiler where big bales of straw are fired directly. The Slagelse is a straw-fired grate boiler, while Amager Unit 2 is a straw and/or wood-fired suspension boiler.

No	Boiler	Type	Capacity	Fuel	Fuel analysis				Probe location	Probe temp.	Flue gas temp.	Exposure time	Deposit formation rate	Ref.
					Ash	K	Cl	Si		°C	°C	h	g/m^2/h	
1[a]	Avedøre 2	Grate fired	105 MW_{th}	Straw	4.7	0.92	0.36	1.10	Convective pass	400	725	24.0	32.0	[15]
2[a]	Avedøre 2	Grate fired	105 MW_{th}	Straw	4.7	0.92	0.36	1.10	Convective pass	400	750	24.0	46.0	[15]
3[a]	Avedøre 2	Grate fired	105 MW_{th}	Straw	4.7	0.92	0.36	1.10	Convective pass	500	770	22.0	36.8	
4[a]	Avedøre 2	Grate fired	105 MW_{th}	Straw	4.7	0.92	0.36	1.10	Convective pass	500	785	27.0	38.0	
5[a]	Avedøre 2	Grate fired	105 MW_{th}	Straw	4.7	0.92	0.36	1.10	Convective pass	550	780	24.0	60.0	[15]
6[a]	Avedøre 2	Grate fired	105 MW_{th}	Straw	5.5	0.69	0.32	–	Furnace	500	940	24.0	113.0	[19]
7	Avedøre 2	Grate fired	105 MW_{th}	Straw	4.7	0.75	0.25	1.18	Furnace	500	1080	3.8	61.8	[29]
8	Avedøre 2	Grate fired	105 MW_{th}	Straw	4.5	0.81	0.26	1.08	Furnace	500	977	4.9	75.6	[29]
9	Avedøre 2	Grate fired	105 MW_{th}	Straw	4.7	0.75	0.25	1.18	Convective pass	650	762	5.3	30.7	[29]
10	Avedøre 2	Grate fired	105 MW_{th}	Straw	4.5	0.81	0.26	1.08	Convective pass	650	640	4.1	18.8	[29]
11	Ensted	Grate fired	39 MW_{th}	Straw	4.4	0.90	0.28	1.10	Near to superheater	650	915	4.5	25.0	[29]
12	Ensted	Grate fired	39 MW_{th}	Straw	4.8	0.90	0.28	1.20	Near to superheater	650	890	4.3	24.3	[29]
13	Haslev	Cigar-burner	23 MW_{th}	Straw	4.1	0.71	0.29	0.96	Superheater	510	650	8.0	6.6	[18]
14	Haslev	Cigar-burner	23 MW_{th}	Straw	4.1	0.71	0.29	0.96	Furnace chamber	510	835	8.0	14.9	[18]
15	Haslev	Cigar-burner	23 MW_{th}	Straw	4.9	1.29	0.52	0.89	Superheater	510	650	8.0	31.3	[18]
16	Haslev	Cigar-burner	23 MW_{th}	Straw	4.9	1.29	0.52	0.89	Furnace chamber	510	835	8.0	61.3	[18]
17	Haslev	Cigar-burner	23 MW_{th}	Straw	5.0	2.05	0.56	–	Superheater	510	650	8.0	92.2	[18]
18	Haslev	Cigar-burner	23 MW_{th}	Straw	5.0	2.05	0.56	–	Furnace chamber	510	835	8.0	68.7	[18]
19	Haslev	Cigar-burner	23 MW_{th}	Straw	4.3	1.15	0.44	–	Superheater	510	650	8.0	22.3	[18]
20	Haslev	Cigar-burner	23 MW_{th}	Straw	4.3	1.15	0.44	–	Furnace chamber	510	835	8.0	71.7	[18]
21	Slagelse	Grate-fired	31 MW_{th}	Straw	6.0	0.41	0.06	2.03	Superheater	510	647	8.0	1.3	[18]
22	Slagelse	Grate-fired	31 MW_{th}	Straw	6.0	0.41	0.06	2.03	Furnace chamber	510	873	8.0	2.6	[18]
23	Slagelse	Grate-fired	31 MW_{th}	Straw	4.5	0.97	0.20	–	Superheater	510	647	8.0	6.2	[18]
24	Slagelse	Grate-fired	31 MW_{th}	Straw	4.5	0.97	0.20	–	Furnace Chamber	510	873	8.0	93.2	[18]
25	Slagelse	Grate-fired	31 MW_{th}	Straw	4.5	1.83	0.32	0.56	Superheater	510	647	8.0	16.6	[18]
26	Slagelse	Grate-fired	31 MW_{th}	Straw	4.5	1.83	0.32	0.56	Furnace Chamber	510	873	8.0	102.9	[18]
27	Slagelse	Grate-fired	31 MW_{th}	Straw	6.5	2.60	0.95	–	Superheater	510	647	8.0	26.2	[18]
28	Slagelse	Grate-fired	31 MW_{th}	Straw	6.5	2.60	0.95	–	Furnace Chamber	510	873	8.0	163.8	[18]
29	Slagelse	Grate-fired	31 MW_{th}	Straw	6.0	1.86	0.51	–	Superheater	510	647	8.0	13.6	[18]
30	Slagelse	Grate-fired	31 MW_{th}	Straw	6.0	1.86	0.51	–	Furnace chamber	510	873	8.0	80.2	[18]
31	Slagelse	Grate-fired	31 MW_{th}	Straw	7.3	2.07	0.86	1.73	Furnace chamber	510	873	8.0	67.4	[18]
32	Slagelse	Grate-fired	31 MW_{th}	Straw	4.9	0.69	0.14	1.59	Superheater	510	647	8.0	6.6	[18]
33	Slagelse	Grate-fired	31 MW_{th}	Straw	4.9	0.69	0.14	1.59	Furnace chamber	510	873	8.0	19.4	[18]
34[b]	Amager 2	Suspension-fired	250 MW_{th}	Straw	5.6	0.90	0.23	1.35	Superheater	480	800–900	12.0	56	[23]
35[a]	Amager 2	Suspension-fired	250 MW_{th}	Straw	5.9	0.83	0.40	1.36	Superheater	500	848	12.0	41.0	
36[a,c]	Amager 2	Suspension-fired	250 MW_{th}	Straw and wood	4.2	0.35	0.15	0.96	Superheater	500	856	12.0	33.0	
37[a,c]	Amager 2	Suspension-fired	250 MW_{th}	Straw and wood	5.4	0.68	0.32	1.24	Superheater	500	863	12.0	33.0	
38[a]	Amager 2	Suspension-fired	250 MW_{th}	Wood	3.3	0.09	0.01	0.75	Tube bank region (after convective pass)	500	586	12.0	~ 1.0	

[a] Measurements with advanced in situ deposit probes.
[b] Mean of three measurements.
[c] Ash, K, Cl and Si contents estimated by using straw share in wood.

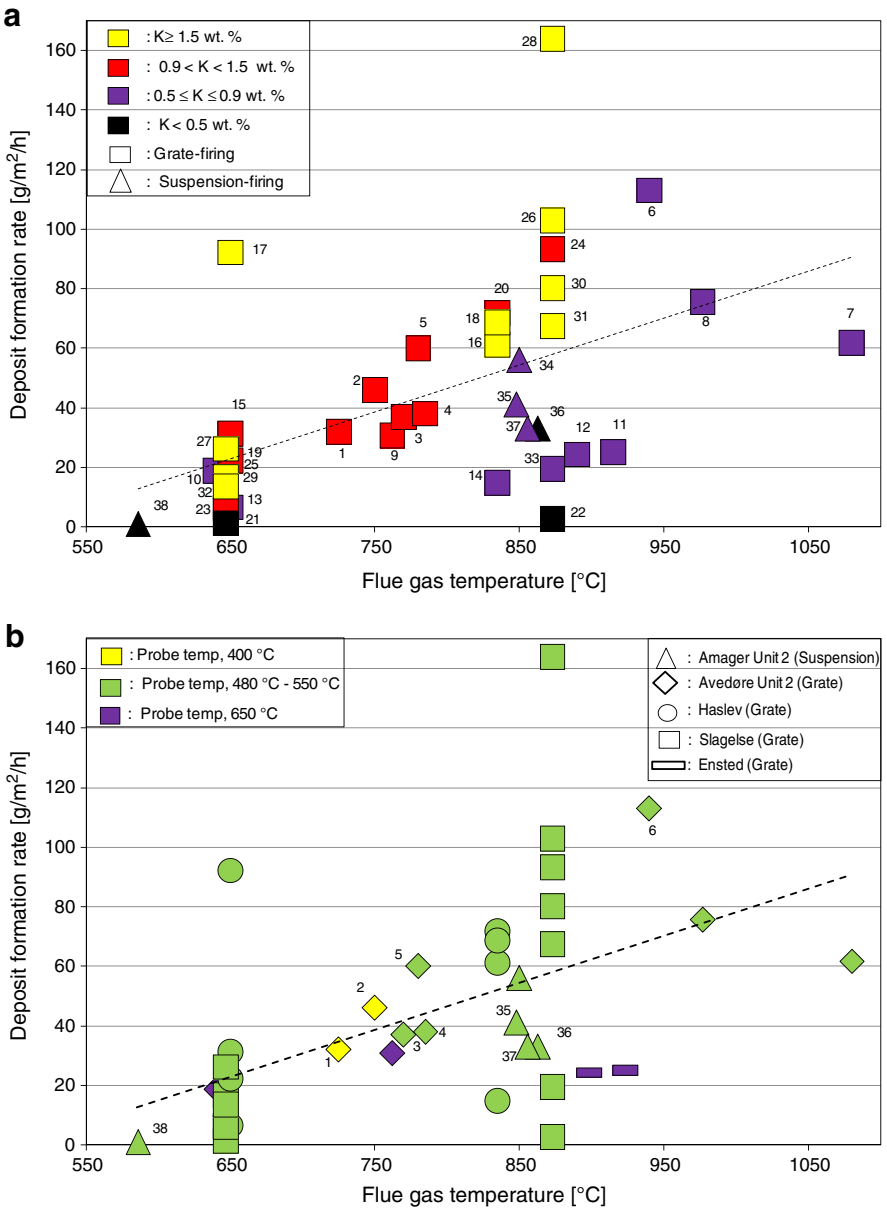

Fig. 7. Impact of flue gas temperature on deposit formation rates, a) four different sets of fuel alkali contents and two types of straw firing technologies, b) different sets of probe surface temperatures and 5 different boilers [15,18,19,23,29]. Amager Unit 2 is a straw and/or wood-fired suspension boiler. Avedøre Unit 2 is a straw-fired grate boiler. Haslev is a cigar type boiler where big bales of straw are fired directly. Slagelse and Ensted are both straw-fired grate boilers. Graph details: a) the color represents the range of fuel alkali in wt.%, while the point shape represents the straw firing technology, b) the color represents the probe surface temperature, while the point shape represents the boiler type.

representative sample was selected for bulk fly ash analysis by ICP-OES. Fly ash samples were also taken from the bag house filter during the AVV2 measurements. The bulk composition of fuel and fly ash samples collected during measurements at AMV2 and AVV2 is shown in Fig. 10. The most remarkable difference is that fly ash from straw suspension firing contains high contents of Si, K and Ca, while fly ash from straw grate firing is rich in the volatile elements K, Cl and S. The depletion in the fly ash of the non-volatile elements such as Al, Fe, Mg, Ca and Si during straw grate firing indicates that these elements are mainly transformed to bottom ash. The enrichment of the volatile elements (K, Cl and S) in the grate-fired fly ash implies that these elements after release from the combustion zone condense as aerosols or are absorbed on the larger fly ash particles. The variation in the distribution of Cl between KCl aerosol and gas phase HCl is dependent upon the K, Cl, Si, Al, Ca and S contents in the biomass fuel. The determination of the exact distribution between KCl and HCl is possible through measurements, which was beyond the scope of the current study. However, previous investigations by Christensen et al. [31] and Zeuthen et al. [32] at straw-fired boilers have shown large amounts of KCl aerosols in the fly ash. Cl influences the deposit formation process because KCl has a relatively low melting temperature and KCl can also be present in the gas phase in the boiler chamber and thereby KCl contributes to the deposit formation process by condensation on boiler surfaces. KCl rarely appears in bottom ash, but are often seen in relatively high concentrations in straw fly ash [31,32].

SEM-EDS analysis was also made to characterize morphology and composition of fly ashes from straw suspension firing (Fig. 11). It can be seen that the fly ash consists of three kinds of particles: 1) flake type Si rich particles (spots 1 and 2), 2) molten or partially molten particles rich in Si, K and Ca with small amounts of Mg, P, and

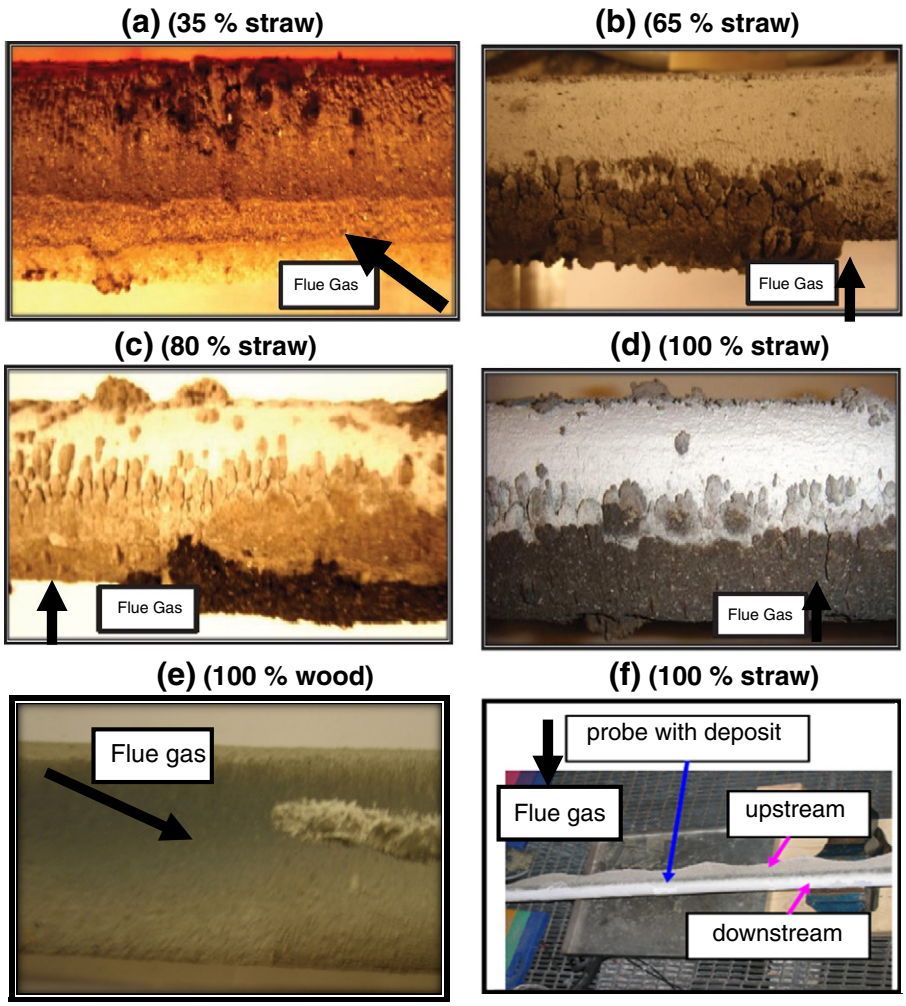

Fig. 8. Pictures of the deposit probe just after the experiments, a) ~20–50 cm from tip of probe (35% straw, test 1 at AMV2), b) ~10–30 cm from tip of probe (65% straw, test 3 at AMV2), c) ~10–30 cm from tip of probe (80% straw, test 2 AMV2), d) ~30–50 cm from tip of probe (100% straw, test 4 at AMV2), e) ~40–60 cm from tip of probe (100% wood, test 5 at AMV2), f) almost complete deposition area of the probe (100% straw, test 1 at AVV2). Black arrows show direction of flue gas flow.

potassium salts on the outer surface (spot 3), and 3) small particles rich in K, Cl and S (aerosols) (spot 4). Overall, the observed fly ash structure matches the data published by Knudsen [30] on biomass ash transformation.

The elemental composition of the main ash forming elements in the deposits is shown in Table 4. It can be seen that during straw suspension firing, the outer layer of upstream deposits contains a significant amount of Si, K and Ca, indicating that large particles impact on and stick on the upstream side of the probe [13,27]. A difference in terms of elemental composition of the upstream outer deposits during 35% and 100% straw firing is evident from Table 4. The Ca and Mg contents were reduced when the straw share was increased, while the K, Cl and Si contents were increased. The possible reason is changes in the ash forming elements of fuels. Morphology and SEM-EDS analysis of the outer layer of upstream deposits collected from straw suspension firing indicate that large molten particles are rich in Si, K and Ca (spot 1, 2 in Fig. 12) with some S, K and Ca enriched small particles on the outer surface (spot 3). The presence of K_2SO_4 particles is evident from spot 4, while spots 5 and 6 show the presence of KCl particles. Si, Ca and Mg contents in the upstream deposits are higher than those in the fly ash during straw grate firing indicating that the predominant phenomenon for ash deposition is inertial impaction.

The downstream side inner deposit during suspension firing has high concentration of Cl and K indicating that possibly KCl has been attached via condensation and/or thermophoresis. The downstream layer formed during straw grate firing was also mainly composed of KCl. The outer layer of deposits in the upstream side shows lesser amount of Cl possibly due to reduction in KCl deposition by condensation at higher deposit surface temperature caused by increase in deposit thickness in the upstream side.

The calculated molar ratios $\psi = (K + Na)/(2S + Cl)$ of fly ashes and deposit samples (Table 4) indicate whether there is sufficient K available to account for all S and Cl in the form of sulfates and chlorides, because Na is available in small amounts in straw and/or wood, compared to K. For ratios smaller than one, all K is probably bound as KCl and K_2SO_4, but some S and Cl must be present in other compounds. For ratios close to or greater than one, KCl and K_2SO_4 probably are the predominant S and Cl containing species, while any excess K likely is found in silicates. The values of ψ for fly ash and deposits are nearly all quite close to 1, although fly ash generated by suspension-fired straw shows a slightly elevated ψ-value that may be due to K containing silicates. A different ψ-value of 1.31 for deposit from 65% straw (AMV2) is the result of unusually low S content, but is probably not much trustworthy since other species also are present in atypical amounts. However, lower 2S/Cl molar ratios of the downstream deposit layers during grate and suspension firing show a significant presence of KCl, possibly deposited through condensation and/or thermophoresis in the downstream side of the probe.

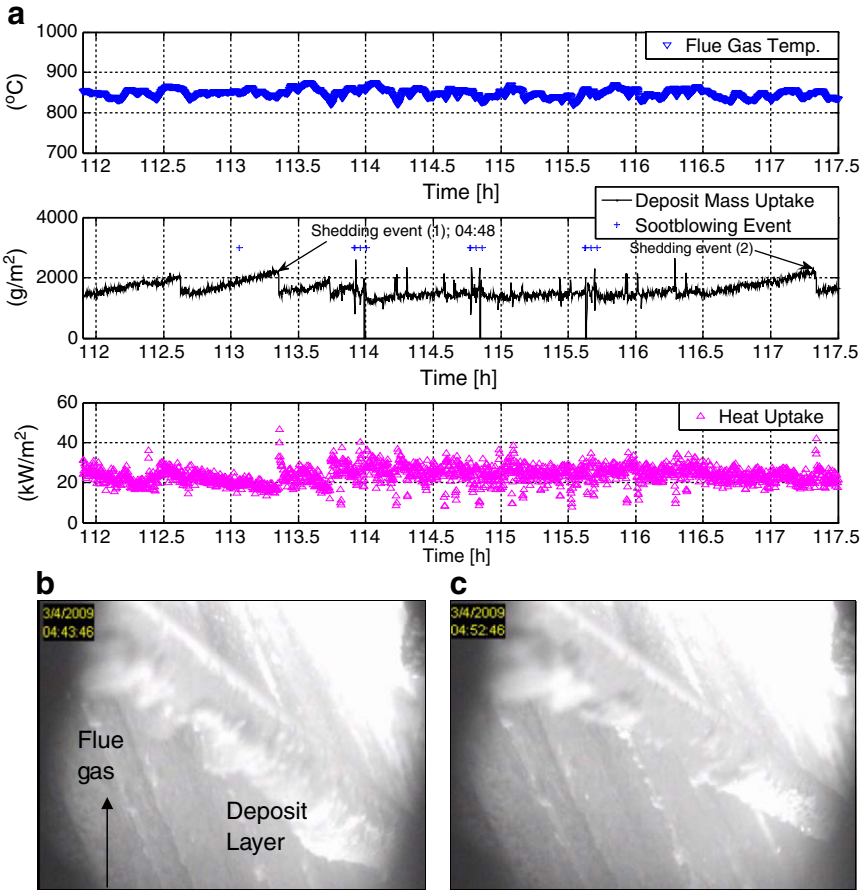

Fig. 9. a) Flue gas temperature, deposit mass uptake and probe heat uptake during 80% straw firing at AMV2 with identified shedding events, b) picture of the deposit probe just before first shedding event (1) at approximately 113.3 h (04:43), c) picture of the deposit probe just after first shedding event (04:52).

3.5. Fly ash melting

A prediction of fly ash melt fraction as function of temperature based on the fly ash compositions in Table 4 was made by using the model proposed by Zhou et al. [33] (Fig. 13). Both grate- and suspension-fired straw fly ash have a first melting temperature (FMT) around 645 °C, but at higher temperatures the melt fraction of fly ash from grate firing is much higher than the melt fraction of the fly ash from suspension firing. This higher melt fraction of fly ash from grate firing leads to a much larger probability of grate-generated fly ash to stick to the probes and other surfaces. This partially explains why the deposit mass uptakes measured for straw grate- and suspension firing are

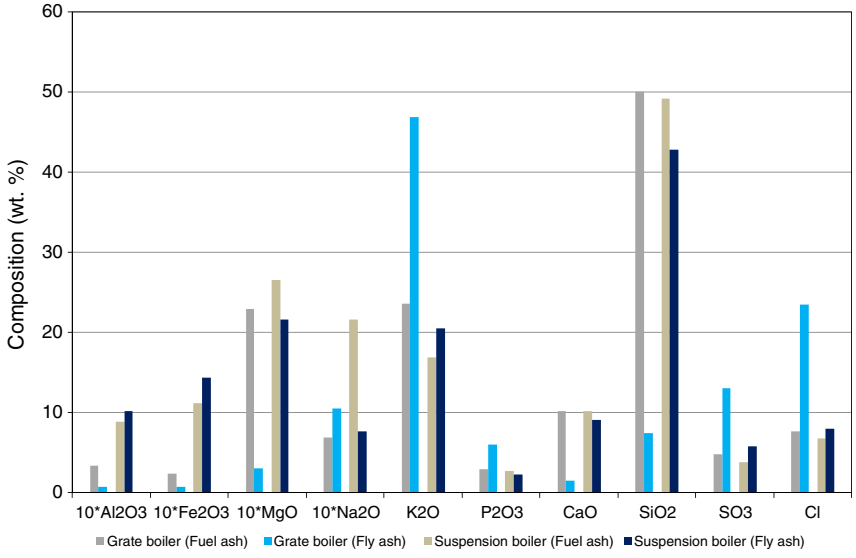

Fig. 10. Ash transformation during straw firing on grate and straw firing in suspension.

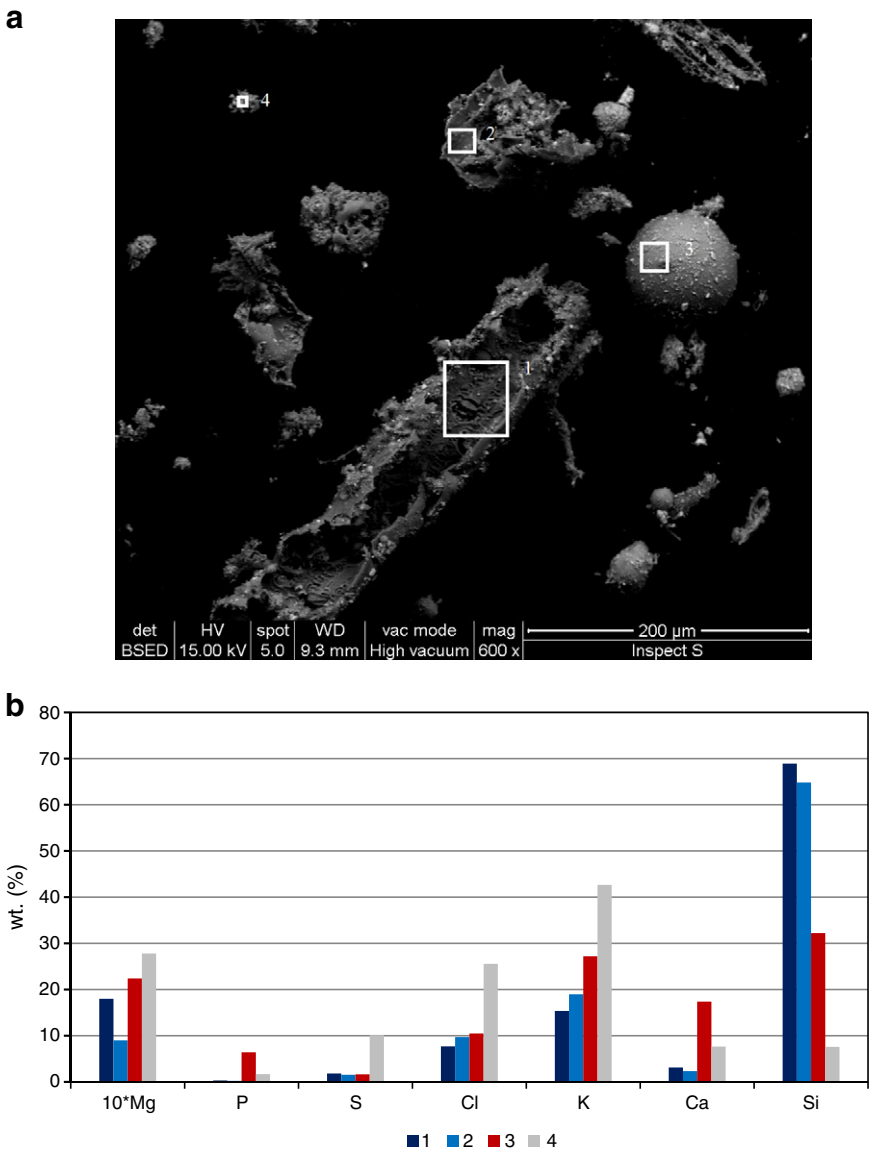

Fig. 11. Morphology and SEM-EDS of fly ash collected from ESP during straw firing in suspension at AMV2.

Table 4
Composition of major elements in the fly ash and deposits formed during AMV2 (suspension) and AVV2 (grate) measurements.

Boiler	AMV2		AVV2	AMV2	AVV2	AMV2				AVV2			
Sample	Fuel ash		Fuel ash	Fly ash	Fly ash	Deposit				Deposit			
Description	Straw	Wood	Straw	ESP	Bag filter	Upstream	Downstream	Upstream	Upstream	Upstream	Upstream	Upstream	Downstream
Layer	–	–	–	–	–	Outer	Inner	Middle	Outer	Outer	Middle	Inner	Overall
Grate/suspension	Suspension		Grate	Suspension	Grate	Suspension				Grate			
Straw (% mass basis)	100	0	100	100	100	35	65	80	100	100	100	100	100
Al_2O_3	0.89	3.64	0.34	1.02	0.08	1.21	0.47	0.76	0.66	–	–	1.00	–
CaO	10.21	9.33	10.12	9.09	1.47	20.99	4.88	12.73	13.85	3.96	3.23	2.14	–
Fe_2O_3	1.12	1.82	0.23	1.43	0.07	2.86	0.19	0.44	0.46	–	–	–	–
K_2O	16.86	3.41	23.58	20.48	46.86	21.68	36.32	32.52	30.12	18.59	16.48	16.13	39.72
MgO	2.65	1.73	2.29	2.16	0.30	4.48	1.16	2.65	3.15	0.91	0.99	1.04	–
Na_2O	2.16	0.98	0.69	0.77	1.05	0.58	6.00	0.80	0.81	0.51	0.22	0.00	0.32
P_2O_3	2.75	0.76	2.93	2.25	6.00	2.75	1.11	2.75	2.52	1.83	1.40	1.21	1.47
SiO_2	49.21	54.78	50.07	42.79	7.40	19.25	18.84	21.39	23.53	11.19	7.89	12.41	0.26
SO_3	3.75	1.34	4.78	5.74	13.03	11.24	4.73	11.24	14.73	12.76	9.36	10.61	6.87
Cl	6.75	0.45	7.62	8.00	23.50	5.30	21.89	16.00	11.00	3.55	6.65	4.08	24.39
Molar: 2S/Cl	0.49	2.60	0.56	0.64	0.49	1.88	0.19	0.62	1.19	3.18	1.25	2.30	0.25
Molar: (K + Na)/(2S + Cl)	1.51	2.25	1.56	1.25	1.04	1.11	1.31	0.98	0.98	0.98	0.85	0.90	0.99

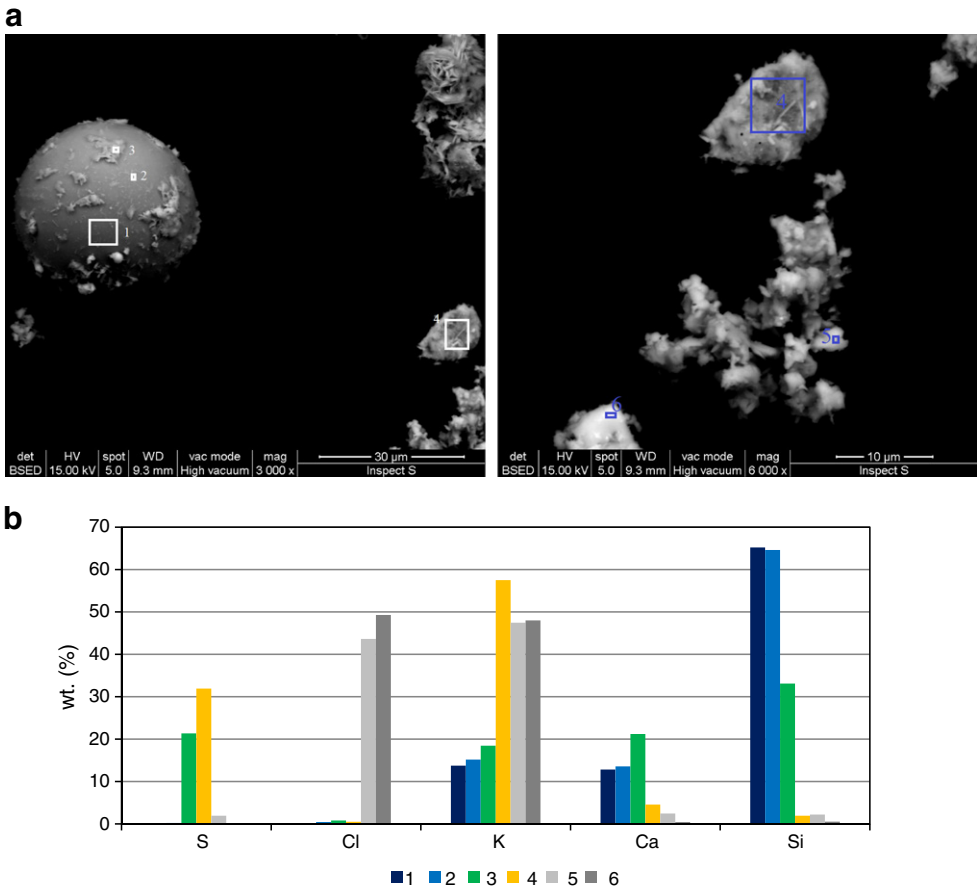

Fig. 12. Morphology and SEM-EDS of outer layer of upstream deposits collected after straw firing in suspension at AMV2 (test 4 at SH).

comparable, even though typically only 10–30% of the fuel ash is transferred to fly ash by stoker and grate firing, compared to a transfer of 80–90% by suspension firing [5]. So, while a higher fly ash concentration is present in suspension boilers than in grate boilers, the larger fraction molten at any temperature above the FMT leads to a greatly increased probability of the fly ash to stick to the deposit probe.

4. Conclusions

A series of full-scale and long duration deposit probe measurements have been conducted in a biomass grate and a biomass suspension boiler to investigate the deposit formation rate, probe heat uptake and ash transformation. It was identified that the deposit

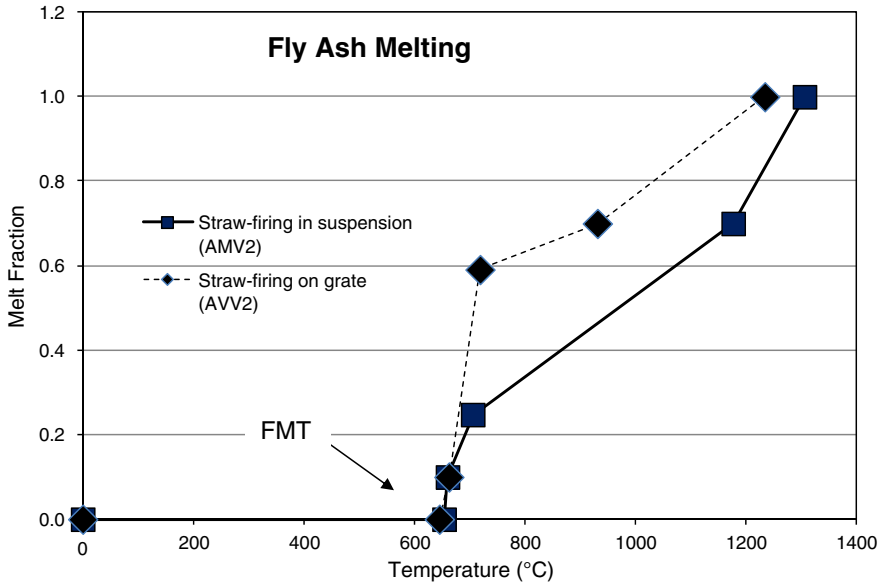

Fig. 13. Prediction of fly ash melt fraction by using the predictive model of Zhou et al. [33]. FMT: first melting temperature.

formation rate increases moderately with straw share increase, when straw is co-fired with wood in a suspension boiler. During 35% straw fuel share on mass basis, a deposit formation rate of 33 g/m^2/h (initial 12 h) was observed, while the corresponding deposit formation rate increased to 41 g/m^2/h when 100% straw was fired. During straw grate firing, the measured deposit formation rate was nearly similar in two tests and approximately 38 g/m^2/h.

The current full-scale measurements data were compared with data from previously conducted deposit probe measurements. The comparison showed an increasing trend in deposit formation rate with increase in flue gas temperature. At a flue gas temperature of 650 °C, the deposit formation rate is typically from 5 to 30 g/m^2/h and at 900 °C, the deposit formation rate is typically 20 to 110 g/m^2/h. At higher fuel alkali contents (K > 0.9 wt.%), the increase in deposit formation rate with flue gas temperature was more significant, compared to the increase in the deposit formation rate at lower fuel alkali contents (K ≤ 0.9 wt.%). An increased flue gas temperature probably increases the fraction of molten ash as well as provides an increased content of gas phase alkali species, and both will lead to an increased deposit formation rate. It was also observed that the deposit formation rates measured in suspension and grate boilers are on similar levels. This was observed even though the concentration of fly ash in the flue gas was significantly higher in the straw-fired suspension boiler.

Shedding events registered by a CCD camera showed that the predominant phenomenon of deposit removal during 80% straw firing in suspension with wood was debonding.

The elemental composition of fly ash generated during straw suspension firing shows higher contents of Si and Ca, compared to grate firing fly ash that is rich in the volatile elements K, Cl and S. SEM-EDS analysis indicated that the fly ashes generated during straw firing in suspension consists of three kinds of particles: 1) flake type Si rich particles, 2) molten or partially molten particles rich in Si, K and Ca with small amounts of Mg, P and potassium salts on the outer surface, and 3) small particles rich in K, Cl and S (aerosols). Chemical analysis of the outer layer of upstream deposits during 35% straw firing and 100% straw firing indicated that by increasing the straw share in the fuel, the K, Cl and Si contents were increased, while Ca and Mg contents were reduced.

It was also found that 35% straw firing with wood does not create severe fouling and slagging on the heat exchanger tubes at the AMV2. The experiences of the operational staff indicate that the boiler operation period may exceed more than one month without deposit related operational problems when firing maximum 50% straw with wood on mass basis. The findings related to deposit management during straw suspension firing are:

- At higher flue gas temperatures (750–950 °C), efficient soot blowing is needed to manage the boiler tube deposits with small superheater tube spacing (113 mm, current case). An increase in superheater tube spacing probably will lead to the absence of tube clogging by ash deposits.
- At flue gas temperatures below 650 °C, deposit formation rate is small and deposits can be easily removed by sootblowers.

Acknowledgements

The financial support by Energinet.DK under the PSO project 7217 and the financial support by Vattenfall A/S are gratefully acknowledged. We would like to thank Vattenfall A/S and DONG Energy A/S for access to their boilers. We are thankful to the operational staff at the Amager Power Station (Vattenfall) and Avedøre Power Station (DONG) for their technical support during the full-scale measurements. Special thanks go to DTU CEN for help in SEM-EDS analysis.

References

[1] L.L. Baxter, Ash deposition during biomass and coal combustion: a mechanistic approach, Biomass and Bioenergy 4 (1993) 85–102.
[2] B.M. Jenkins, L.L. Baxter, T.R. Miles Jr., T.R. Miles, Combustion properties of biomass, Fuel Processing Technology 54 (1998) 17–46.
[3] L. Hansen, Melting and sintering of ashes, PhD Thesis, Technical University of Denmark, (1998), ISBN 87-90142-31-4.
[4] L.L. Baxter, T.R. Miles Jr., T.R. Miles, B.M. Jenkins, T. Milne, D. David, R.W. Bryers, L.L. Oden, The behavior of inorganic material in biomass-fired power boilers: field and laboratory experiences, Fuel Processing Technology 54 (1998) 47–78.
[5] H.P. Nielsen, Deposition and high temperature corrosion in biomass-fired boilers, PhD Thesis, Technical University of Denmark, (1998), ISBN 87-90142-47-0.
[6] T.R. Miles, T.R. Miles Jr., L.L. Baxter, R.W. Bryers, B.M. Jenkins, L.L. Oden, Boiler deposits from firing biomass fuels, Biomass and Bioenergy 10 (1996) 125–138.
[7] L.L. Baxter, Influence of ash deposit chemistry and structure on physical and transport properties, Fuel Processing Technology 56 (1998) 81–88.
[8] P.A. Jensen, B. Sander, K. Dam-Johansen, Removal of K and Cl by leaching of straw char, Biomass and Bioenergy 20 (2001) 447–457.
[9] K.H. Andersen, F.J. Frandsen, P.F. Hansen, K. Wieck-Hansen, I. Rasmussen, P. Overgaard, K. Dam-Johansen, Deposit formation in a 150 MWe utility PF-boiler during co-combustion of coal and straw, Energy & Fuels 14 (2000) 765–780.
[10] P.A. Jensen, F.J. Frandsen, J. Hansen, K. Dam-Johansen, N. Henriksen, S. Hörlyck, SEM investigation of superheater deposits from biomass-fired boilers, Energy & Fuels 18 (2004) 378–384.
[11] L.A. Hansen, H.P. Nielsen, F.J. Frandsen, K. Dam-Johansen, S. Hørlyck, A. Karlsson, Influence of deposit formation on corrosion at a straw-fired boiler, Fuel Processing Technology 64 (2000) 189–209.
[12] F.J. Frandsen, Utilizing biomass and waste for power production—a decade of contributing to the understanding, interpretation and analysis of deposits and corrosion products, Fuel 84 (2005) 1277–1294.
[13] F.J. Frandsen, Ash formation, deposition and corrosion when utilizing straw for heat and power production, Doctoral Thesis, Technical University of Denmark, (2011), ISBN 978-87-92481-40-5.
[14] P.A. Jensen, H. Zhou, F.J. Frandsen, J. Hansen, Ash deposits removal in biomass power plant boilers, Proceeding of 15th European Biomass Conference and Exhibition, Berlin, Germany, 07–11 May, 2007.
[15] H. Zhou, F.J. Frandsen, P.A. Jensen, P. Glarborg, PSO Project 4106, CHEC Report R0603, CHEC Research Centre, Technical University of Denmark, 2006.
[16] A. Zbogar, F. Frandsen, P.A. Jensen, P. Glarborg, Shedding of ash deposits, Progress in Energy and Combustion Science 35 (2009) 31–56.
[17] D. Nordgren, H. Hedman, N. Padban, D. Boström, M. Öhman, Ash transformations in pulverised fuel co-combustion of straw and woody biomass, Fuel Processing Technology (2011), doi:10.1016/j.fuproc.2011.05.027.
[18] P.A. Jensen, M. Stenholm, P. Hald, Deposition investigation in straw-fired boilers, Energy & Fuels 11 (1997) 1048–1055.
[19] A. Zbogar, P.A. Jensen, F.J. Frandsen, J. Hansen, P. Glarborg, Experimental investigation of ash deposit shedding in a straw-fired boiler, Energy & Fuels 20 (2006) 512–519.
[20] H.P. Mickelsen, F.J. Frandsen, K. Dam-Johansen, O.H. Larsen, Deposition and high temperature corrosion in a 10 MW straw fired boiler, Fuel Processing Technology 54 (1998) 95–108.
[21] M.S. Bashir, P.A. Jensen, F.J. Frandsen, S. Wedel, K. Dam-Johansen, T. Wolfe, S.T. Pedersen, J. Wadenbäck, Characterization and quantification of deposits buildup and removal in biomass suspension-fired boilers, Proceedings of 18th European Biomass Conference and Exhibition, Lyon, France, 03–07 May, 2010.
[22] M. Theis, B.-J. Skrifvars, M. Hupa, H. Tran, Fouling tendency of ash resulting from burning mixtures of biofuels. Part 1: deposition rates, Fuel 85 (2006) 1125–1130.
[23] L. Tobiasen, R. Skytte, L.S. Pedersen, S.T. Pedersen, M.A. Lindberg, Deposit characteristics after injection of additives to a Danish straw-fired suspension boiler, Fuel Processing Technology 88 (2007) 1108–1117.
[24] B.-J. Skrifvars, T. Lauren, M. Hupa, R. Korbee, P. Ljung, Ash behaviour in a pulverized wood fired boiler—a case study, Fuel 83 (2004) 1371–1379.
[25] M. Berg, S.T. Pedersen, G. Rhode, Experience with straw dust firing at Amager 2, VGB Powertech 87 (Nr. 5) (2007) 93–95.
[26] IFRF Suction Pyrometer, user information document, International Flame Research Foundation, Netherlands, 2007.
[27] H. Wu, P. Glarborg, F.J. Frandsen, K. Dam-Johansen, P.A. Jensen, Dust-firing of straw and additives: ash chemistry and deposition behavior, Energy & Fuels 25 (2011) 2862–2873.
[28] S.S. Lokare, J.D. Dunaway, D. Moulten, D. Rogers, D.R. Tree, L.L. Baxter, Investigation of ash deposition rates for a suite of biomass fuels and fuel blends, Energy & Fuels 20 (2006) 1008–1014.
[29] J. Hansen, P.A. Jensen, P. Glarborg, Deposit probe measurements in the Avedøre and Ensted straw-fired grate boilers, CHEC Report R0705, CHEC Research Centre Technical University of Denmark, 2007.
[30] J.N. Knudsen, Volatilization of inorganic matter during combustion of annual biomass, PhD Thesis, Technical University of Denmark, (2004), ISBN 87-91435-11-0.
[31] K.A. Christensen, M. Stenholm, H. Livbjerg, The formation of submicron aerosols particles, HCl and SO_2 in straw-fired boilers, Journal of Aerosol Science 29 (1998) 421–444.
[32] J.H. Zeuthen, P.A. Jensen, J.P. Hansen, H. Livbjerg, Aerosol formation during combustion of straw with addition of sorbents, Energy & Fuels 21 (2007) 699–709.
[33] H. Zhou, P.A. Jensen, F.J. Frandsen, Dynamic mechanistic model of superheater deposit growth and shedding in a biomass fired grate boiler, Fuel 86 (2007) 1519–1533.

September. 2012, DTU no. 50530

Appendix A4

Journal paper: Suspension-Firing of Biomass. Part 1: Full-scale Measurements of Ash Deposit Build-up. Energy & Fuels 2012, 26, 2317-2330

Energinet.dk project no. 7217

Characterization and quantification of deposits build up and removal in straw suspension fired boilers

Muhammad Shafique Bashir, Peter Arendt Jensen, Flemming Frandsen, Stig Wedel, Kim Dam-Johansen, Johan Wadenbäck, Søren Thaaning Pedersen

Department of Chemical and Biochemical Engineering

Technical University of Denmark

Søltofts Plads, Building 229, DK-2800 Lyngby, Denmark

CHEC no. R1301

energy&fuels

Article

pubs.acs.org/EF

Suspension-Firing of Biomass. Part 1: Full-Scale Measurements of Ash Deposit Build-up

Muhammad Shafique Bashir,[†] Peter Arendt Jensen,*[,†] Flemming Frandsen,[†] Stig Wedel,[†] Kim Dam-Johansen,[†] Johan Wadenbäck,[‡] and Søren Thaaning Pedersen[‡]

[†]DTU Chemical and Biochemical Engineering, Technical University of Denmark, Building 229, DK-2800 Lyngby, Denmark

[‡]Vattenfall A/S, Amager Power Plant, Kraftværksvej 37, DK-2300 Copenhagen S, Denmark

ABSTRACT: This paper is Part 1 in a series of two describing probe measurements of deposit build-up and removal (shedding) in a 350 MW_{th} suspension boiler, firing straw and wood. The influence of fuel type (straw share in wood), probe exposure time, probe surface temperature (500, 550, and 600 °C), and flue gas temperature (600−1050 °C) on ash deposit formation rate has been investigated. Investigations of deposit formation rate were made by use of an advanced online deposit probe that allowed nearly continuous measurement of the deposited mass. Two different measures of deposit formation rate are used in the analysis of the data. The first is the integral deposit formation rate (IDF-rate) found by dividing the integral mass change over integral time intervals (of order several hours) by the time interval. The IDF-rate is similar to deposit formation rates based on total deposit mass uptake divided by probe exposure time reported in previous full-scale investigations, but it is a relatively crude measure that includes all deposit shedding in addition to actual deposit formation. To remove major shedding events from the determination of deposition rates a second measure, the derivative-based deposit formation rate (DDF-rate), was devised. This was determined by averaging the deposit mass uptake signals over short time intervals (on the order of minutes), calculating the local values of the time derivative of the mass uptake, removing large negative values signifying major shedding events, and finally time smoothing the derivatives to remove excessive noise. The DDF-rate was influenced by flue gas temperature and straw share, while changes in probe surface temperature had no significant influence. The IDF-rate, qualitatively related to the ratio between the time-integrated DDF-rate and the integration time, followed the same trends. Ash transformation was investigated by bulk ash analysis of the fuel, fly, and bottom ash during straw and/or wood suspension firing. Bulk ash analysis of fly ashes showed that the contents of volatile elements (K, Cl, S) were slightly greater than in the fuel ash, while Ca and Si remained either in the same proportion or were slightly reduced. It was also found that, with an increase in fuel ash K/Si molar ratio, the concentration of the volatile elements, K, Cl, and, to some extent, S, increased in the fly ash. The bottom ash was dominated by Si and Ca, with almost no S and Cl, possibly as a result of the high volatility of S and Cl during combustion at higher temperatures.

1. INTRODUCTION

By the end of 2009, there were eight biomass and five biomass cofired power plants in Denmark.[1] Utilization of biomass in power plants is an attractive option to lower CO_2 emissions and to make the energy supply independent of fossil fuels. However, the use of biomass, especially straw, constitutes a serious technical challenge as a result of the presence of large amounts of alkali metals and chlorine.[2−8] The presence of alkali metals and chlorine may induce large operational problems due to boiler ash deposition and subsequent corrosion.[6,8−11] To minimize deposition problems, different strategies can be employed, for example, use of additives that can convert the vaporized inorganic species to less harmful forms, pretreatment of fuels by leaching out alkali, cofiring with coal, and use of effective deposit shedding techniques.[4−8,10,12−18]

Some full-scale experimental studies on ash deposit build-up and removal conducted in biomass grate-fired boilers can be found in the literature.[16−19] Potentially, most suspension-fired boilers have a better electrical efficiency (46−48%) than traditional grate-fired systems (25−30%),[8] but only limited ash deposition data from biomass suspension firing are availabe.[10,14,15,20−25] In biomass suspension firing, pulverized biomass typically from pellets crushed in the coal mills (roller mills) is blown into the burners, where the fuel particles are burned in suspension. Quantification of deposit formation rates in biomass suspension-fired boilers is an area where relatively limited accurate knowledge is available, and improved knowledge on the transient deposit formation and removal is wanted to optimize design and operation.[14,20−22,24] Compared to grate-fired units, the deposit flux may increase during suspension firing because a larger part of the fuel ash is transformed to fly ash.[2] In addition, fuel particle residence times are on the order of a few seconds, and peak flame temperatures are higher, compared to grate firing conditions.[23] Investigations by Nordgren et al.[20] indicate that, during biomass (straw and/or woody biomass) dust combustion at higher temperatures, significant ash deposition formation may appear. Investigations of biomass suspension combustion at both pilot-scale and full-scale have shown higher deposit formation rate during straw firing, compared to straw and wood cofiring, possibly due to dilution and/or chemical interations.[20,24,25] However, only few full-scale measurements are reported for 100% straw and/or wood combustion in suspension-fired boilers, and most of these studies have been based on short testing time (up to 12 h),[14,22] while more

Received: October 28, 2011
Revised: February 21, 2012
Published: March 20, 2012

dx.doi.org/10.1021/ef201680k | *Energy Fuels* 2012, 26, 2317−2330

extensive full-scale measurements are rare.[24] Therefore, detailed and extensive full-scale studies on transient deposit formation processes when firing straw and wood will improve our understanding of ash deposit formation processes.

The aim of this study is to provide long-time, full-scale data on ash deposit formation in a 350 MW_{th} suspension-fired boiler, firing straw and wood. Furthermore, an analysis is carried out, giving quantitative information about deposit formation rates as functions of operating conditions. The influence of fuel type (straw share in wood), probe exposure time, probe surface temperature (500, 550, and 600 °C) and flue gas temperature (600−1050 °C) on ash deposit formation rate has been investigated.

2. EXPERIMENTAL SECTION

2.1. Boiler. The probe measurements were conducted at Amager Power Station, Unit 1 (AMV1), firing biomass in suspension. The AMV1 boiler, a multifuel suspension-fired boiler, was commissioned in 2009 to use pulverized biomass with varying shares of straw and wood. The annual biomass consumption (AMV1) is approximately 300 000 tons wood pellets and 100 000 tons straw pellets. The 350 MW_{th} boiler is front wall-fired with 12 burners at 3 levels. The fuel is introduced as particles and is combusted while being suspended in the air stream. Due to an expected increase in the corrosion rate with respect to temperature, the final steam temperatures of the superheaters are limited to approximately 540 °C.[26] The overall boiler operational data can be found in Table 1, while the boiler drawings with identified probe measuring position are shown in Figure 1. Only one probe position was selected. The probe measuring position was selected because of significant deposit build-up during straw firing in that boiler position. The selected probe measuring position was in the most contaminated area in the boiler.

Table 1. Brief Operational Data of the AMV1 Boiler

param. (steam)	unit	high pressure (HP) superheater	reheater (RH)
temp.	°C	540 (biomass)	540
pressure	bar	185	75
flow	kg/s	138.4	123

2.2. Ash Deposition Probe. The deposit probe used during the measurements is shown schematically in Figure 2a and b. The probe is made of stainless steel, is about 3 m long, and has an outer diameter of 40.5 mm. The probe was cooled by water and air, whereby it was possible to determine heat uptake by the probe and keep a stable surface temperature. The probe hung on a hinge connected to a flange. A balance at the rear was used to oppose fluctuations in the boiler and to keep the probe aligned horizontally. A load cell was used to detect the force caused by the mass of deposit on the probe. The deposit mass was calculated by using the following balance:

$$m_{dg} = (m_{t0} - m_{t1})g\frac{L_1}{L_2} \quad (1)$$

where m_d is the deposit mass (g), g is the gravitational acceleration (m/s^2), m_{t0} is the initial mass signal of the load cell (g), m_{t1} is the final mass signal of the load cell (g), and L_1 and L_2 are the distances (mm) from the hinge to the balance (784 mm) and to the mass center of the deposit (1460 mm), respectively. The deposit mass signals were then divided by the probe surface area to get a measure of the deposit mass uptake.

In each horizontal position of the probe (TC position 1, 2, and 3), four thermocouples provided temperatures at the N, E, S, and W positions (Figure 2b). A CCD (charge-coupled device) camera registered the deposit formation and removal processes on the probe. The flue gas temperature near the probe was continuously measured, using a simple thermocouple in a protective shell. In addition, a suction pyrometer (International Flame Research Foundation (IFRF) model[27]) was also used for some periods during each test. Due to strong radiation effects in the probe measuring area, a significant difference was identified between the flue gas temperature measured by the thermocouple and the suction pyrometer. A schematic of the port used during the measurements is shown in Figure 2c. In the large port, a small port for the deposit probe, a port for the thermo-element, a CCD camera port, and a port for the suction pyrometer and artificial sootblowing probe can be seen. The thermocouple was placed just above the suction pyrometer port.

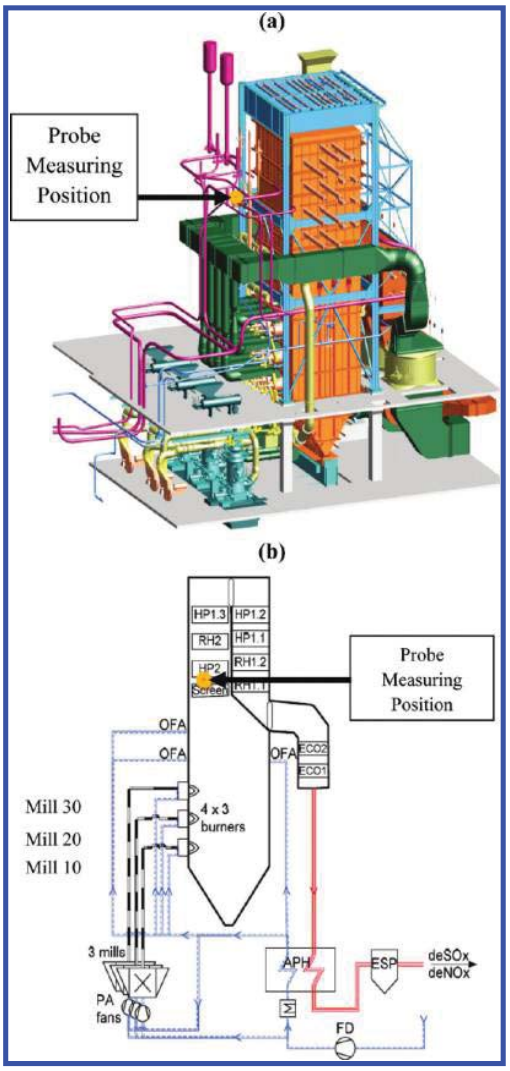

Figure 1. Drawings of AMV1 boiler with identified probe measuring position, just above the screen tubes: (a) overall boiler configuration, (b) schematic presentation of the boiler. (Modified with permission from ref 26. Copyright 2006, Power-Gen Europe.) Top: mill 30. Middle: mill 20. Bottom: mill 10. HP: high pressure. RH: reheater. OFA: over fire air. ECO: economizer. APH: air preheater.

2.3. Fuels. The compositions and analysis methods of some of the fuels fired during the full-scale measurements are shown in Table 2. It is seen that the straw ash has a high content of Si, K, and Ca. During the experiments, the fuels were continuously sampled before the burners and then analyzed. The ash contents of the fuel from all test runs were analyzed, and thereby, the straw fuel fractions were determined based on the total ash contents. The detailed ash analysis was done on samples from test 1 and test 5, as shown in Table 2.

Overall, eight test runs were carried out, and the mean straw share during each test is shown in Table 3. In Table 3, mean values of each complete test are shown, while in Table 2 values are shown for a

dx.doi.org/10.1021/ef201680k | Energy Fuels 2012, 26, 2317−2330

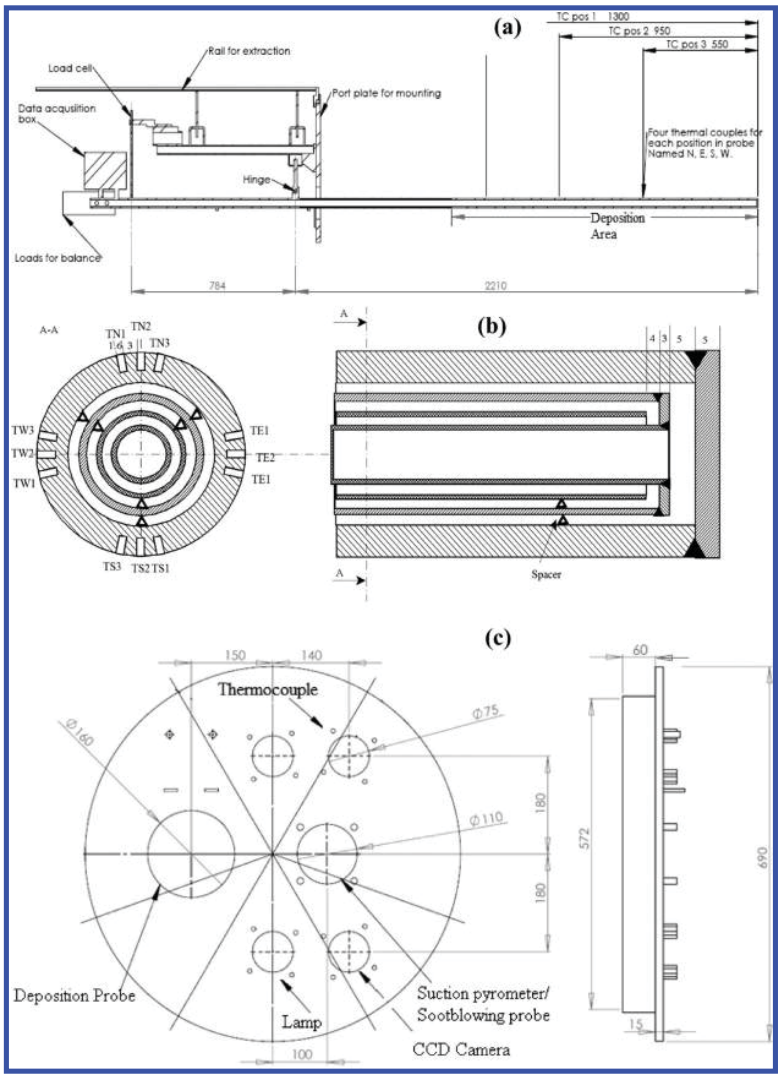

Figure 2. Schematic presentation of the probe and the complete port: (a) schematic view of the probe with identified positions of temperature measurements, deposition area, port plate for mounting, hinge, load cell, and rail for pulling out the probe, (b) cross-sectional view perpendicular to probe axis and cross-sectional view along axis of annuli, (c) schematic drawings of the port plate used during the measurements.

sample collected just before the burners. This causes a slight difference in fuel ash contents reported in Tables 2 and 3. It should be mentioned that the pure straw and wood fuel samples shown in Table 2 were collected from the fuel silos, while fuel sample just before the burners was collected almost daily during each test.

The particle size distribution of the fuel particles collected just before the burners showed that close to 50% of the particles were below 500 μm (Figure 3), while about 10 wt % of the particles had a size between 1.2 and 3.1 mm.

2.4. Procedure of Experiments. A series of probe measurements were conducted in the superheater region, just above the screen tubes. The influence of fuel type, probe exposure time, flue gas temperature and probe surface temperature on deposit formation rate was investigated. The fuel contained from 0 to 85 wt % straw share in wood. Each measurement lasted 2−18 days. The deposition probe was exposed to flue gas temperatures from 600 to 1050 °C. Probe surface temperatures were varied between 500 and 600 °C in order to investigate ash deposit formation rate at different probe surface temperatures. A complete summary of all the conducted measurements is presented in Table 3.

Retractable steam soot blowers were used for 5−10 min (each soot blower) at regular intervals during boiler operation, typically at 8 h intervals. The soot blower located nearest to the probe measuring position (approximately 1 m to the left) was shut down during tests 1−5, while soot blowers located further away from the measuring position were in operation during all the tests.

Ash transformation was investigated by elemental analysis of inorganic elements in the fuel ash, residual ash and deposit samples for different straw shares in wood by ICP-IC (inductively coupled plasma-ion chromatography) analysis. Fly ash was collected from electrostatic precipitators by using a spear to collect a representative sample. Bottom ash was collected from the water and ash pit at the bottom of the furnace.

3. RESULTS AND DISCUSSION

3.1. Data Treatment. The results represented in this paper are from full-scale measurements on a large operating power plant boiler. Hence, full control over all conditions influencing measurements cannot be achieved. In particular, two aspects of the measurements will be considered.

One aspect is the influence of operating conditions on temperature measurements, where the primary data were thermocouple readings of the flue gas temperature. Radiation, flow fluctuations, and particulates in the gas phase can all influence

dx.doi.org/10.1021/ef201680k | *Energy Fuels* 2012, 26, 2317−2330

Table 2. Analysis of Straw and Wood Pellets Used at AMV1[a]

param.	procedure	straw (Køge)	wood (Kunda*)	80−85% straw (test 1)	65−70% straw (test 5)	60−65% straw (test 5)	60−65% straw (test 5)	40−45% straw (test 5)
day/month/year (time)				22/03/2010	19/04/2010	20/04/2010 (13:00)	20/04/2010 (17:00)	21/04/2010
ash contents (wt %, a.r.)	EN 14775:2009	6.03	0.80	5.26	4.32	3.56	3.63	2.74
ash contents (wt %, d.b.)	EN 14775:2009	6.54	0.86	5.63	4.57	3.78	3.84	2.88
moisture (wt %, a.r.)	EN 14774-3:2009	7.86	6.83	6.67	5.61	5.94	5.55	5.03
higher heating value (MJ/kg, d.b.)	EN 14918:2010	18.71	20.47	17.62	19.68	19.39	19.35	19.87
volatiles (wt %, d.b.)	EN 15148:2009	80.91	85.24	82.87	82.58	82.15		83.11
C (wt %, d.b.)	CEN/TS 15104:2006	50.52	55.54	51.16	52.44	52.89	52.57	53.91
S (wt %, d.b.)	CEN/TS 15289:2006	0.15	0.035	0.121	0.105	0.095	0.093	0.068
N (wt %, d.b.)	DS/EN ISO 10304-1:2009	0.59	0.73	0.8	0.62	0.63	0.68	0.75
H (wt %, d.b.)	EN 14918:2010 calcd.	5.79	6.15	5.85	5.92	5.97	5.96	6.02
O (wt %, d.b.)	EN 14918:2010 calcd.	36.11	36.68	36.43	36.19	36.45	36.67	36.28
Cl (wt %, d.b.)	DS/EN ISO 10304-1:2009	0.290	0.003		0.155	0.184	0.191	0.093
				Ash Analysis (wt %, d.b.)				
Al_2O_3	DIN 51729/ ASTM3682	0.66		0.95	1.88	1.30	0.97	2.11
CaO	DIN 51729/ ASTM3682	14.56		8.30	9.97	11.05	11.80	17.69
Fe_2O_3	DIN 51729/ ASTM3682	0.50		0.47	6.81	1.03	0.58	1.13
K_2O	DIN 51729/ ASTM3682	17.88		15.25	12.58	15.92	20.41	13.96
MgO	DIN 51729/ ASTM3682	3.39		2.25	2.11	2.29	2.54	2.90
Na_2O	DIN 51729/ ASTM3682	0.69		0.57	0.59	0.87	1.04	1.03
P_2O_5	DIN 51729/ ASTM3682	5.56		2.47	2.17	2.46	2.60	2.13
SO_3	DIN 51729/ ASTM3682	2.43		2.36	2.03	2.16	1.88	2.43
SiO_2	DIN 51729/ ASTM3682	44.51		52.05	44.89	49.15	46.95	36.87
TiO_2	DIN 51729/ ASTM3682	0.05		0.06	0.11	0.10	0.06	0.13

[a]a.r.: as received, d.b.: dry basis. * one type out of four.

the readings, but in rather unpredictable ways. Hence, some suction pyrometer readings were taken, and together with determinations of other operating conditions, these measurements allowed a correction of the thermocouple values. The procedure is discussed in detail in section 3.1.1.

The other aspect is the deposit formation rate determinations. In an ideal world, where deposited mass is monitored continuously with little or only insubstantial noise and no deposit shedding, there is no doubt that the time derivative of the mass uptake signal is the true deposit formation rate. However, the measuring probe mass uptake signal, on which this paper is based, includes noise, larger shedding events, and eventually some smaller (minor) shedding events, with a magnitude on the same level as the noise. The shedding events may therefore be divided into two classes: one type of events, macro-events, with so much shedding that the event times mark points across which deposit formation rate calculations cannot be done by averaging, and another type, microevents, that are not clearly distinguishable from externally generated noise contributions, across which it is necessary to do averaging when calculating something that is representative of the true deposit formation rate.

With this kind of measured data, it is necessary to use a terminology that clearly distinguishes between (a) (true) deposition rate, (b) a measure of the deposition rate found as an average of the time derivative over periods that do not include major shedding events but do include some minor shedding events in addition to noise (called derivative-based deposit formation rate, DDF-rate), and finally (c) the overall measure where the difference in deposit mass at two different times is divided by the time difference and, in this case, with no particular concern about the presence or absence of even major shedding events (called integral deposit formation rate, IDF-rate). Each of these measures of deposition rate has its use, but it is important in the discussion of the data to distinguish between them.

The DDF-rate is determined by calculating a smoothed time derivative of the short time averaged deposit mass uptake signals. The time interval for smoothing includes minor shedding events that cannot *a priori* be distinguished from measurement noise but excludes larger shedding events. A more detailed description of the

Table 3. Experimental Summary of Conducted Measurements

test no.	1	2	3	4	5	6	7	8
day/month/year	22/03/2010 −25/03/2010	27/03/2010 −29/03/2010	29/03/2010 −06/04/2010	06/04/2010 −09/04/2010	15/04/2010 −22/04/2010	07/05/2010 −25/05/2010	25/05/2010 −08/06/2010	08/06/2010 −18/06/2010
straw (wt %)	80−85	60−65	30−35	40−50	40−50	0−10	0−10	0−10
fuel ash content (wt %)	~5.2	~4.0	~2.4	~3.4	~3.4	~1.0	~1.0	~1.0
probe temp. (°C)	500	600	500	500	500 (600)	550	550	550 (600)
exposure time (h)	56	45	185	73	168	434	335	212

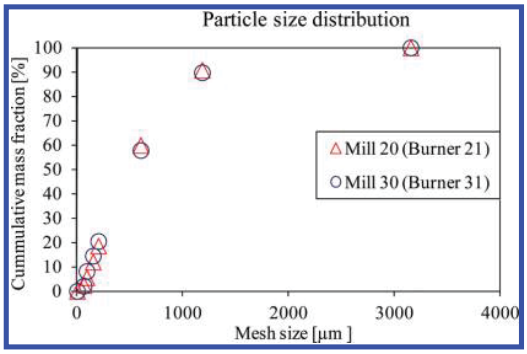

Figure 3. Particle size distribution of fuel collected from two burners connected to two different mills (test 1, 22/03/2011). The particle size distribution was determined by a sieve analysis.

procedure is given in section 3.1.2. Since the averaging time is relatively short, and since a time smoothed derivative is the result, we settled on this measure to be called DDF-rate: derivative-based deposit formation rate. DDF-rates should represent fairly characteristic net-deposition rates, allowing its dependence on operating conditions to be determined.

The IDF-rate is a cruder measure of deposit formation rate determined as the mass deposited on the probe over large time intervals divided by the time interval length. The IDF-rate includes both minor and major shedding events of any kind and is similar to deposit formation rates determined from previous full-scale probe measurement data.[14,24] More details about the procedure are given in section 3.1.3.

3.1.1. Corrected Flue Gas Temperature. The flue gas temperature near the probe was continuously measured, using a simple thermocouple in a protective shell, while suction pyrometer based temperature measurements were only conducted for a limited time during each experiment. The suction pyrometer measurements were conducted for 0.5 to 2 h, ranging from 1 to 3 measurements during each test. During suspension firing of biomass, the radiation effects were stronger compared to biomass grate firing,[17,18] and a typical higher flue gas temperature in the range 50−200 °C was observed by the suction pyrometer. The presence of deposits in the experimental region may cause a difference between thermocouple and suction pyrometer measurements due to changed radiation conditions. Other possible factors responsible for a temperature difference can be the fuel flow through mills located in the top positions (mill 30, top; mill 20, middle; Figure 1) leading to a change in flame position, fuel oil loading, and overall boiler load. These physical causes provided the basis for the initiation of the following empirical model relating a prediction of the gas temperature, Y_{calc}, to the actual measured thermocouple temperature, Y_{TC}:

$$Y_{calc} = Y_{TC} + \mathrm{Diff}_{pred} \quad (2)$$

$$\mathrm{Diff}_{pred} = A + BX_{ash} + CX_{oilload} + DX_{boilerload} + EX_{mill20} + FX_{mill30} \quad (3)$$

X_i in eq 3 represent measured operational parameters likely to influence the difference between the suction pyrometer temperature (Y_{meas}) and the thermocouple temperature (Y_{TC}). X_{ash} (0.70−5.26, wt %) represents the fuel ash content, $X_{oilload}$ (0.0−160.7, MW_{th}) is the fuel oil loading, $X_{boilerload}$ (59.0−93.4, %) is the relative boiler load, and X_{mill} (0.0−7.2, kg/s) denotes the fuel flow rate through the mill indicated. Parameters A−F are empirical constants determined through fitting of the above equations to the true temperatures, Y_{meas}, measured by the suction pyrometer. The fitting was carried out by minimizing the sum of squares (SS). Not all of these operational parameters may have a significant influence on the correction. Hence, we used the methods outlined by Kittrell[28] and Pritchard et al.,[29] based on the variance−covariance matrix, to assess which parameters were most important. The final result of the fitting procedure was that the predicted temperature difference could be described well by eq 4.

$$\mathrm{Diff}_{pred} = BX_{ash} + CX_{oilload} + DX_{boilerload} + EX_{mill20} \quad (4)$$

with the parameters shown in Table 4. The plot of predicted flue gas temperature versus the measured suction pyrometer temperature is shown in Figure 4. It can be seen that the predicted temperature values are close to the measured temperature values.

Table 4. Calculated Constants for Flue Gas Temperature Prediction Model with Estimated Confidence Intervals

constant	value
B	23.11 ± 1.25
C	0.195 ± 0.041
D	0.084 ± 0.068
E	4.78 ± 0.48

dx.doi.org/10.1021/ef201680k | *Energy Fuels* 2012, 26, 2317−2330

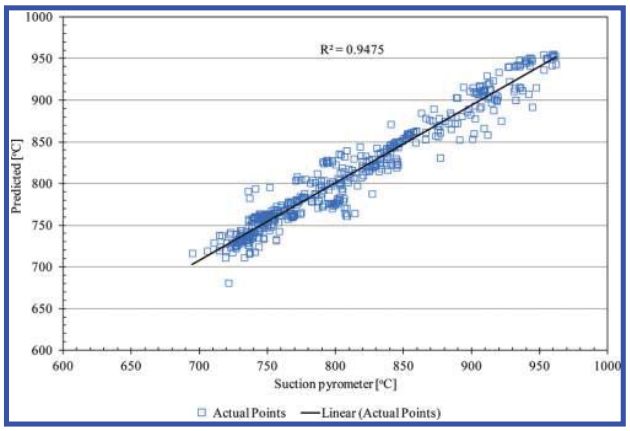

Figure 4. Comparison of measured (suction pyrometer) and calculated flue gas temperature. The predicted points are calculated from the thermo-element temperature and boiler operational data using eqs 2, 3, and 4.

3.1.2. Derivative-Based Deposit Formation Rate (DDF-Rate). The amount of deposit collected on the probe is a function of both the deposit formation process and shedding events. An example of raw data of flue gas temperature, deposit mass uptake, and heat uptake of test 1 is shown in Figure 5. The flue gas temperatures measured using a thermocouple are between 500 and 800 °C. The deposit mass uptake signals show both natural and plant sootblowing shedding events (observed as a sudden deposit mass loss on the curve). The deposit is influenced by several processes: large shedding events, minor shedding events, a relatively slow deposit build-up process, and some noise mainly caused by boiler fluctuations. Boiler fluctuations could be mechanical vibrations or large changes in boiler flow dynamics. The most severe fluctuations are observed when the boiler plant soot blowers were in operation. Even though the plant soot blower nearest to the probe was shutdown, the thermal and mechanical fluctuations were induced by the rest of the soot blowers and that could cause some shedding. To analyze data systematically under these conditions where noise and small and large shedding events are present, a deposit mass uptake signal treatment method is developed and applied to the measuring data. The method allows us to identify shedding events and can quantify the deposit formation rate between major shedding events. The idea is to average out the noise in the deposit mass uptake signals and to identify the larger shedding events. When the plant (and probe) artificial soot blowers are used, the probe mass signal noise level increased, and therefore, the DDF-rate determinations were not done on mass uptake signal data obtained during plant soot blower operation.

The steps involved in the deposit mass signal treatment to calculate the DDF-rate are based on Matlab procedures[30−33] as follows:

Step A: The deposit mass uptake signals are filtered using a 10 point resampling method implemented in Matlab.[30] This effectively smooths the data over 10 points, returning one resampled data point for further use.

Step B: Slope calculations are done using a moderately low order polynomial (3rd order, current case) that is

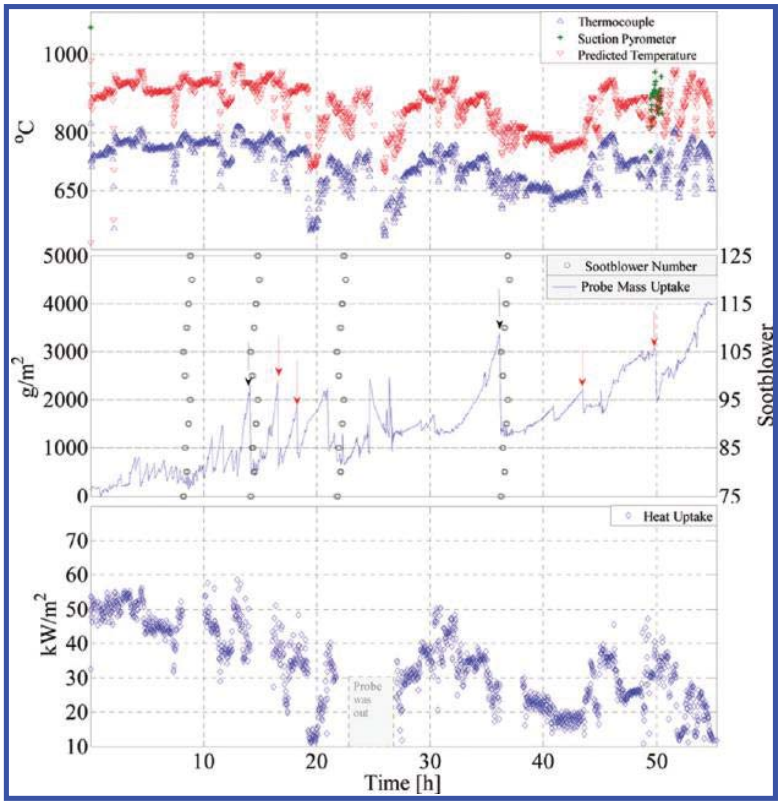

Figure 5. Raw data of flue gas temperature, deposit mass uptake, plant sootblowing events (specific number of soot blower in operation) and probe heat uptake during test 1. Red arrows with continuous line indicate natural deposit sheddings, while black arrows with discontinuous line indicate deposit shedding through plant sootblowing. The soot blower number represents a specific soot blower in the superheater region as seen on the secondary *y*-axis (middle figure).

dx.doi.org/10.1021/ef201680k | *Energy Fuels* 2012, 26, 2317−2330

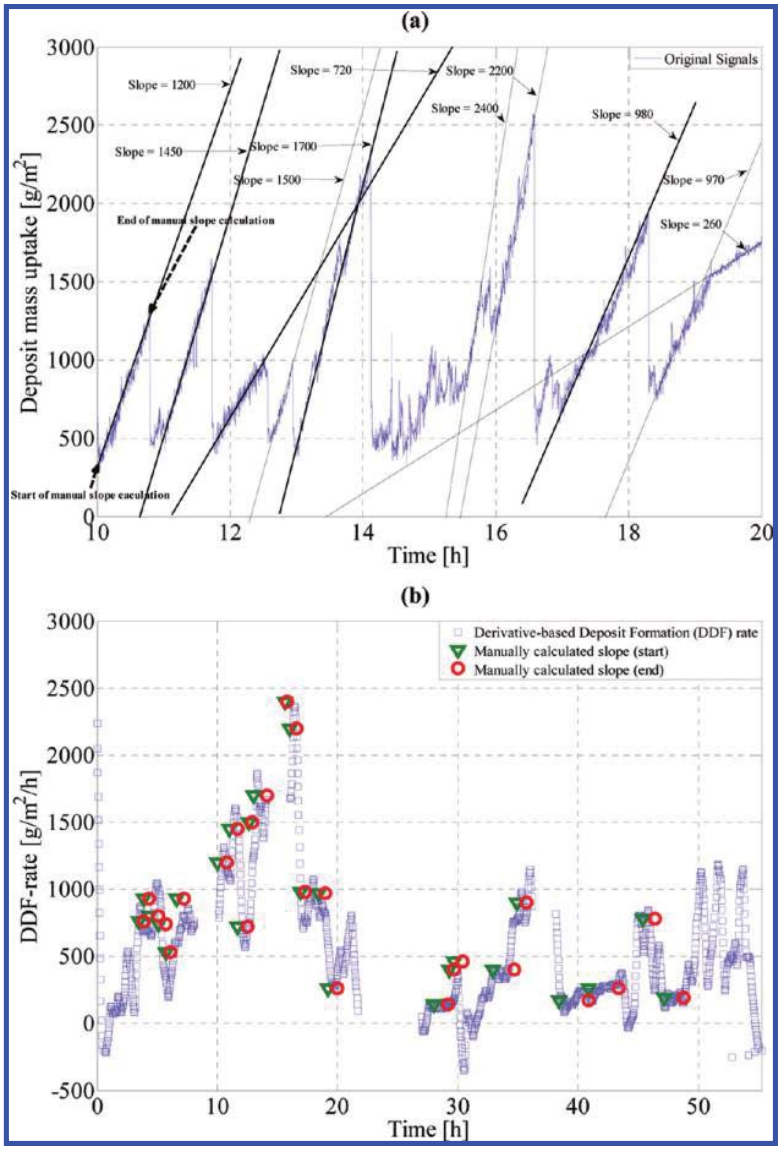

Figure 6. (a) Approximate manually calculated slopes of deposit mass uptake signals during 10−20 h of exposure time during test 1; (b) comparison of manually calculated slopes and slopes calculated by the mathematical procedure (DDF-rate) for complete test 1.

fitted to the data in a sliding window (5 data points), and finally, differentiation of the model is performed.[31]

Step C: Cut off of negative slope values is made to remove major shedding events. The cut off level is adjusted to determine the number of major shedding events accurately while still giving a satisfactory prediction of apparent deposit formation rates. A high cut off level (e.g. −200 g/(m^2·h)) may count some noise as shedding events, which results in higher deposit formation rate values. A low cut off (e.g. −6000 g/(m^2·h)) will include some shedding in the DDF-rate calculation and results in lower deposit formation rate values. The selected cut off level was −3800 g/(m^2·h) for all the tests. This represents a subjective judgment that strikes a balance between determining the most shedding events (a high cut off level is needed) and not removing selectively a negative noise contribution to the DDF-rate determination (a low cut off level is needed).

Step D: Smoothing of the raw slope calculations is made using a moving average filter over 31 points.[32] Our choice of 15 data points on each side of the *i*th data point represents a subjective judgment that balances effective smoothing against undesired removal of minor, but significant, variations in the deposit formation rate. The result of the smoothed data is the DDF-rate.

This complete procedure was validated. It should be kept in mind that our aim is to treat all data systematically once the subjective judgments of steps C and D have been made, thus avoiding the pitfall of seeing or not seeing trends from case to case based on incomparable criteria. To validate the above described procedure of deposit formation rate determination as DDF-rates, manual slope calculations were done on the original deposit mass uptake signals of test 1. Test 1 is appropriate for comparison because the probe mass uptake signals during this test cover three kinds of behavior: (1) with small but frequent shedding events (3−10 h), (2) with large but more frequent shedding events (10−20 h), and (3) with less frequent

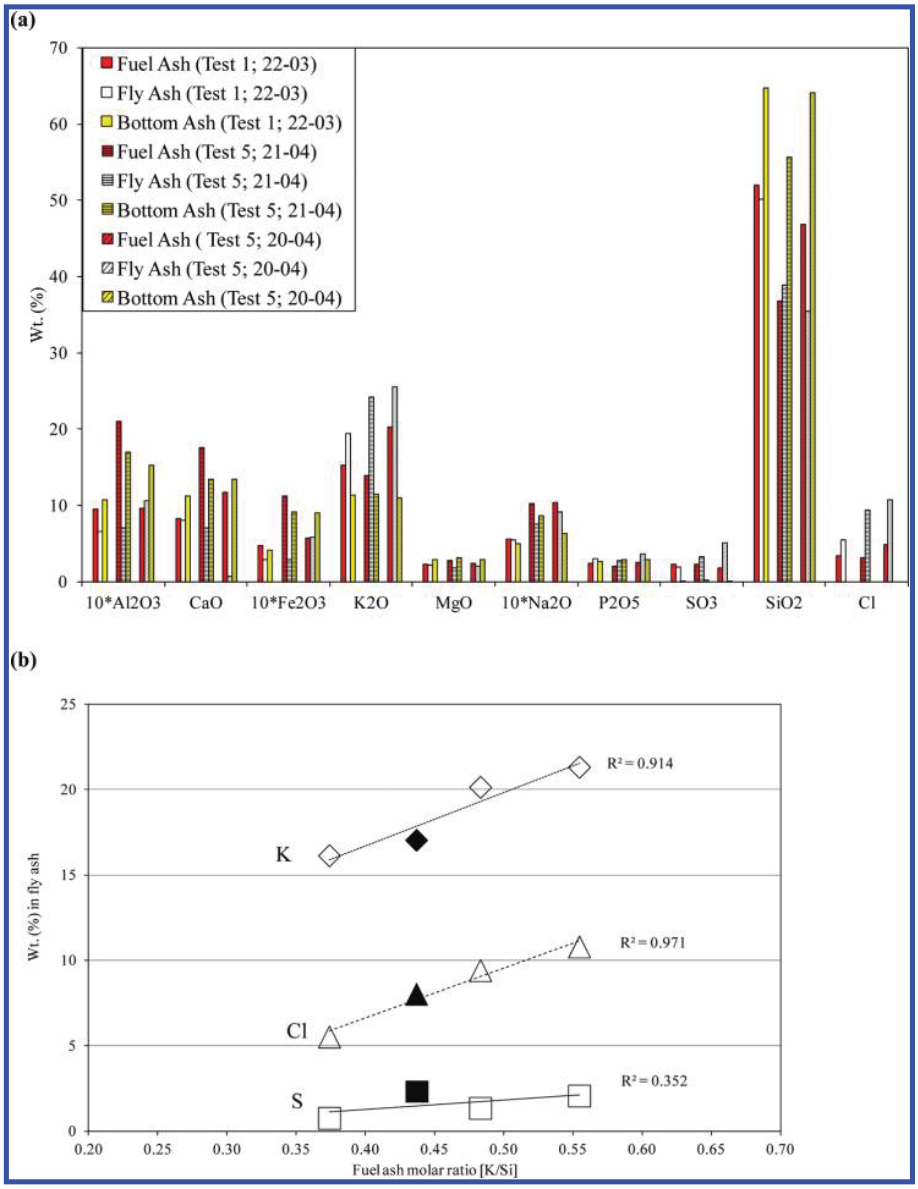

Figure 7. Ash transformation during straw and wood (straw > 46 wt %) suspension combustion: (a) comparison of fuel, fly, and bottom ash samples from tests 1 and 5; (b) impact of molar K/Si ratio in fuel ash on the content of K, Cl, and S in the fly ash. The filled points show data from straw suspension-fired measurements at Amager Unit 2,[24] while the rest of the points are from the current measurements.

shedding events (28−55 h) (Figure 5). The approximate manually calculated slopes of the 10−20 h interval during test 1 are shown in Figure 6a, and a comparison of these slopes and the calculated DDF-rates using the procedure described above is shown in Figure 6b for complete test 1. It is clear that the DDF-rates calculated by steps A through D are in good agreement with manually calculated average deposition rates. Since smoothing in step D is across shedding events, just excluding the most negative slopes in step C, the procedure results in a continuous change between the discrete levels determined by the manual procedure. This is an acceptable price to pay to get a consistent analysis of all data points and test series. The above procedure is thus adopted for the first five tests (Table 3), and the results are used to identify the influence of experimental conditions and boiler operational conditions on DDF-rates.

3.1.3. Integral Deposit Formation Rate (IDF-Rate). The deposit formation rate (g/(m^2·h)) can also be determined based on the mass increase divided by a given probe exposure time, and we have called this the integral deposit formation rate (IDF-rate). The IDF-rate is then the result of both the deposit formation rate and shedding events in a given period. In this work, IDF-rates were determined using 12 h intervals. The IDF-rate is similar to deposit formation rates determined from previous full-scale measuring data.[14,24] The latter were calculated by taking the probe out, collecting the deposits, and dividing the amount of deposits by the time the probe was inside the boiler.

3.2. Chemical Compositions of Fuel Ash, Residual Ash, and Deposits. Representative samples of the fly ashes were collected from electrostatic precipitators by using a spear, while the bottom ash was collected from the water and ash pit at the bottom of the furnace. ICP-IC analysis was used to

dx.doi.org/10.1021/ef201680k | *Energy Fuels* 2012, 26, 2317−2330

determine the concentration of major elements in the fuel, fly, and bottom ash and deposit samples. The bulk ash compositions of the fly ashes obtained from two days (22/03/2010 and 23/03/2010) during test 1 were almost identical under almost identical operating conditions, thereby supporting the reliability of the measurements. The bulk compositions of fuel, fly, and bottom ash samples collected during test 1 and 5 are shown in Figure 7a. It is seen that the content of the most of the volatile elements (K, Cl, S) in the fly ash (colorless bars) are greater than in the fuel ash (red bars), while Ca and Si remained either almost in the same proportion or were reduced. It can also be seen that bottom ashes (yellow bars) are dominated by Si and Ca, with almost no S and Cl, possibly caused by the high volatility of S and Cl during straw and wood combustion at higher temperatures.[8,15,20,34] Compared to the fly ash from a straw grate-fired system that is rich in volatile elements, K, Cl and S, the fly ash from straw suspension firing is dominated by K, Si, and Ca.[17,19] It can also be seen that, with an increase in fuel ash K/Si molar ratio, the concentration of volatile elements, K, Cl, and, to some extent, S, increased in the fly ash (Figure 7b). This suggests that the presence of Si tends to retain K as K−silicate in the ash and residual K can bind Cl and S in the fly ash as KCl and K_2SO_4. It has also previously been reported that the fraction of water-soluble K (KCl and K_2SO_4) in the fly ash increases with increased fuel ash K/Si molar ratio.[8,34]

The composition of the probe upstream and downstream deposit layers is shown in Figure 8. The inner layers (on the upstream and on the downstream side) were rich in K, Cl, and S. K, S, and Cl were found in higher proportions on the downstream side of the probe indicating that thermophoresis and/or condensation of KCl and K_2SO_4 is important for the deposit formation process on the downstream side. The upstream side deposit outer layers contain large amounts of Si, K, and Ca, indicating that larger particles predominantly impact on and stick to the upstream side of the probe.

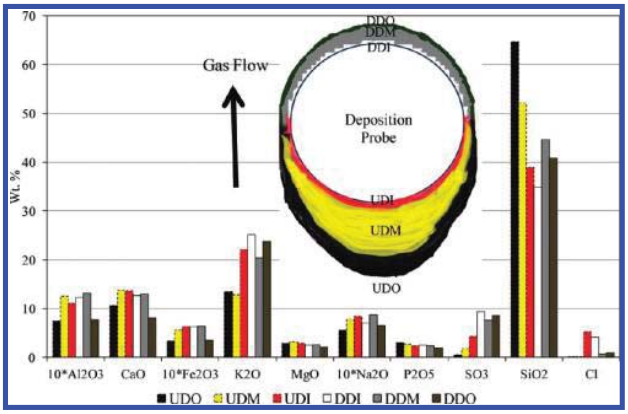

Figure 8. Bulk ash analysis of deposit layers removed from the probe after it was taken out of the boiler (straw share > 46 wt %, tests 1 and 5). UDO, upstream deposits outer layer; UDM, upstream deposits middle layer; UDI, upstream deposits innermost layer; DDI, downstream deposits innermost layer; DDM, downstream deposits middle layer; DDO, downstream deposits outer layer.

3.3. Comparison of Results with Previously Conducted Probe Measurements. Probe deposit formation measurements performed on biomass-fired boilers can be found in literature.[14,16,19,22] The ash deposit formation rates in these measurements were determined by dividing the collected amount of the probe deposit with the probe exposure time. A comparison of these previously determined probe deposit formation rates and the IDF-rates from this study (tests 1−8) is presented in Figure 9. The IDF-rate in the present study was calculated from the deposit mass uptake signals after initial 12 h to obtain data that can be compared with previous biomass suspension-fired deposit measurements.[14,24] The deposit formation rates determined in the previous full-scale measurements are also reported as IDF-rates for a better comparison.

As seen in Figure 9a, there is a general tendency that an increased alkali content in the fuel (or increased straw share in wood) and an increased flue gas temperature results in an increased IDF-rate. The trend is seen both for grate firing and suspension firing. At a flue gas temperature of 650 °C, the IDF-rate is typically from 5 to 30 g/(m^2·h) and at 900 °C, the IDF-rate is typically 20 to 110 g/(m^2·h). Skrifvars et al.[22] measured IDF-rate of 40 g/(m^2·h) at 920 °C and 7 g/(m^2·h) at 750 °C in a wood fired pulverized fuel boiler. Bashir et al.[24] measured IDF-rate of 1 g/(m^2·h) during wood suspension firing at a flue gas temperature of 586 °C, while IDF-rates of 41 g/(m^2·h) and 56 g/(m^2·h) have been measured during straw suspension firing at flue gas temperatures of about 850 °C.[14,24] Overall, the IDF-rates during straw firing in suspension and grate boilers are on similar levels, as indicated in Figure 9a. This is seen even though the percentage of fuel ash retained as fly ash can be considerably higher during suspension firing, compared to grate firing.[2]

It can be seen in Figure 9a that when firing a fuel with high alkali contents (K > 0.9 wt %, yellow and red points), the increase in IDF-rate with flue gas temperature is steeper compared to the increase in the IDF-rate with a fuel with low alkali contents (K ≤ 0.9 wt %, violet and black points). Possibly the content of gas phase alkali and the fraction of molten ash increased at increased flue gas temperatures, and both will lead to an increased deposit formation rate. It is also seen that the probe surface temperature has no significant influence on the IDF-rate (Figure 9b). The changed probe surface temperatures in the range from 400 to 650 °C do not seem to have significant influence on the deposit formation rate.

The calculated overall derivative-based deposit formation (DDF) rates were between 234 to 3105 g/(m^2·h) during tests 1−5, which are much higher than the IDF-rates. This is in agreement with expectations since IDF-rates are influenced by all shedding events during the time interval of the deposit collection. The IDF-rates provide deposit formation values that will approximately be experienced by the boiler operation personal. However, to provide more detailed information and to test models that separate the deposit formation and shedding processes, the DDF-rates data are needed.

3.4. Influence of Local Conditions on the DDF-Rate. To make it possible to investigate the influence of different operational parameters on the DDF-rates, each test was divided into further subtests based on the number of hours (usually 6 h). A significant number of data points thus allowed us to analyze the influence of local flue gas temperature and boiler operational parameters on the DDF-rates. The DDF-rate as a function of flue gas temperature is shown in Figure 10a. The figure also shows information about the applied probe temperature, straw share in wood, and deposit mass load. No significant influence of changed probe surface temperature on the DDF-rates is seen. There is observed an increase in DDF-rates with increase in flue

dx.doi.org/10.1021/ef201680k | Energy Fuels 2012, 26, 2317−2330

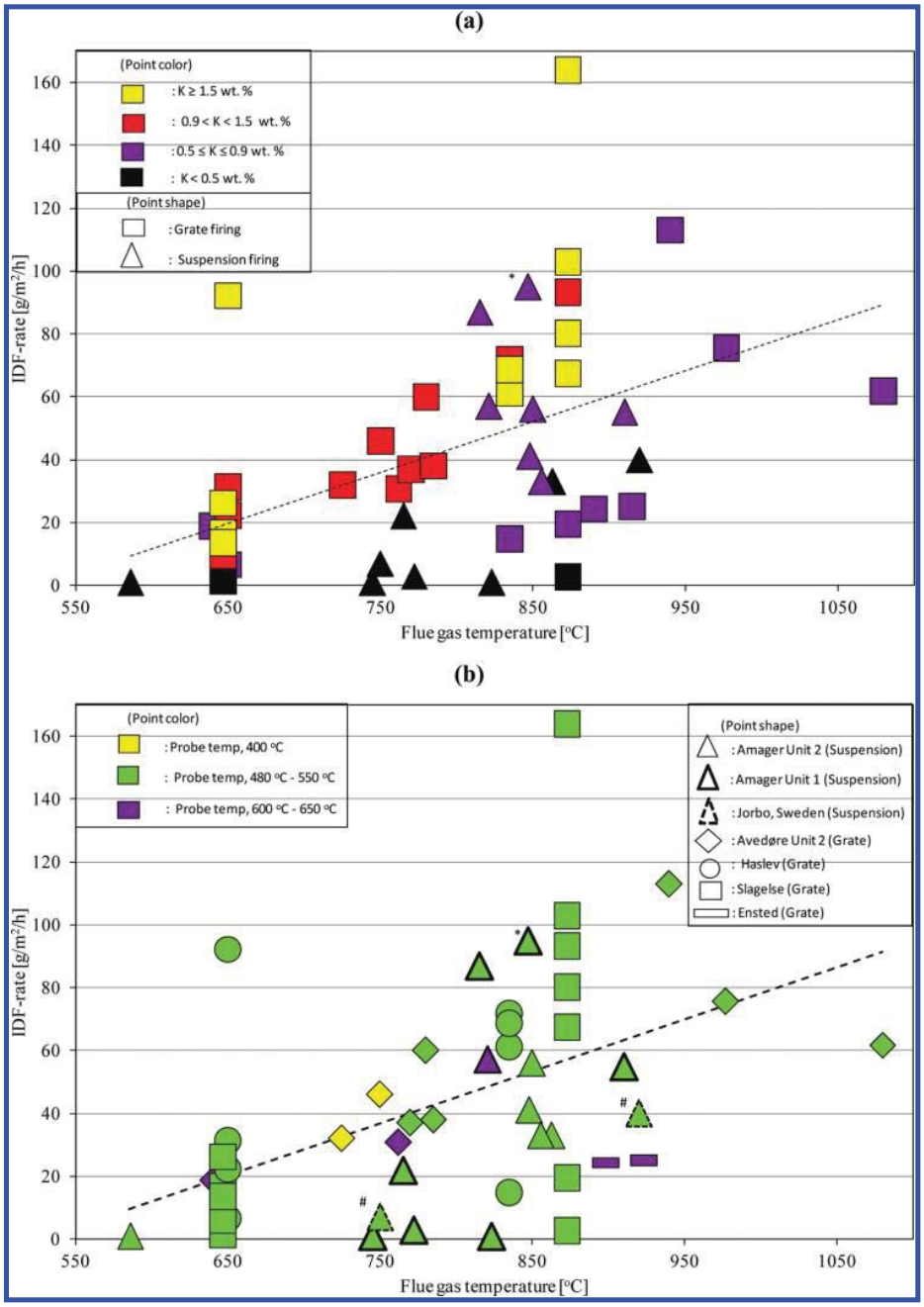

Figure 9. Impact of flue gas temperature on IDF-rates (12 h): (a) comparison of deposit probe measurements data at different fuel alkali levels and two types of straw firing technologies; (b) comparison of the some data set with marking of the probe surface temperature and boiler where the measurements were preformed. Amager Unit 2 and Unit 1 are straw and/or wood-fired suspension boilers. Jorbo, Sweden is a down-fired pulverized fuel boiler. Avedøre Unit 2, Slagelse and Ensted are straw-fired grate boilers. Haslev is a cigar type boiler where big bales of straw are fired directly.[14,16−19,22,24] Graph details: (a) the color represents the range of fuel alkali in wt %, while the particular point shape represents the straw firing technology; (b) the color represents the probe surface temperature, while the particular point shape represents the boiler type. * indicates the point where IDF-rate was calculated after 6 h. # indicates the point where the IDF-rate was measured with the short-term (about 2 h) deposit probe. For grate-fired boilers, the IDF-rate was calculated between 4 to 27 h. (Modified with permission from ref[24]. Copyright 2012, Elsevier. (Additional data of current measurements and data from Jorbo boiler were added.))

gas temperature. It can be seen that the DDF-rates increased strongly above a flue gas temperatures ranging 850−880 °C. There is only one exception and that is data from the 16/04/2010 (test 5), where a fuel particle grindability problem occurred in mill 20, and this probably caused the observed high DDF-rates. A possible reason for the increased DDF-rate at higher flue gas temperatures could be that the K−silicate and K−Ca−silicate particles hitting the probe to a higher degree are molten, and thereby a larger fraction of the impacted ash particles sticks to the deposit probe. A similar trend of increase in DDF-rate with increase in flue gas temperature was seen for the overall mean DDF-rate of each test, as shown in Figure 10b. Increased deposit

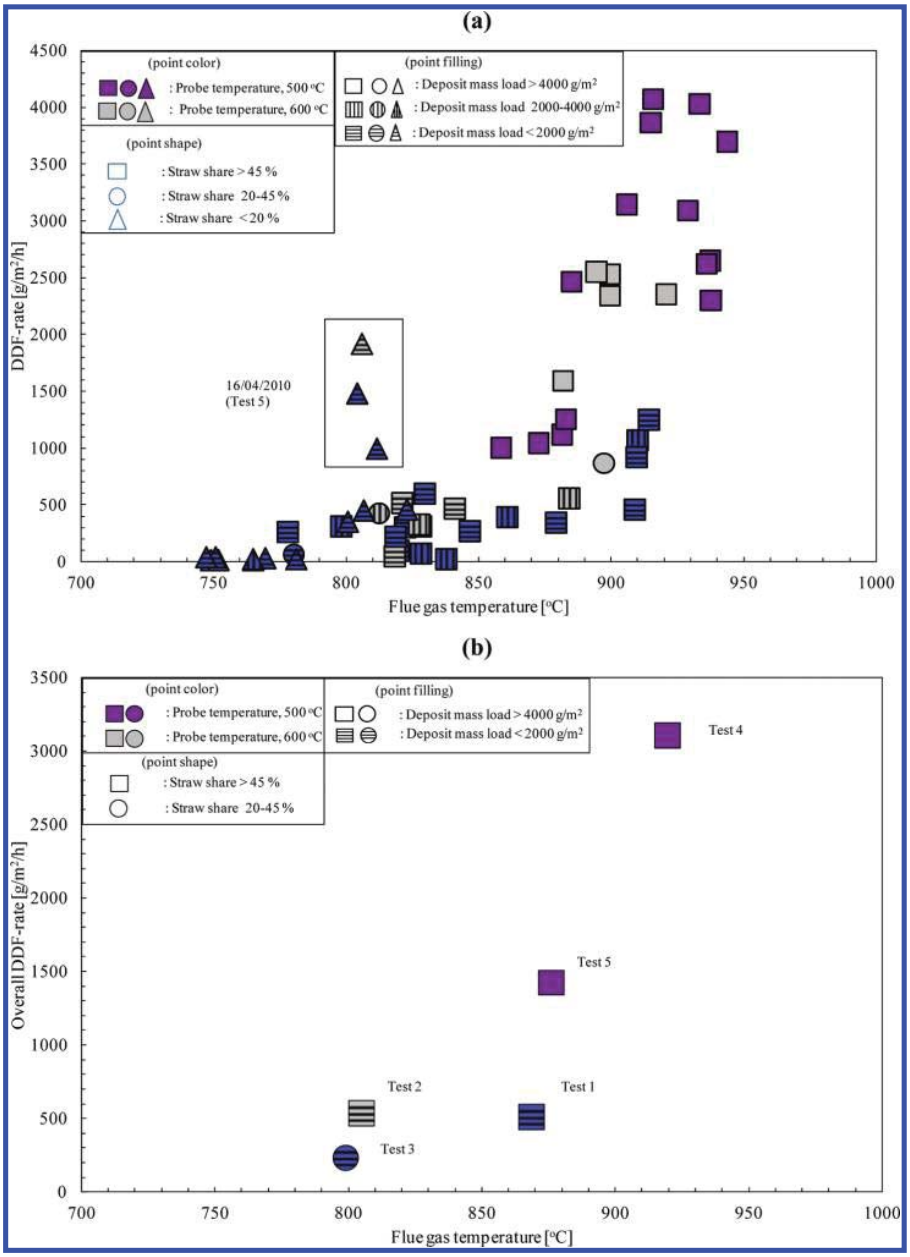

Figure 10. Impact of flue gas temperature on (a) the DDF-rate, data points from tests 1−5 and (b) overall DDF-rate, tests 1−5. Graph details: the color represents the probe surface temperature; the particular point shape represents the straw share with wood in wt %, while the particular point filling indicates the deposit mass load.

formation rate with increased flue gas temperature has also been seen in the previous full-scale measurements conducted at different straw grate-fired boilers.[14,16−19] The DDF-rate is lower at lower straw shares in wood and higher at high straw shares possibly due to the changed total fuel ash content level and changed melting properties of the fly ash. Reduced ash deposit formation rates during straw cofiring with woody biomass, compared to pure straw suspension firing have been observed by Nordgren et al.,[20] Bashir et al.,[24] and Lokare et al.[25] Lower ash deposit formation rates have been shown in previous full-scale measurements at straw grate-fired boilers for reduced alkali contents in straw.[14,16−19]

The very steep increases in the DDF-rates above approximately 850 °C are suggestive of an exponential, Arrhenius-like dependence on temperature. In Figure 11a, the logarithm of the DDF-rate is shown as function of the reciprocal of the absolute temperature. A straight line limit below which the majority of data lies is shown, but clearly a large spread is evident. The general trend is, however, followed by all points, and it appears that the data points all lie in a band between two straight lines. A similar Arrhenius-like trend is seen for overall mean DDF-rate of each test, as shown in Figure 11b. The equation of the straight line is

$$\ln(\text{DDF-rate}) = \frac{-23400}{T} + 28 \quad (5)$$

Since the full-scale measurements have been conducted in a commercial boiler, the information presented in Figures 10 and 11

dx.doi.org/10.1021/ef201680k | Energy Fuels 2012, 26, 2317−2330

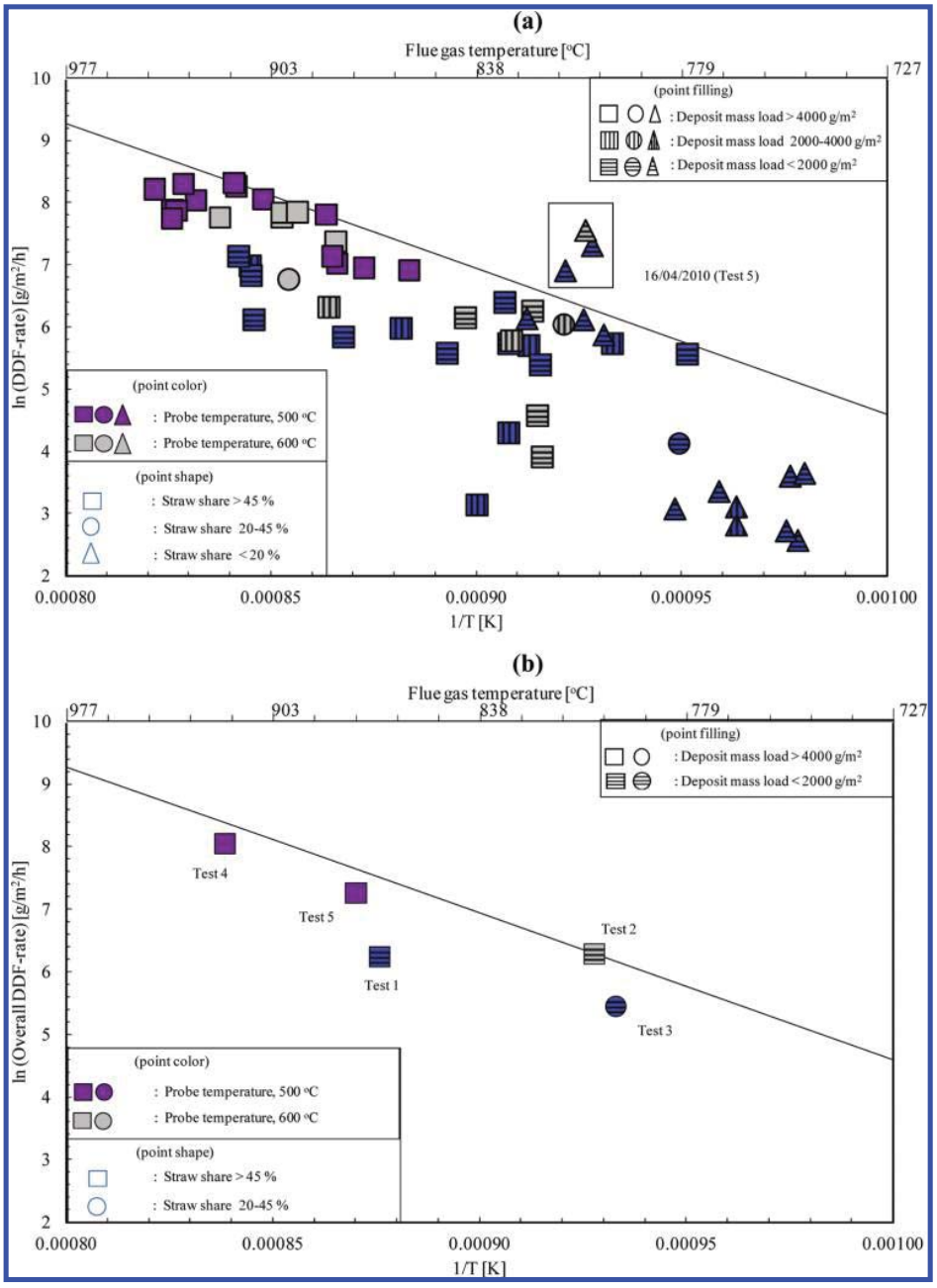

Figure 11. Logarithm of the (a) DDF-rate as a function of reciprocal of absolute flue gas temperature, data points from tests 1−5 and (b) overall DDF-rate as a function of reciprocal of absolute flue gas temperature, tests 1 to 5. Graph details: the color represents the probe surface temperature; the particular point shape represents the straw share with wood in wt %, while the particular point filling indicates the deposit mass load. The flue gas temperature in degrees Celsius is shown in the secondary *x*-axis.

may be used to predict the deposit formation rate levels in the superheater region of a biomass suspension-fired boiler. The information can be used to estimate deposit formation levels as a function of surface temperature, flue gas temperature, and fuel alkali content. Regarding the practical implications for the boiler operation personnel, the increase in probe surface temperature from 500 to 600 °C will not be a significant concern, but a higher fuel alkali contents in addition to higher fuel ash K/Si molar ratio and a flue gas temperature higher than 880 °C can result in significant deposit formation on the superheater tubes.

A prediction of fly ash melt fraction as a function of temperature based on the fly ash compositions was made by using the model proposed by Zhou et al.[35] (Figure 12). The fly ashes have a first melting temperature (FMT) between 640 and 645 °C, but at higher temperatures (>800 °C), a significant fraction of molten fly ash is seen, and this could lead to a greatly increased probability of the fly ash to stick to the deposit probe. This probably induces the higher DDF-rates at higher flue gas temperatures (Figure 10). The higher melt fraction of fly ash from test 5 may lead to a larger probability of the generated fly ash to stick to probe, causing a higher overall DDF-rate

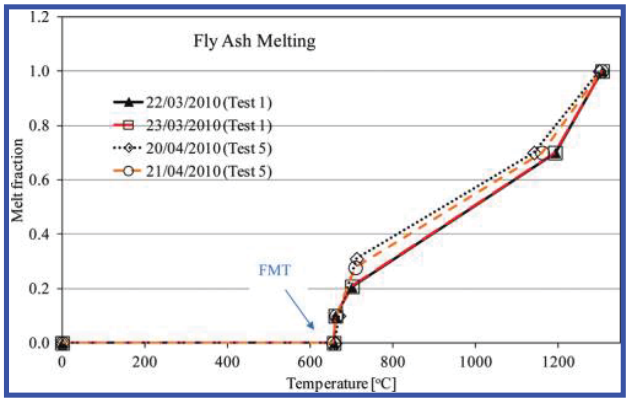

Figure 12. Fly ash melt prediction using predictive model of Zhou et al.[35]

measured for test 5 compared to test 1 (Figure 10b). The influence of fly ash composition on the melting curves indicates that the presence of the elements K, Cl, and S strongly influences the ash melt fraction.[35]

4. CONCLUSIONS

A series of full-scale probe measurements have been conducted in a biomass suspension-fired boiler to investigate ash deposit formation when firing straw and wood. The influence of fuel type, probe exposure time, probe surface temperature, and flue gas temperature on ash deposit formation rate has been investigated. A systematic procedure to determine deposit formation rate from probe measuring deposit data was developed and termed the derivative-based deposit formation rate (DDF-rate). A comparison with previously conducted probe measurements at different straw-fired boilers was made based on another measure of deposit formation rate—integral deposit formation rate (IDF-rate). Ash transformation was investigated by bulk ash analysis of the fuel ash, residual ash, and deposit layers. The overall conclusions are the following:

- The bulk chemical composition of straw and wood suspension-fired fly ash shows relatively higher contents of Si, and Ca and lower contents of volatile elements (K, Cl, and S), compared to grate firing conditions. However, it was also found that with an increase in fuel ash K/Si molar ratio the concentration of volatile elements, K, Cl, and, to some extent, S, increased in the fly ash.
- The upstream side deposit outer layers on the probe contain high concentration of Si, K, and Ca, indicating that larger particles impact on and stick to the probe on the upstream side. K, S, and Cl were found in higher proportions on the downstream side deposit layers indicating that the downstream deposits to a greater extent are formed by thermophoresis and/or condensation of KCl and K_2SO_4. The innermost layers were rich in K, Cl, and S.
- The IDF-rate increases with increased fuel K contents (straw share in wood) and with increase in flue gas temperature, but probe surface temperatures have no significant influence on the IDF-rate. The IDF-rates determined from biomass grate and suspension firing are comparable.
- The DDF-rate increases with increased straw share in wood and with increase in flue gas temperature, but probe surface temperatures have no significant influence on the measured DDF-rates.
- The overall mean DDF-rate also increases with increase in flue gas temperature and deposit formation levels between 234 to 3105 g/(m^2·h) were observed.

AUTHOR INFORMATION

Corresponding Author

*Phone: +45 45252849. Fax: +45 45882258. E-mail: paj@kt.dtu.dk.

Notes

The authors declare no competing financial interest.

ACKNOWLEDGMENTS

The financial support by Energinet.DK under the PSO project 7217 and the financial support by Vattenfall A/S are gratefully acknowledged. Special thanks to Vattenfall A/S for providing access to their boiler. In addition, we are thankful to the operational staff at the Amager Power Plant for their technical support during the power plant boiler measurements.

NOMENCLATURE

A, B, C, D, E, F = empirical constants for flue gas temperature prediction
CCD = charge-coupled device
DDF-rate = derivative-based deposit formation rate (g/(m^2·h))
$Diff_{pred}$ = predicted difference between thermocouple based flue gas temperature measurements and suction pyrometer based flue gas temperature measurements (°C)
FMT = first melting temperature (°C)
ICP-IC = inductively coupled plasma-ion chromatography
IDF-rate = integral deposit formation rate (g/(m^2·h))
IFRF = International Flame Research Foundation
g = gravitational acceleration (m/s^2)
L_1 = distance from the hinge to the balance (m)
L_2 = distance from the hinge to the mass center of the deposit (m)
m_d = deposit mass (g)
m_{t0} = initial signal of the load cell (g)
m_{t1} = final signal of the load cell (g)
T = flue gas temperature (K)
X_i = operational parameter for flue gas temperature prediction
Y_{calc} = predicted flue gas temperature (°C)
Y_{meas} = measured suction pyrometer flue gas temperature (°C)
Y_{TC} = measured thermocouple flue gas temperature (°C)

REFERENCES

(1) Montgomery, M.; Jensen, S. A.; Borg, U.; Biede, O.; Vilhelmsen, T. Experiences with high temperature corrosion at straw-firing power plants in Denmark. *Mater. Corros.* **2011**, *62*, 593−605.
(2) Nielsen, H. P. Deposition and high temperature corrosion in biomass-fired boilers. PhD Thesis, Technical University of Denmark. 1998; ISBN 87-90142-47-0.
(3) Jenkins, B. M.; Baxter, L. L.; Miles, T. R. Jr.; Miles, T. R. Combustion properties of biomass. *Fuel Process. Technol.* **1998**, *54*, 17−46.
(4) Munir, S.; Nimmo, W.; Gibbs, B. M. Co-combustion of agricultural residues with coal: turning waste into energy. *Energy Fuels* **2010**, *24*, 2146−2153.
(5) Shao, Y.; Xu, C.; Zhu, J.; Preto, F.; Wang, J.; Tourigny, G.; Badour, C.; Li, H. Ash deposition during cofiring biomass and coal in a fluidized-bed combustor. *Energy Fuels* **2010**, *24*, 4681−4688.
(6) Sander, B.; Henriksen, N.; Larsen, O. H.; Skriver, A.; Ramsgaard-Nielsen, C.; Jensen, J. N.; Stærkind, K.; Livberg, H.; Thellefsen, M.;

Dam-Johansen, K.; Frandsen, F. J.; van der Lans, R.; Hansen, J. Emissions, corrosion, and alkali chemistry in straw-fired combined heat and power plants. *Proceedings of 1st World Conference on Biomass for Energy and Industry*, Sevilla, June 5−9, 2009.
(7) Jensen, P. A.; Sander, B.; Dam-Johansen, K. Removal of K and Cl by leaching of straw char. *Biomass Bioenergy* **2001**, *20*, 447−457.
(8) Frandsen, F. J. Ash formation, deposition, and corrosion when utilizing straw for heat and power production. Doctoral Thesis, Technical University of Denmark. 2011; ISBN 978-87-92481-40-5.
(9) Baxter, L. L. Ash deposition during biomass and coal combustion: A mechanistic approach. *Biomass Bioenergy* **1993**, *4*, 85−102.
(10) Andersen, K. H.; Frandsen, F. J.; Hansen, P. F. B.; Wieck-Hansen, K.; Rasmussen, I.; Overgaard, P.; Dam-Johansen, K. Deposit formation in a 150 MWe utility PF-boiler during co-combustion of coal and straw. *Energy Fuels* **2000**, *14*, 765−780.
(11) Jensen, P. A.; Frandsen, F. J.; Hansen, J.; Dam-Johansen, K.; Henriksen, N.; Hörlyck, S. SEM investigation of superheater deposits from biomass-fired boilers. *Energy Fuels* **2004**, *18*, 378−384.
(12) Zbogar, A.; Frandsen, F.; Jensen, P. A.; Glarborg, P. Shedding of ash deposits. *Prog. Energy Combust. Sci.* **2009**, *35*, 31−56.
(13) Jensen, P. A.; Zhou, H.; Frandsen, F. J.; Hansen, J. Ash deposits removal in biomass power plant boilers. *Proceeding of 15th European Biomass Conference and Exhibition*, Berlin, Germany, May 7−11, 2007.
(14) Tobiasen, L.; Skytte, R.; Pedersen, L. S.; Pedersen, S. T.; Lindberg, M. A. Deposit characteristics after injection of additives to a Danish straw-fired suspension boiler. *Fuel Process. Technol.* **2007**, *88*, 1108−1117.
(15) Wu, H.; Glarborg, P.; Frandsen, F. J.; Dam-Johansen, K.; Jensen, P. A. Dust-firing of straw and additives: Ash chemistry and deposition behavior. *Energy Fuels* **2011**, *25*, 2862−2873.
(16) Jensen, P. A.; Stenholm, M.; Hald, P. Deposition investigation in straw-fired boilers. *Energy Fuels* **1997**, *11*, 1048−1055.
(17) Zhou, H.; Frandsen, F. J.; Jensen, P. A.; Glarborg, P. *PSO Project 4106, CHEC Report R0603*; CHEC Research Centre, Technical University of Denmark: Kongens Lyngby, Denmark, 2006.
(18) Zbogar, A.; Frandsen, F. J.; Jensen, P. A.; Hansen, J.; Glarborg, P. Experimental investigation of ash deposit shedding in a straw-fired boiler. *Energy Fuels* **2006**, *20*, 512−519.
(19) Hansen, J.; Jensen, P. A.; Glarborg, P. *Deposit Probe Measurements in the Avedøre and Ensted Straw-Fired Grate Boilers*, CHEC Report R0705, CHEC Research Centre, Technical University of Denmark: Kongens Lyngby, Denmark, 2007.
(20) Nordgren, D.; Hedman, H.; Padban, N.; Boström, D.; Öhman, M. Ash transformations in pulverised fuel co-combustion of straw and woody biomass. *Fuel Process. Technol.* **2011**, DOI: 10.1016/j.fuproc.2011.05.027.
(21) Theis, M.; Skrifvars, B. J.; Hupa, M.; Tran, H. Fouling tendency of ash resulting from burning mixtures of biofuels. Part 1: Deposition rates. *Fuel* **2006**, *85*, 1125−1130.
(22) Skrifvars, B.-J.; Lauren, T.; Hupa, M.; Korbee, R.; Ljung, P. Ash behavior in a pulverized wood fired boiler—A case study. *Fuel* **2004**, *83*, 1371−1379.
(23) *IFRF Handbook*, ISSN: 1607-9116. Available online: www.handbook.ifrf.net/handbook/index.html (accessed: Jan. 30, 2009).
(24) Bashir, M. S.; Jensen, P. A.; Frandsen, F.; Wedel, S.; Dam-Johansen, K.; Wadenbäck, J.; Pedersen, S. T. Ash transformation and deposit build-up during biomass suspension and grate firing: Full-scale experimental studies. *Fuel Process. Technol.* **2012**, *97*, 93−106.
(25) Lokare, S. S.; Dunaway, J. D.; Moulten, D.; Rogers, D.; Tree, D. R.; Baxter, L. L. Investigation of ash deposition rates for a suite of biomass fuels and fuel blends. *Energy Fuels* **2006**, *20*, 1008−1014.
(26) Gjernes, E. Fuel flexibility at Amager unit 1 using pulverized fuels. *Proceedings of Power-Gen Europe*, Cologne, Germany, 2006.
(27) *IFRF Suction Pyrometer, User Information Document*; International Flame Research Foundation: 2007.
(28) Kittrel, J. R. *Adv. Chem. Eng.* **1970**, *8*, 97−183.
(29) Pritchard, D. J.; Bacon, D. W. Prospects for reducing correlation among parameters estimates in kinetics models. *Chem. Eng. Sci.* **1978**, *33*, 1539−1543.
(30) *Matlab, Signal Processing Toolbox*. http://www.mathworks.com/help/toolbox/signal/resample.html (Accessed: March 31, 2011).
(31)http://www.mathworks.com/matlabcentral/fileexchange/16997-movingslope (Accessed: Dec. 16, 2010).
(32) Smith, S. W. *The Scientist and Engineer's Guide to Digital Signal Processing*; Califonial Technical Publishing: San Diego, CA, 1997−1998; Chapter 15, pp 277−284. Available online: http://www.dspguide.com/ (Accessed: Dec. 31, 2010).
(33) *Matlab, Curve Fitting Toolbox*. http://www.mathworks.com/help/toolbox/curvefit/bq_6yqb.html (Accessed: March 31, 2011).
(34) Zheng, Y.; Jensen, P. A.; Jensen, A. D.; Sander, B.; Junker, H. Ash transformation during co-firing coal and straw. *Fuel* **2007**, *86*, 1008−1020.
(35) Zhou, H.; Jensen, P. A.; Frandsen, F. J. Dynamic mechanistic model of superheater deposit growth and shedding in a biomass fired grate boiler. *Fuel* **2007**, *86*, 1519−1533.

September. 2012, DTU no. 50530

Appendix A5

Journal paper: Suspension-Firing of Biomass. Part 2: Boiler Measurements of Ash Deposit shedding. Energy & Fuels 2012, 26, 5241-5255

Energinet.dk project no. 7217

Characterization and quantification of deposits build up and removal in straw suspension fired boilers

Muhammad Shafique Bashir, Peter Arendt Jensen, Flemming Frandsen, Stig Wedel, Kim Dam-Johansen, Johan Wadenbäck

Department of Chemical and Biochemical Engineering

Technical University of Denmark

Søltofts Plads, Building 229, DK-2800 Lyngby, Denmark

CHEC no. R1301

energy&fuels

Article

pubs.acs.org/EF

Suspension-Firing of Biomass. Part 2: Boiler Measurements of Ash Deposit Shedding

Muhammad Shafique Bashir,[†] Peter Arendt Jensen,*[,†] Flemming Frandsen,[†] Stig Wedel,[†] Kim Dam-Johansen,[†] and Johan Wadenbäck[‡]

[†]DTU Chemical and Biochemical Engineering, Building 229, Technical University of Denmark, DK-2800 Lyngby, Denmark

[‡]Vattenfall A/S, Amager Power Plant, Kraftværksvej 37, DK-2300 Copenhagen S, Denmark

ABSTRACT: This paper is the second of two papers, describing probe measurements of deposit buildup and removal (shedding), conducted in a 350 MW_{th} suspension-fired boiler, firing straw and wood. Investigations of deposit buildup and shedding have been made by use of an advanced online deposit probe and a sootblowing probe. The influences of feedstock (i.e., straw share in wood), flue gas temperature (600−1050 °C), probe surface temperature (500 and 600 °C), and probe exposure time on deposit shedding have been quantified. Quantification of naturally occurring deposit shedding and deposit shedding during plant sootblowing was made via deposit mass uptake signals obtained from the deposit probe. The deposit shedding process was characterized by calculation of the amount of deposit removed at a shedding event (g/m^2) and the frequency of the shedding events (h^{-1}). The results showed that the shedding process is stochastic and that the amount of deposit shed varies even at constant local conditions. However, the deposit shedding rates showed an increasing trend with increase in flue gas temperatures and probe deposit mass loads. The deposit shedding rate was in most cases higher at a probe temperature of 500 °C than at a probe temperature of 600 °C. A possible reason for this is partial melting and/or sintering of the innermost deposit layer (rich in K, Cl, and S) at higher probe surface temperature. This could cause the adhesion strength of the deposit to the probe to increase at the higher probe temperature. Quantification of the necessary peak impact pressure (PIP) needed to remove the deposit was also made by use of a sootblowing probe in conjunction with the deposit probe. Results of deposit removal by artificial sootblowing showed that the deposits formed on a 500 °C probe temperature and at exposure times of <91 h can be removed with a PIP of <55 kPa. However, increase in probe exposure time and/or probe surface temperature (600 °C) significantly increases the PIP needed to remove the deposits.

INTRODUCTION

The focus on substituting fossil resources by biomass has significantly increased the interest in efficient use of biomass for electricity production, and this includes the use of wood or straw in large suspension-fired boilers. However, especially straw constitutes a serious technical challenge with respect to deposit formation and corrosion, due to the large content of K and Cl in straw.[1−9] Deposit formation and corrosion problems limit the maximum applicable superheater temperature and, thereby, limit the electrical efficiency. In the case of severe ash deposition, boiler shutdown and expensive manual cleaning of the heat transfer surfaces may be needed. To minimize deposition problems, different strategies can be employed, for example, the use of additives that can convert gaseous inorganic species to less harmful forms, pretreatment of fuels by leaching out alkali, cofiring with coal, and the use of effective deposit-shedding techniques.[10−16] Use of additives and pretreatment of fuels by leaching are less cost-effective compared to the use of effective deposit shedding techniques.[7,10−14]

Ash deposit buildup during biomass combustion is a dynamic process consisting of both deposit formation[14,15] and shedding.[12,14,16] The most common industrial methods used to shed deposits from superheater tubes include sootblowing, mechanical vibrations, detonation wave techniques, shot-cleaning methods, thermal tensions, and rapping gear systems. Shedding may be initiated at the surface of the deposit, along the deposit tube interface, or inside the deposit depending on the local boiler conditions and the deposit properties. Important mechanisms of ash deposit shedding are[14,16] (1) erosion, when nonsticky, relatively large, and sharp-edged fly ash particles often rich in quartz collide with nonsticky areas on a deposit surface causing deformation (ductile deposits) and a cutting action (brittle deposits); (2) gravity shedding, when the gravity force exceeds the tube adhesion strength; (3) through temperature changes and differences in the thermal expansion coefficients of the tube and deposit; local temperature changes may be caused by sootblowing or boiler load fluctuations; and (4) mechanically induced tension in the deposit typically caused by vibrations or sootblowing.

These mechanisms include both naturally occurring and artificially induced shedding. Natural shedding includes processes such as surface melting, erosion, and thermal shock. Steam, water, and air sootblowing are the most common artificial shedding techniques applied to remove deposits from superheater tubes. Biomass-fired boilers often have several sootblowers depending on the local flue gas temperature, deposit-sintering characteristics, and deposit quantity.[14,16] The cleaning effectiveness depends on the sootblower location, the cleaning media applied, and the peak impact pressure (PIP) reached when sootblowing is performed.[16−19] Sootblowers

Received: April 11, 2012
Revised: July 9, 2012
Published: July 9, 2012

effectively remove fouling deposits, but to ensure maximum boiler thermal efficiency, cost-effective use of sootblowers is also important, because these may consume a significant percentage of the boiler steam production.[20] In addition, a high superheater temperature (>550 °C) is needed due to the corresponding increased electrical efficiency, and therefore deposit shedding at elevated superheater temperatures is of significant interest.[20] Optimization of plant sootblowing and other deposit shedding conditions is important to facilitate efficient removal of deposits from biomass-fired boilers.

Full-scale deposition and shedding measurements provide useful and real information with respect to better understanding of deposit shedding and minimizing fouling and slagging in biomass-fired boilers. Ash deposit shedding through surface melting in the high-temperature superheater region at the Avedøre straw grate-fired boiler was investigated by Zbogar et al.[21] The results showed that deposit surface melting is the main mechanism of straw ash deposit shedding, at flue gas temperatures >1000 °C. Deposit shedding in the Avedøre straw grate-fired boiler was investigated by Zhou et al.[20] by using an artificial sootblowing probe in the superheater region nearer the convective pass at flue gas temperatures between 700 and 800 °C. Most deposit shedding studies have been based on measurements in laboratory-scale equipment,[18,22] grate-fired boilers,[20,21] and Kraft recovery boilers,[23] whereas only a limited amount of data is available from biomass suspension-firing.[24−27]

The aim of this study was to investigate deposit buildup and shedding in a 350 MW_{th} suspension-fired boiler, firing straw and wood. Paper 1 in this series[24] dealt with deposit formation, whereas this paper deals with shedding. An advanced probe was used to collect ash deposits and shedding data, which are then used to quantify naturally occurring shedding and shedding caused by plant sootblowing.

EXPERIMENTAL SECTION

Boiler. The probe measurements were conducted at Amager Power Station, Unit 1 (AMV1). The AMV1 boiler is a multifuel suspension-fired boiler, which was commissioned in 2009 to fire pulverized biomass (in the shape of crushed pellets) with various shares of straw and wood. The annual biomass consumption (at AMV1) is approximately 300,000 tons of wood pellets and 100,000 tons of straw pellets. The 350 MW_{th} boiler is front wall-fired, having 12 burners located in three levels. Due to an expected increase in the corrosion rate with respect to temperature, the final steam temperatures of the superheaters are limited to approximately 540 °C.[28] The boiler data are shown in Table 1, whereas a schematic drawing of the boiler is shown in Figure 1 (more details can be seen in paper 1[24]).

Ash Deposition and Sootblowing Probe. The advanced deposit probe was made of stainless steel, about 3 m long with an outer diameter of 40.5 mm. More details of the deposit probe can be found in other publications.[21,24]

The flue gas temperature near the probe was continuously measured, using a simple thermocouple in a protective shell. In addition, a suction pyrometer (International Flame Research Foundation model, IFRF[29]) was also used for shorter periods in each test, to find the difference between the thermocouple flue gas temperature measurements and the true flue gas temperature measurements. On the basis of these data, corrected thermocouple temperatures were calculated (see paper 1[24]). A charge-coupled device (CCD) camera was used to register the deposit formation and shedding processes on the probe. A schematic of the complete port setup used during the measurements can be seen in paper 1.[24]

An artificial sootblowing probe with an external diameter of 42.2 mm and a length of 3 m was used for in situ removal of deposits. The schematic drawing of the sootblowing probe is shown in Figure 2a, and the detailed sootblower nozzle drawing can be seen in Figure 2b. The air pressure to the sootblowing probe was measured by using a pressure gauge, and the air pressure was increased in steps. The sootblowing probe was cooled by water. In the large port (please refer to part 1 of the current series of paper[24]), a small port for the ash deposition probe, a port for the thermoelement, a CCD camera port, and a port for artificial sootblowing probe were placed. The sootblowing probe was placed parallel to the deposit probe. The sootblower probe nozzle was of convergent−divergent shape, and air at a supply pressure of 6.0 bar was fully expanded.[17] The sootblower nozzle was fixed at the end of the probe. The PIP of the nozzle was measured along the axial centerline as a function of the supplied air

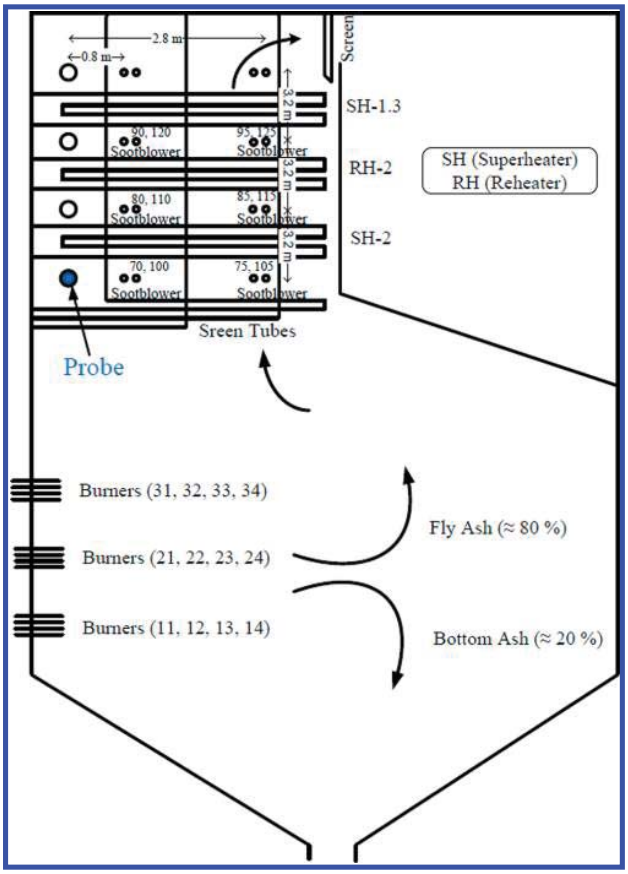

Figure 1. Schematic drawing of the AMV1 boiler outlining the position of the plant sootblowing near the experimental setup. In total, 12 sootblowers affect the deposit shedding process, 6 along the left wall of the boiler and 6 along the right wall of the boiler. The distance of each sootblower from the probe measuring position is also shown. Sootblower 70 was very near the probe measuring position (1 m to the left) and was shut down during tests 1−5. The first number in a pair of two numbers shows the sootblowers located on the same wall where the probe is located (left wall, burner location), whereas the second number shows the sootblowers located on the opposite wall (right wall, burner location).

Table 1. Brief Operational Data of the AMV1 Boiler

boiler cross-sectional area (at probe measuring position)	5.75 × 12.5 ∼12 m^2	
parameter (steam)	high-pressure (HP) superheater	reheater (RH)
temperature (°C)	540 (biomass)	540
pressure (bar)	185	75
flow (kg/s)	138.4	123

dx.doi.org/10.1021/ef300611v | Energy Fuels 2012, 26, 5241−5255

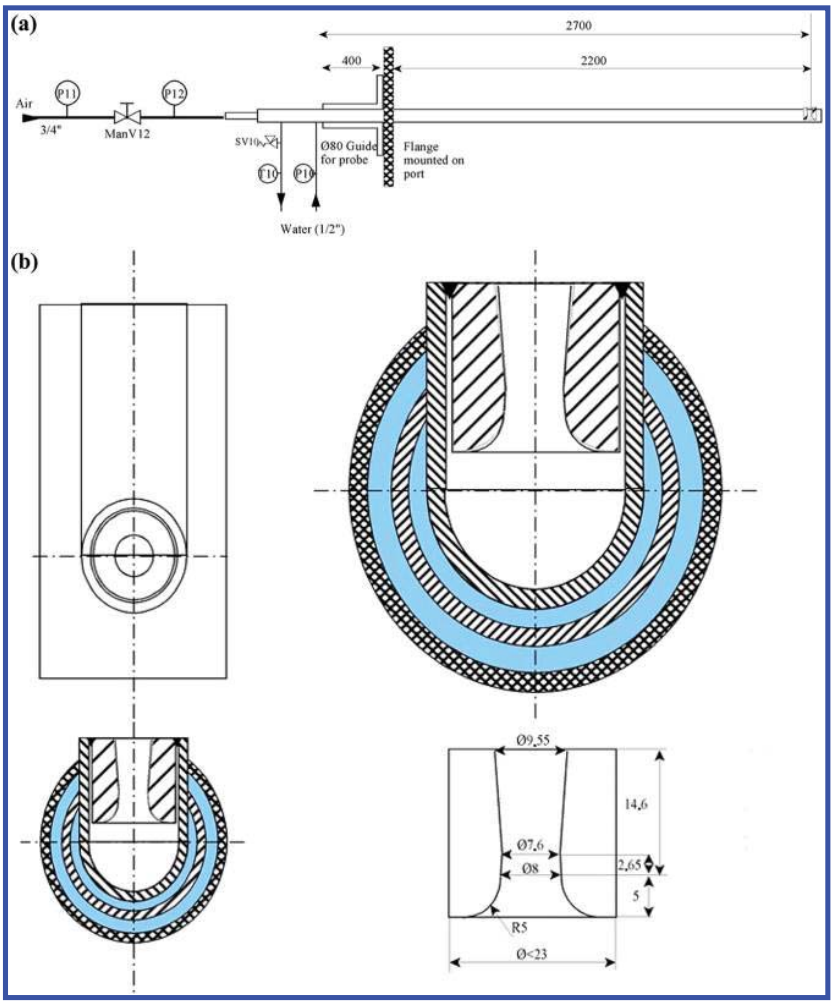

Figure 2. (a) Schematic of sootblowing probe with water and air flow description: P10, P11, and P12 are pressure gauges for air, P10 is a pressure gauge for water (to act as a cooling medium), and T10 is temperature indicator. (b) Detailed drawings of the sootblowing nozzle.

pressure in the laboratory at room temperature. The PIP of the jet, defined as the centerline stagnation pressure of the jet, was used to define the removal of deposits by the sootblowing probe.[17] The measured values of PIP are shown in Figure 3, and it is important to note that these values are measured at room temperature. In the applied range of PIP, there can be a minor impact of flue gas temperature on PIP, but the measurement of PIP at temperatures close to the flue gas temperature was not possible. The measured PIP increases with the supplied air pressure and drops off quickly with the axial distance from the nozzle exit (Figure 3).

Fuels. During the measurements, fuels were continuously sampled before the burners. The total ash contents of the fuel samples collected from all test runs were analyzed, and thereby the straw fuel fractions were determined on the basis of the total ash contents. In some cases also detailed ash analysis was made as shown in Table 2. The analysis methods and the detailed ash analysis of pure fuels and some samples from tests 1 and 5 are shown in Table 2. It is seen that the straw ash has high contents of Si, K, Cl, and Ca.

Overall, eight test runs were carried out, and the mean straw share during each test is shown in Table 3. The slight difference in fuel ash contents shown in Tables 2 and 3 is due to the fact that in Table 3 mean values of each complete test are shown, whereas in Table 2, values are shown for a sample collected just before the burners. It is also important to mention that pure straw and wood fuel samples shown in Table 2 were collected from the fuel silos, whereas fuel sample just before the burners was collected almost each day during each test. In the start of test 5, the fraction of straw in fuel was low (about 14 wt %, not shown in Table 2); therefore, the overall percentage of straw in fuel was low compared to the fuel samples of test 5 shown in Table 2.

Procedure of Experiments. *Ash Deposition Experiments.* Measurements were conducted in the superheater region, just above the screen tubes (Figure 1). The influence of fuel type (straw share in wood), flue gas temperature (600−1050 °C), probe surface temperature (500 and 600 °C), and deposit mass load on ash deposit formation rate was investigated. Description of ash deposition equipment and detailed interpretation of results can be found in paper 1.[24]

Evaluation of probe heat uptake as a function of deposit mass load was also made for each test. A complete overview of all the conducted measurements is presented in Table 3. Additional information, for example, air flow rate, fuel flow rate, ash flux, etc., of each test is also shown in Table 3.

Artificial Sootblowing Experiments. Three different methods were used to quantify the PIP needed to remove the deposits on the probe (see Figure 4). In method 1, the sootblowing probe was placed parallel to the ash deposition probe and artificial sootblowing was started from the tip of the deposition probe with air pressure ranging from 0.5 to 4.0 bar. Method 2 is actually a continuation of method 1, where the sootblowing probe was slightly pulled out (approximately 20 cm) to remove remaining layers of the deposits by using the same principle adopted in method 1. This procedure was repeated until the nozzle of the sootblowing probe reached a distance of 1.5 m from the tip of the ash deposition probe. If the amount of deposits removed was not

dx.doi.org/10.1021/ef300611v | *Energy Fuels* 2012, 26, 5241−5255

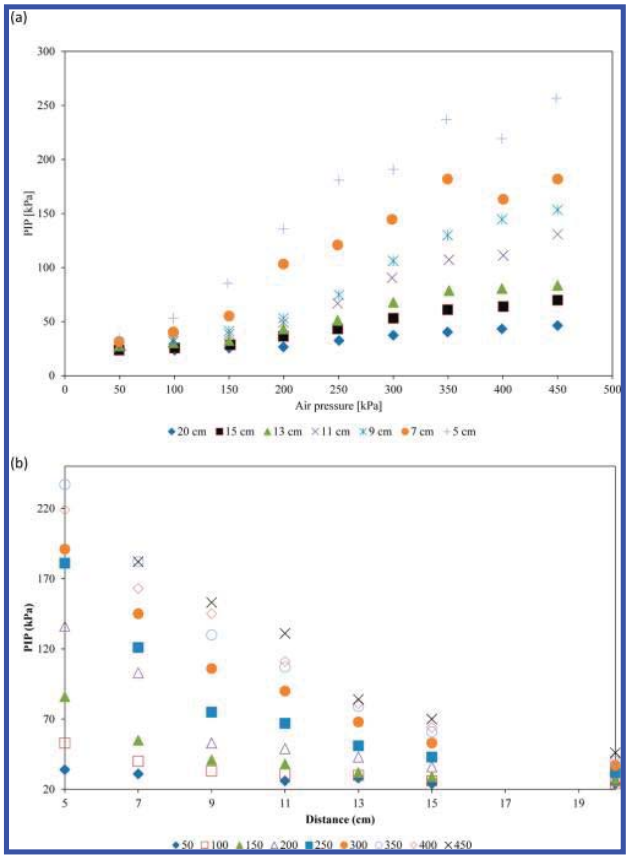

Figure 3. Measured peak impact pressure (PIP) as a function of (a) applied air pressure at various downstream distances from the nozzle exit to the deposit probe at room temperature and (b) distance from the nozzle exit to the deposit probe at various pressures at room temperature.

significant, method 3 was applied by reducing the distance between the nozzle and the deposition probe in the range of 5−20 cm, to achieve maximum values of PIP. In each position, the impact of air on the deposit probe was from a couple of seconds to a minute. In addition, in each method, the air pressure was increased in steps. The sootblowing probe was not rotated and was only pulled or moved closer to the deposit probe. During the artificial sootblowing, camera images were collected to confirm the observed changes in the deposit mass uptake signals.

Plant Sootblowing. In the superheater region area of the boiler, retractable steam sootblowers were used for a time of 5−10 min (each sootblower) at regular intervals during boiler operation, typically at 8 h intervals. Six sootblowers were placed along the left wall of the boiler and six along the right wall of the boiler as shown in Figure 1. The sootblower located nearest the probe measuring position (approximately 1 m to the left) was shut down during tests 1−5, whereas the rest of the sootblowers located farther away from the probe measuring position were in operation during all tests.

RESULTS AND DISCUSSION

Ash Deposit Formation Rate. The total amount of deposit collected on the probe is a function of both the deposit formation process and shedding events. Two different measures of deposit formation rate were used in the analysis of the data. The first is the integral deposit formation rate (IDF rate) found by dividing the integral mass change over integral time intervals (on the order of several hours) by the time interval. A second measure, the derivative-based deposit formation rate (DDF rate), was determined by averaging the deposit mass uptake signals over short time intervals (on the order of minutes), calculating the local values of the time derivative of the mass uptake, removing large negative values signifying major shedding events, and finally time smoothing the derivatives to remove excessive noise. Further details about the deposit formation rate determinations are presented in paper 1.[24]

Video Observations of Shedding Events. The deposit mass uptake signals were continuously monitored, and deposit-shedding events were confirmed by video recordings. The deposit mass uptake signals during test 1 are shown in Figure 5. We have divided the shedding events into naturally occurring events and sootblowing-initiated shedding events. Even when the nearby sootblower is turned off, the increased thermal and mechanical fluctuations induced by the rest of the sootblowers may increase the shedding rate. No artificial probe sootblowing measurements were conducted during test 1.

Confirmation of some deposit shedding events was made using the images collected at 20−30 s intervals. It was found that deposit shedding was primarily through debonding from the surface of the deposit probe; an example of a deposit shedding event is shown in Figure 6. No deposit shedding through surface melting was seen in the videos collected from any of the tests, even though a flue gas temperature of >1000 °C was observed during tests 4 and 5. Earlier investigations by Zbogar et al.[21] showed shedding through surface melting in a straw grate-fired boiler, at local flue gas temperatures >1000 °C. Possibly the high contents of Si and Ca in the fly ash of the AMV1 boiler, and the relatively lower concentrations of the inorganic volatile elements (K, Cl, and S), cause a higher melting temperature of the ash deposits generated by the suspension-cofiring of straw and wood.[24,30]

Monitoring of deposit shedding from inspection holes very close to the port position revealed a small amount of deposit shedding through erosion when nonsticky, relatively large, and sharp-edged SiO_2-rich fly ash particles collide with nonsticky areas on a deposit surface. A significant amount of Si in the fly ash formed during straw and wood suspension-firing has been reported.[24,30] Generally, most of the deposits were removed by debonding, where larger pieces detached from the tube surface.

Deposit Removal (Shedding). As discussed in paper 1,[24] during the calculation of DDF rates, a particular negative slope cutoff level was selected to determine major shedding events accurately while still giving a satisfactory prediction of apparent DDF rates. The selected cutoff level was −3800 g/m^2/h for all tests.[24] This cutoff level strikes a balance between including larger shedding events in the analysis and preventing deposit mass signal noise from being counted on a shedding event.[24] The selected minimum magnitude of a shedding event included in the analysis was −105 g/m^2, and this was calculated by eq 1.

$$\begin{aligned}&\text{minimum shedding event magnitude}\\&= \text{slope cutoff level} \times \text{sampling interval}\\&= -3800\frac{\text{g}}{(\text{m}^2\text{h})}\frac{\text{h}}{(3600\text{s})} \times 100\text{s}\\&= -105\frac{\text{g}}{\text{m}^2}\end{aligned} \quad (1)$$

The flue gas temperature and deposit probe mass uptake signals are shown in Figure 5 for test 1. The temperature measurements by the thermocouple show temperature fluctuations in the range of 500−800 °C. The deposit mass

dx.doi.org/10.1021/ef300611v | *Energy Fuels* 2012, 26, 5241−5255

Table 2. Analysis of Straw and Wood Pellets Used at AMV1[a]

parmeter	procedure	straw, Køge	wood, Kunda[b]	80−85% straw, test 1	65−70% straw, test 5	60−65% straw, test 5	60−65% straw, test 5	40−45% straw, test 5
date				March 22, 2010	April 19, 2010	April 20, 2010 (1:00 p.m.)	April 20, 2010 (5:00 p.m.)	April 21, 2010
ash contents (wt %, ar)	EN 14775:2009	6.03	0.80	5.26	4.32	3.56	3.63	2.74
ash contents (wt %, db)	EN 14775:2009	6.54	0.86	5.63	4.57	3.78	3.84	2.88
moisture (wt %, ar)	EN 14774-3:2009	7.86	6.83	6.67	5.61	5.94	5.55	5.03
higher heating value (MJ/kg, db)	EN 14918:2010	18.71	20.47	17.62	19.68	19.39	19.35	19.87
volatiles (wt %, db)	EN 15148:2009	80.91	85.24	82.87	82.58	82.15		83.11
C (wt %, db)	CEN/TS 15104:2006	50.52	55.54	51.16	52.44	52.89	52.57	53.91
S (wt %, db)	CEN/TS 15289:2006	0.15	0.035	0.121	0.105	0.095	0.093	0.068
N (wt %, db)	DS/EN ISO 10304-1:2009	0.59	0.73	0.8	0.62	0.63	0.68	0.75
H (wt %, db)	EN 14918:2010 calculated	5.79	6.15	5.85	5.92	5.97	5.96	6.02
O (wt %, db)	EN 14918:2010 calculated	36.11	36.68	36.43	36.19	36.45	36.67	36.28
Cl (wt %, db)	DS/EN ISO 10304-1:2009	0.290	0.003		0.155	0.184	0.191	0.093
ash analysis (wt %, db)								
Al_2O_3	DIN 51729/ASTM3682	0.66		0.95	1.88	1.30	0.97	2.11
CaO	DIN 51729/ASTM3682	14.56		8.30	9.97	11.05	11.80	17.69
Fe_2O_3	DIN 51729/ASTM3682	0.50		0.47	6.81	1.03	0.58	1.13
K_2O	DIN 51729/ASTM3682	17.88		15.25	12.58	15.92	20.41	13.96
MgO	DIN 51729/ASTM3682	3.39		2.25	2.11	2.29	2.54	2.90
Na_2O	DIN 51729/ASTM3682	0.69		0.57	0.59	0.87	1.04	1.03
P_2O_5	DIN 51729/ASTM3682	5.56		2.47	2.17	2.46	2.60	2.13
SO_3	DIN 51729/ASTM3682	2.43		2.36	2.03	2.16	1.88	2.43
SiO_2	DIN 51729/ASTM3682	44.51		52.05	44.89	49.15	46.95	36.87
TiO_2	DIN 51729/ASTM3682	0.05		0.06	0.11	0.10	0.06	0.13

[a]ar, as received; db, dry basis. [b]One type of four.

Table 3. Experimental Summary

	test 1	test 2	test 3	test 4	test 5	test 6	test 7	test 8
date	March 22−25, 2010	March 27−29, 2010	March 29−April 6, 2010	April 6−9, 2010	April 15−22, 2010	May 7−25, 2010	May 25−June 8, 2010	June 8−18, 2010
straw (wt %)	80−85	60−65	30−35	40−50	40−50	0−10	0−10	0−10
fuel ash content (wt %)	∼5.2	∼4.0	∼2.4	∼3.4	∼3.4	∼1.0	∼1.0	∼1.0
fuel flow (kg/s)	12.1	11.4	12.9	17.3	12.7	14	12	12
air flow (kg/s)	114	103	106	130	107	124	116	112
ash flux (approx) ($g/m^2/h$)	25334	19382	12780	23741	17105	4439	4826	4272
probe temperature (°C)	500	600	500	500	500 (600)	550	550	550 (600)
exposure time (h)	56	45	185	73	168	434	335	212
probe heat uptake investigation	yes	yes	yes	yes	yes	yes	yes	yes
artificial sootblowing	no	yes	yes	yes	yes			
naturally occurring deposit shedding events	yes	yes	yes	yes	yes			
plant sootblowing	yes[a]	yes[a]	yes[a]	yes[a]	yes[a]	yes	yes	yes

[a]Plant sootblower very near the ash deposition probe (about 1 m to the left) was closed.

uptake signals show both natural and plant sootblowing shedding events. The deposit mass uptake signal is influenced by several processes: large shedding events, smaller shedding events (observed as a sudden deposit mass loss on the curve), a relatively slow deposit buildup process, and some noise mainly caused by boiler fluctuations. Boiler fluctuations could be mechanical vibrations or large changes in boiler flow dynamics. The most severe fluctuations are observed when the boiler plant sootblowers were used. Even though the plant sootblower very near the probe was shut down, the rest of the sootblowers to some extent induced fluctuations that could cause some shedding. All shedding events are marked showing both natural

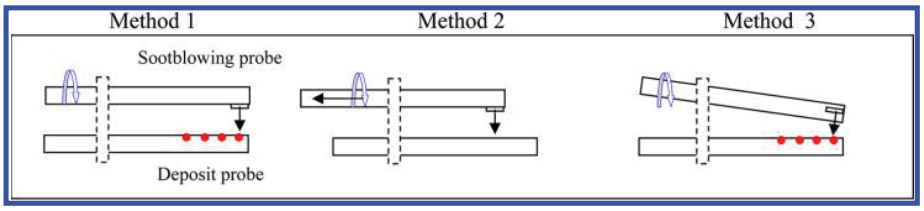

Figure 4. Experimental methods applied for artificial sootblowing.

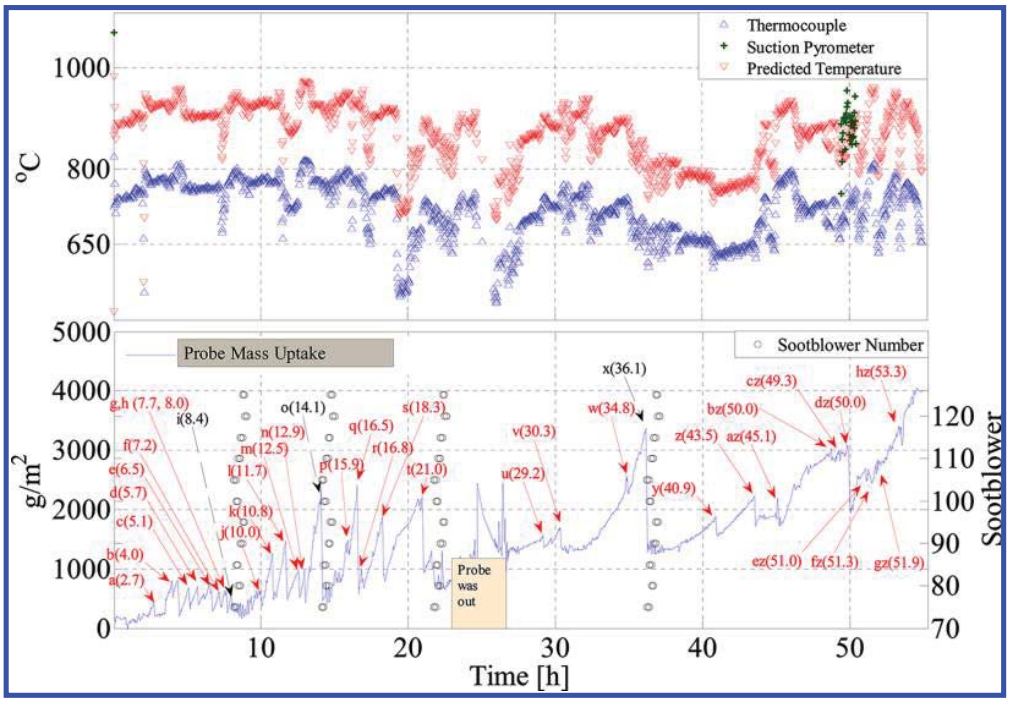

Figure 5. Data of flue gas temperature (thermocouple, suction pyrometer, and predicted[24]), probe mass uptake, and plant sootblowing events (specific number of sootblower in operation as seen on the secondary *y*-axis) during test 1 with identified shedding events. Red arrows with continuous line show natural deposit shedding events, whereas black arrows with discontinuous line show deposit shedding through plant sootblowing. Sootblower number shown on the secondary *y*-axis represents a specific sootblower in the superheater region shown in Figure 1. The number attached to each event specifies the time of the shedding event.

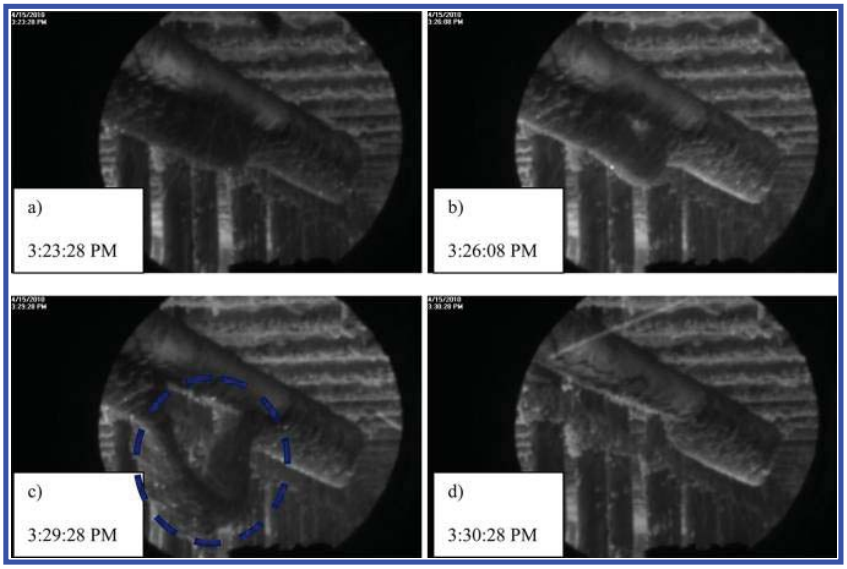

Figure 6. Images of the ash deposition probe during test 5 on May 15, 2010 (about 4 h of exposure time). From panels a to d, the process of natural deposit shedding through debonding can be clearly seen.

dx.doi.org/10.1021/ef300611v | *Energy Fuels* 2012, 26, 5241−5255

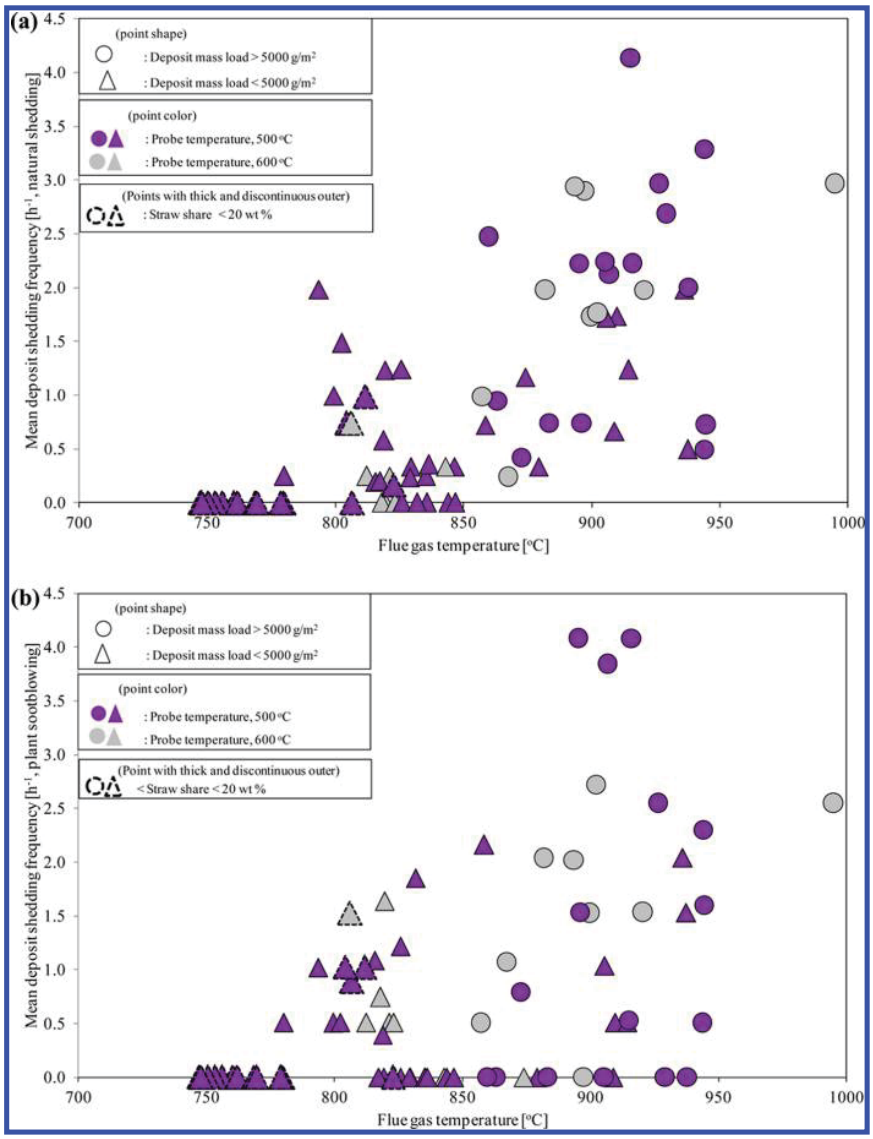

Figure 7. Impact of flue gas temperature on (a) mean natural deposit shedding frequency and (b) mean plant sootblowing shedding frequency. Data points are from tests 1−5. The particular point shape represents the deposit mass load, and the color represents the probe surface temperature, whereas points (larger in size) with thick and discontinuous outer edges are representative of straw share in wood.

and plant sootblowing-induced shedding events. The naturally occurring shedding was defined to occur when the plant sootblowers were not in operation, and no artificial sootblowing tests were made. Sootblowing-induced shedding events can occur when the plant sootblowers are in operation. Typically, a plant sootblowing operation lasts for about 1−2 h. The lengths of intervals between naturally occurring shedding incidents are very variable as seen in Figure 5. In the first 10−12 h, natural shedding occurs often, but with only small amounts of material. From about 12 to 21 h, the intervals between shedding events become longer, and the amounts removed in the single events are also larger compared to the previous period. Finally, from 29 to 55 h, natural shedding is infrequent, but the shedding amount is again relatively small. These changes in behavior may be related to varying boiler operation parameters, but it is worth noting that during the full 55 h, the baseline of deposited mass on the probe increased slowly from 0 to about 2500 g/m^2. Similar behavior was observed in most of the other tests also.

Under these conditions, analysis and quantification of natural shedding during the long time test is done by averaging over shorter time intervals. These are long enough that short time random behavior does not influence results unduly, but short enough that local operating and probe conditions may be considered fairly constant. Thus, each test was divided into sections of 6 h, which were used for the data analysis to characterize the deposit shedding by means of magnitude of events (g/m^2) and the incidence rate (deposit shedding frequency, h^{-1}). With regard to natural shedding, this allowed us to calculate mean incidence rates (mean natural deposit shedding frequency), $f_{nat,6}$, as the number of shedding events in a 6 h interval divided by the interval time. It should be noted that for each 6 h interval, the period of plant sootblowing was excluded in the evaluation of the natural shedding events. The mean deposit shedding frequency by natural shedding was calculated by eq 2.

dx.doi.org/10.1021/ef300611v | *Energy Fuels* 2012, 26, 5241−5255

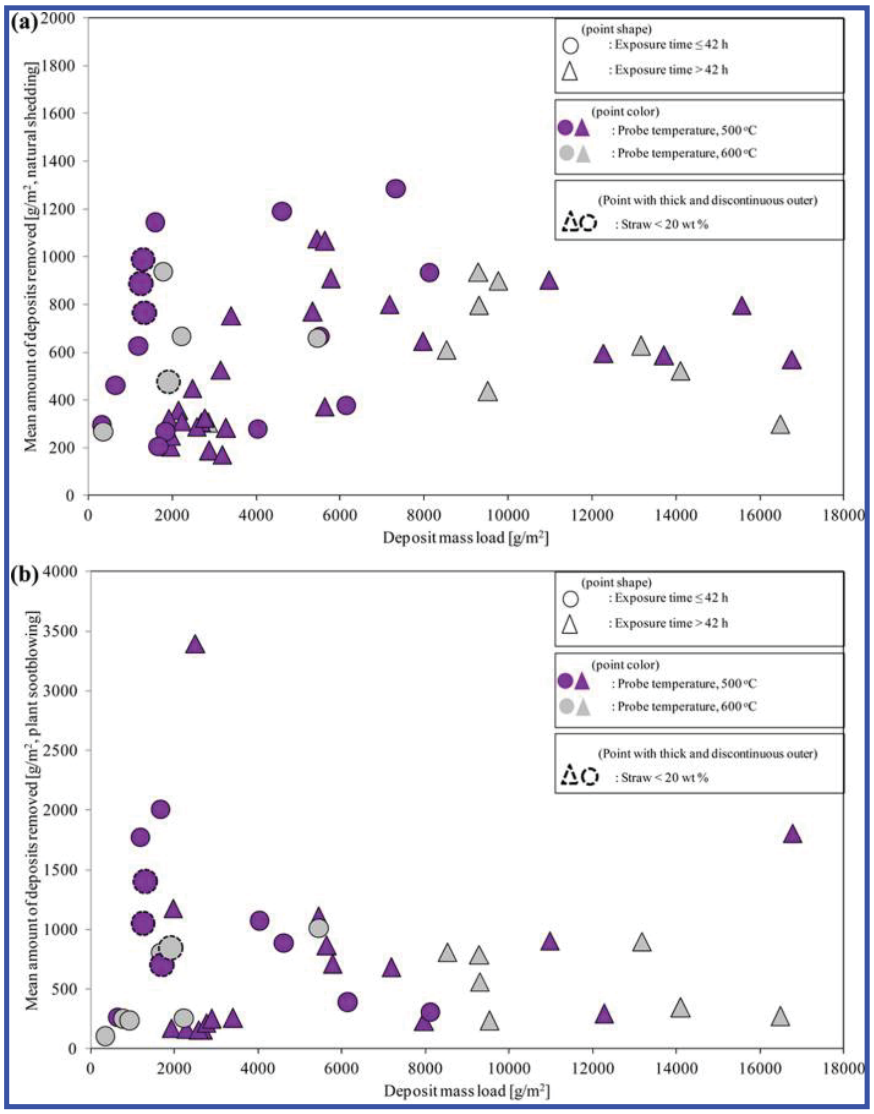

Figure 8. Impact of deposit mass load on (a) the mean amount of deposits removed naturally and (b) the mean amount of deposits removed by plant sootblowing. Data points are from tests 1−5. The particular point shape represents the exposure time, and the color represents the probe surface temperature, whereas points (larger in size) with thick and discontinuous edges are representative of straw share in wood.

$$\text{mean natural deposit shedding frequency } (f_{\text{nat},6}) = \frac{\text{no. of natural shedding events in a 6 h interval}}{\text{total time without plant sootblowing during a 6 h interval}} \quad (2)$$

The mean plant sootblowing deposit shedding frequency was calculated by eq 3,

$$\text{mean plant sootblowing deposit shedding frequency } (f_{\text{soot},6}) = \frac{\text{no. of plant sootblowing shedding events in a 6 h interval}}{\text{total time of plant sootblowing during a 6 h interval}} \quad (3)$$

Influence of Different Parameters on the Shedding Process. The shedding frequency (h^{-1}) and the shedding event size (g/m^2) are shown in Figures 7 and 8. The mean values for 6 h periods with similar conditions are presented in Tables 4 (natural shedding) and 5 (sootblowing induced shedding). The shedding data are divided into groups to make it possible to analyze the influence of changed conditions in flue gas temperature (above or below 850 °C), probe surface temperature (500 or 600 °C), straw fuel share (weight fraction of straw in the fuel above or below 20%), and deposit mass load (above or below 5000 g/m^2). The selected criterion of flue gas temperature is based on the results presented in paper 1,[24] where it was found that the deposit formation rate increases significantly when the flue gas temperature exceeds 850 °C. The second criterion was the probe surface temperature to investigate the influence of probe surface temperature on deposit shedding. The selected number (5000 g/m^2) for the deposit mass load is an arbitrary number, which was introduced to find any impact of deposit amount on the probe on deposit shedding. As seen in Tables 4 and 5 several of the combinations of operating conditions are without data. In two cases (straw < 20 wt %, deposit mass load < 5000 g/m^2, flue gas temperature < 850 °C, probe surface temperature = 600 °C; and straw > 20 wt %, deposit mass load < 5000 g/m^2, flue gas temperature >850 °C, probe surface temperature = 600 °C) only one 6 h period is presented. These cases are highlighted in italic type in Tables 4 and 5, and statistically it is difficult to use those data because of

dx.doi.org/10.1021/ef300611v | *Energy Fuels* 2012, 26, 5241−5255

Table 4. Summary of the Analysis of Natural Deposit Shedding for Two Different Sets of Flue Gas Temperature, Probe Surface Temperature, Straw Share, and Deposit Load

natural deposit shedding		flue gas temperature:	<850 °C		>850 °C	
fuel straw share	probe deposit mass load	probe surface temperature:	500 °C	600 °C	500 °C	600 °C
>20 wt %	>5000 g/m^2	mean DDF rate (g/m^2/h)			2691	1934
		no. of 6 h periods			16	9
		no. of shedding events			134	70
		mean size of shedding event (g/m^2)			854	730
		mean deposits removed (%)			10	7
		mean shedding frequency (h^{-1})			1.89	1.92
		mean shedding rate (g/m^2/h)			1612	1403
	<5000 g/m^2	mean DDF rate (g/m^2/h)	234	313	1245	*577*
		no. of 6 h periods	19	6	8	*1*
		no. of shedding events	42	4	38	*7*
		mean size of shedding event (g/m^2)	343	702	632	*305*
		mean deposits removed (%)	15	34	27	*10*
		mean shedding frequency (h^{-1})	0.47	0.15	1.04	*1.17*
		mean shedding rate (g/m^2/h)	160	107	660	*356*
<20 wt %	>5000 g/m^2	mean DDF rate (g/m^2/h)				
		no. of 6 h periods				
		no. of shedding events				
		mean size of shedding event (g/m^2)				
		mean deposits removed (%)				
		mean shedding frequency (h^{-1})				
		mean shedding rate (g/m^2/h)				
	<5000 g/m^2	mean DDF rate (g/m^2/h)	221	*1913*		
		no. of 6 h periods	17	*1*		
		no. of shedding events	8	*3*		
		mean size of shedding event (g/m^2)	910	*476*		
		mean deposits removed (%)	44	*28*		
		mean shedding frequency (h^{-1})	0.11	*0.74*		
		mean shedding rate (g/m^2/h)	101	*353*		

the limited data points. Below the influence of local changes and changes in probe conditions on the shedding characteristics is discussed.

(a) Increased Deposit Load on the Probe. The mean amount of deposit removed at a shedding event is 716 g/m^2 during natural shedding and 805 g/m^2 during sootblowing-initiated shedding as seen in Figure 8. There are seen large fluctuations in the amount of deposit removed in a single shedding event (6 h mean) from 180 to 1400 g/m^2 during natural shedding, but there is not observed any strong influence of the total deposit mass load on the amount of deposit removed in the single event (see Figure 8). In most cases, the probe deposit mass increases over time, and in the later stages of the experiments more than 5000 g/m^2 deposits are collected on the probe.

Two sets of data with similar conditions except for an increase in deposit load are available only for a flue gas temperature >850 °C, a probe temperature of 500 °C, and a straw fuel share >20 wt % (as seen in Tables 4 and 5). Going from a deposit mass below 5000 g/m^2 to above 5000 g/m^2 changed the mean shedding event mass from 632 to 854 g/m^2 during natural shedding and from 935 to 849 g/m^2 during sootblowing-induced shedding. Again, this shows that even though the deposit mass level has a tendency to increase through time, this does not strongly influence the amount of deposit released at a shedding event. The shedding frequency is increased from 1.04 to 1.89 h^{-1} during natural shedding and from 1.29 to 1.56 h^{-1} during sootblower-induced shedding for the change from a deposit mass below 5000 g/m^2 to above 5000 g/m^2. There is also seen a clear increase in DDF rate when the deposit mass load is increased, and because the shedding frequency increases, the shedding rate (g removed/h/m^2) increases with the increasing deposit mass load.

Because the amount of deposit removed at a shedding event is approximately independent of the amount of deposits on the probe, the relative amount of deposits removed (relative to total amount on the probe) is larger at low probe deposit mass. In addition, video recordings of deposit removal by plant sootblowing indicate that for shorter probe exposure time, plant sootblowing removes deposits from the entire surface of the probe, whereas a complete or partial layer of deposits is removed at higher exposure times.

With regard to the shedding properties, an increased amount of deposits on the probe leads not to a significant change in the amount of deposit lost at a shedding event but to an increase in the shedding frequency and thereby the shedding rate.

(b) Changed Probe Surface Temperature. For two sets of data (temperature < 850 °C, deposit mass < 5000 g/m^2, and a straw fuel share > 20 wt %; and temperature > 850 °C, deposit mass > 5000 g/m^2, and a straw fuel share > 20 wt %) in Tables 4 and 5, the influence of a change in probe temperature from 500 to 600 °C is illustrated. However, no clear tendencies are observed, and a systematic change in the amount of deposit shed in an event or the deposit frequency cannot be observed when the probe temperature is changed from 500 to 600 °C. However, if one looks at the mean shedding rate, then the shedding rate is in most cases higher at a probe temperature of

dx.doi.org/10.1021/ef300611v | *Energy Fuels* 2012, 26, 5241−5255

Table 5. Summary of the Analysis of Shedding during Sootblower Operation for Two Different Sets of Flue Gas Temperatures, Probe Surface Temperatures, Straw Shares, and Deposit Loads

sootblowing deposit shedding		flue gas temperature:	<850 °C		>850 °C	
fuel straw share	probe deposit mass load	probe surface temperature:	500 °C	600 °C	500 °C	600 °C
>20 wt %	>5000 g/m^2	mean DDF rate (g/m^2/h)			2691	1934
		no. of 6 h periods			16	9
		no. of shedding events			39	30
		mean size of shedding event (g/m^2)			849	688
		mean deposits removed (%)			10	9
		mean shedding frequency (h^{-1})			1.56	1.71
		mean shedding rate (g/m^2/h)			1322	1176
	<5000 g/m^2	mean DDF rate (g/m^2/h)	234	313	1245	
		no. of 6 h periods	19	6	8	
		no. of shedding events	9	5	15	
		mean size of shedding event (g/m^2)	750	332	935	
		mean deposits removed (%)	20	32	42	
		mean shedding frequency (h^{-1})	0.37	0.51	1.29	
		mean shedding rate (g/m^2/h)	278	170	1208	
<20 wt %	>5000 g/m^2	mean DDF rate (g/m^2/h)				
		no. of 6 h periods				
		no. of shedding events				
		mean size of shedding event (g/m^2)				
		mean deposits removed (%)				
		mean shedding frequency (h^{-1})				
		mean shedding rate (g/m^2/h)				
	<5000 g/m^2	mean DDF rate (g/m^2/h)	221	*1913*		
		no. of 6 h periods	17	*1*		
		no. of shedding events	8	*3*		
		mean size of shedding event (g/m^2)	965	*845*		
		mean deposits removed (%)	69	*46*		
		mean shedding frequency (h^{-1})	0.27	*1.53*		
		mean shedding rate (g/m^2/h)	260	*1293*		

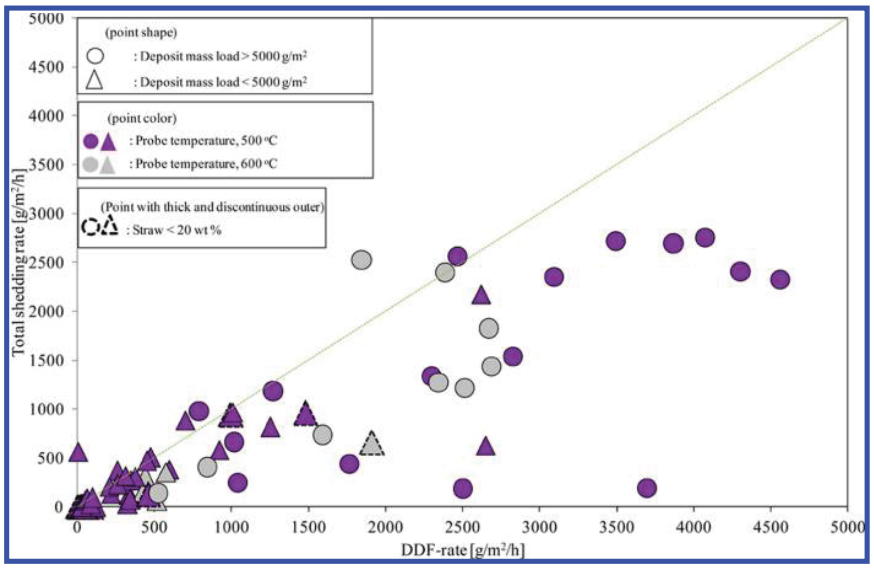

Figure 9. Total deposit shedding rate as a function of the DDF rate. Data points are from tests 1−5. The particular point shape represents the deposit mass load, and the color represents the probe surface temperature, whereas points (larger in size) with thick and discontinuous edges are representative of straw share in wood.

500 °C than at a probe temperature of 600 °C, possibly due to partial melting and/or sintering of the innermost deposit layer (rich in K, Cl, and S)[24] at higher probe surface temperature.

(c) Changed Flue Gas Temperature. As seen in Figure 7 an increased flue gas temperature leads to an increased deposit shedding frequency; even there is seen a very large spread in the data points. By comparison of the data sets with similar

dx.doi.org/10.1021/ef300611v | *Energy Fuels* 2012, 26, 5241−5255

Table 6. Mean DDF Rates and Mean Net Deposit Accumulation Rates for Two Different Sets of Flue Gas Temperatures, Probe Surface Temperatures, Straw Shares, and Deposit Loads

		flue gas temperature:	<850 °C		>850 °C	
fuel straw share	probe deposit mass load	probe surface temperature:	500 °C	600 °C	500 °C	600 °C
		mean flue gas temperature			(909)[b]	(902)[b]
>20 wt %	>5000 g/m^2 (9403)[a]	mean DDF rate (g/m^2/h)			2691	1934
		no. of 6 h periods			16	9
		mean total deposit shedding rate (g/m^{2}h)			1537	1329
		mean net deposit accumulation rate (g/m^2/h)			1155	605
		mean net deposit accumulation rate (g/m^2/h)[c]			957	
	<5000 g/m^2 (2447)[a]	mean flue gas temperature	(823)[b]	(823)[b]	(906)[b]	*(874)*[b]
		mean DDF rate (g/m^2/h)	234	313	1245	*577*
		no. of 6 h periods	19	6	8	*1*
		mean total deposit shedding rate (g/m^2/h)	185	124	793	*356*
		mean net deposit accumulation rate (g/m^2/h)	49	189	452	*221*
		mean net deposit accumulation rate (g/m^2/h)[c]	83		426	
<20 wt %	>5000 g/m^2	mean DDF rate (g/m^2/h)				
		no. of 6 h periods				
		mean total deposit shedding rate (g/m^2/h)				
		mean net deposit accumulation rate (g/m^{2}h)				
		mean net deposit accumulation rate (g/m^2/h)[c]				
	<5000 g/m^2 (792)[a]	mean flue gas temperature	(773)[b]	*(806)*[b]		
		mean DDF rate (g/m^2/h)	221	*1913*		
		no. of 6 h periods	17	*1*		
		mean total deposit shedding rate (g/m^2/h)	147	*660*		
		mean net deposit accumulation rate (g/m^2/h)	73	*1253*		
		mean net deposit accumulation rate (g/m^2/h)[c]	139			

[a]Mean value of the deposit mass load. [b]Mean value of the flue gas temperature. [c]Mean value irrespective of probe surface temperature.

conditions (probe temperature = 500 °C, deposit mass < 5000 g/m^2, and a straw fuel share > 20 wt %) in Tables 4 and 5 but with different flue gas temperatures (below and above 850 °C), there is seen an increase in shedding frequency, and a small increase in shedding mass is also observed when the flue gas temperature is increased.

(d) Increased Fraction of Straw in the Fuel. Changes in fuel straw fraction in the fuel (from above to below 20 wt %) for the data sets with (probe temperature = 500 °C, deposit mass < 5000 g/^{2}, and flue gas temperature < 850 °C) show an increased shedding amount with decreased straw share. However, the mean shedding rate is low at lower straw fraction.

To summarize the main observations, the mean deposit shedding rate (shedding event amount times the shedding frequency) can be used as shown in Tables 4 and 5.

(1) The deposit shedding rates increased at high flue gas temperatures (>850 °C) and high probe deposit mass loads (>5000 g/m^2), at which also high deposit formation rates are observed (DDF rate).

(2) The shedding rate is in most cases higher at a probe temperature of 500 °C than at a probe temperature of 600 °C. A possible reason could be partial melting and/or sintering of the innermost deposit layer (rich in K, Cl, and S)[24] at higher probe surface temperature. This could cause the adhesion strength of the deposit to increase at the higher probe surface temperatures.

(3) The deposit shedding process is a stochastic process, for which the amount of deposit shed varies, even at constant conditions (Figure 8). The deposit amount removed is probably strongly related to the strength of the innermost salt-rich deposit layer.

Net Deposit Accumulation Rate. The total deposit shedding rate was calculated by using eq 4:

$$\text{total deposit shedding rate} = (\text{natural shedding rate} \times F) + (\text{sootblowing shedding rate} \times (1 - F)) \quad (4)$$

Here, F is the fraction of time of the 6 h interval when plant sootblowers were not in operation. The total deposit shedding rate as a function of the DDF rate is shown in Figure 9. It can be seen that with an increase in DDF rate, the total deposit shedding rate slightly increases. It is also evident that the total deposit shedding rate is lower than the DDF rate in most cases. This causes an accumulation of deposit mass on the probe with the passage of time. The accumulation of the deposits can be presented in the form of net deposit accumulation rate, a measure of the difference between the total shedding rate and the DDF rate. In addition, it is of interest for the plant operators to quantify deposit amount finally remaining on the superheater tubes as a common result of buildup and shedding. The net deposit accumulation rate was calculated by eq 5:

$$\text{net deposit accumulation rate} = \text{DDF rate} - \text{total deposit shedding rate} \quad (5)$$

The calculated net deposit formation rate is shown in Table 6 for the changed conditions in flue gas temperature (above or below 850 °C), probe surface temperature (500 or 600 °C), straw fuel share (weight fraction of straw in the fuel above or below 20%), and deposit mass load (above or below 5000 g/m^2). The main observations are the following.

dx.doi.org/10.1021/ef300611v | Energy Fuels 2012, 26, 5241−5255

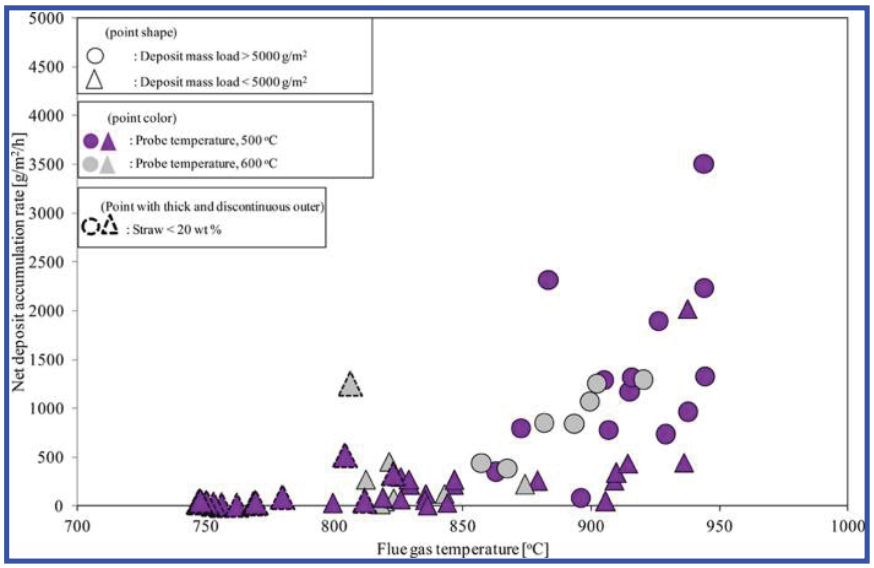

Figure 10. Impact of flue gas temperature on the net deposit accumulation rate. Data points are from tests 1−5. The particular point shape represents the deposit mass load, and the color represents the probe surface temperature, whereas points (larger in size) with thick and discontinuous edges are representative of straw share in wood.

(1) The net deposit accumulation rate increases with increase in flue gas temperature (see Figure 10). Increased flue gas temperatures increase the fraction of molten ash as well as provide an increased content of gas phase alkali species, and both will lead to an increased deposit formation rate. The increase in DDF rate was larger than the increase in deposit shedding rate with increased flue gas temperature as shown in Table 6.

(2) The net deposit accumulation rate is low (452 g/m^2/h) at lower deposit mass load (<5000 g/m^2) on the probe, compared to a value of 1155 g/m^2/h for deposit mass load > 5000 g/m^2 (Table 6, probe temperature = 500 °C, flue gas temperature about 900−910 °C, and straw share > 20 wt %).

(3) Generally, no clear tendency for the impact of probe surface temperature on net deposit accumulation rate was seen.

Deposit Removal by Using an Artificial Sootblowing Probe. The PIP needed in the sootblower jet to remove the probe deposits at different conditions was investigated using all three methods (1−3), and the results are summarized in Figure 11. It can be seen that increasing both probe surface temperatures and exposure times increased the PIP necessary to remove the deposits. It is also clear that deposits formed at a 500 °C probe temperature and with exposure time of <91 h could be removed with a PIP of <55 kPa. With an increase in probe surface temperature from 500 to 600 °C, the PIP needed to remove the deposits significantly increased. It is also interesting to note that the PIP seems to be independent of exposure time at the higher probe temperature. The higher probe surface temperature may cause partial melting and/or sintering of the innermost deposit layer (rich in K, Cl, and S).[24] This would enhance the adhesion between the deposit and superheater tube. At higher probe surface temperatures (>550 °C) and longer probe exposure times, a 2−10 mm thick layer formed on the downstream probe surface. The layer grew to make contact with the thick upstream layer. This ring-shaped layer will be more difficult to remove, because the ring must be broken by the sootblower. At lower surface temperatures (500 °C), the layer formed on the downstream side of the probe was thin, and the distinct upstream layer was easy to remove using the artificial sootblower.

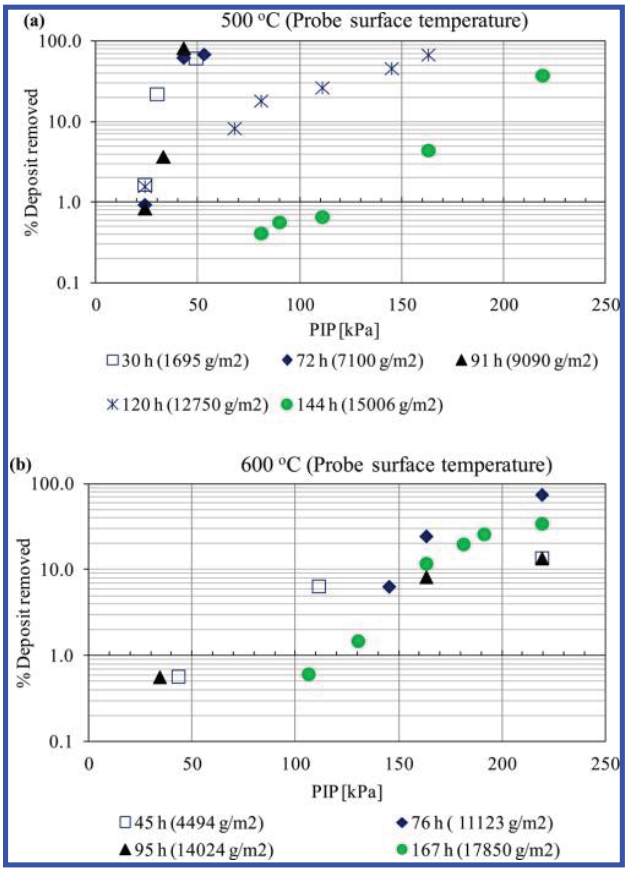

Figure 11. Percentage of deposits removed as a function of applied peak impact pressure (PIP) at different probe exposure times and deposit mass loads: (a) probe surface temperature = 500 °C; (b) probe surface temperature = 600 °C.

dx.doi.org/10.1021/ef300611v | *Energy Fuels* 2012, 26, 5241−5255

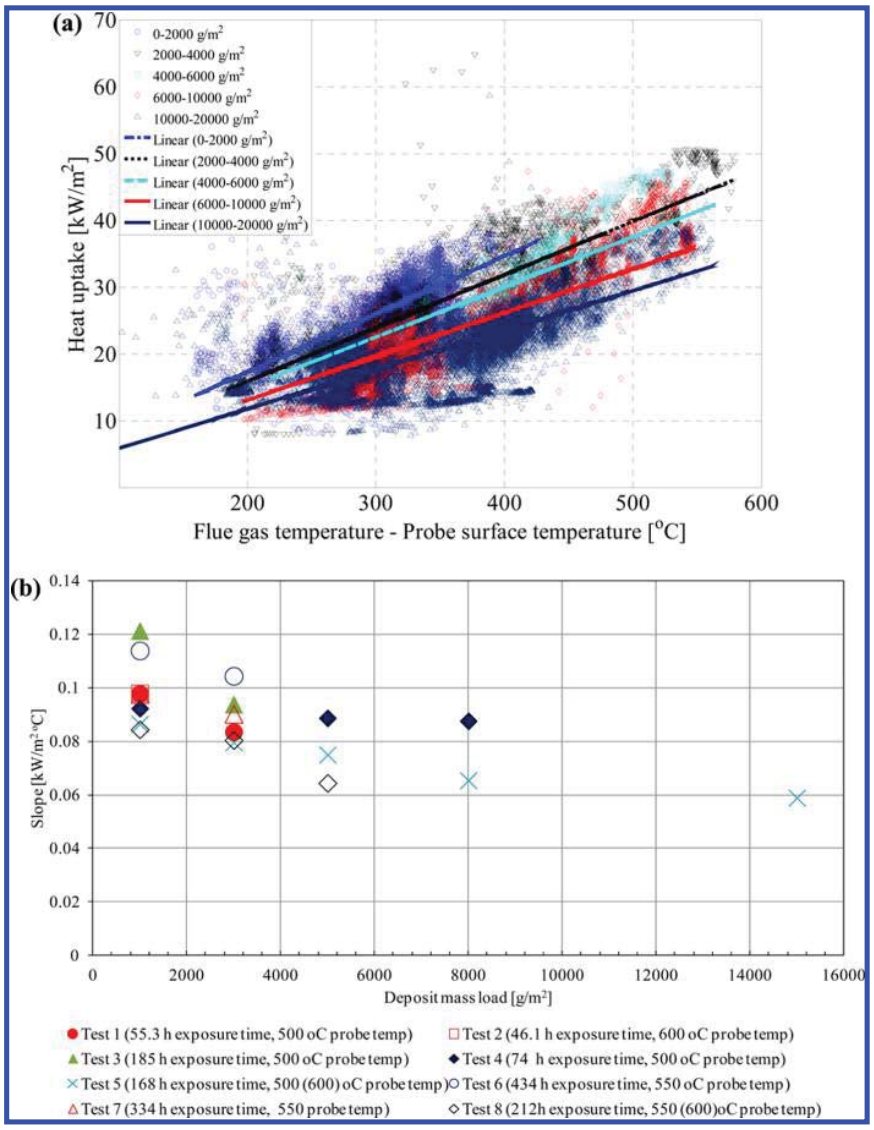

Figure 12. (a) Impact of temperature difference between flue gas and probe surface on heat uptake for different deposit mass loads for test 5. The slope is calculated by a linear fit using the equation $y = bx$. (b) Sensitivity of heat uptake with change in temperature difference between flue gas and probe surface for different deposit mass loads for all tests (1−8).

Probe Heat Uptake. The heat uptake in the probe, for different deposit mass loads during test 5, is shown Figure 12a as a function of the difference between flue gas temperature and probe surface temperature. It can be seen that when the deposit mass load is higher (>5000 g/m^2), the slope slightly decreases due to the insulation effect of the deposit layers. The slope for different deposit loads for each test was calculated, and the combined slopes for all tests for different probe mass loads are shown in Figure 12b. A moderate reduction in the probe heat uptake was observed with increase in mass load of deposits on the probe. All of the tests provided reasonably similar results. Additionally, it can be seen that up to a deposit mass load of 5000 g/m^2 the reduction in heat transfer is steeper, whereafter the steepness of the curve is reduced. This is consistent with the deposit layer being more pronounced on the upstream side, so that most of the heat uptake will occur through the downstream side.

CONCLUSIONS

The overall conclusions are the following:

(1) Video recordings revealed that deposit shedding was primarily through debonding, where a deposit layer is being removed due to a breakoff of the deposit from the tube surface.

(2) It was observed that the shedding process is a stochastic process, where the amounts of deposit shed are highly variable even at constant conditions. We believe the amount of deposit shed is strongly related to the strength of the innermost salt-rich deposit layer.

(3) The deposit shedding process was characterized by calculation of the average amount of deposit removed at a shedding event (g/m^2) and the frequency of the shedding events (h^{-1}) in 6 h periods. The average shedding event magnitude was 716 g/m^2 during natural deposit shedding and 805 g/m^2 during plant sootblowing-induced shedding events. The shedding frequencies were 0.81 and 0.89 h^{-1} during natural deposit shedding and plant sootblowing-induced

dx.doi.org/10.1021/ef300611v | *Energy Fuels* 2012, 26, 5241−5255

shedding events, respectively. On the basis of the shedding magnitude and frequency, it was possible to calculate a shedding rate ($g/m^2/h$).

(4) The deposit shedding rates increased at high flue gas temperatures (>850 °C) and high probe deposit mass loads (>5000 g/m^2) at which also high deposit formation rates are observed (DDF rate).

(5) The shedding rate is in most cases higher at a probe temperature of 500 °C than at a probe temperature of 600 °C.

(6) The net deposit accumulation rate increases with increase in flue gas temperature. Increased flue gas temperatures increase the fraction of molten ash as well as provide an increased content of gas phase alkali species, and both will lead to an increased deposit formation rate. The increase in DDF rate was larger than the increase in deposit-shedding rate with increased flue gas temperature.

(7) The net deposit accumulation rate is low (452 $g/m^2/h$) at lower deposit mass load (<5000 g/m^2) on the probe, compared to a value of 1155 $g/m^2/h$ for deposit mass load > 5000 g/m^2 (probe temperature = 500 °C, flue gas temperature about 900−910 °C, and straw share > 20 wt %).

(8) Generally, no clear tendency for the impact of probe surface temperature on net deposit accumulation rate was seen.

(9) A sootblower probe was used to investigate the needed PIP to remove the deposits. At lower temperatures (500 °C), the deposits formed at a exposure time of <91 h could be removed with a PIP of <55 kPa. At higher probe surface temperature (>550 °C), the PIP needed to remove the probe deposits significantly increases.

AUTHOR INFORMATION

Corresponding Author

*Phone: +45 45 25 28 49. Fax: +45 45 88 22 58. E-mail: paj@kt.dtu.dk.

Notes

The authors declare no competing financial interest.

ACKNOWLEDGMENTS

The financial support by Energinet.DK under the PSO Project 7217 and the financial support by Vattenfall A/S are gratefully acknowledged. We give special thanks to Vattenfall A/S for providing access to their boiler. In addition, we are thankful to the operational staff at the Amager Power Plant for their technical support during the full-scale measurements.

NOMENCLATURE

CCD = charge-coupled device

DDF rate = derivative-based deposit formation rate ($g/m^2/h$)

F = time fraction of 6 h period with no sootblower operation

$f_{nat,6}$ = mean natural deposit shedding frequency (h^{-1})

$f_{soot,6}$ = mean plant sootblowing deposit shedding frequency (h^{-1})

IDF rate = integrated deposit formation rate ($g/m^2/h$)

IFRF = International Flame Research Foundation

PIP = peak impact pressure (kPa)

REFERENCES

(1) Baxter, L. L. Ash deposition during biomass and coal combustion: a mechanistic approach. *Biomass Bioenergy* **1993**, *4*, 85−102.

(2) Nielsen, H. P. Deposition and high temperature corrosion in biomass-fired boilers. Ph.D. Thesis, Technical University of Denmark. 1998; ISBN 87-90142-47-0.

(3) Jenkins, B. M.; Baxter, L. L.; Miles, T. R., Jr.; Miles, T. R. Combustion properties of biomass. *Fuel Process. Technol.* **1998**, *54*, 17−46.

(4) Miles, T. R.; Miles, T. R., Jr.; Baxter, L. L.; Bryers, R. W.; Jenkins, B. M.; Oden, L. L. Boiler deposits from firing biomass fuels. *Biomass Bioenergy* **1996**, *10*, 125−138.

(5) Baxter, L. L. Influence of ash deposit chemistry and structure on physical and transport properties. *Fuel Process. Technol.* **1998**, *56*, 81−88.

(6) Sander, B.; Henriksen, N.; Larsen, O. H.; Skriver, A.; Ramsgaard-Nielsen, C.; Jensen, J. N.; Stærkind, K.; Livberg, H.; Thellefsen, M.; Dam-Johansen, K.; Frandsen, F. J.; van der Lans, R.; Hansen, J. Emissions, corrosion and alkali chemistry in straw-fired combined heat and power plants. *Proceedings of the 1st World Conference on Biomass for Energy and Industry*, Sevilla, Spain, June 5−9; James and James (Science Publishers): London, UK, 2009.

(7) Jensen, P. A.; Sander, B.; Dam-Johansen, K. Removal of K and Cl by leaching of straw char. *Biomass Bioenergy* **2001**, *20*, 447−457.

(8) Andersen, K. H.; Frandsen, F. J.; Hansen, P. F. B.; Wieck-Hansen, K.; Rasmussen, I.; Overgaard, P.; Dam-Johansen, K. Deposit formation in a 150 MWe utility PF-boiler during co-combustion of coal and straw. *Energy Fuels* **2000**, *14*, 765−780.

(9) Jensen, P. A.; Frandsen, F. J.; Hansen, J.; Dam-Johansen, K.; Henriksen, N.; Hörlyck, S. SEM investigation of superheater deposits from biomass-fired boilers. *Energy Fuels* **2004**, *18*, 378−384.

(10) Jensen, P. A.; Sørensen, L. H.; Hu, G.; Holm, J. K.; Frandsen, F.; Henriksen, U. B. Combustion experiments with biomass fuels and additives in a suspension fired entrained flow reactor − test of Ca and P rich additives used to minimize deposition and corrosion. *PSO Project: Biomass Dust Firing*; CHEC Report R0504, CHEC Research Centre, Technical University of Denmark: Lyngby, Denmark, 2005.

(11) Wu, H.; Glarborg, P.; Frandsen, F. J.; Dam-Johansen, K.; Jensen, P. A. Dust-firing of straw and additives: ash chemistry and deposition behavior. *Energy Fuels* **2011**, *25*, 2862−2873.

(12) Jensen, P. A.; Zhou, H.; Frandsen, F. J.; Hansen, J. Ash deposits removal in biomass power plant boilers. *Proceeding of 15th European Biomass Conference and Exhibition*, Berlin, Germany, May 7−11; ETA-Florence Renewable Energies: Florence, Italy, 2007.

(13) Tobiasen, L.; Skytte, R.; Pedersen, L. S.; Pedersen, S. T.; Lindberg, M. A. Deposit characteristics after injection of additives to a Danish straw-fired suspension boiler. *Fuel Process. Technol.* **2007**, *88*, 1108−1117.

(14) Frandsen, F. J. Ash formation, deposition and corrosion when utilizing straw for heat and power production. Doctoral Thesis, Technical University of Denmark, 2011; ISBN 978-87-92481-40-5.

(15) Jensen, P. A.; Stenholm, M.; Hald, P. Deposition investigation in straw-fired boilers. *Energy Fuels* **1997**, *11*, 1048−1055.

(16) Zbogar, A.; Frandsen, F.; Jensen, P. A.; Glarborg, P. Shedding of ash deposits. *Prog. Energy Combust. Sci.* **2009**, *35*, 31−56.

(17) Jameel, M. I.; Cormack, D. E.; Tran, H.; Moskal, T. E. Sootblowing optimization, Part 1: Fundamental hydrodynamics of a soootblower nozzle and jet. *Tappi J.* **1994**, *77*, 135−142.

(18) Ebrahimi-Sabet, S. A. A laboratory study of deposit removal by debonding and its application to fireside deposits in Kraft boilers. Ph.D. Thesis, Department of Chemical Engineering and Applied Chemistry, University of Toronto, 2001; ISBN 0-612-58923-4.

(19) Stitt, S. J.; Junker, H.; Baxter, L. L. Optimization of deposit removal in biofueled boilers: review of control systems, technologies and mechanisms, Report 02-1036. *Tech-wise* **2002**, 1−27.

(20) Zhou, H.; Frandsen, F. J.; Jensen, P. A.; Glarborg, P. PSO Project 4106, CHEC Report R0603, CHEC Research Centre, Technical University of Denmark, 2006.

(21) Zbogar, A.; Frandsen, F. J.; Jensen, P. A.; Hansen, J.; Glarborg, P. Experimental investigation of ash deposit shedding in a straw-fired boiler. *Energy Fuels* **2006**, *20*, 512−519.

(22) Pophali, A.; Emamia, B.; Bussmanna, M.; Tran, H. Studies on sootblower jet dynamics and ash deposit removal in industrial boilers. *Fuel Process. Technol.* **2011**, DOI: 10.1016/j.fuproc.2011.04.034.

(23) Kaliazine, A.; Cormack, D. E.; Ebrahimi-Sabet, A.; Tran, H. The mechanics of deposit removal in kraft recovery boilers. *J. Pulp Paper Sci.* **1999**, *25*, 418−424.
(24) Bashir, M. S.; Jensen, P. A.; Frandsen, F.; Wedel, S.; Dam-Johansen, K.; Wadenbäck, J.; Pedersen, S. T. Suspension-firing of biomass. Part 1: Full-scale measurements of ash deposit build-up. *Energy Fuels* **2012**, *26*, 2317−2330.
(25) Bashir, M. S.; Jensen, P. A.; Frandsen, F. J.; Wedel, S.; Dam-Johansen, K.; Pedersen, S. T.; Wadenbäck, J. Quantification of ash deposit build-up and removal in a straw and wood suspension-fired boiler. *Proceedings of 19th European Biomass Conference and Exhibition*, Berlin, Germany, June 6−10; ETA-Florence Renewable Energies: Florence, Italy, 2011.
(26) Nordgren, D.; Hedman, H.; Padban, N.; Boström, D.; Öhman, M. Ash transformations. *Fuel Process Technol.* **2011**, DOI: 10.1016/j.fuproc.2011.05.027.
(27) Frandsen, F. J. Utilizing biomass and waste for power production − a decade of contributing to the understanding, interpretation and analysis of deposits and corrosion products. *Fuel* **2005**, *84*, 1277−1294.
(28) Gjernes, E. Fuel flexibility at Amager unit 1 using pulverized fuels. *Proceedings of Power-Gen Europe*, Cologne, Germany, 2006.
(29) *IFRF Suction Pyrometer, User Information Document*; International Flame Research Foundation: Livorno, Italy, 2010.
(30) Bashir, M. S.; Jensen, P. A.; Frandsen, F.; Wedel, S.; Dam-Johansen, K.; Wadenbäck, J.; Pedersen, S. T. Ash transformation and deposit build-up during biomass suspension and grate firing: full-scale experimental studies. *Fuel Process. Technol.* **2012**, *97*, 93−106.

June. 2012, DTU no. 50530

Appendix A6

Suspension-firing of wood with coal ash addition: Probe measurements of ash deposit build-up at Avedøre Power Plant (AVV2)

Energinet.dk project no. 7217

Characterization and quantification of deposits build up and removal in straw suspension fired boilers

Muhammad Shafique Bashir, Peter Arendt Jensen, Flemming Frandsen, Stig Wedel, Kim Dam-Johansen.

Department of Chemical and Biochemical Engineering

Technical University of Denmark

Søltofts Plads, Building 229, DK-2800 Lyngby, Denmark

CHEC no. R1301

Contents

Abstract

This report is about full-scale probe measurements of deposit build-up and removal conducted at the Avedøreværket Unit 2, a 800 MW_{th} suspension boiler, firing wood and natural gas with the addition of coal ash. Coal ash was used as an additive to capture potassium (K) from wood-firing. Investigations of deposit formation rate were made by use of an advanced online ash deposition/shedding probe. Quantification of ash deposition and shedding was made via deposit mass uptake signals obtained from the deposit probe. The influence of coal ash, flue gas temperature, probe surface temperature and boiler load on ash deposition propensity was investigated. Results of ash deposition propensity showed increasing trend with increasing flue gas temperature. Video monitoring revealed that the deposits formed were not sticky and could be easily removed, and even at very high flue gas temperatures (> 1350 ^{o}C), deposit removal through surface melting was not identified. SEM-EDS analysis of the deposits showed significant presence of Ca, Al and Si, indicating that a significant amount of K has been captured by coal ash to form deposits rich in calcium-aluminum-silicates, and possible release of Cl to the gas phase as HCl(g). Effect of boiler operational parameters on gas emissions has also been investigated.

Keywords: *Dust-firing, coal ash as additive, deposits, deposit formation rate, deposit removal (shedding).*

1 INTRODUCTION

The focus on substituting fossil resources by biomass has significantly increased the interest in efficient use of biomass for heat and electricity production, and this includes the use of wood in suspension-fired boilers. In the recent decades, the focus to substitute fossil fuels by wood has significantly increased the interest in efficient use of wood in large suspension-fired boilers. However, the presence of alkali metals (K) and chlorine (Cl) in wood – even in small amount – may induce operational problems due to ash deposit formation, corrosion and deactivation of SCR catalyst [1-4]. Strategies to handle ash deposit related problems include use of additive to chemically capture potassium (K), leaching of potassium (K) from fuel, inhibition of sintering and effective deposit shedding techniques [5-12].

Some full-scale experimental studies on deposit build-up have been reported on measurements in biomass grate and fluidized-bed boilers [13-16]. Only limited data is available from wood suspension-firing where improved knowledge on the transient deposit formation and removal is needed to optimize design and operation [17-19]. Fewer full-scale pulverized wood-firing investigations are reported in the literature and the most recent ones are by Jensen et al. [5], Skrifvars et al. [19] and Bashir et al. [17, 20]. In addition, most of these studies have been based on short testing time (up to couple of hours) [5,19], while more extensive full-scale measurements are rare to find [17, 20]. Therefore, more detailed and extensive full-scale studies on transient deposit formation rate when firing wood with coal ash addition will improve our understanding of deposit formation and shedding processes.

This report aims to provide long time, full-scale data on ash deposit formation at the Avedøreværket Unit 2, a 800 MW_{th} suspension boiler, firing wood and natural gas with the addition of coal ash. The boiler was operated with coal fly ash addition to minimize problems of deposit formation, corrosion and deactivation of SCR catalyst. Possibly the alumina silicates present in the coal ash may react with potassium chloride, where HCl is released, and potassium (K) is bound in alumina silicates with relatively high melting temperatures. Furthermore, quantitative information on ash deposition propensity as functions of operating conditions is provided. The influence of coal ash to wood ash ratio, probe exposure time, probe surface temperature (500 ^{o}C, 550 ^{o}C), boiler load and flue gas temperature (750-1450 ^{o}C) on ash deposition propensity have been investigated. Effect of boiler operational parameters on gas emissions has also been investigated.

2 EUIPMENTS, MATERIALS AND METHODS

2.1 Boiler

The probe measurements were conducted at Avedøre Power Station, unit 2 (AVV2), firing wood and natural gas in suspension. The AVV2 boiler, located in the Copenhagen area, is a multi-fuel suspension-fired boiler that can apply wood, natural gas and heavy fuel oil as fuel. The boiler drawing is shown in Figure 1. The AVV2 boiler is a 80 meter high Benson type boiler with a thermal capacity of 800 MW_{th}. Overall, there are three sub-units, a straw-

fired grate boiler, a suspension-fired boiler and lastly two gas turbines [5]. In the lower part of the boiler tower is the combustion chamber, which has 16 burners in four levels (see Figure 1). There are three mills used to grind wood pellets, and the pulverized wood after being ground in the mills is blown into the burners, where the fuel particles are burned in suspension. Above the combustion chamber is a radiation shield, followed by the superheaters and economizers. The probe measuring position was situated at a level of ~48.9 m, meaning that the probe was inserted below the radiation shield (Appendix A). The AVV2 boiler is being able to operate in a pure condensing mode, a pure back pressure mode or any combination. Operating in pure condensing mode, an electrical efficiency of 48 % is obtainable. If operated in pure back pressure mode, using the thermal energy of the condensed steam for district heating, the total efficiency can be as high as 94 % [5].

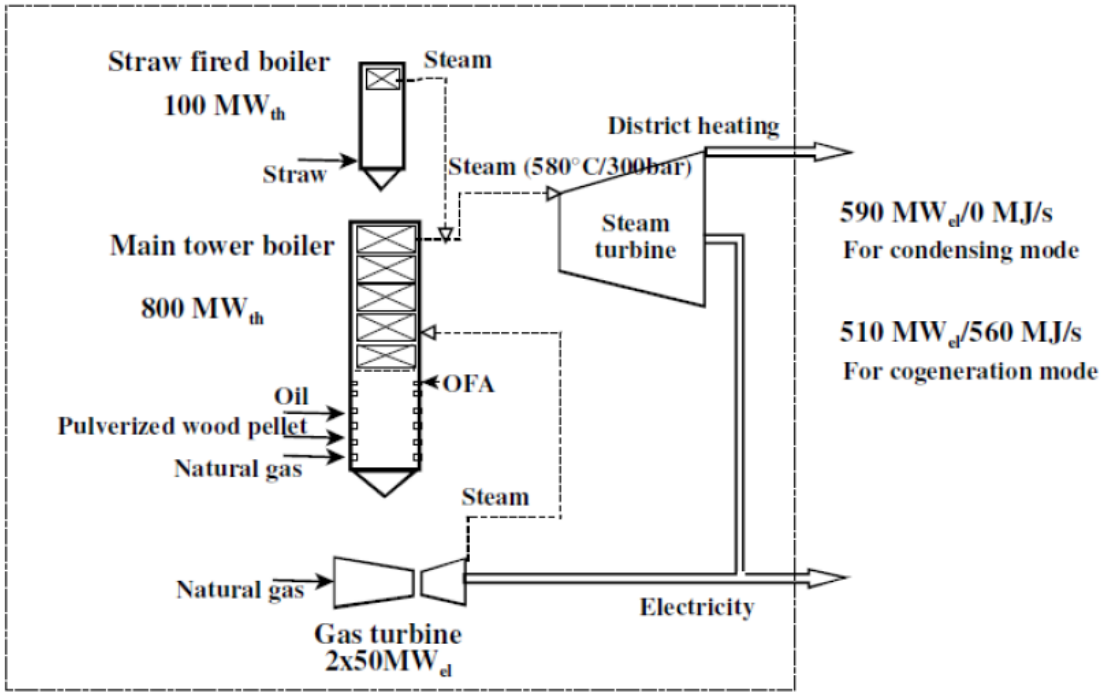

Figure 1: Flow chart of the Avedøre Power Station, unit 2. [5]

2.2 Ash deposition probe

The deposit probe system used for the measurements is shown schematically in Figure 2. The probe was made of stainless steel, about 3 m long and having an outer diameter of 40.5 mm. The deposit probe was cooled by water and air, whereby it was possible to determine heat uptake by the probe and keep a stable surface temperature. The probe was placed in an acoustic pyrometer port on the boiler wall. In the start of the current measurements, due to higher flue gas temperature (>1250 ^{o}C), it was not possible to keep the probe surface temperature between 500 and 600 ^{o}C. A possible reason was that the boiler was running with a high wood-fuel input leading to high flue gas temperatures at the probe measuring position. The problem of keeping the probe surface temperature at the desired levels was then solved by mounting the probe somewhat retracted. A special port extension pipe was installed to keep the probe only 772 mm inside the boiler (Figure 2 (a, b)). This solution believed to work satisfactory if the probe is inserted slowly in the boiler because with the formation of a small layer of deposits on the probe, the probe surface temperature fluctuations were considerably reduced.

(a)

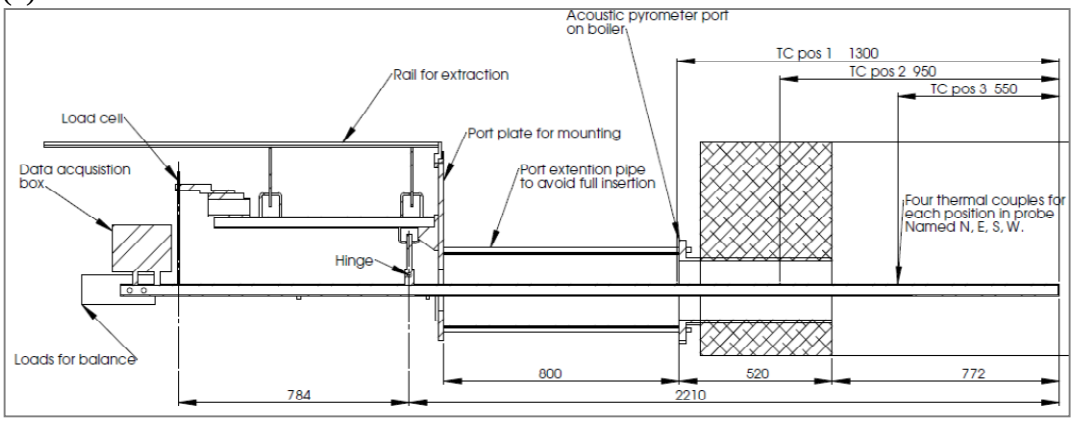

(b)

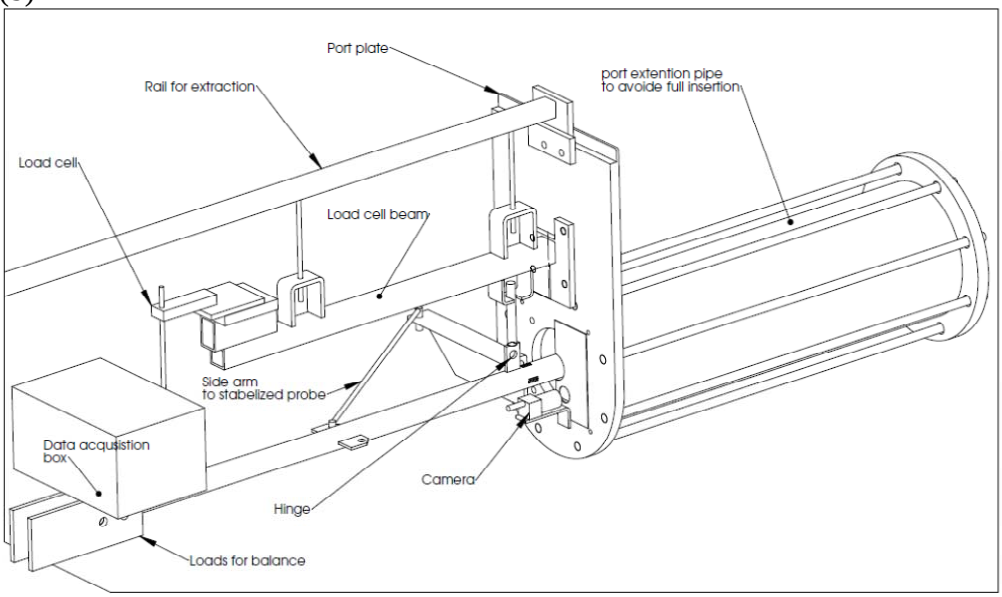

(c)

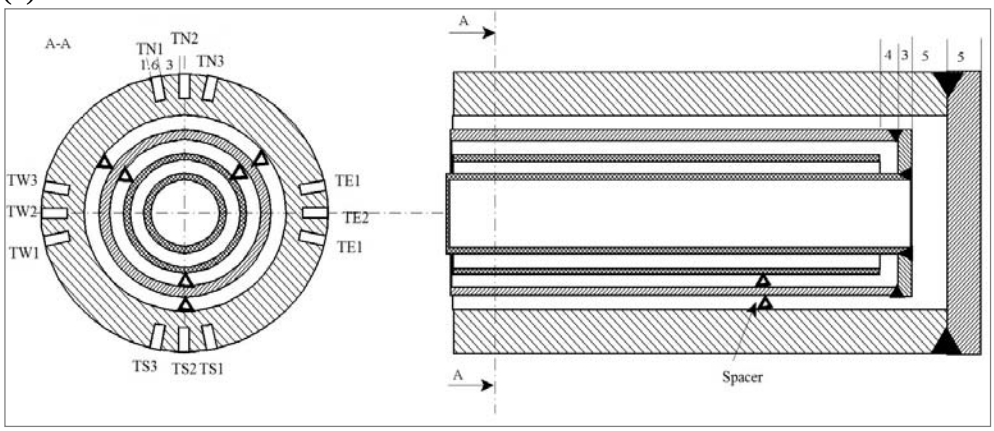

Figure 2: a) Schematic drawing of the probe with identified positions of temperature measurements, deposition area, port extension pipe, port plate for mounting, hinge, load cell and rail for pulling out the probe, b) layout of the complete probe set up, c) cross-sectional view perpendicular to the probe axis and cross-sectional view along the axis of annuli.

In total, 12 thermocouples were placed inside the outer probe metal tube with four thermo-elements at three different horizontal positions (Figure 2 (c)). In each horizontal position, the thermocouple provided temperature information at the N, S, E and W position of the probe. However, due to the modifications with the extension pipe, probe temperature measurements only at horizontal position 3 were possible.

The flue gas temperature near the probe was measured using a simple thermocouple in a protective shell. In addition, a suction pyrometer (International Flame Research Foundation model, IFRF [22]) was also used for some periods to find the difference between the thermocouple flue gas temperature measurements and suction pyrometer flue gas temperature measurements.

It was tried to make a special port for video monitoring functional at the right wall of the probe measuring position in order to have a better angle of view, but due to problems in maintaining the port temperature at the required levels (< 50 ^{o}C), a CCD (charge-coupled device) camera was placed below the probe to register the deposit formation and removal processes on the probe (Figure 2 (b)).

2.2.1 Probe heat uptake

The water and air flow to the probe was measured by flow meters at the inlets of the probe. The temperatures of the water and air were measured by 4 thermocouples at the inlet and outlet positions. The probe heat uptake was then calculated under steady state conditions using:

$$Q = \frac{\dot{m}_w C_{p,w}\left(T_{w,out} - T_{w,in}\right) + \dot{m}_a C_{p,a}\left(\overline{T}\right)\left(T_{a,out} - T_{a,in}\right)}{s} \qquad (1)$$

Where Q is the heat uptake (W/m^2), $\dot{m}$ is the flow rate (kg/s), C_p is the heat capacity (J/kg/K), T is the temperature (K), while in the superscripts w and a represent water and air, respectively. In the above equation (1), s represents the effective probe surface area.

2.2.2 Deposit mass uptake

The deposit mass uptake was calculated by using the following torque balance:

$$m_d g = \left(m_{to} - m_{t1}\right) g \frac{L_1}{L_2} \qquad (2)$$

Where m_d is the deposit mass (g), m_{to} is the initial signal of the load cell, m_{t1} is the final signal of the load cell, g is the gravitational acceleration (m/s^2), while L_1 and L_2 are the distances (mm) from the hinge to the balance and to the mass center of the deposit, respectively.

2.3 Fuels

The fuels fired during the measurements were wood-dust and natural gas. As it was not possible to obtain fuel samples, the composition of the applied fuels is adopted from previous measurements at AVV2 ([5], Table 1). Fuel analysis shows that the wood fuel has

small content of potassium (K) and chlorine (Cl), while calcium (Ca) and silica (Si) are present in significant amounts. The natural gas analysis shows a large content of CH_4 and C_2H_6.

The coal ash used as an additive contains significant content of aluminum (Al) and silicon (Si), indicating possible potential of the coal ash to capture potassium (K) formed during wood combustion.

Table 1: Analysis of the fuels fired and added coal ash. [5] ar: as received, db: dry basis

Parameter	Wood	Coal ash	Parameter	Units	Natural gas
Ash contents (wt% ar), assumed	1.0	--	--	--	--
Moisture (wt%)	5.80	--	--	--	--
Higher Heat Value (MJ/kg db)	17.0	--	Heating value	MJ/kg	48.07
C (wt% db)	46.84	--	CH_4	mol. %	89.06
S (wt% db)	0.009	0.26	C_2H_6	mol. %	6.08
N (wt% db)	0.094	--	C_3H_8	mol. %	2.47
H (wt% db)	5.91	--	iC_4H_{10}	mol. %	0.39
O (wt% db)	40.53	--	nC_4H_{10}	mol. %	0.54
Cl (wt% db)	0.0043	0.0	C_5H_{12}	mol. %	0.11
Al (wt% db)	0.014	14.0	nC_5	mol. %	0.08
Ca (wt% db)	0.14	5.2	C_{5+}	mol. %	0.05
Fe (wt% db)	0.013	2.3	N_2	mol. %	0.29
K (wt% db)	0.048	0.45	CO_2	mol. %	0.91
Mg (wt% db)	0.024	0.91	--	--	--
Na (wt% db)	0.005	0.11	--	--	--
P (wt% db)	0.0058	0.81	--	--	--
Si (wt% db)	0.17	20.0	--	--	--

2.4 Procedure of experiments

A series of deposit probe measurements were conducted in a region just below the radiation shield. In the measurements, varying ratio of coal ash to the wood ash was used. Each measurement lasted 1-5 days (all measurements from 04 April to 15 April, 2011). The influence of coal ash, boiler load, probe surface temperature and flue gas temperature on ash deposition propensity was investigated. The target probe surface temperatures were varied between 500 and 550 ^oC in order to investigate ash deposition at two different probe surface temperatures. The deposition probe was exposed to flue gas temperatures from 750 to 1450 ^oC. The overall experimental summary is shown in Table 2. The first three tests are at higher boiler loads with varying biomass loads, while test four is long due to the fact that the boiler was running smoothly for a longer period at lower overall boiler load and biomass load, while test 5 is based on measurements at moderate boiler load.

In each measurement, boiler operational data was collected to make it possible to analyze the influence of boiler operational parameters on ash deposition and gas emissions (CO, NO_x and SO_2). Biomass load was calculated by using equation (3),

$$Biomass\ Load\ (\%) = \frac{Wood\ fuel\ flow\ rate \cdot Heating\ value\ of\ wood}{800 MW_{th}} \cdot 100 \quad (3)$$

The sootblowers located very near to the probe measuring position (0.8 m to the right on the same wall and about 3 m to the right on the right wall) were shut down during all the tests, while the rest of the sootblowers in the probe measuring position were still in operation.

Table 2: Experimental summary. W: wood, NG: natural gas

Test no.	**1**	**2**	**3**	**4**	**5**
Start date-	**05/04-**	**05/04-**	**06/04-**	**08/04-**	**13/04-**
End date	**06/04**	**06/04**	**07/04**	**13/04**	**15/04**
Fuel	W and NG	W and NG	W and NG	W and NG	W and NG
Boiler load (%)	91	98	88	41	76
Biomass load (%)	44	81	72	18	59
Target probe temperature (°C)	550	550	550	500	500
Exposure time (h)	26	16	28	116	52

3 RESULTS AND DISCUSSION

3.1 Probe functionality

A great deal of information was collected by using the deposition probe. However, there were some technical issues regarding control of the air flow to the probe and to keep the probe surface temperature at the required level. In the start of the measurements, due to high flue gas temperature (>1250 °C), it was not possible to keep the probe surface temperature between 500 and 600 °C. A possible reason was that the boiler was running with a high wood-fuel input leading to high flue gas temperatures at the probe measuring position. The problem of keeping the probe surface temperature at the desired levels was then solved by mounting the probe somewhat retracted. A special port extension pipe was installed to keep the probe only 772 mm inside the boiler. However, even though only 772 mm probe was inside the boiler, due to the higher flue gas temperature, there were still fluctuations in the probe surface temperature. The control parameters for the air flow to the probe added additional problems. However, by adjusting the air pressure to the controller (air) and finding appropriate PID parameters for the controller (air), the fluctuations in the probe surface temperature were reduced. The load cell worked well to quantify the deposit build-up. Due to high flue gas temperature, it was not possible to cool the camera port. Therefore, the camera was placed just below the probe instead of in a separate port. The

video quality and angle of view were therefore not the same as were planned. However, still we were able get some good images to identify the deposit formation and shedding processes.

3.2 Data treatment

A large set of data was obtained from the Power Plant and the probe measurements, and a data treatment procedure was adopted for each test. As an example, the detailed signals of flue gas temperature, deposit mass uptake, events of plant sootblowing and probe heat uptake during test 3 are shown in Figure 3, while fuel flow and boiler load are shown in Figure 4. The thick black line along with the deposit mass uptake signals (Figure 3) indicate the events when the nearby plant sootblowers were in operation. It was observed that even though the plant sootblowers located very near to the probe measuring position (0.8 m to the right on the same wall and about 3 m to the right on the right wall) were closed, the rest of the sootblowers were to some extent effective in causing smaller fluctuations to the deposit mass uptake. The information about the activeness of the surrounding plant sootblowers was provided by DONG energy.

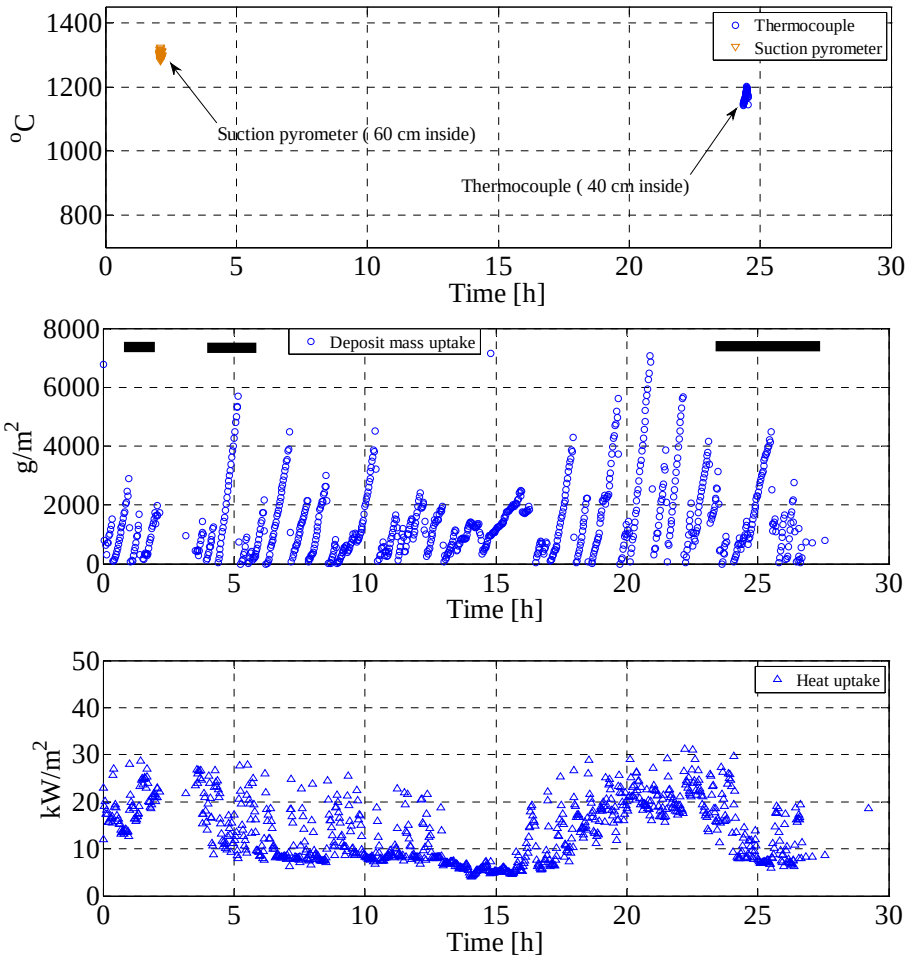

Figure 3: Flue gas temperature, deposit mass uptake, plant sootblowing and probe heat uptake during test 3. The thick black line in the middle figure shows the time when the surrounding sootblowers were in operation.

During test 3, the boiler was running at a mean load of 88.5 %. The biomass (wood) load was more than 80 % in the first 5 h and then slowly decreased to about 70 % in the next 5 h, and between 13 to 17 h, the biomass load fluctuated at approximately 50 %. The flue gas temperature measured during this test was around 1300±75 ^{o}C based on flue gas temperature measurements with suction pyrometer for a short period. The flue gas temperature for the rest of the test was estimated based on the thermocouple readings and difference between temperature measured by suction pyrometer and thermocouple, and boiler load information. The deposit mass uptake signals indicate a number of events with steep increase and then a sudden drop due to shedding of deposits (Figure 3). It can be seen that at higher biomass and boiler load, the deposit mass uptake curve is steeper during time with lower biomass and boiler load, possibly due to changes induced by flue gas temperature and biomass ash flux (Figure 4). The probe heat uptake fluctuations are also evident at higher biomass and boiler load due to larger amount of air needed to keep the probe surface temperature close to the target temperature.

The fuel (wood) flow through each mill during test 3 is shown in Figure 5. The coal ash flow and ratio of coal ash to fuel ash is also shown in the figure. It can be seen that during the 13 to 17 h period, mill 10 was not in operation, thereby causing a reduced biomass load and a slight increase in coal ash to wood ash ratio. The deposit mass uptake signals during this interval are less steeper compared to the events when mill 10 was in operation.

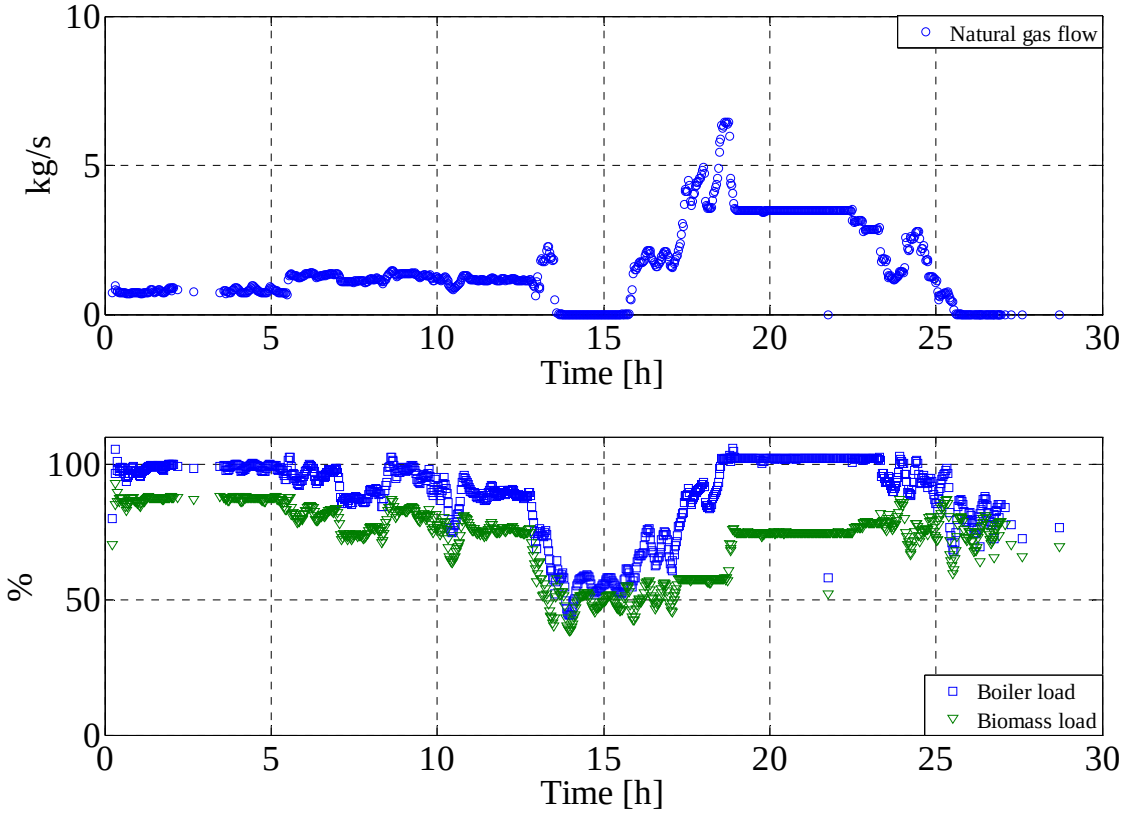

Figure 4: Natural gas flow, overall boiler load and biomass load during test 3.

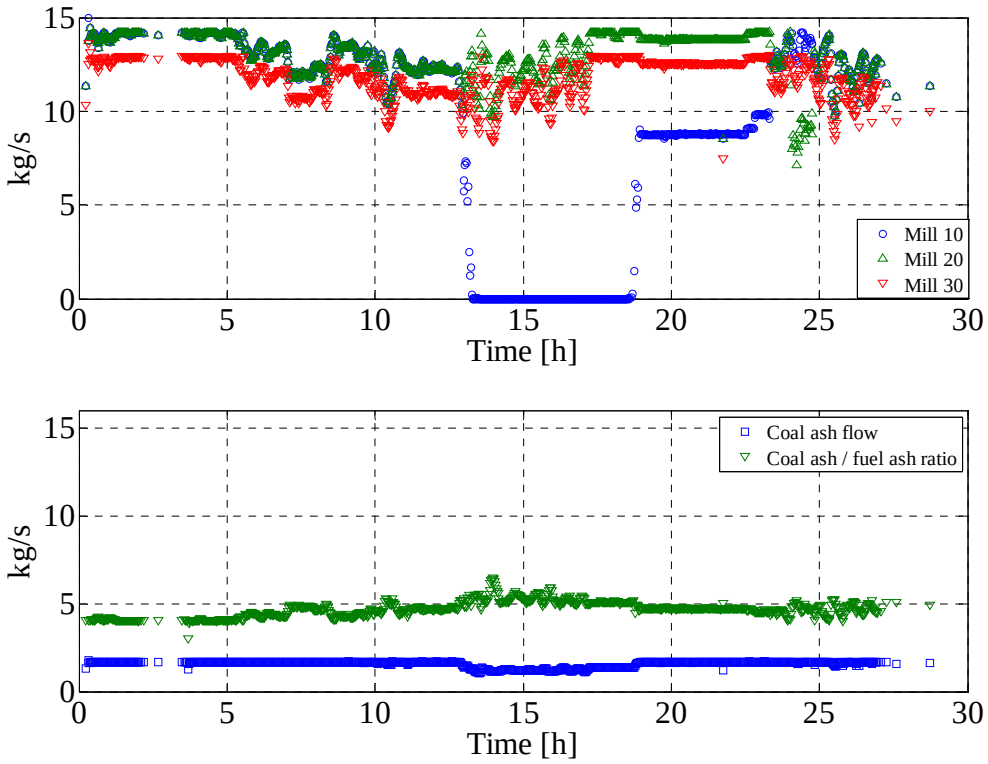

Figure 5: Fuel flow (wood) through each mill of the boiler, coal ash flow (kg/s) and ratio between coal ash and wood ash flow during test 3. It is assumed that wood fuel contains 1.0 wt. % ash.

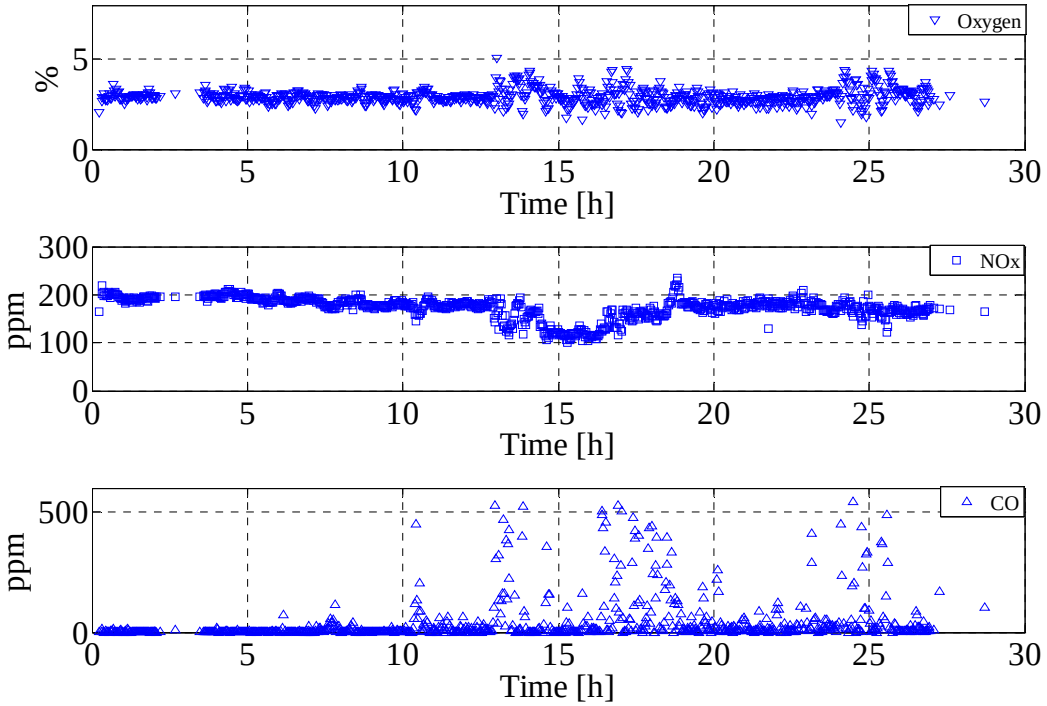

Figure 6: Oxygen level, NOx level before DeNOx and CO level during test 3.

The gas emissions (CO and NO_x) are shown in Figure 6. It is clear that NO_x emissions were reduced at lower biomass and boiler load. The CO emissions indicate fluctuations during the 13-20 h and 23-27 h period, possibly caused by fluctuations in the fuel flow through mills during these periods. CO emissions are generally low at smoother fuel flow to the boiler.

The probe temperatures were continuously monitored and the measured signals of four thermo-elements at position 3 are shown in Figure 7. The S3 position was used as target probe temperature. The water and air flow needed to keep the probe surface temperature stable and close to the target are shown in Figure 8. There is a seen significant drop in probe surface temperatures from 13 to 17 h of exposure time due to reduced boiler load. However, this trend indicates that further improvement in the air flow control is needed to keep the probe surface temperature close to the target temperature with least fluctuations, even at low and high flue gas temperatures. The detailed signals of flue gas temperature, mass uptake, heat uptake, fuel flow, boiler load, biomass load, probe surface temperatures and coolant flow to the probe for the rest of the tests can be found in Appendix B.

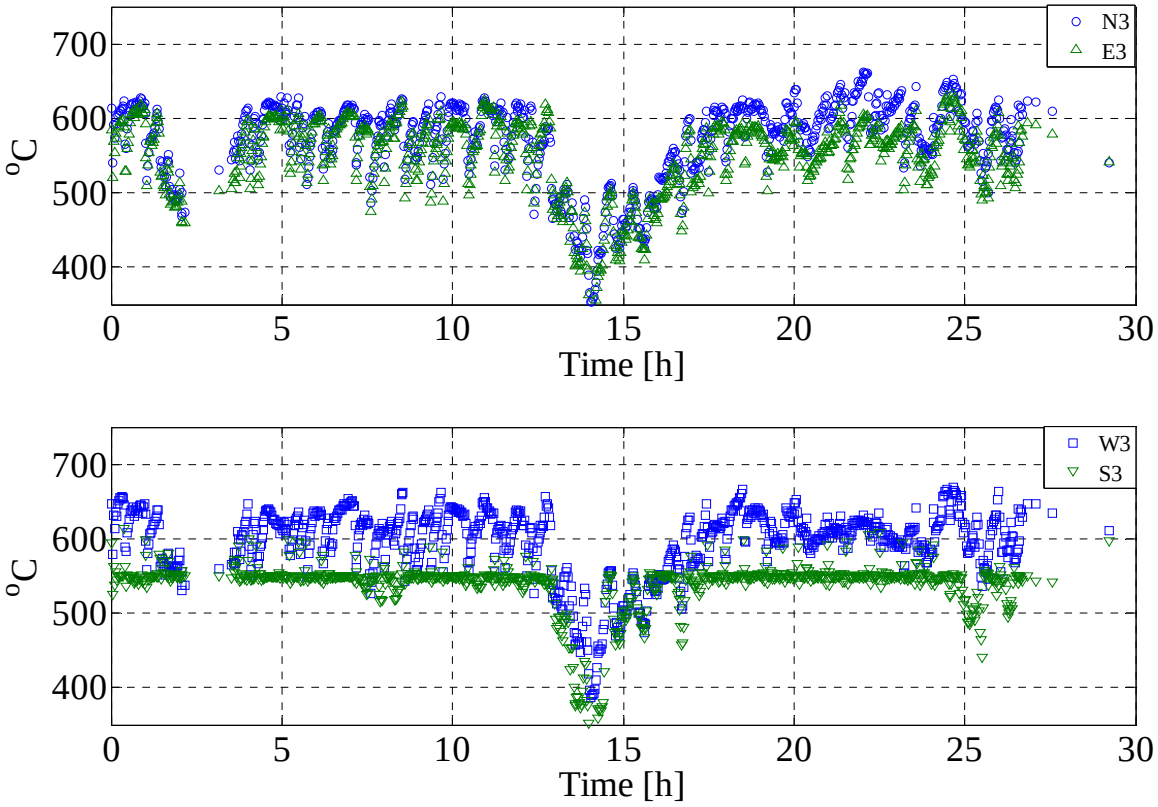

Figure 7: Measured probe surface temperatures during test 3.

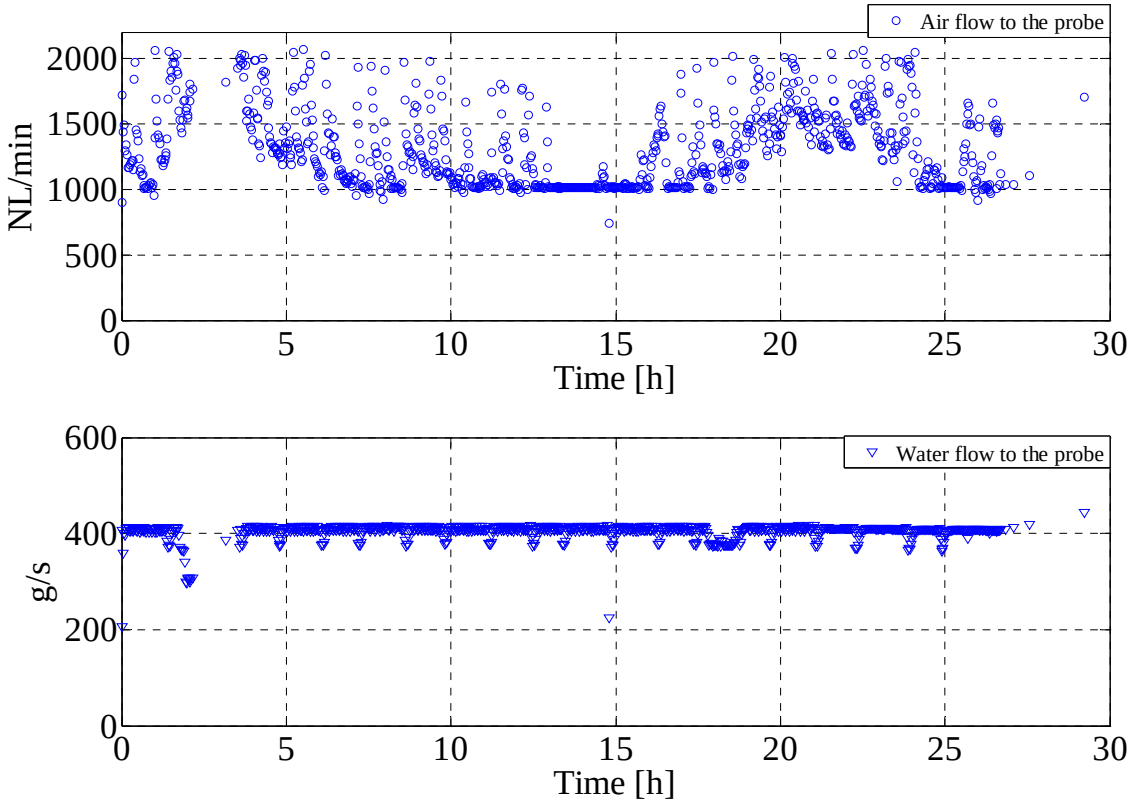

Figure 8: Water and air flow to the probe measured during test 3.

3.2.1 Ash deposition propensity

The amount of deposit collected on the probe is a function of both the deposit formation process and shedding events as shown in Figure 3. As an example, significant amount of deposits formed even after 50 minutes as is evident from Figure 9. Apart from deposit build-up, there are different kinds of deposit shedding, natural and caused by plant sootblowing. To handle this kind of data, two different measures of deposit formation rate are used in the analysis of the data. The first is the integral deposit formation rate (IDF-rate) found by dividing the integral mass change over integral time intervals (of order several hours) by the time interval. The IDF-rate is similar to deposit formation rates based on total deposit mass uptake divided by probe exposure time reported in previous full-scale investigations, but it is a relatively crude measure that includes all deposit shedding in addition to actual deposit formation. In order to remove major shedding events from the determination of deposition rates a second measure, the derivative-based deposit formation rate (DDF-rate), was devised. This was determined by averaging the deposit mass uptake signals over short time intervals (of order minutes), calculating the local values of the time derivative of the mass uptake, removing large negative values signifying major shedding events, and finally time smoothing the derivatives to remove excessive noise. The complete procedure used to calculate the DDF-rate is shown in Appendix C. Looking at the deposit mass uptake data in the different tests, following observations were made:

Test 1. A lot of build-up and fast shedding of all the deposits up to 14 h of exposure time. About 20 events in the first 14 h can be found where all of the deposits attached to the probe are removed naturally. After 15 h the deposit level is constant at 4,000 g/m^2.

Test 2. During all the measuring time (total 15 h) there were observed fast deposit build-up to maximum 6,000 g/m^2 and then sudden shedding of all deposit. A lot of shedding events were observed.

Test 3. A similar deposit build-up behavior as in test 2, but the probe was placed in the boiler for 27 h.

Test 4. A slow deposit formation process up to 10 h and then there are observed a constant amount of deposit build-up to a probe residence time of 110 h. The boiler was running at lower biomass and boiler load.

Test 5. Only small amounts of deposits are observed on the probe in most of the time (less than 200 g/m^2). Several cases of fast deposit build-up and deposit shedding appear sometimes.

The DDF-rate may be influenced by the coal ash flow rate. Therefore, ash deposition propensity provides useful information about the fraction of total ash actually depositing on the deposit probe. The ash deposition propensity in the present case was calculated by dividing the DDF-rate with the total ash flux. The DDF-rate represents the transient deposit build-up meaning that if the DDF-rate is equal to the total ash flux, all of the ash the probe will experience is going to stick to the deposit probe.

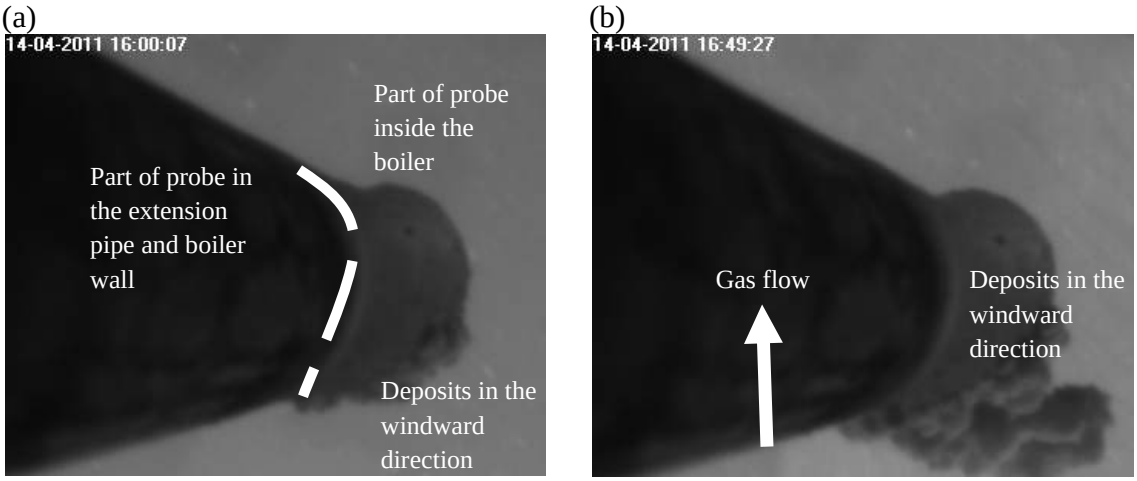

Figure 9: Deposit build-up in just 50 minutes during test 5 (total exposure time of 31.3 h).

The calculated DDF-rate was then used to determine ash deposition propensity using the following correlation [21],

$$\text{Ash deposition propensity}\,(\%) = \text{Impaction efficiency} \times \text{Capture efficiency} = \frac{\text{Transient deposition flux}}{\text{Ash flux}} \cdot 100 = \frac{\text{DDF-rate}}{\text{Ash flux}} \cdot 100 \quad (4)$$

$$\text{Ash flux (g/m}^2\text{/h)} = \frac{m_f X_a}{A_r} + \frac{ash_{coal}}{A_r} \quad (5)$$

In the above equation (5), m_f represents the wood fuel flow to the boiler, X_a represents fraction of ash in dry wood fuel, ash_{coal} represents the coal ash flow and A_r represents the cross-sectional area of the boiler at the probe measuring position.

The calculated DDF-rate during test 3 is shown in Figure 10. It is clear that DDF-rate decreases at decreased biomass load and boiler load (between 13 to 17 h). The DDF-rate

shows a big peak after the introduction of fuel through mill 10 after 17 h of exposure time, when the natural gas flow was relatively larger (~ 4 kg/h). The calculated ash deposition propensity almost follows the same trend as the DDF-rate (Figure 11). The calculated DDF-rates and ash deposition propensity for each test can be found in Appendix B. For test 3, it is seen that when the boiler is approximately near full load, the deposit formation rate is above 3,500 g/m^{2}h.

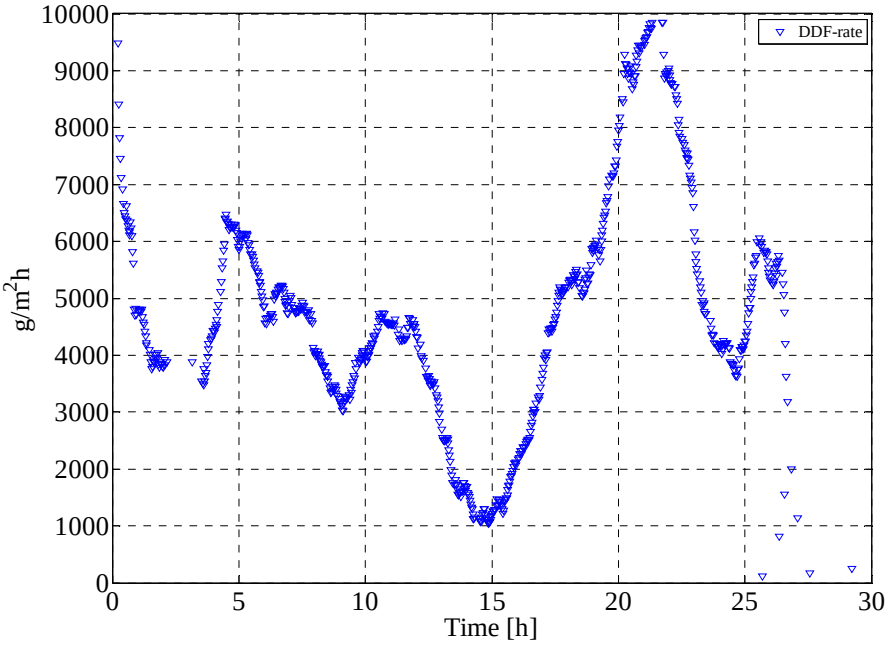

Figure 10: Calculated Derivative-based Deposit Formation (DDF) rate during test 3.

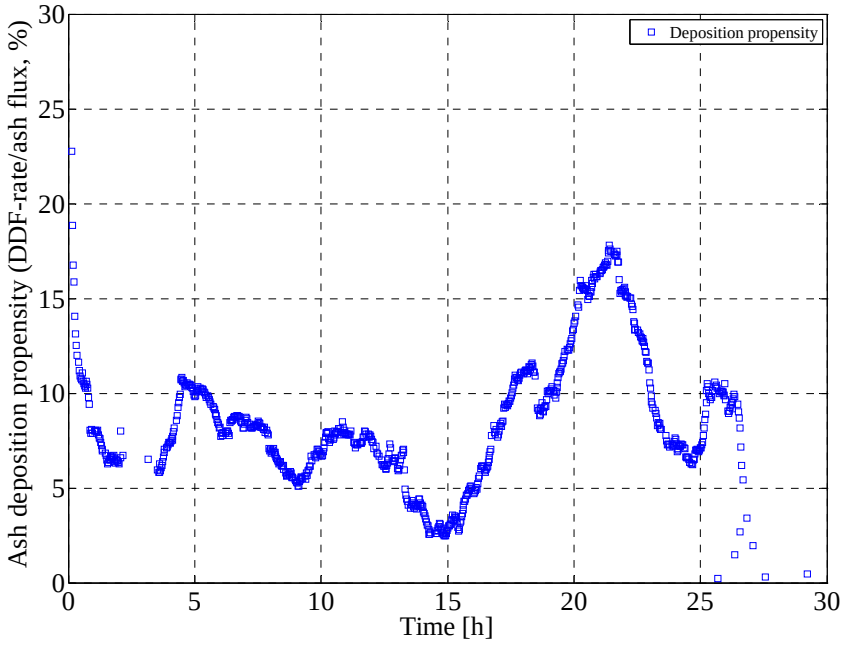

Figure 11: Calculated ash deposition propensity during test 3.

3.3 Influence of local conditions on deposition propensity

To make it possible to investigate the influence of different operational parameters on ash deposition propensity, mean values of each test were determined. Five data points were generated and it was possible to analyze the influence of probe surface temperature, local flue gas temperature and boiler operational parameters on ash deposition propensity and gas emissions. Table 3 provides an overview of the conducted measurements. The mean flue gas temperature in the range of 950 to 1350 ^{o}C can be seen, while the impact of flue gas temperature on ash deposition propensity is shown in Figure 12. It can be seen that ash deposition propensity increased with increasing flue gas temperature. The possible reason for increased ash deposition propensity at higher flue gas temperatures could be that the particles hitting the probe are partially molten, whereby a larger fraction of impacted ash particles sticks to the deposit.

Table 3: Summary of all main results of the measurements. [a] standard deviation.

	Unit	Test 1	Test 2	Test 3	Test 4	Test 5
Exposure time	h	26	16	28	116	52
Biomass load	%	44.10	81.16	72.18	18.20	59.24
Boiler load	%	91.22	97.63	88.47	41.37	76.28
Natural gas flow	kg/s	7.86	2.55	1.62	3.87	2.53
Probe surface temperature (mean of N3, E3, S3, W3)	^{o}C	577	583	561	483	525
Coal ash to wood ash ratio	--	3.63	4.35	4.69	7.35	5.79
Ash flux (wood with 1 wt. % ash + coal ash)	g/m^{2}h	28886	58782	54931	20580	45571
Flue gas temperature	^{o}C	1350 ± 75	1250 ± 75	1300 ± 75	950 ± 75	1075 ± 75
Deposit mass uptake (mean)	g/m^2	2648	1589	1370	1691	375
DDF-rate (st. dev.)[a]	g/m^{2}h	4717 (23051)	4501 (3473)	4849 (2603)	96 (647)	653 (1055)
IDF-rate (deposition rate) (initial 12 h)	g/m^{2}h	212	156	53	128	30
Ash deposition propensity ,DDF-rate/ash flux (st. dev.)[a]	%	16.33 (79.8)	7.66 (5.91)	8.83 (4.73)	0.47 (3.14)	1.43 (2.31)
Heat uptake	kW/m^2					
Mean	kW/m^2	--	20.61	13.55	8.10	18.37
Deposit mass uptake < 1500 g/m^2	kW/m^2	--	22.52	13.82	8.25	--
Deposit mass uptake > 1500 g/m^2	kW/m^2	--	18.23	13.03	6.38	--
NO_x (6% O_2)	ppm	170	191	172	99	118
CO	ppm	48	5.0	37	1	20
O_2	%	2.41	2.79	2.90	3.29	2.95
SO_2	ppm	0.33	4.82	8.23	--	4.32

The mean probe heat uptake for each measurement is shown in Table 3 along with the impact of ash deposits on probe heat uptake for two different set of deposit mass loads on the probe (less than and greater than 1,500 g/m^2). It can be seen that probe heat uptake is reduced when the deposit mass load is increased; however, the probe heat uptake reduction is different for each test possibly due to flue gas temperature and probe surface temperature differences. In addition, due to problems at the temperature measuring position of air and water inlet to the probe, the heat uptake was not accurately calculated during test 1. Also, during test 5, due to unstable probe temperature, the results of probe heat uptake are not included.

Some of the parameters in Table 3 cannot be regarded as independent. The coal ash injection flows were to some extent kept constant. However, an increase in the biomass load seems to have induced an increase flue gas temperature and decreased the coal to wood ash ratio. The impact of coal ash to fuel ash ratio on ash deposition propensity is shown in Figure 13 (a) at different probe surface temperatures. It can be seen that deposition propensity increased with decrease in coal ash to fuel ash ratio. However, as shown in Figure 13 (b), the points with high coal ash to wood ash ratio also have low biomass and boiler load. Changes in boiler load influence the flue gas temperature, and the coal ash to wood ash ratio was lowest in the tests with high flue gas temperature. With the few measuring points available and the limited variation in the ash ratio (coal ash to wood ash), it is difficult to determine the influence of this parameter.

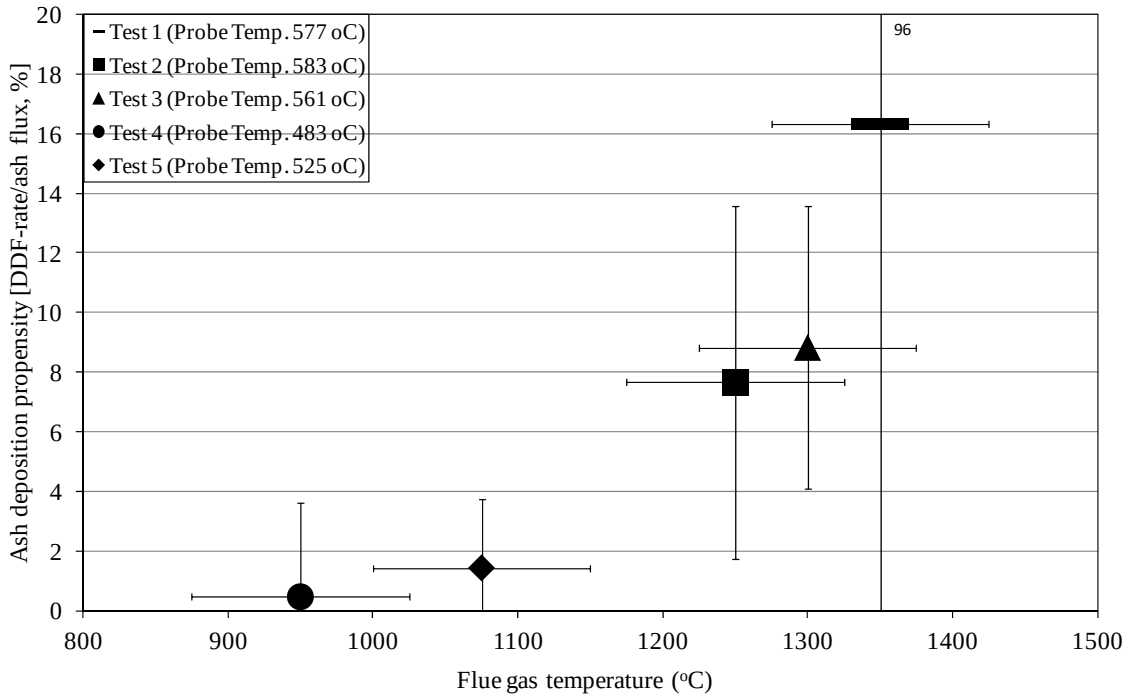

Figure 12: Impact of flue gas temperature on ash deposition propensity (deposition flux/ash flux, %). The error bars indicate possible variation of the flue gas temperature due to the fact that the suction pyrometer was used only for small periods to find the true flue gas temperature.

Based on the experiences from previous measurements, we believe that when high deposition flux to ash flux ratio is observed, the main cause is the flue gas temperature.

(a)

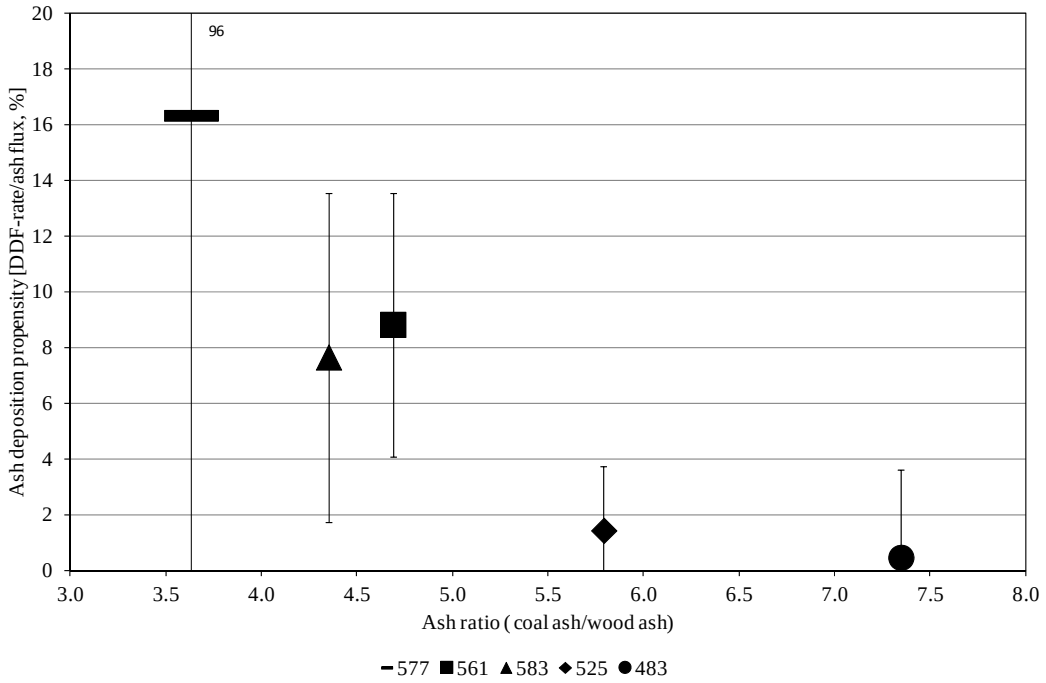

(b)

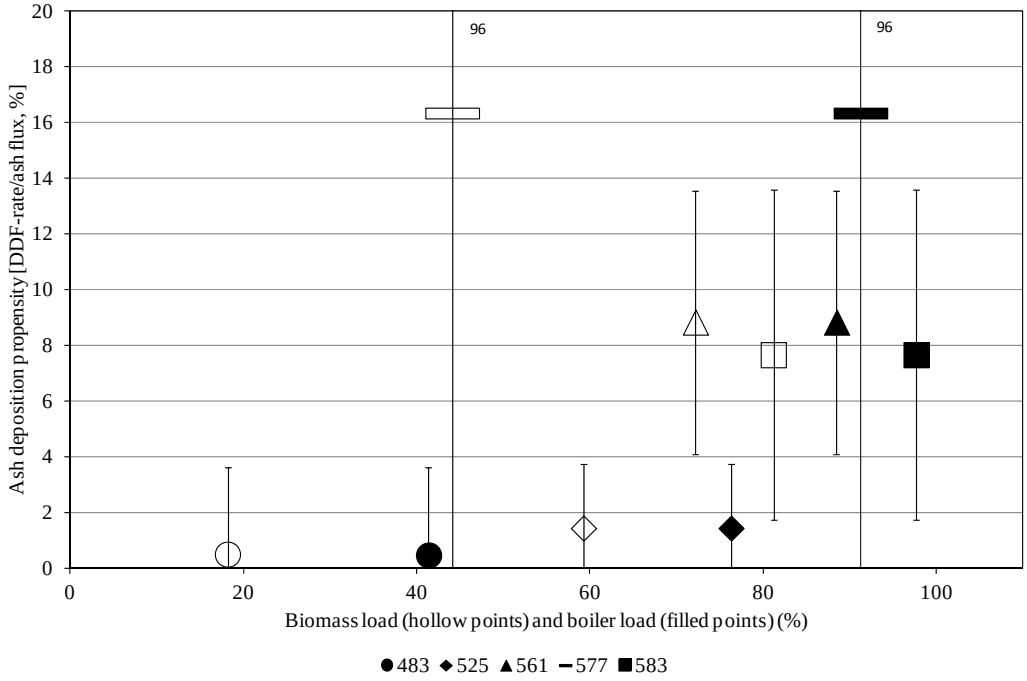

Figure 13: a) Impact of coal ash to fuel ash ratio on ash deposition propensity at different probe surface temperatures, b) impact of biomass load (hollow points) and boiler load (filled points) on ash deposition propensity at different probe surface temperatures.

3.4 Comparison of results with previously conducted probe measurements

The deposit formation rate (g/m^2/h) can also be determined based on the mass increase divided by a given probe exposure time and we have called this the integrated deposit formation rate (IDF-rate). In mathematical terms, let $m(t)$ be the continuously monitored probe mass uptake. If the probe signal was noise free and no shedding events of any kind occurred, the true deposit formation rate would be the derivative $m'(t)$. However, the signal is not noise free, and both minor and major shedding events occur, so that the derivative $m'(t)$ represents the net deposit accumulation rate at any time. We defined IDF- and DDF-rates corresponding to the mathematical expressions

$$\text{IDF-rate} = \frac{\int_{t_1}^{t_2} m'(t)\,dt}{t_2 - t_1} = \frac{m(t_2) - m(t_1)}{t_2 - t_1} \quad (6)$$

$$\text{DDF-rate} = \langle m'(t) \rangle \quad (7)$$

where $\langle m'(t) \rangle$ represents a moving average over short time intervals without major shedding events.

In previously conducted measurements at straw and/or wood-fired boilers, the deposit formation rates were calculated by inserting the probe inside the boiler for 2-12 h [11,19]. In the current measurements, the deposit mass uptake signal after 12 h was measured and then divided by 12 h to get the IDF-rate. However, the IDF-rate can be influenced by shedding events during the time interval of the deposit collection. This could also happen when people report deposit formation rate when they took the probe out and divide the deposit amount collected by the probe exposure time, but the deposit mass can be significantly lower because of shedding. The values of IDF-rate calculated for the current study are therefore just representing arbitrary numbers. The deposit build-up pattern observed in tests 1, 2, 3 and 5 makes the calculated IDF-rate quite random. The deposit mass uptake at 12 h can be anywhere between 0 and 6,000 g/m^2, which implies that in the case with a lot of fast shedding, IDF-rate data are not meaningful. However, a comparison of previous full-scale deposit probe measurements was made for different wood-fired boiler measurements and the current measurements (see Table 4 and Figure 14). The data points, even those at approximately the same conditions, have a large spread, which is a result of the difficulties of keeping all operational parameters constant during full-scale measurements. However, within the range of deposit formation rates, some systematic tendencies can be observed. Previous probe measurements at AVV2 unit 2 showed deposit formation values in the range of 5-13 g/m^2/h during wood dust and natural gas firing (may be oil firing also), with and without the addition of coal ash. Skrifvars et al. [19] measured deposit formation rate in the range of 12-74 g/m^2/h (mean 40 g/m^2/h of 4 measurements) at 920 ^{o}C and between 3 to 15 g/m^2/h (mean 7 g/m^2/h of four measurements) at 750 ^{o}C in a wood pulverized fuel boiler. Overall, it is observed that an increased flue gas temperature and straw addition in wood (increased K contents) cause an increased deposit formation rate, while a changed probe surface temperature seems not to cause any systematic change. Moreover, the present measurements indicate increased deposit formation rates compared to previous measurements at the same boiler [5], possibly due to higher flue gas temperatures. In addition, the IDF-rates may be severely influenced by uncontrolled fluctuations and shedding events in the initial 12 h period.

Table 4: Ash deposition data from the previous and current full-scale measurements. Amager Unit 2 (AMV2) and Unit 1 (AMV1) are straw and/or wood-fired suspension boilers. Jorbo, Sweden is a down-fired pulverized fuel boiler. Avedøre Unit 2 (AVV2) is a wood and natural gas fired suspension boiler.

No.	Boiler	Fuel (+ additive)	Fuel ash	Probe position	Probe surface temp.	Flue gas temp.	Exposure time	IDF-rate	Ref.
		--	% wt.	--	^{o}C	^{o}C	h	g/m^{2}h	
1	AVV2	Wood + natural gas (+ coal ash)	1.0	Just below radiation shield	577	1350	12.0	212	
2	AVV2	Wood + natural gas (+ coal ash)	1.0	Just below radiation shield	583	1250	12.0	156	
3	AVV2	Wood + natural gas (+ coal ash)	1.0	Just below radiation shield	561	1300	12.0	53	
4	AVV2	Wood + natural gas (+ coal ash)	1.0	Just below radiation shield	483	950	12.0	128	
5	AVV2	Wood + natural gas (+ coal ash)	1.0	Just below radiation shield	525	1000	12.0	30	
6	AVV2	Wood + natural gas	0.6	Near radiation shield	500	923	~4.0	5	[5]
7	AVV2	Wood + natural gas	0.6	Near radiation shield	476	930	~5.0	13	[5]
8	AVV2	Wood + natural gas	1.2	Near radiation shield	491	918	~2.4	10.5	[5]
9	AVV2	Wood + natural gas	1.2	Near radiation shield	500	929	~4.5	4.5	[5]
10	AVV2	Wood + natural gas + oil	0.67	Near radiation shield	504	885	--	6.5	[5]
11	AVV2	Wood + oil (+coal ash)	--	Near radiation shield	503	955	~3.5	10	[5]
12	AVV2	Wood (+coal ash)	--	Near radiation shield	474	938	~2.5	12.5	[5]
13	Jorbro	Wood	0.55	Superheater	520	920	~2.0	40	[19]
14	Jorbro	Wood	0.55	Superheater	520	750	~2.0	7	[19]
15	AMV1	Straw + wood	5.1	Superheater	493	910	12.0	55	[17]
16	AMV1	Straw + wood	5.0	Superheater	593	821	13.5	57	[17]
17	AMV1	Straw + wood	1.3	Superheater	481	765	12.0	22	[17]
18	AMV1	Straw + wood	3.4	Superheater	479	847	6.0	95	[17]
19	AMV1	Straw + wood	1.6	Superheater	494	815	12.0	87	[17]
20	AMV1	Straw + wood	1.0	Superheater	563	823	12.0	1	[17]
21	AMV1	Straw + wood	0.85	Superheater	538	772	12.0	3	[17]
22	AMV1	Straw + wood	0.8	Superheater	539	745	12.0	1	[17]
23	AMV2	Straw + wood	5.4	Superheater	500	863	12.0	33	[20]
24	AMV2	Straw + wood	4.2	Superheater	500	856	12.0	33	[20]
25	AMV2	Wood	3.3	Superheater	500	586	12.0	1	[20]

(a)

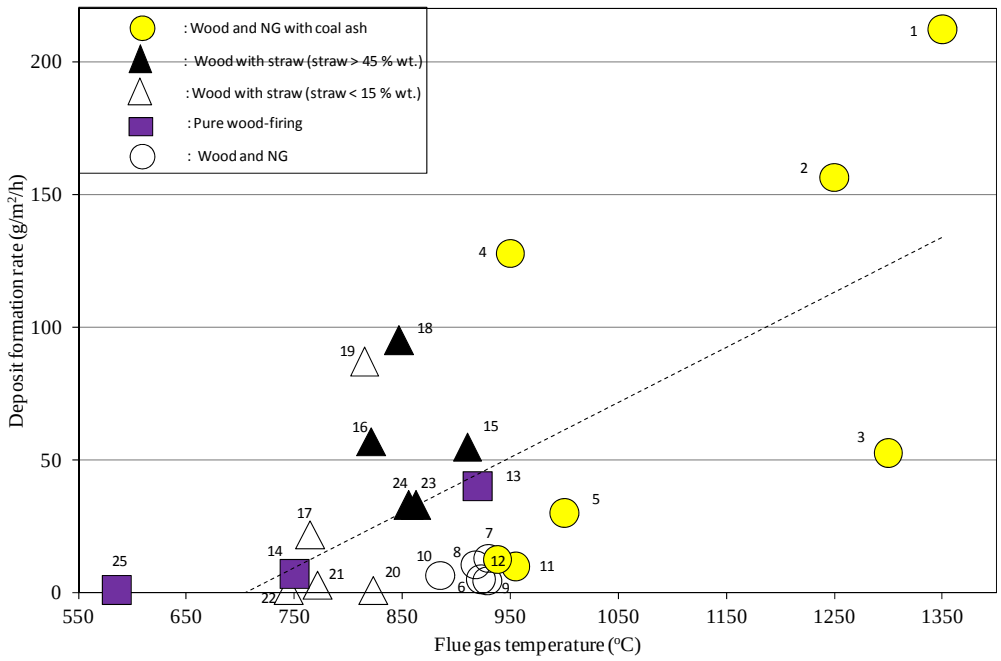

(b)

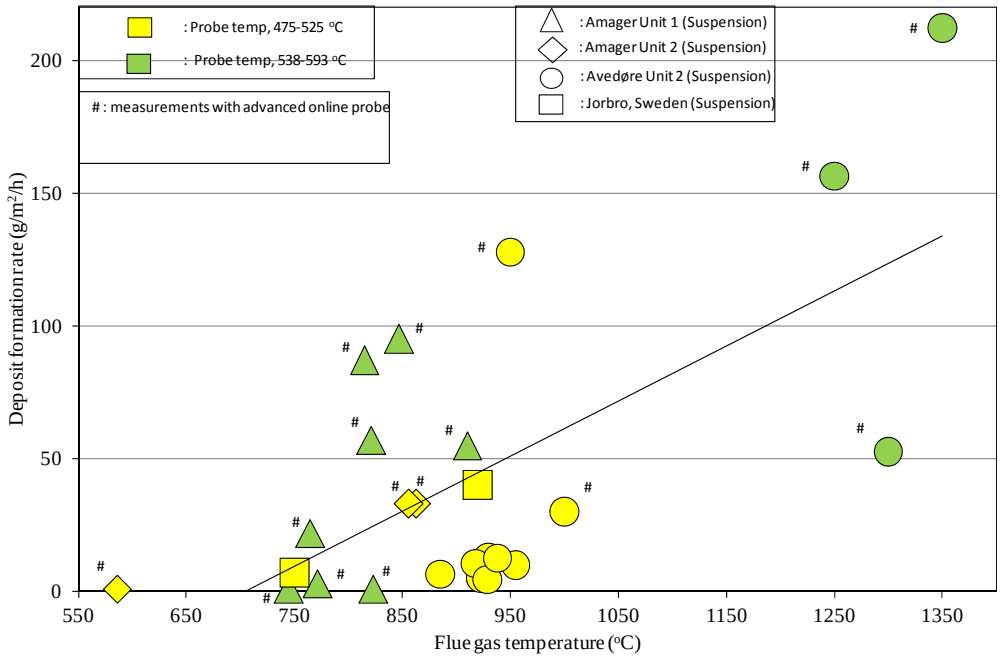

Figure 14: Impact of flue gas temperature on deposit formation rates (IDF-rates), a) comparison of deposit probe measurements data for wood-firing with and without co-firing wood in combination with other fuels, b) comparison of data set with marking of the probe surface temperature and the boilers where the measurements were preformed [5,17,19,20.] Graph details: NG is meant for natural gas, a) the number on each point represents the corresponding number in Table 4. b) the color represents the probe surface temperature, while point shape represents the boiler type. # indicates points where measurements were conducted with advanced probe. Amager Unit 2 (AMV2) and Unit 1 (AMV1) are straw and/or wood-fired suspension boilers. Jorbro is a down-fired pulverized fuel boiler. Avedøre Unit 2 (AVV2) is a wood, oil and natural gas fired suspension boiler. Furnace oil was fired in addition to wood and natural gas during points 10 and 11 mentioned in Figure 14 a).

3.5 Deposit shedding

The deposit mass uptake signals were continuously monitored along with video monitoring in order to identify shedding events. The larger shedding events appear as a sudden decrease in the deposit mass uptake signal and a corresponding increase in the probe heat uptake signal. Video monitoring during almost all the tests revealed that the deposits were not sticky and were easy to remove (see Figure 15), even at very high flue gas temperatures (> 1350 ^{o}C). Deposit removal through surface melting was not identified. This indicates that potassium (K) has been captured by coal ash rich in aluminum-silicates whereby an ash with a high melting temperature is formed. A typical example of a deposit shedding event is shown in Figure 15. It can be seen that the deposits are not strongly attached to the probe and were removed naturally. The deposits are loosely attached as shown in Figure 15 (a), and after just 2 minutes, a significant amount of deposit was removed from the upstream side of the probe (see Figure 15 (d)). It was seen that deposit were removed through debonding when a complete/partial deposit layer is detached from the probe. Similar results were seen after finishing the new measurements at AVV2, where two cameras were used. The deposit removal was caused by both naturally occurring shedding events and shedding events caused by plant sootblowing (see Figure 3).

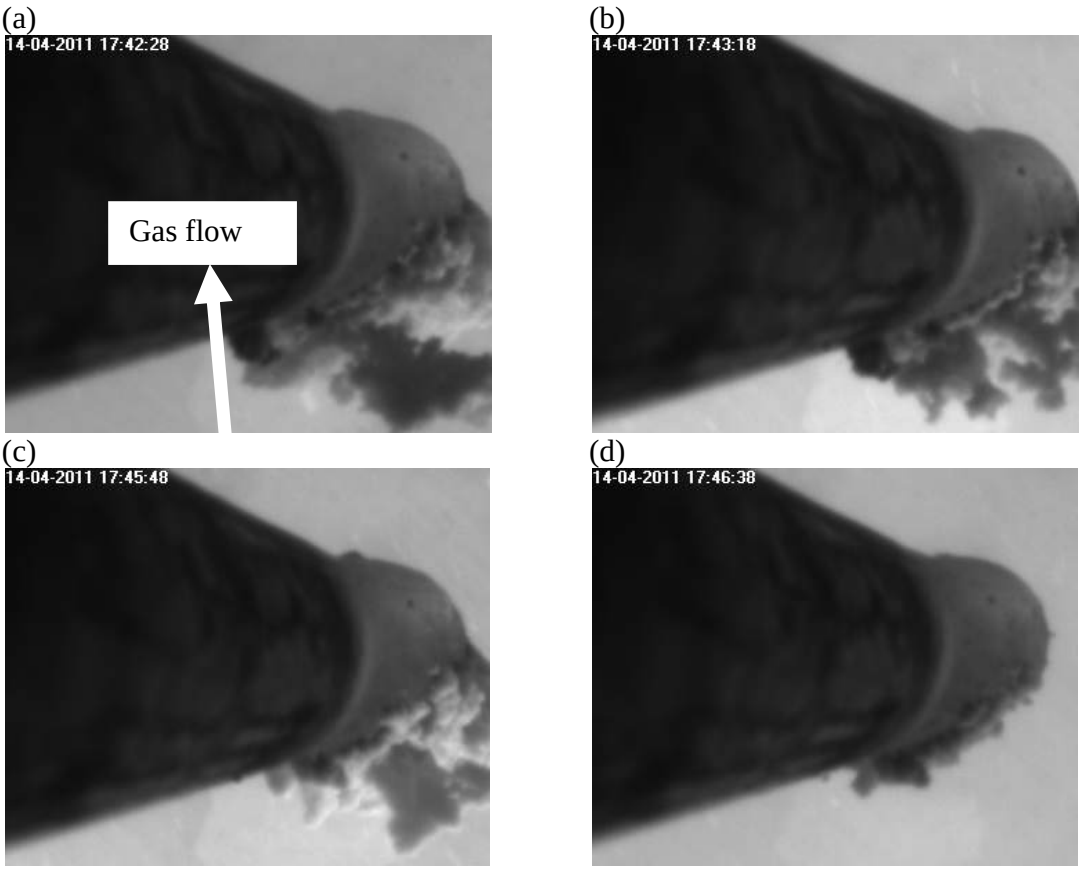

Figure 15: Images of probe before and after deposit shedding during test 5 (30.3 h exposure time).

During the calculation of DDF-rates, a particular negative slope cut off level was selected to determine major shedding events accurately, while still giving a satisfactory prediction of apparent DDF-rates. The selected cut off level was -3,800 g/m^2/h for all the tests.[17] This cut off level strikes a balance between including larger shedding events in the analysis and preventing deposit mass signal noise from being counted on a shedding event. The selected minimum magnitude of a shedding event included in the analysis was -105 g/m^2 and this was calculated by equation (8).

$$\text{minimum shedding event magnitude} = \text{slope cut off level} \cdot \text{sampling interval} = -3800 \frac{\text{g}}{(\text{m}^2\text{h})} \frac{\text{h}}{(3600\ \text{s})} \cdot 100\ \text{s} = -105 \frac{\text{g}}{\text{m}^2} \quad (8)$$

To make it possible to investigate the influence of different operational parameters on the ash deposition and shedding, each test was divided into further sub-tests based on the number of hours (usually 6 hours). A significant number of data points thus allowed us to analyze the influence of local boiler operational parameters on deposition rate and deposit shedding. The results are summarized in Table 5. For a complete test there can be seen a difference between the DDF-rate and the deposit shedding rate (mean deposit removal multiplied by deposit removal frequency) even though the deposit mass uptake signals indicate a little amount of deposits accumulated on the probe at the end of most of the tests. This difference is probably due to the fact the selected number of minimum shedding event is -105 g/m^2, and any shedding event less than that will potentially cause an error.

Table 5: Overall summary of ash deposition and deposit shedding.

Test	Exposure time (h)	Boiler load (%)	Biomass load (%)	Gas temp (^{o}C)	Probe temp (S3) (^{o}C)	Deposit mass uptake (g/m^2)	Heat uptake (kW/m^2)	DDF-rate (g/m^{2}h)	Ash flux (g/m^{2}h)	Deposition propensity (%)	St. dev. (deposition propensity)	Max deposit drop (g/m^2)	Mean deposit drop (g/m^2)	Mean deposit removed (%)	Deposit removal frequency (hr^{-1})
Test 1	1-6	89.64	77.07	--	555.32	395.44	--	14312	57608	24.84	83.92	4437	1723	--	2.00
Test 1	6-12	91.71	64.99	--	540.21	1860.64	--	4201	50141	8.38	2.21	5447	2187	75.36	1.50
Test 1	12-18	92.67	3.27	--	610.91	3948.13	--	855	7369	11.61	16.75	966	952	22.52	0.33
Test 1	18-25.10	90.74	38.90	1314	570.24	3811.31	--	1481	9558	15.50	36.91	1770	1770	39.90	0.17
Test 1	Overall test	91.22	44.10	1350 ± 75	570.39	2648.00	--	4717	28886	16.33	79.80	5447	1835	--	0.96
Test 2	1-6	94.22	79.09	--	553.90	1719.01	20.97	5343	58374	9.15	8.96	6303	2972	89.56	1.00
Test 2	6-12	99.75	80.99	--	553.00	1585.31	20.92	4194	58762	7.14	0.90	5168	2006	70.46	1.83
Test 2	12-15.15	100.38	85.71	--	550.61	1333.62	19.28	3381	59651	5.67	1.48	2683	1346	70.20	1.33
Test 2	Overall test	97.63	81.16	1250 ± 75	552.89	1589.30	20.61	4501	58782	7.66	5.91	6303	2027	74.96	1.65
Test 3	1-6	98.30	86.39	--	550.32	1034.58	17.83	5730	59583	9.62	6.27	5817	1900	98.10	1.67
Test 3	6-12	91.23	77.33	--	545.94	1198.73	10.84	4291	58291	7.36	0.99	4400	1492	70.75	2.33
Test 3	12-18	68.02	53.45	--	501.44	1195.90	8.24	2595	44757	5.80	2.80	4264	1174	63.44	2.17
Test 3	18-24	100.48	73.93	--	549.43	1960.68	19.80	7224	57179	12.63	3.25	7777	2938	83.94	2.00
Test 3	24-26.70	85.09	74.48	--	530.81	1402.54	10.49	4608	57260	8.05	1.84	2897	1310	83.86	1.50
Test 3	Overall test	88.47	72.18	1300 ± 75	535.26	1369.55	13.55	4874	54931	8.87	4.71	7777	1762	78.59	2.17

Test	Exposure time (h)	Boiler load (%)	Biomass load (%)	Gas temp (°C)	Probe temp (S3) (°C)	Deposit mass uptake (g/m^2)	Heat uptake (kW/m^2)	DDF-rate (g/m^2h)	Ash flux (g/m^2h)	Deposition propensity (%)	St. dev. (deposition propensity)	Max deposit drop (g/m^2)	Mean deposit drop (g/m^2)	Mean deposit removed (%)	Deposit removal frequency (hr^{-1})
Test 4	1-6	39.20	18.07	--	496.50	573.03	6.30	872	35861	2.43	7.25	0	0	0.00	0.00
Test 4	6-12	39.22	18.09	--	499.74	1453.85	6.66	96	24546	0.39	0.56	0	0	0.00	0.00
Test 4	12-18	38.85	18.09	--	499.64	1592.29	7.04	124	19188	0.64	1.21	0	0	0.00	0.00
Test 4	18-24	38.99	18.09	--	499.79	1642.61	7.44	9	19027	0.04	0.11	0	0	0.00	0.00
Test 4	24-30	39.03	18.09	--	499.63	1648.21	7.86	172	19357	0.89	1.30	0	0	0.00	0.00
Test 4	30-36	39.04	18.09	--	499.62	1664.08	7.42	4	19591	0.02	0.10	0	0	0.00	0.00
Test 4	36-42	38.90	18.09	--	499.75	1703.40	7.60	8	19477	0.04	0.10	0	0	0.00	0.00
Test 4	42-48	43.45	18.09	--	499.81	1771.23	9.19	158	18789	0.84	1.40	0	0	0.00	0.00
Test 4	48-54	44.11	18.09	--	499.79	1919.17	10.35	17	19408	0.09	0.16	0	0	0.00	0.00
Test 4	54-60	42.43	18.09	--	499.49	1931.84	10.16	--	19129	--	--	224	224	12.44	0.17
Test 4	60-66	43.62	18.09	--	499.53	1814.75	11.07	99	20035	0.50	0.50	0	0	0.00	0.00
Test 4	66-72	43.17	18.08	--	499.63	1685.38	6.64	61	19187	0.32	1.18	0	0	0.00	0.00
Test 4	72-78	42.08	18.09	--	499.55	1721.72	7.08	12	19343	0.06	0.14	0	0	0.00	0.00
Test 4	78-84	41.49	18.09	--	499.79	1754.44	7.19	0	19964	0.00	0.08	261	261	15.48	0.17
Test 4	84-90	42.28	18.09	--	499.59	1809.54	6.88	182	19400	0.94	1.17	0	0	0.00	0.00
Test 4	90-96	42.66	18.09	--	499.79	1891.19	7.76	--	19389	--	--	0	0	0.00	0.00
Test 4	96-102	43.02	18.83	--	499.78	1885.18	9.30	--	19702	--	--	0	0	0.00	0.00
Test 4	102-108	42.73	19.18	--	499.69	1909.02	10.06	8	19862	0.04	0.04	0	0	0.00	0.00
Test 4	108-110	42.36	19.14	--	495.58	1798.28	6.98	--	19575	--	--	232	190	10.13	0.33
Test 4	Overall test	41.37	18.20	950 ± 75	499.45	1691.41	8.10	96	20580	0.47	3.14	261	216	12.05	0.04
Test 5	1-6	43.13	19.18	970	499.57	80.27	9.57	384	19626	1.96	11.09	0	0	0.00	0.00
Test 5	6-12	57.11	23.93	--	531.70	121.34	12.18	68	22473	0.30	0.84	0	0	0.00	0.00
Test 5	12-18	84.57	70.66	--	563.47	463.79	18.19	561	53104	1.06	0.87	1687	848	75.75	0.50
Test 5	18-24	87.06	73.69	--	569.21	512.86	19.42	476	55756	0.85	0.87	1896	708	51.59	0.67
Test 5	24-30	89.35	75.11	1214	574.12	387.78	22.53	661	58071	1.14	0.66	487	338	51.71	1.67
Test 5	30-36	94.85	81.96	--	563.57	493.95	24.98	1458	58638	2.49	1.68	805	445	53.35	2.67
Test 5	36-42	68.24	59.35	--	516.34	392.48	16.06	669	45817	1.46	2.24	1017	486	55.14	1.83
Test 5	42-48	81.22	67.37	--	541.84	417.12	21.21	712	50069	1.42	1.48	889	490	48.10	1.17
Test 5	48-51.50	91.33	73.80	--	568.34	662.07	25.61	1280	53673	2.39	1.00	1352	468	50.51	1.83
Test 5	Overall test	76.28	59.24	1075 ± 75	546.09	374.87	18.37	653	45571	1.43	2.31	1896	481	53.28	1.20

All the measurements are summarized in Table 5, while in Figure 16 is shown the deposition propensity as a function of boiler load. Flue gas temperature measurements are not available for most of the six hour periods and changed deposit behavior as a function of flue gas temperature can therefore not be plotted. In Figure 17, Figure 18 and Figure 19 are shown the shedding frequency and the amount of the deposit removed in a single shedding period (6 h), as a function of boiler load. From Figure 16 is seen a weak increase in deposition propensity with increasing boiler load, probably caused by the increased local flue gas temperature. It is observed in Figure 17, Figure 18 and Figure 19 that both the shedding frequency and the amount of deposit removed in an actual event increases with increasing boiler load.

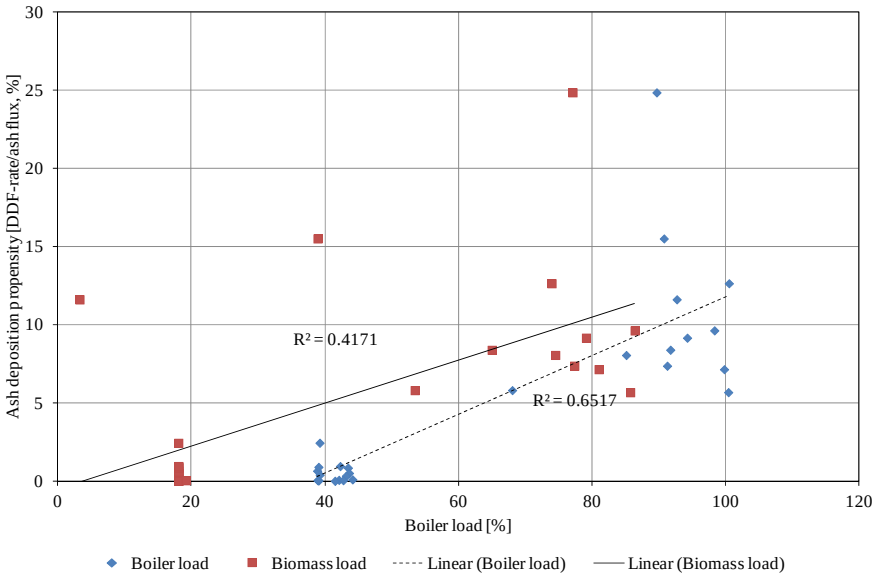

Figure 16: Impact of boiler load and biomass load on ash deposition propensity. Data of each 6 hours from test 1 to 4. Test 5 is excluded due to difficulties in keeping probe surface temperature constant.

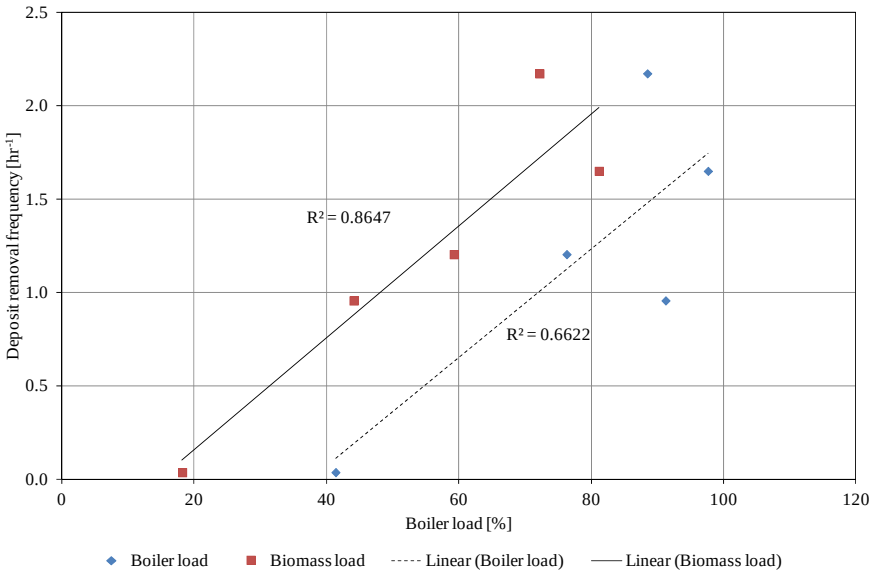

Figure 17: Impact of boiler load and biomass load on deposit removal frequency. Data of each test.

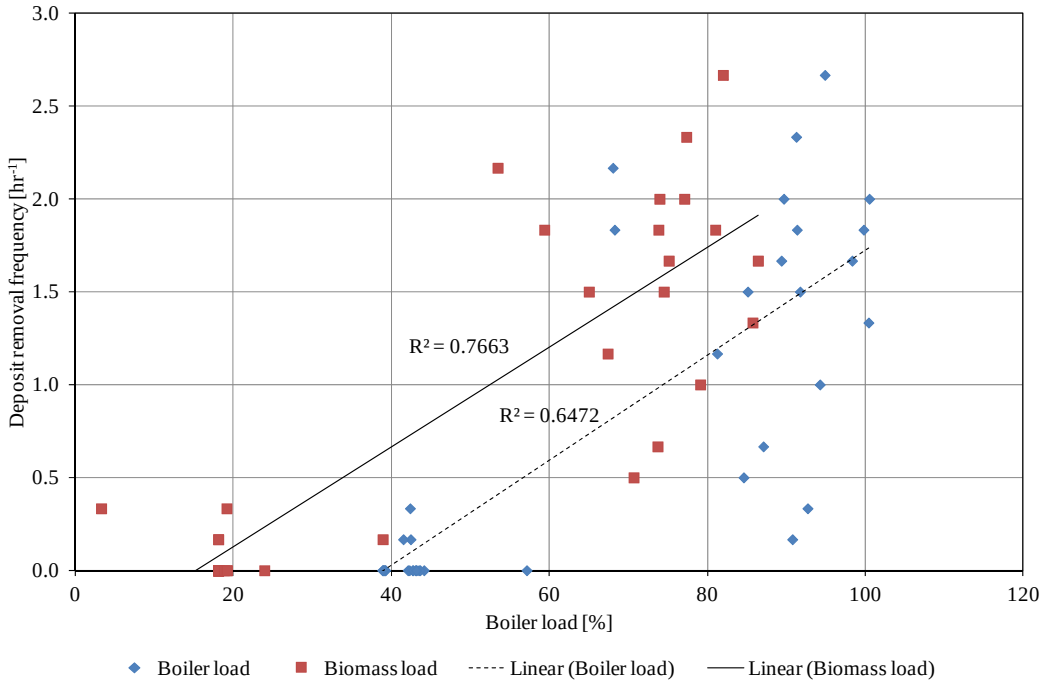

Figure 18: Impact of boiler load and biomass load on deposit removal frequency. Data of each 6 hours from test 1 to 5.

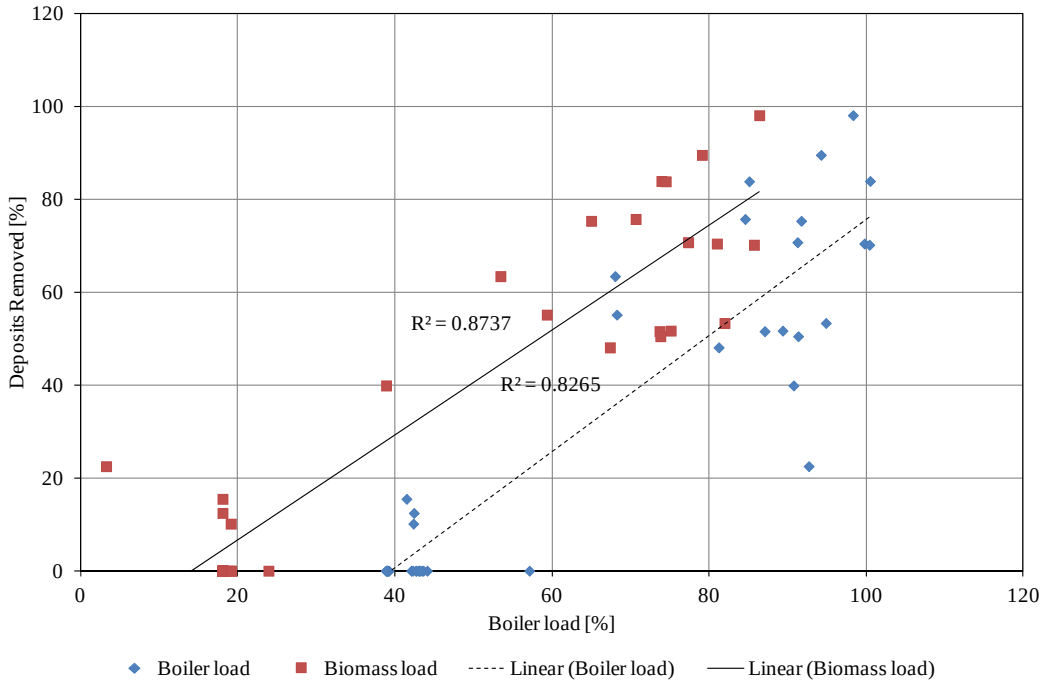

Figure 19: Impact of boiler load and biomass load on percentage of deposits removed. Data of each 6 hours from test 1 to 5.

3.6 Morphology and chemical composition of deposits

At the end of the experiment, the probe was carefully taken out of the boiler; the deposits were removed, photographed and finally an overall representative sample was selected for SEM-EDS analysis to characterize morphology and composition of deposits. Deposits from the downstream and upstream side of the probe were collected separately for later SEM-EDS analysis. The results of SEM-EDS analysis of only two tests (test 3 and test 5) are discussed based on the morphology and elemental composition of deposits on the upstream and downstream side of the probe. A typical image of upstream deposits from test 3 is shown in Figure 20, while the SEM-EDS results of upstream and downstream deposits are shown in Figure 21 and Figure 22, respectively. The chemical composition of the upstream deposits shows that the particles are primarily rich in Si, Al and Ca, while K is found in small amounts. The bigger particles contain lesser Ca, compared to small particles as observed in spot 4 and 5. The chemical composition of the downstream side deposits also shows a high content of Ca, Si and Al. In addition, Cl is not found either on the upstream side or on the downstream side of the probe. Therefore, potentially Cl has been released to the gas phase as HCl(g).

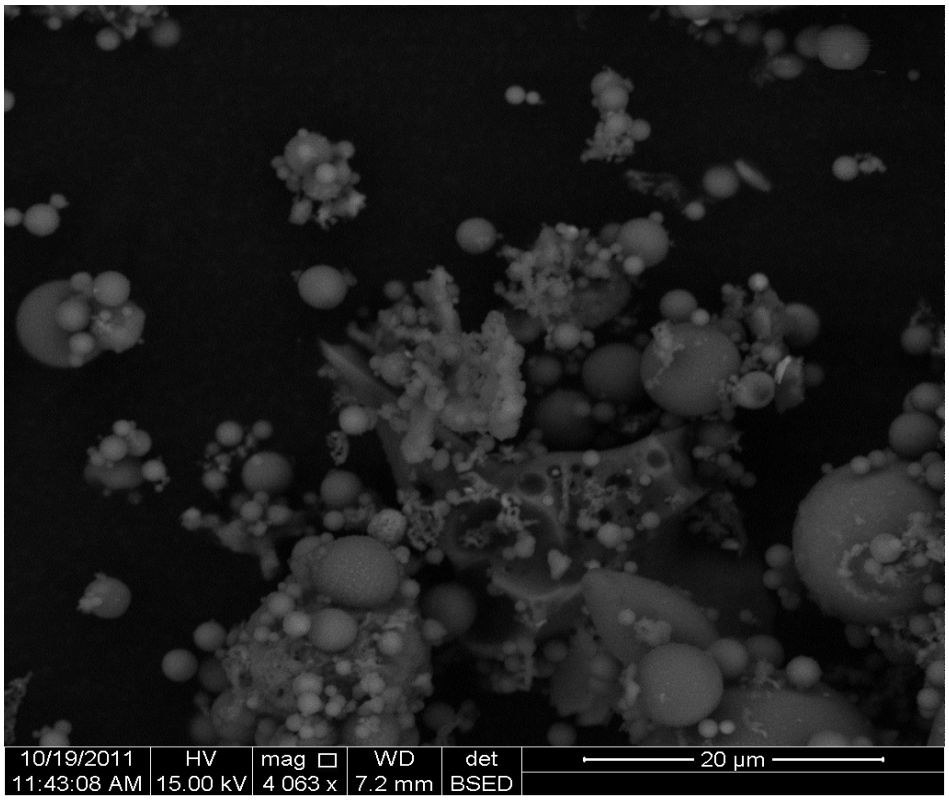

Figure 20: Morphology of upstream deposits from test 3.

(a)

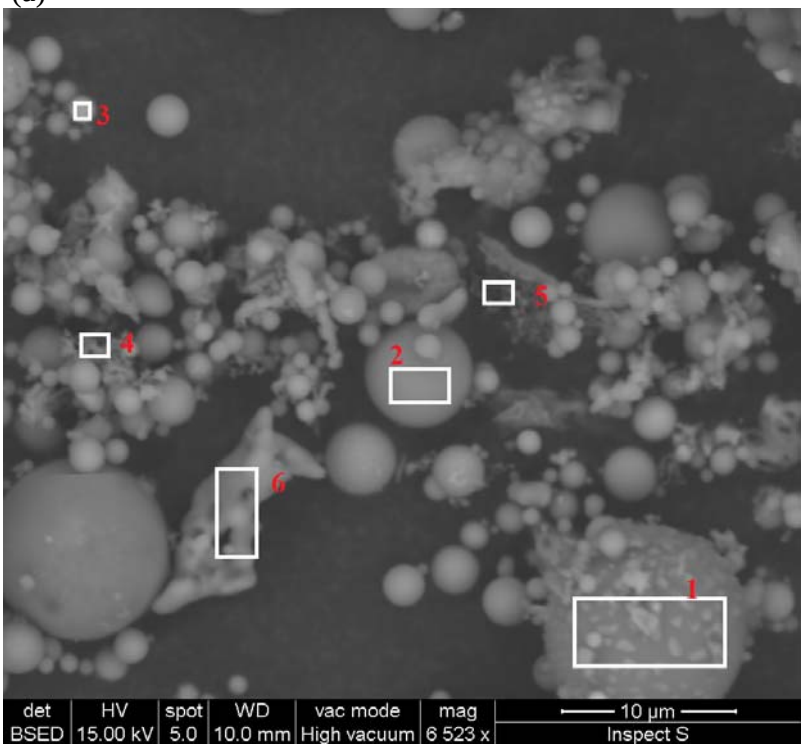

(b)

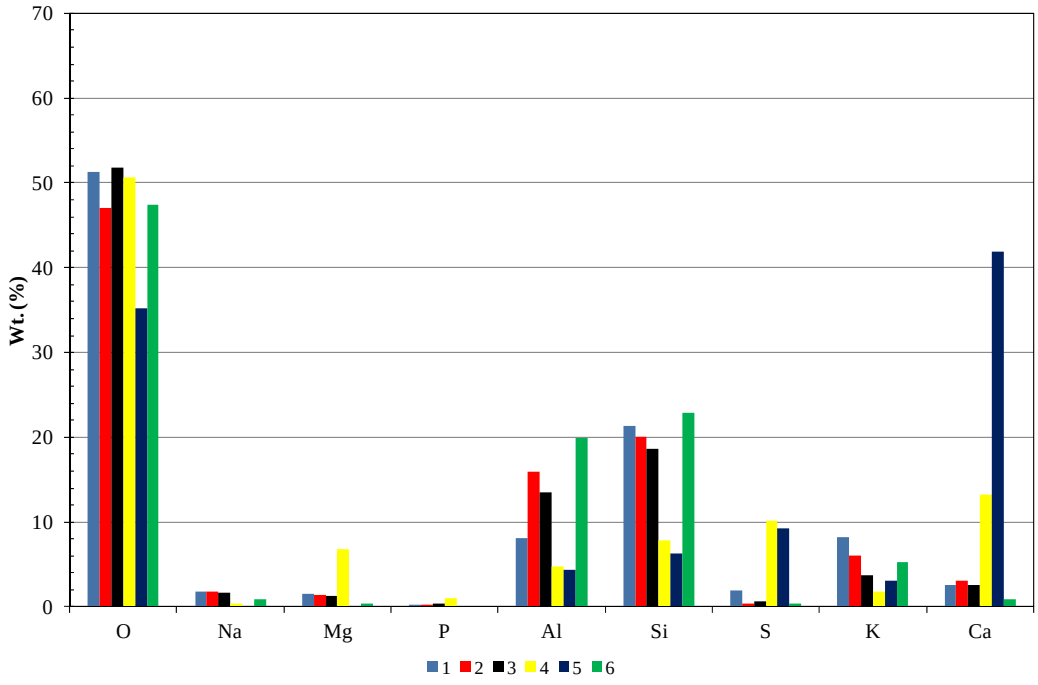

Figure 21: Morphology and composition of upstream side deposits formed during test 3.

(a)

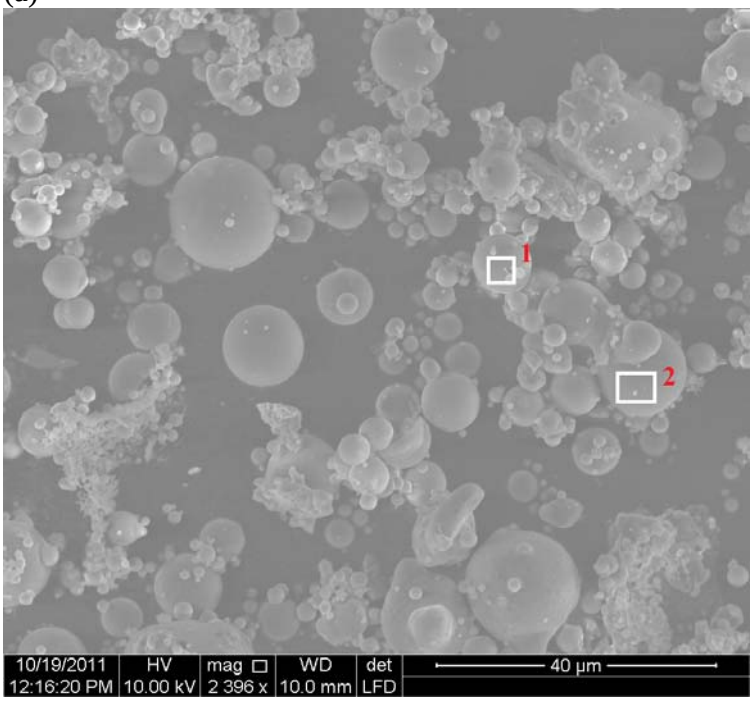

(b)

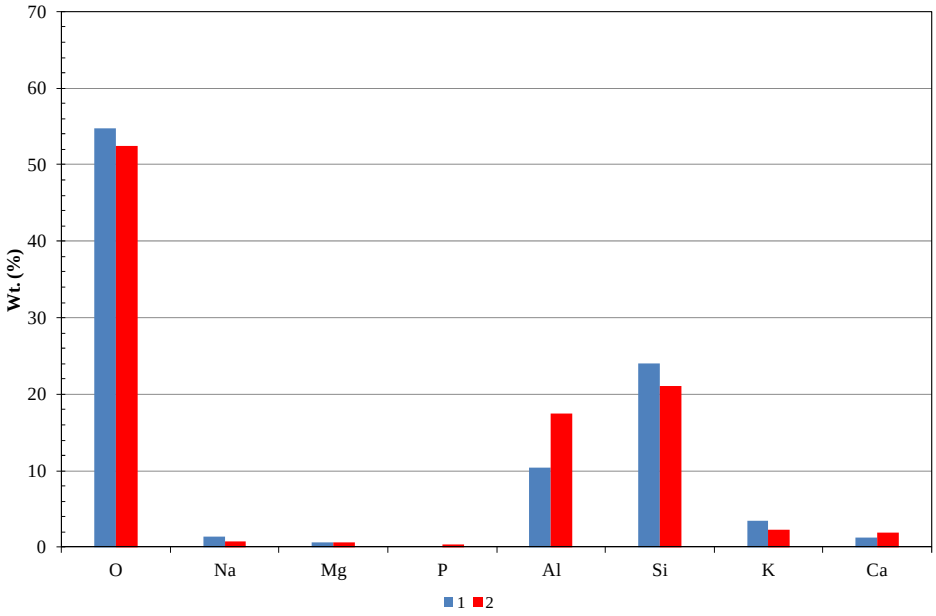

Figure 22: Morphology and composition of downstream side deposits formed during test 3.

An image and spot analysis of upstream deposits collected during test 5 is shown in Figure 23. I can be seen that most of the particles have a high content of Ca, Si and Al. Spot 5 and 6 contain more Na and K, compared to other spots possibly due to the fact that the very small particles adhered on large particles. The image and spot analysis of downstream deposits collected during test 5 is shown in Figure 24. The downstream deposits are rich in Ca, Si and Al. It is also interesting to note that spot 1, 2, 3 and 9 shows higher contents of K and Na compared to other spots, indicating that the small particles on these spots have a

high content of alkali metals. However, the composition of the deposits from both tests does not show a high concentration of K and Na. It is also worthwhile to note that Cl is not found either on the upstream or on the downstream side of the probe during test 5.

(a)

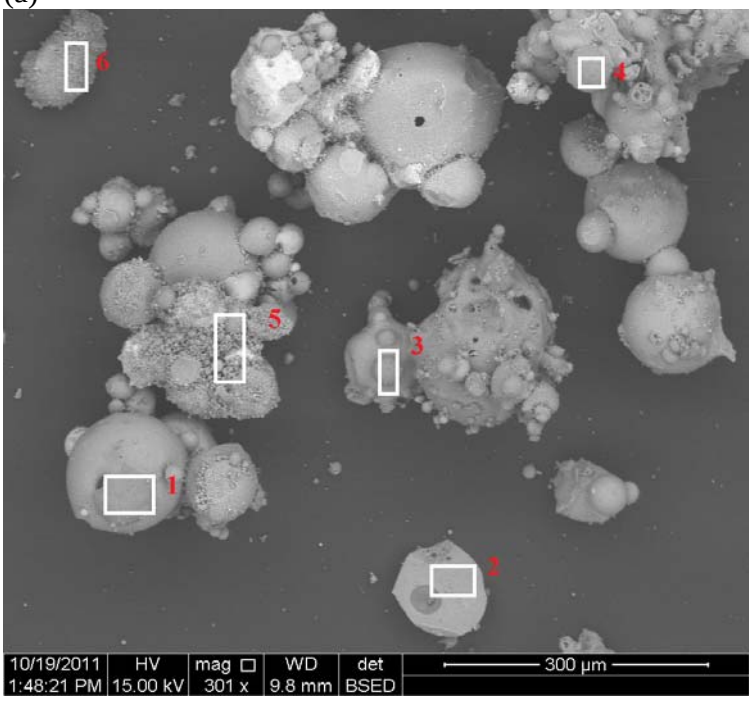

(b)

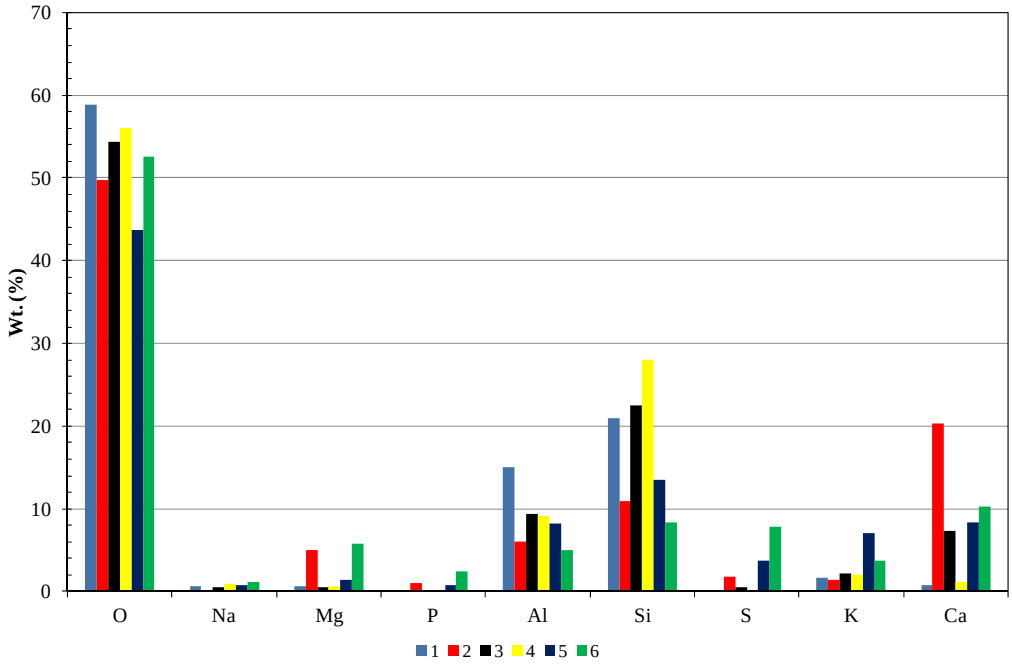

Figure 23: Morphology and composition of upstream side deposits formed during test 5.

(a)

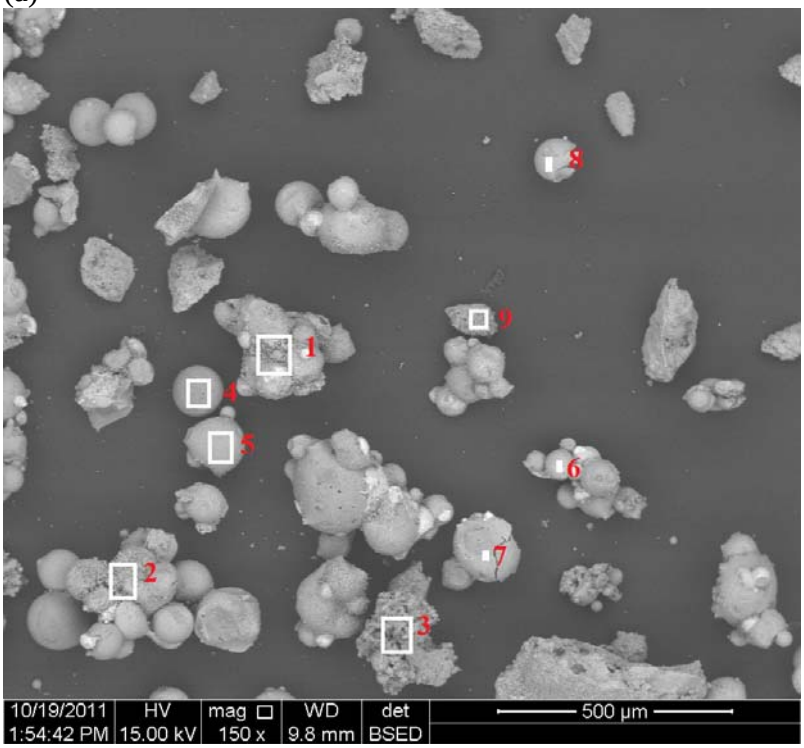

(b)

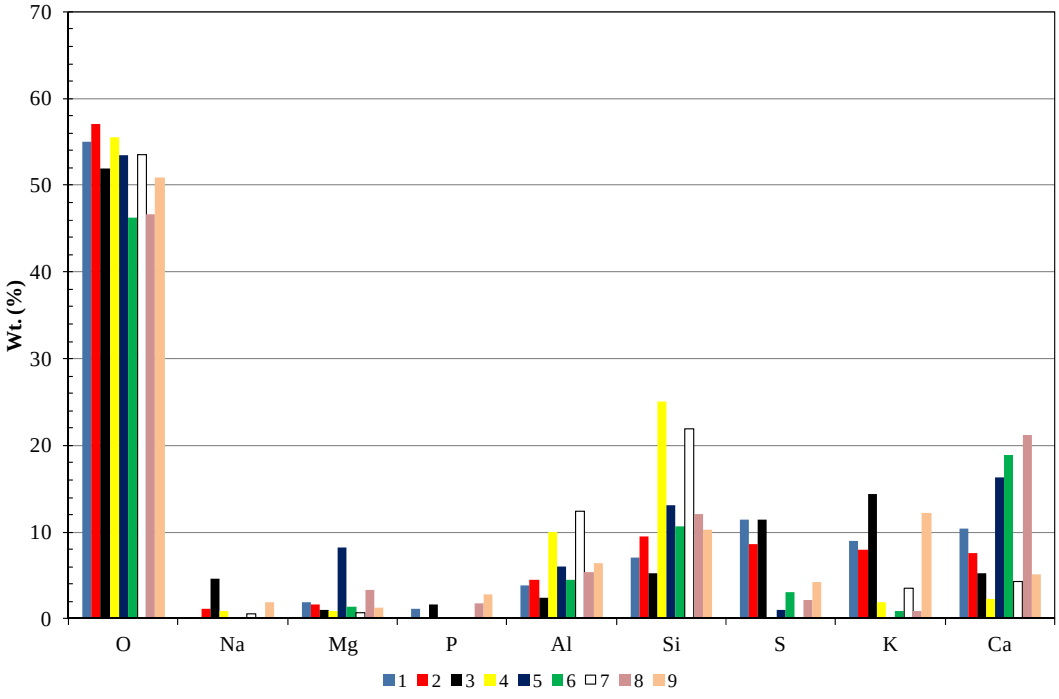

Figure 24: Morphology and composition of downstream side deposits formed during test 5.

3.7 Effect of operating parameters on the emissions of NO, SO_2 and CO

The effect of operating parameters on NO, SO_2 and CO emissions was also studied. The impact of biomass load and boiler load on NO_x emissions is shown in Figure 25, while impact of flue gas temperature on NO_x emissions is shown in Figure 26. It can be seen that NO_x emissions increased with increasing boiler load contrary to the previous full-scale measurements at the same boiler [5]. However, there is no clear tendency of increase of NO_x emissions with increase in biomass load. There is seen an increased NO_x emissions at higher flue gas temperatures, possibly due to formation of thermal NO_x.

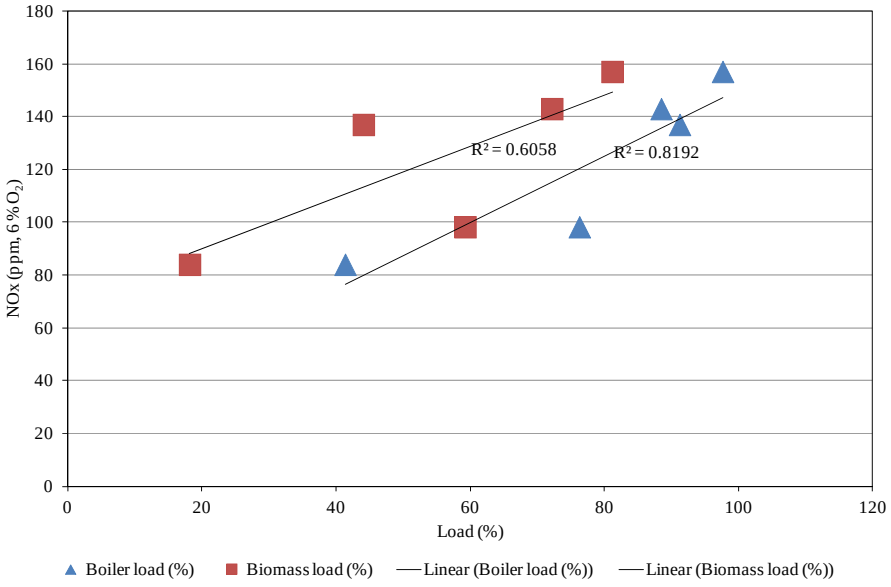

Figure 25: Impact of biomass load and boiler load on NOx emissions.

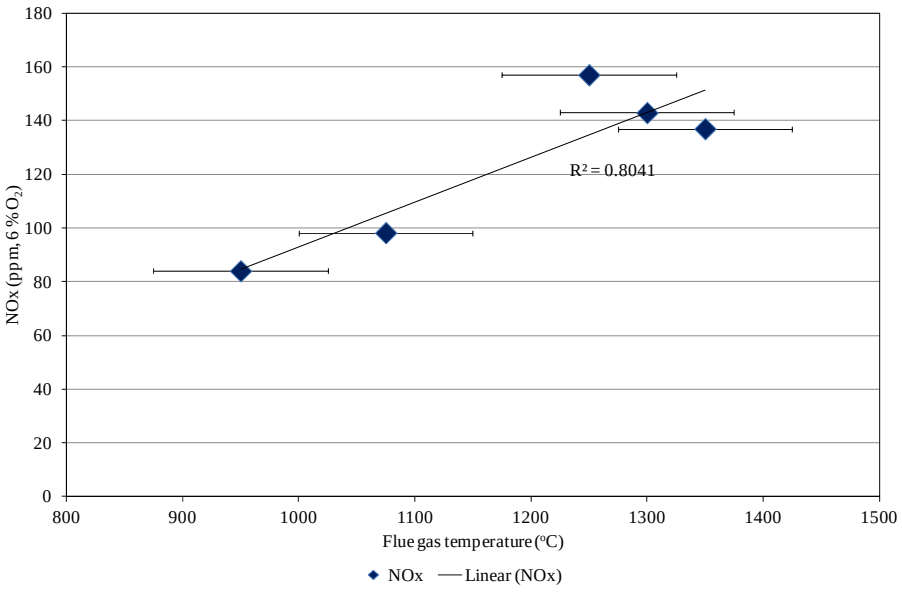

Figure 26: Impact of flue gas temperature on NOx emissions.

The impact of biomass load and boiler load on CO emissions is shown in Figure 27. There is not seen a correlation between biomass and boiler load on CO emissions. However, a relation between oxygen level and CO emissions can be seen in Figure 28. It can be seen that CO emissions increased at reduced oxygen levels, and a maximum value of 48 ppm is evident at 2.4 % O_2. The SO_2 emissions were observed to be very small in all the measurements and a maximum value of 8.2 ppm was seen during test 3.

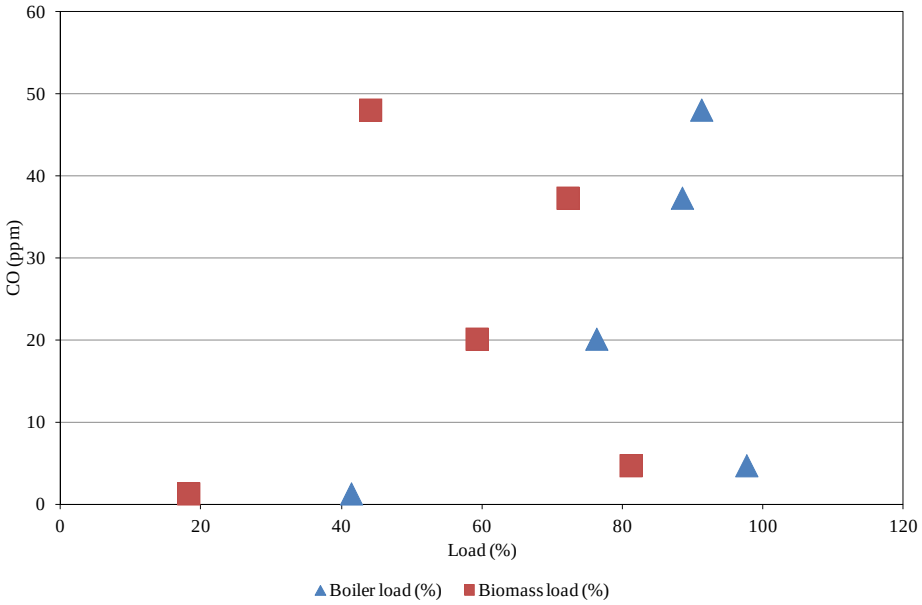

Figure 27: Impact of biomass load and boiler load on CO emissions.

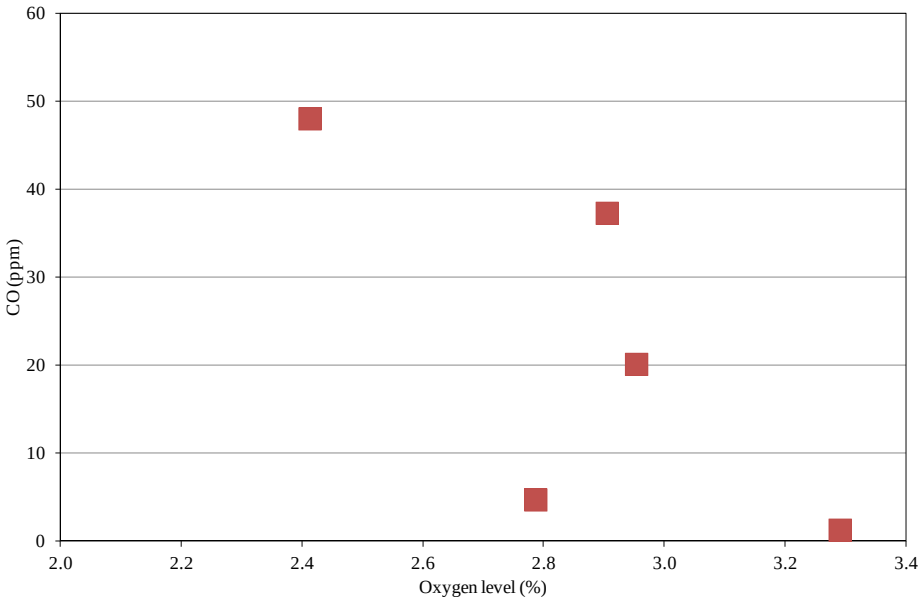

Figure 28: Relation between oxygen level and CO emissions.

4 SUMMARY AND CONCLUSIONS

A series of deposit probe boiler measurements were conducted at Avedøre Unit 2, a wood and natural gas suspension-fired boiler, to investigate ash deposition with coal ash addition. The probe was placed just below the radiation shield in the top of the boiler chamber. The measurements included deposit mass, heat uptake, flue gas temperature and video registration. The overall conclusions are summarized in the following points:

- Changes in biomass boiler load lead to some degree to changes in boiler flue gas temperature and the used coal ash to wood ash ratio. It is therefore difficult to determine which changes that causes the observed large changes in the deposit formation rate. However, a high increase in local flue gas temperature increased the deposit formation rate in this study, and this has also been observed in other previous deposit probe biomass boiler studies.
- Video monitoring revealed that the deposits formed were not sticky and could be easily removed by gravity shedding, and even at very high flue gas temperatures (> 1350 ^{o}C), deposit removal through surface melting was not identified. This indicates that potassium (K) has been captured by coal ash to form deposits with high melting temperatures.
- The percentage of deposits removed at a shedding event and deposit removal frequency increases to some extent with increasing boiler load and biomass load.
- NO_x emissions increased with increase in flue gas temperature, possibly due to formation of thermal NO_x.
- CO emissions reduced with increase in O_2 level. However, CO emissions were very small even at lower O_2 level (48 ppm at 2.4 % O_2).
- SO_2 emissions in all the measurements were very small with a maximum value of 8 ppm.
- SEM-EDS analysis of deposits shows significant presence of Ca, Al and Si, indicating that K has been captured by the coal ash to form deposits rich in calcium-aluminum-silicates. Cl was not found either on the upstream side or on the downstream side of the probe, and potentially Cl has been released to the gas phase as HCl(g).

ACKNOWLEDGEMENTS

The financial support by DONG Energy is gratefully acknowledged. We are thankful to the operational staff at the Avedøre Power Station, for their technical support during the full-scale measurements.

References

(1) Frandsen, F. J. Ash formation, deposition and corrosion when utilizing straw for heat and power production. Doctoral Thesis, Technical University of Denmark. **2011**, ISBN 978-87-92481-40-5.

(2) Baxter, L. L. Ash deposition during biomass and coal combustion: A mechanistic approach. *Biomass and Bioenergy* **1993**, 4, 85-102.

(3) Nielsen, H. P. Deposition and high temperature corrosion in biomass-fired boilers. PhD Thesis, Technical University of Denmark. **1998**, ISBN 87-90142-47-0.

(4) Montgomery, M.; Jensen, S. A.; Borg, U.; Biede, O.; Vilhelmsen, T. Experiences with high temperature corrosion at straw-firing power plants in Denmark, *Materials and Corrosion* **2011**, 62, 593-605.

(5) Jensen, P. A.; Dall'ora, M.; Lin, W.; Clausen, S.; Hansen, J.; Simonson, P.; Berg, M.; Jensen, A. D. Measurements on the 800 MW_{th} Avedøre oil, gas and wood co-fired suspension-boiler-Analysis of emission, burnout, deposit and FTIR measurements from April 2005 (Appendix E), CHEC Research Centre, Technical University of Denmark, **2008**.

(6) Jensen, P. A.; Sander, B.; Dam-Johansen, K. Removal of K and Cl by leaching of straw char. *Biomass and Bioenergy* 2001, 20, 447-457.

(7) Andersen, K. H.; Frandsen, F. J.; Hansen, P. F.; Wieck-Hansen, K.; Rasmussen, I.; Overgaard, P.; Dam-Johansen, K. Deposit formation in a 150 MWe utility PF-boiler during co-combustion of coal and straw, *Energy Fuels* **2000**, 14, 765-780.

(8) Zbogar, A.; Frandsen, F.; Jensen, P. A.; Glarborg, P. Shedding of ash deposits, *Prog. Energy Combust. Sci.* **2009**, 35, 31-55.

(9) Jensen, P. A.; Sørensen, L. H.; Hu, G.; Holm, J. K.; Frandsen, F.; Henriksen, U. B. Combustion experiments with biomass fuels and additives in a suspension fired entrained flow reactor – Test of Ca and P rich additives used to minimize deposition and corrosion. PSO Project, CHEC Research Centre, Technical University of Denmark. **2006.**

(10) Jensen, P. A.; Zhou, H.; Frandsen, F. J.; Hansen, J. Ash deposits removal in biomass power plant boilers, Proceeding of 15th European Biomass Conference and Exhibition. Berlin, Germany, 07-11 May, **2007**.

(11) Tobiasen, L.; Skytte, R.; Pedersen, L. S.; Pedersen, S. T.; Lindberg, M. A. Deposit characteristics after injection of additives to a Danish straw-fired suspension boiler. *Fuel Process Technol.* **2007**, 88, 1108-1117.

(12) Wu, H.; Glarborg, P.; Frandsen, F. J.; Dam-Johansen, K.; Jensen, P. A.; Dust-firing of straw and additives: Ash chemistry and deposition behavior, *Energy Fuels* **2011**, 25, 2862-2873.

(13) Åmand, L. E.; Leckner, B.; Eskillson, D.; Tullin, C. Ash deposition on heat transfer tubes during demolition wood, *Energy and Fuels* **2006**, 20, 1001-1007.

(14) Jensen, P. A.; Stenholm, M.; Hald, P. Deposition investigation in straw-fired boilers. *Energy Fuels* **1997**, 11, 1048-1055.

(15) Zhou, H.; Frandsen, F. J.; Jensen, P. A.; Glarborg, P. PSO Project 4106, CHEC report R0603, CHEC Research Centre, Technical University of Denmark. **2006**.

(16) Zbogar, A.; Frandsen, F. J.; Jensen, P. A.; Hansen, J.; Glarborg, P., Experimental investigation of ash deposit shedding in a straw-fired boiler. *Energy Fuels* **2006**, 20(2), 512-519.

(17) Bashir, M. S.; Jensen, P. A.; Frandsen, F.; Wedel, S.; Dam-Johansen, K.; Wadenbäck, J.; Pedersen, S. T.; Suspension-firing of biomass. Part 1: Full-scale measurements of ash deposit build-up, *Energy Fuels* **2012**, 26, 2317-2330.
(18) Nordgren, D. et al., Ash transformations in pulverised fuel co-combustion of straw and woody biomass. *Fuel Process Technol.* **2011**, doi:10.1016/j.fuproc.2011.05.027.
(19) Skrifvars, B-J.; Lauren, T.; Hupa, M.; Korbee, R.; Ljung, P. Ash behavior in a pulverized wood fired boiler - a case study. *Fuel* **2004**, 83, 1371-1379.
(20) Bashir, M. S.; Jensen, P. A.; Frandsen, F.; Wedel, S.; Dam-Johansen, K.; Wadenbäck, J.; Pedersen, S. T.; Ash transformation and deposit build-up during biomass suspension and grate-firing: Full-scale experimental studies. *Fuel Process Technol.* **2012**, 97, 93-106.
(21) Lokare, S. S.; Dunaway, J. D.; Moulten, D.; Rogers, D.; Tree, D. R.; Baxter, L. L. Investigation of ash deposition rates for a suite of biomass fuels and fuel blends. *Energy Fuels* **2006**, 20, 1008-1014.
(22) IFRF Suction Pyrometer, User Information Document, International Flame Research Foundation.
(23) IFRF Handbook, ISSN 1607-9116 www.handbook.ifrf.net/handbook/index.html
(24) Biomass energy centre, www.biomassenergycentre.org.uk (29-09-2011).
(25) Dam-Johansen, K.; Frandsen, F. J.; Jensen, P. A.; Jensen, A.D.; Co-firing of coal with biomass and waste in full-scale suspension-fired boilers. 7th international symposium on coal combustion, Harbin, China, July 17-20, **2011**.

Appendices

A: Boiler drawings

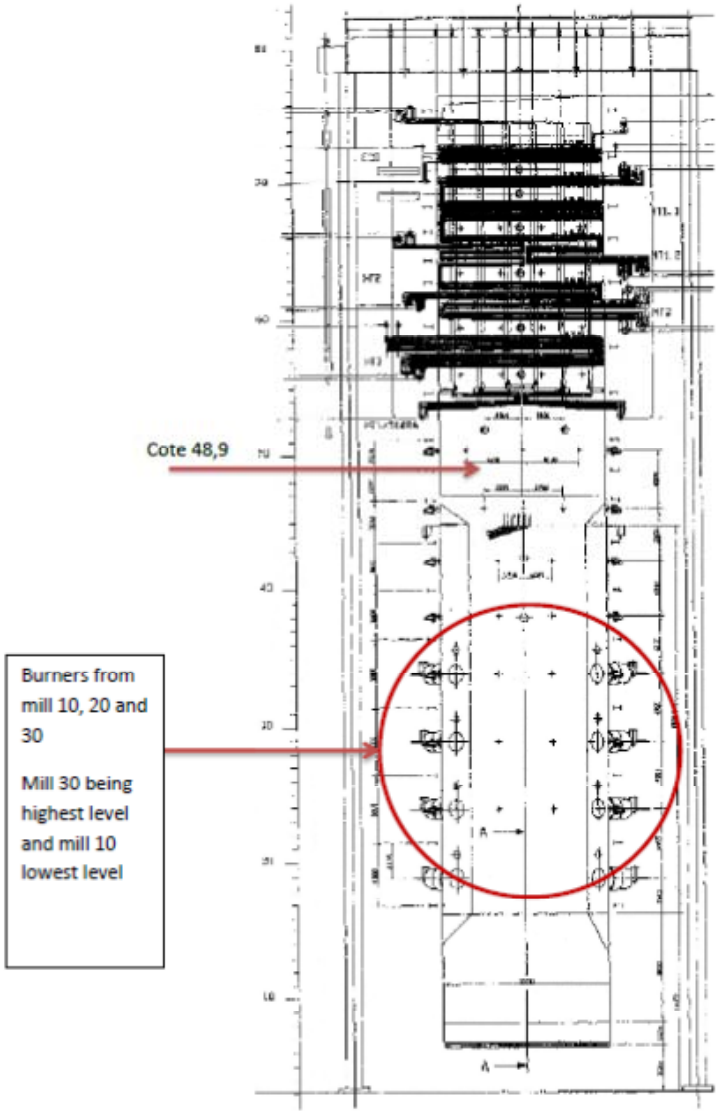

Figure A 1: Drawings of AVV2 boiler with identification of probe measuring position [5].

Appendix B: Flue gas temperature, deposit mass uptake signals, probe heat uptake, boiler operational conditions and ash deposition propensity during each test.

Test 1

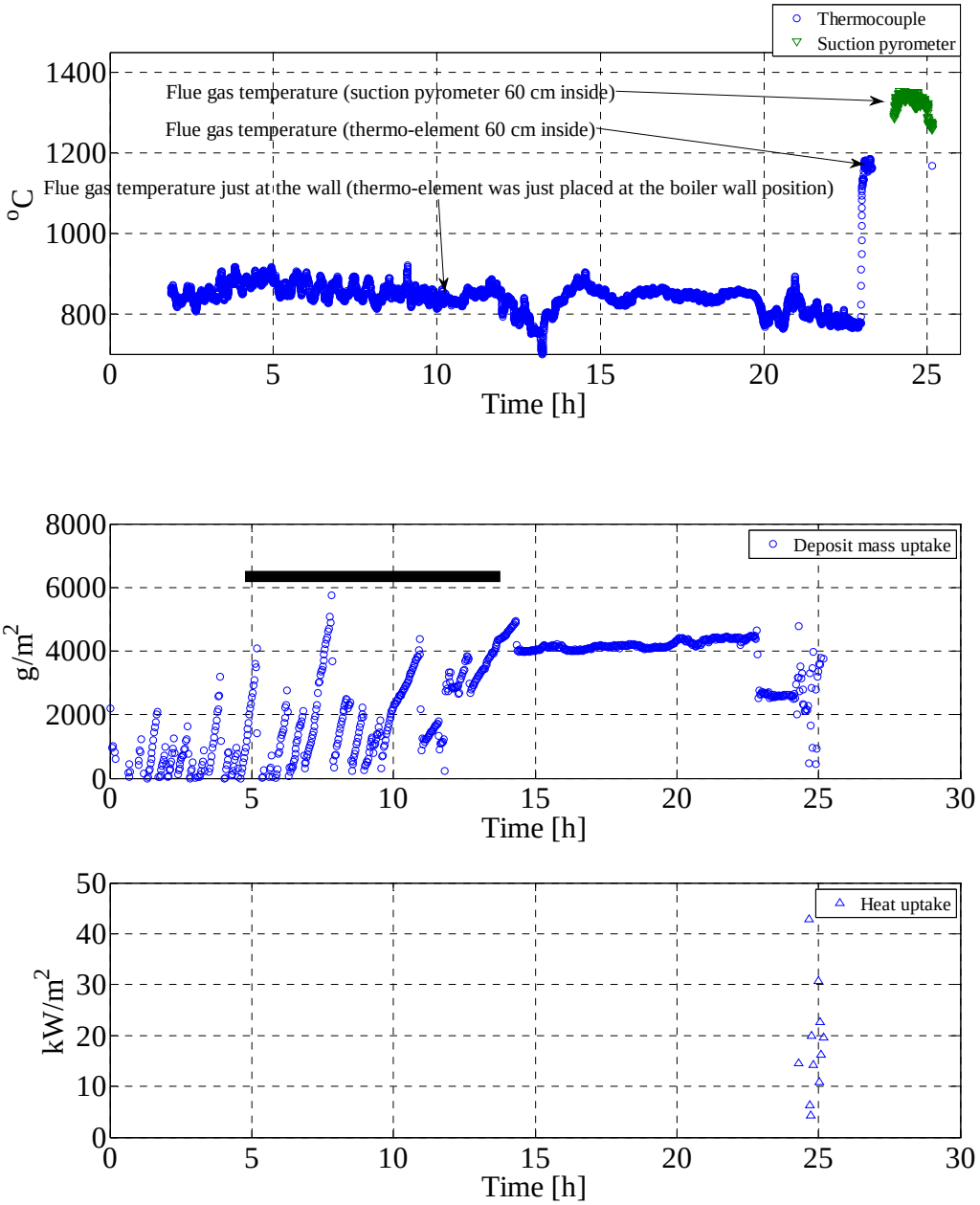

Figure B 1: Flue gas temperature, deposit mass uptake, sootblowing events and probe heat uptake during test 1. The black line in the middle figure shows the time when the surrounding sootblowers were in operation.

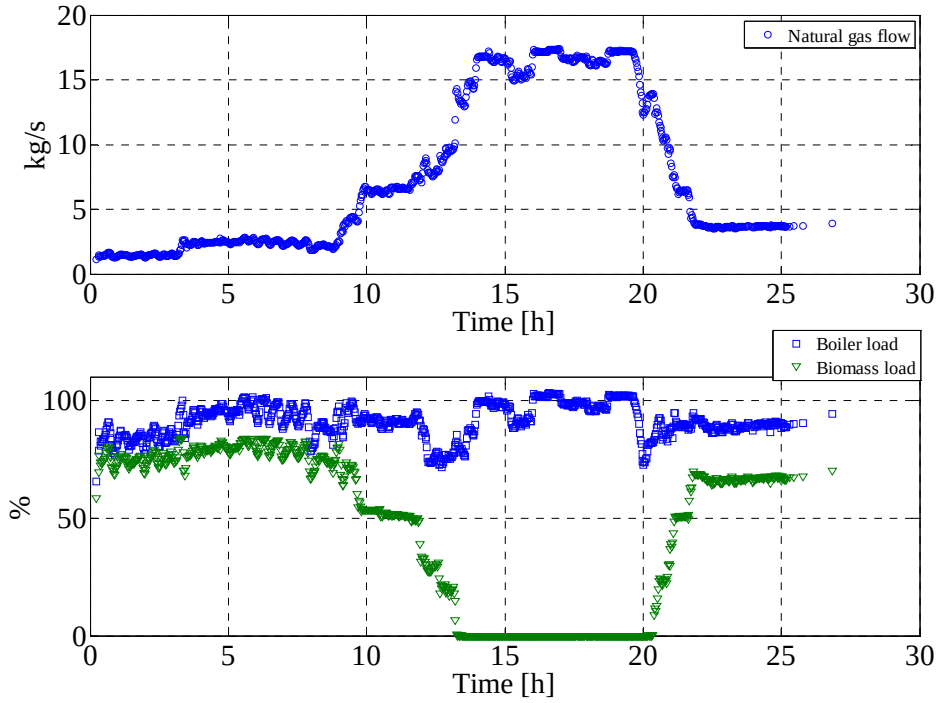

Figure B 2: Natural gas flow, overall boiler load and biomass load during test 1.

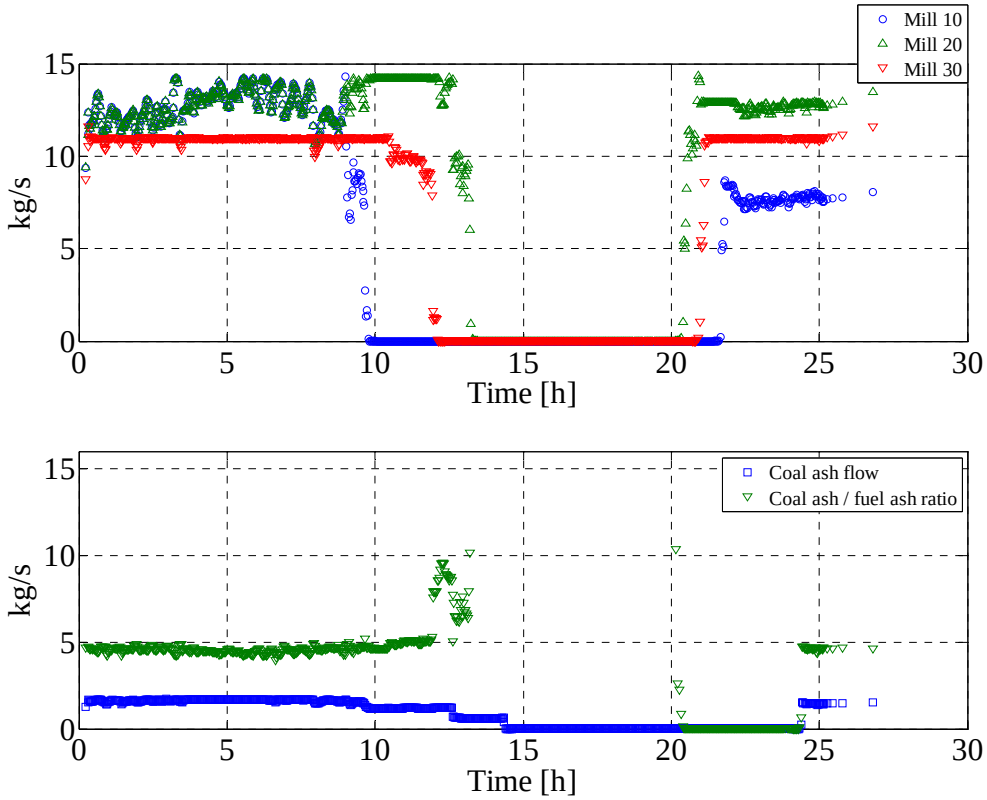

Figure B 3: Fuel flow (wood) through each mill, coal ash flow (kg/s) and ratio between coal ash and wood ash during test 1.

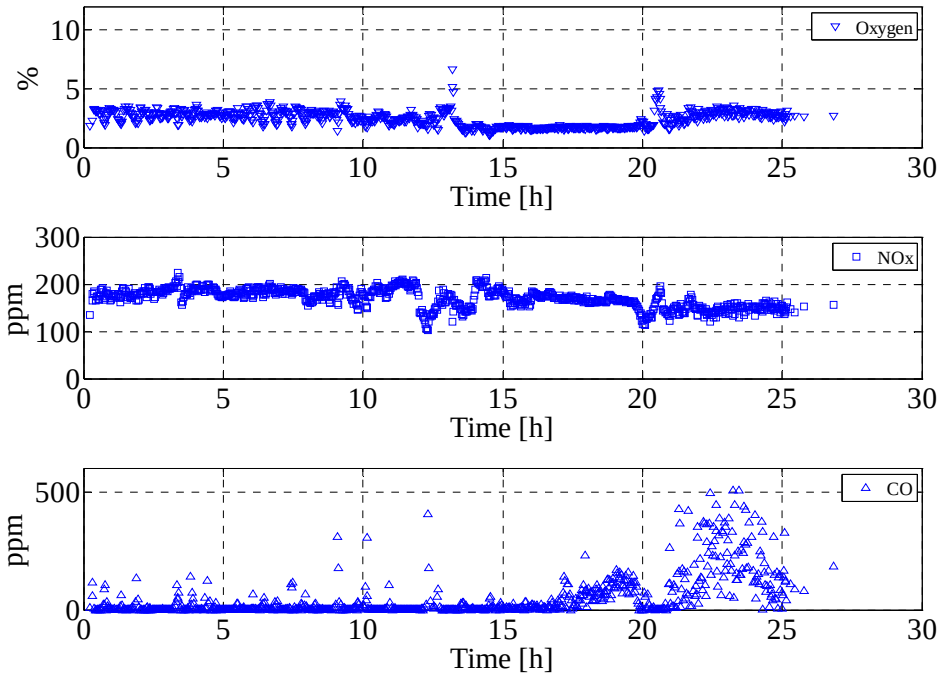

Figure B 4: Oxygen level, NOx level before DeNOx and CO level during test 1.

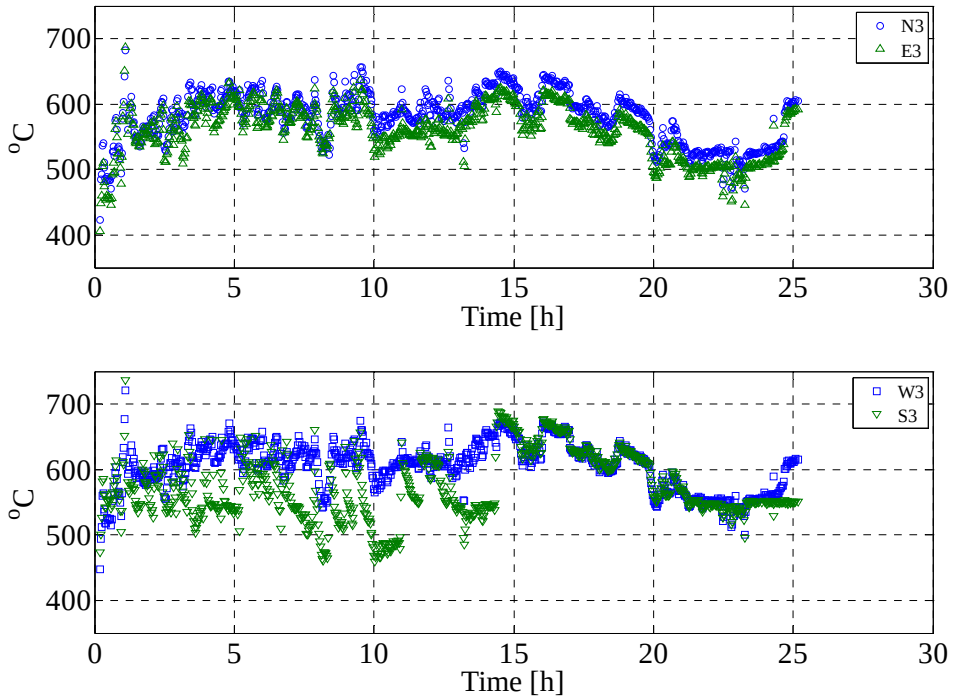

Figure B 5: Measured probe surface temperatures during test 1.

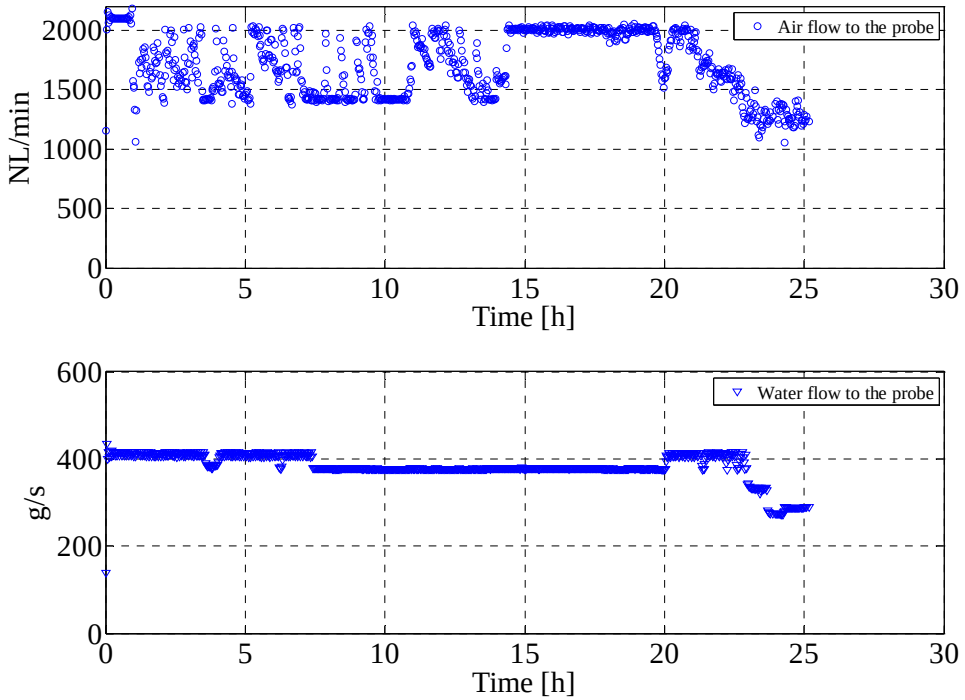

Figure B 6: Water and air flow to the probe measured during test 1.

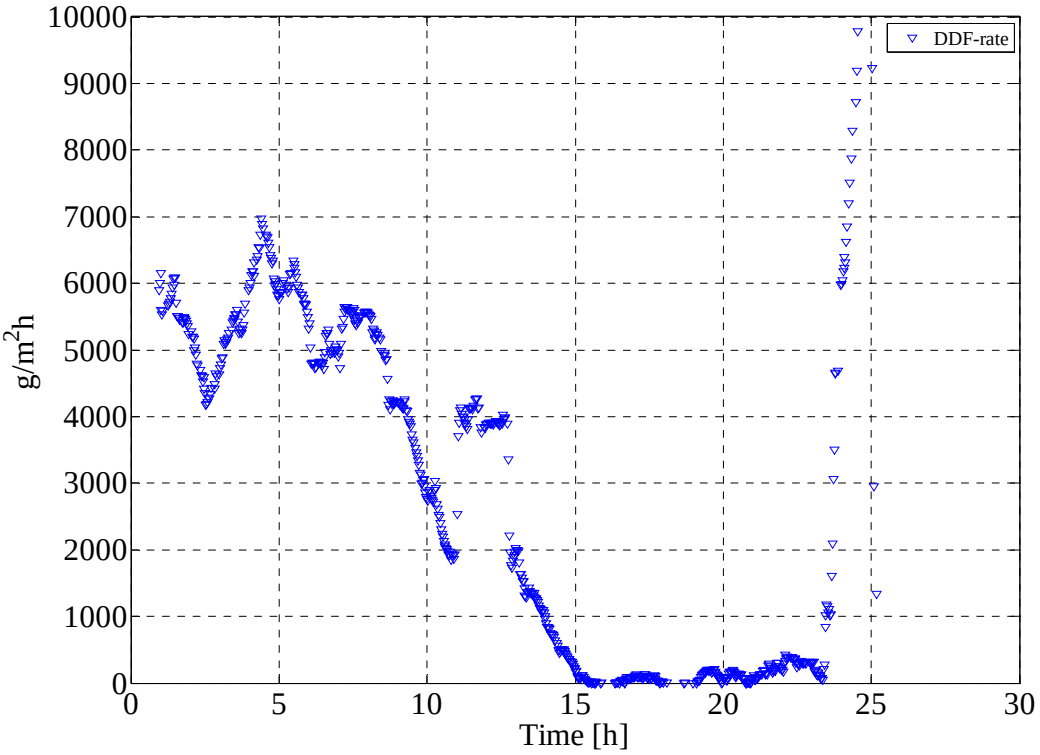

Figure B 7: Calculated Derivative-based Deposit Formation (DDF) rate during test 1.

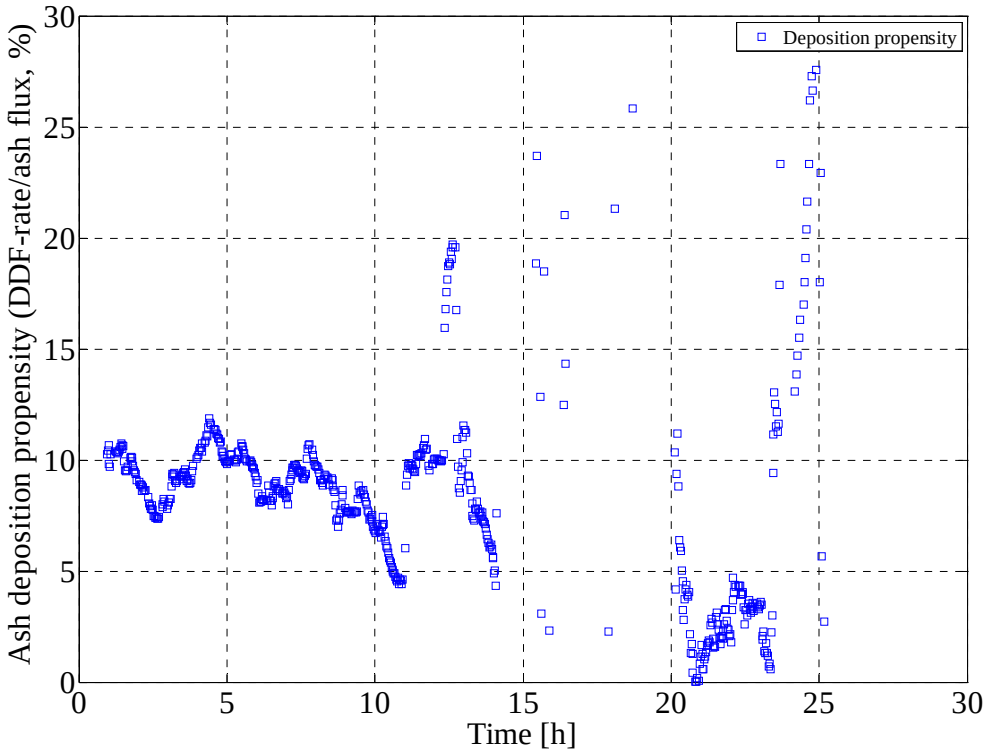

Figure B 8: Calculated ash deposition propensity during test 1.

Test 2

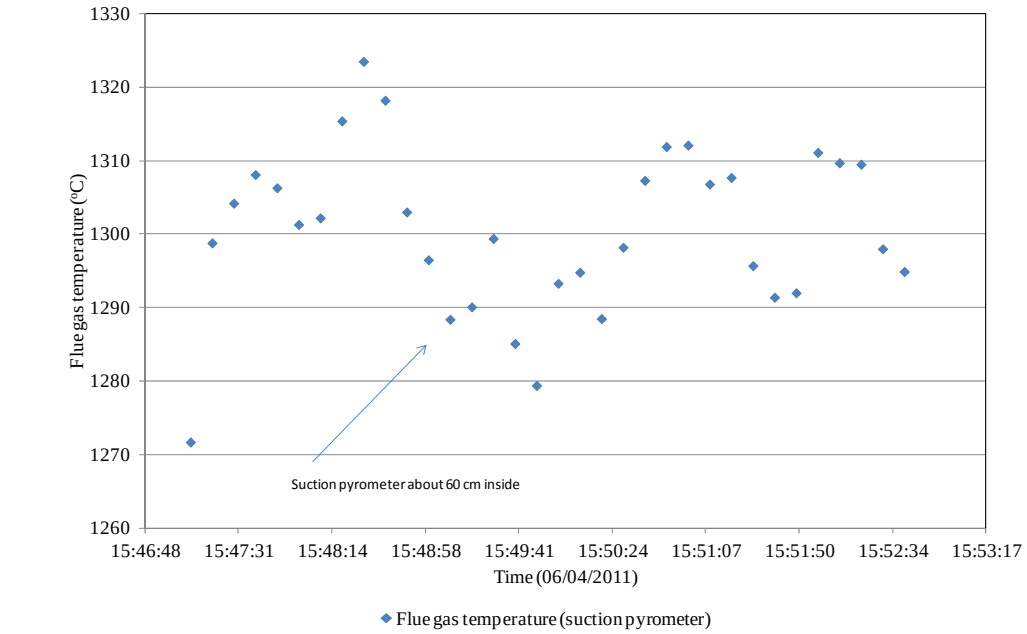

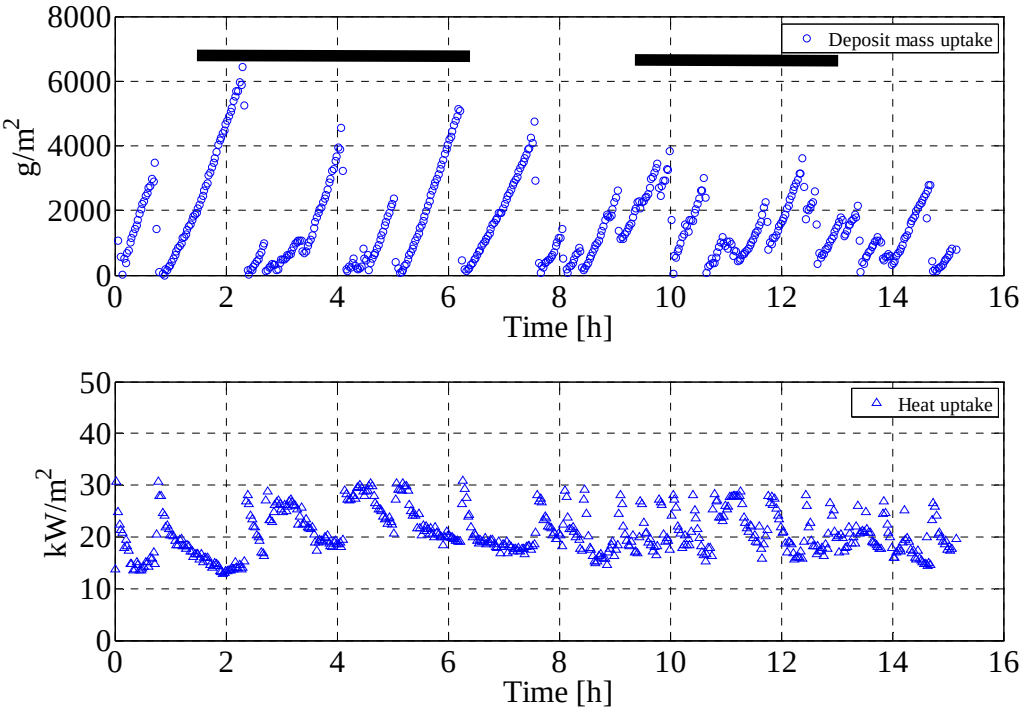

Figure B 9: Flue gas temperature (just after 2-3 hours of test 2) by suction pyrometer, deposit mass uptake, sootblowing events and probe heat uptake during test 2. The black lines in the middle figure show the time when the surrounding sootblowers were in operation.

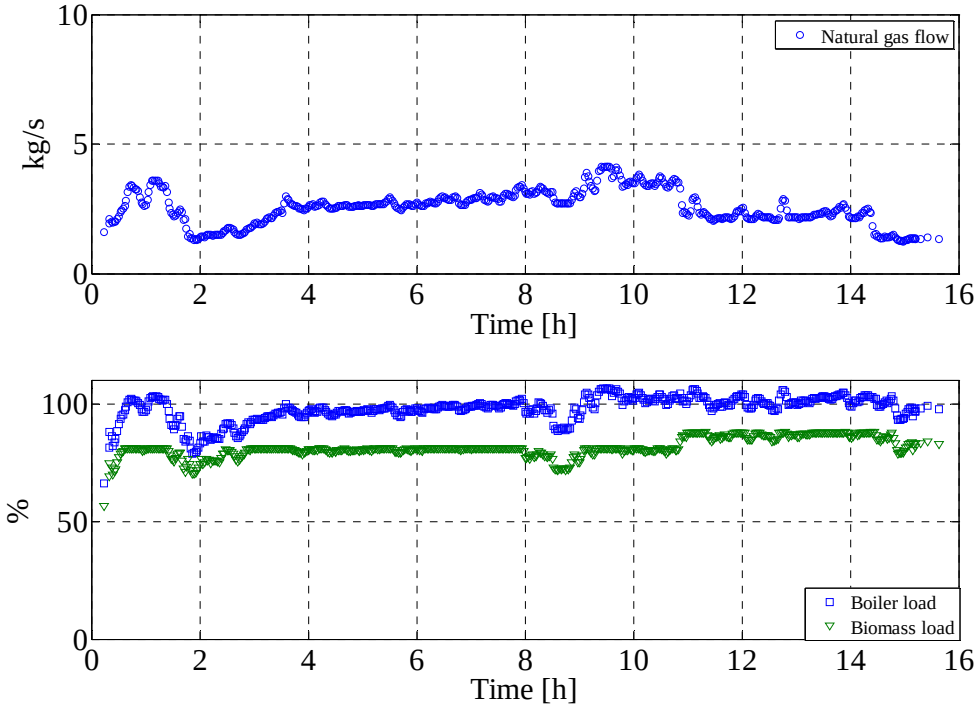

Figure B 10: Natural gas flow, overall boiler load and biomass load during test 2.

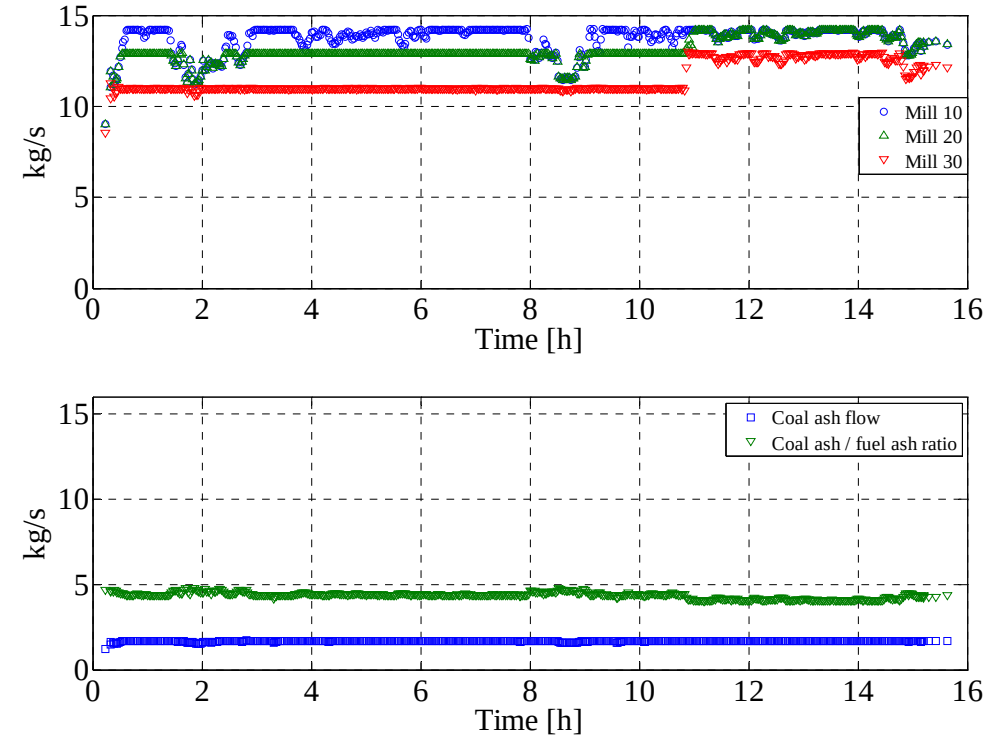

Figure B 11: Fuel flow (wood) through each mill, coal ash flow (kg/s) and ratio between coal ash and wood ash during test 2.

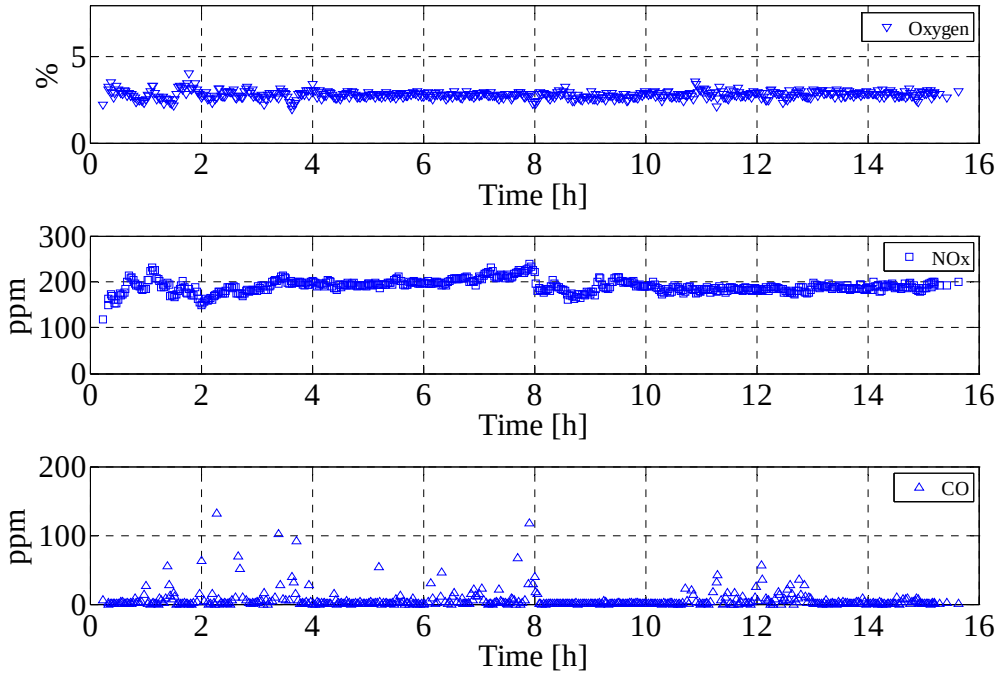

Figure B 12: Oxygen level, NOx level before DeNOx and CO level during test 2.

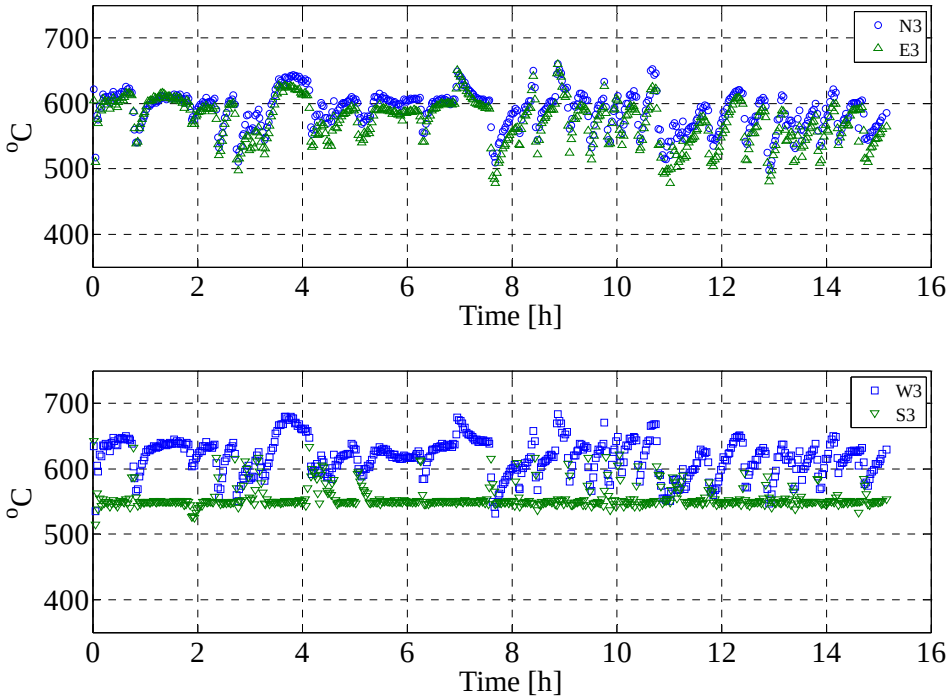

Figure B 13: Measured probe surface temperatures during test 2.

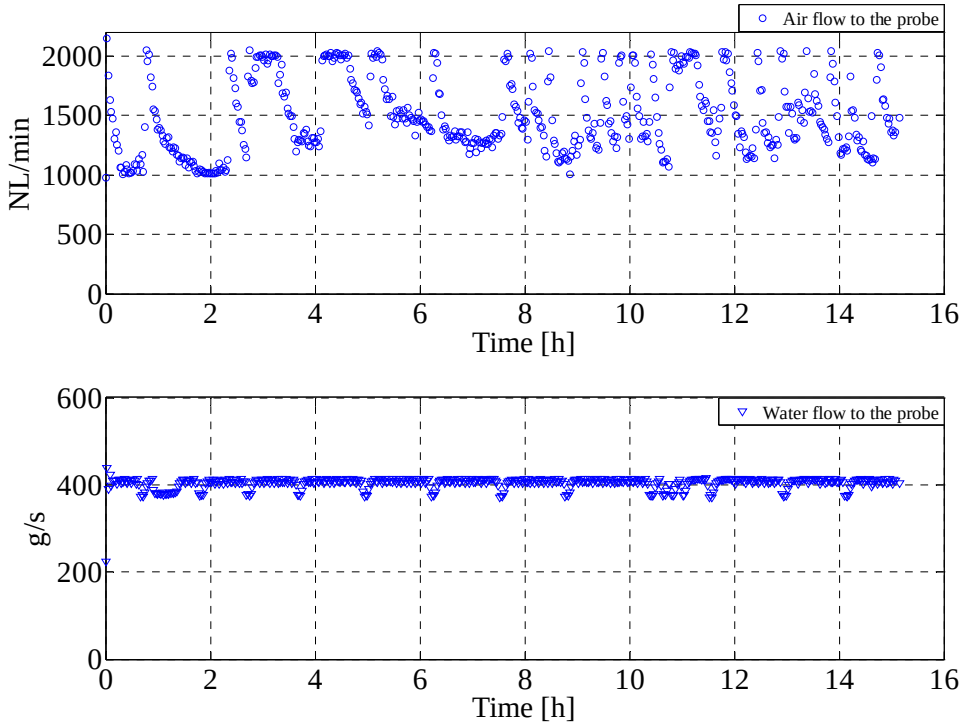

Figure B 14: Water and air flow to the probe measured during test 2.

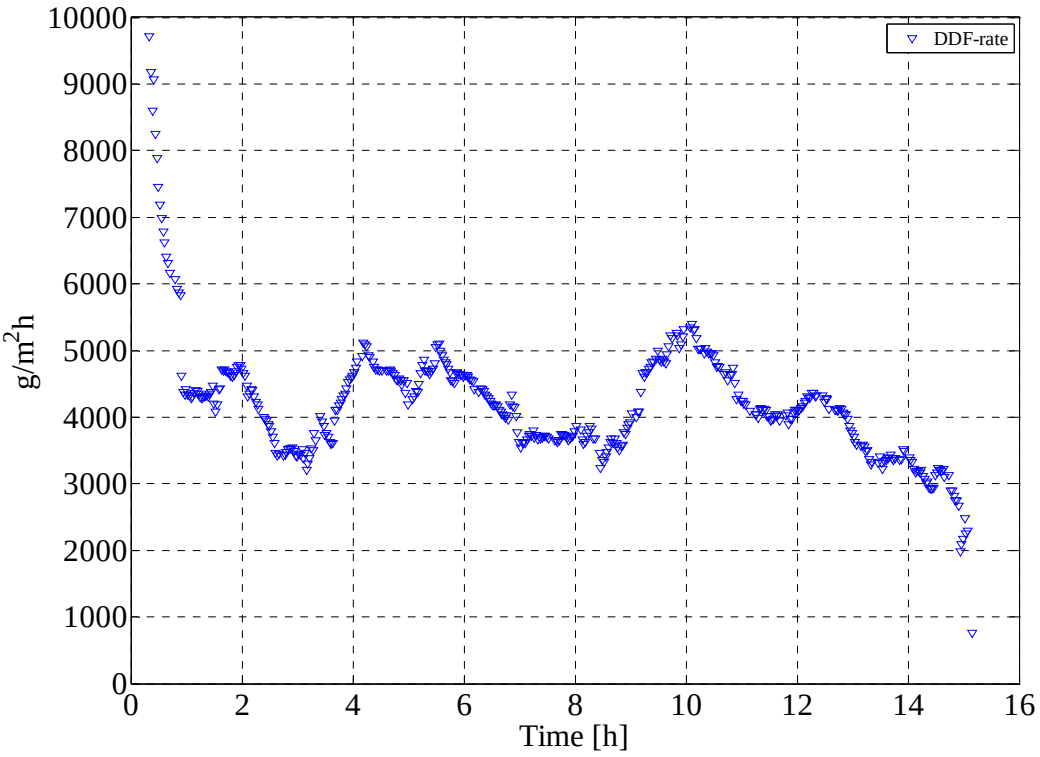

Figure B 15: Calculated Derivative-based Deposit Formation (DDF) rate during test 2.

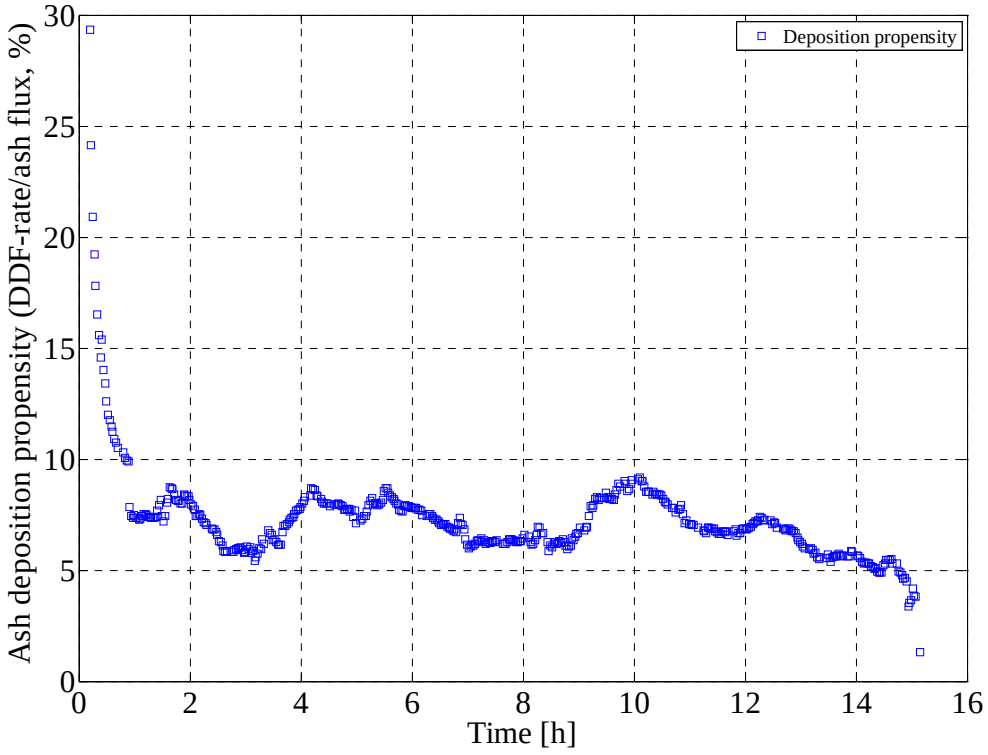

Figure B 16: Calculated ash deposition propensity during test 2.

Test 4

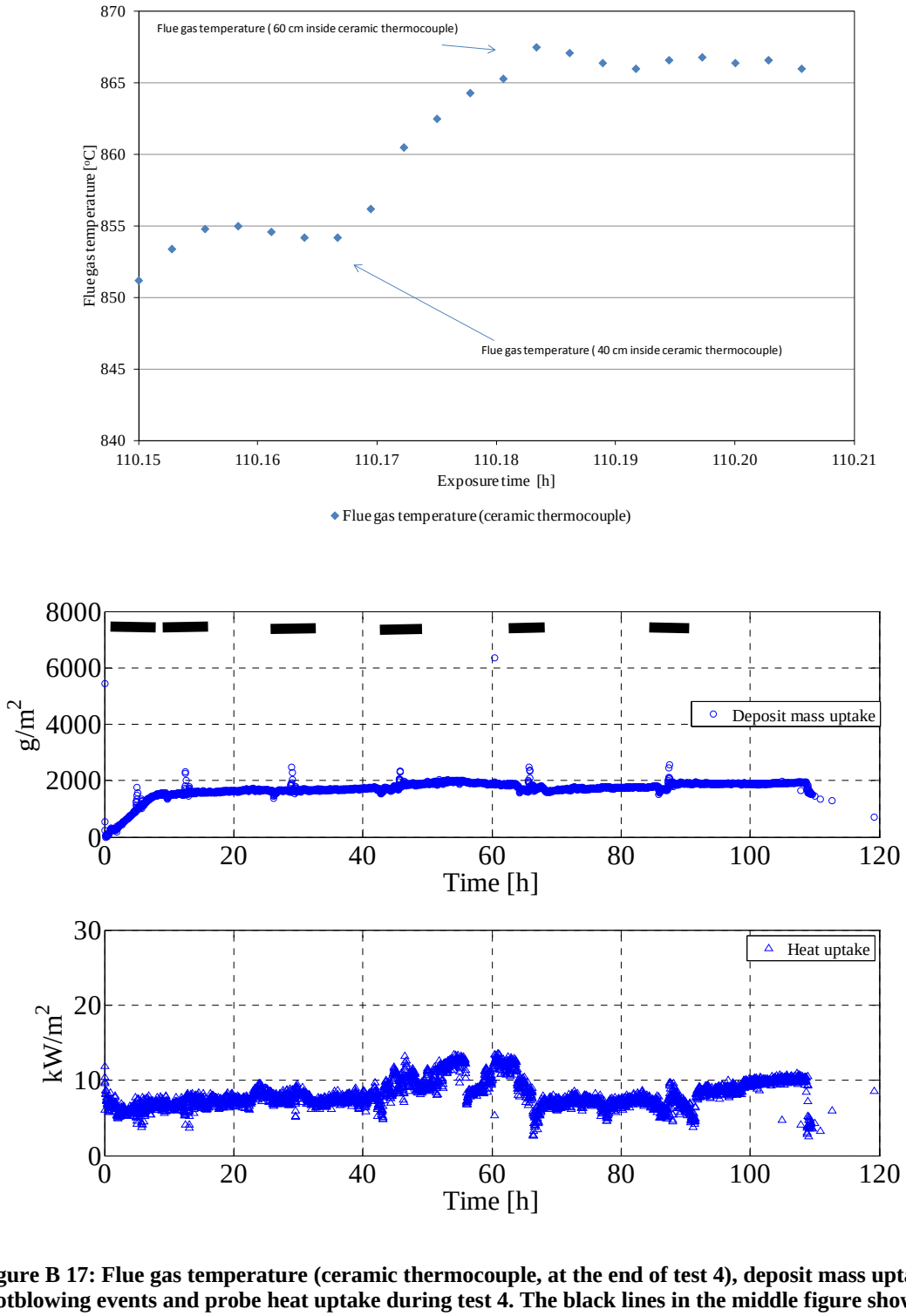

Figure B 17: Flue gas temperature (ceramic thermocouple, at the end of test 4), deposit mass uptake, sootblowing events and probe heat uptake during test 4. The black lines in the middle figure show the time when the surrounding sootblowers were in operation.

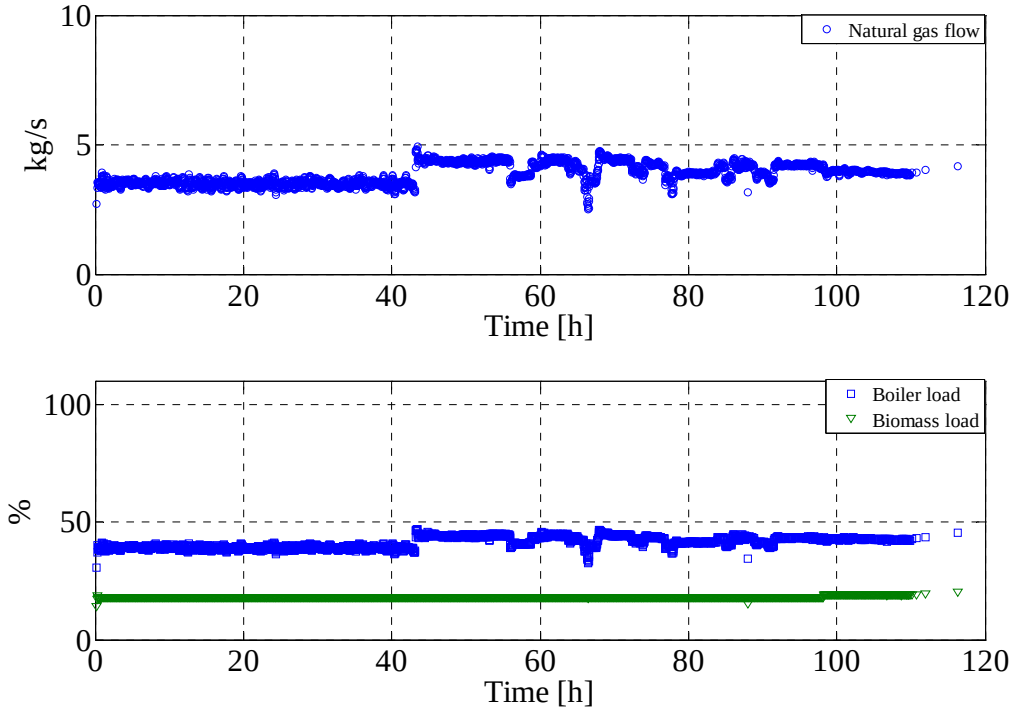

Figure B 18: Natural gas flow, overall boiler load and biomass load during test 4.

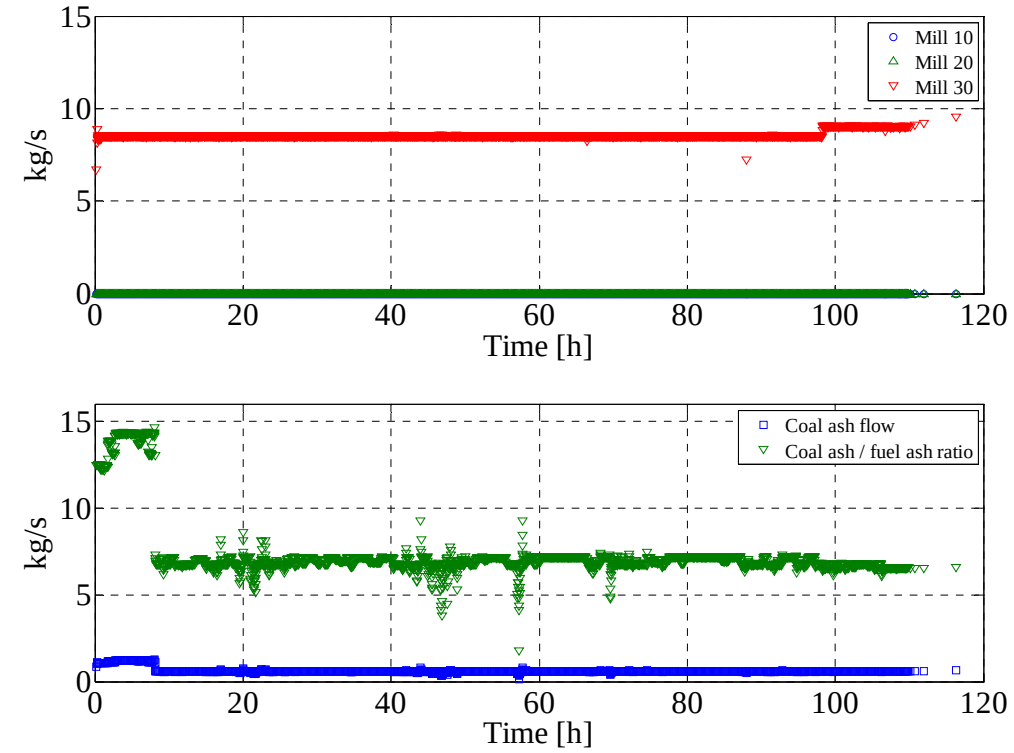

Figure B 19: Fuel flow (wood) through each mill, coal ash flow (kg/s) and ratio between coal ash and wood ash during test 4.

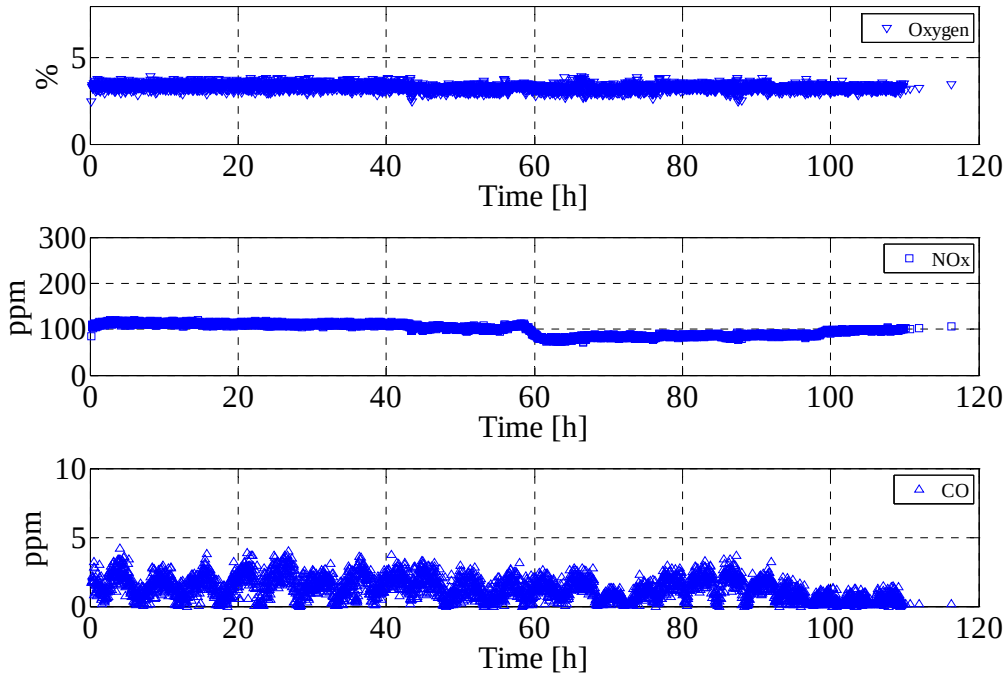

Figure B 20: Oxygen level, NOx level before DeNOx and CO level during test 4.

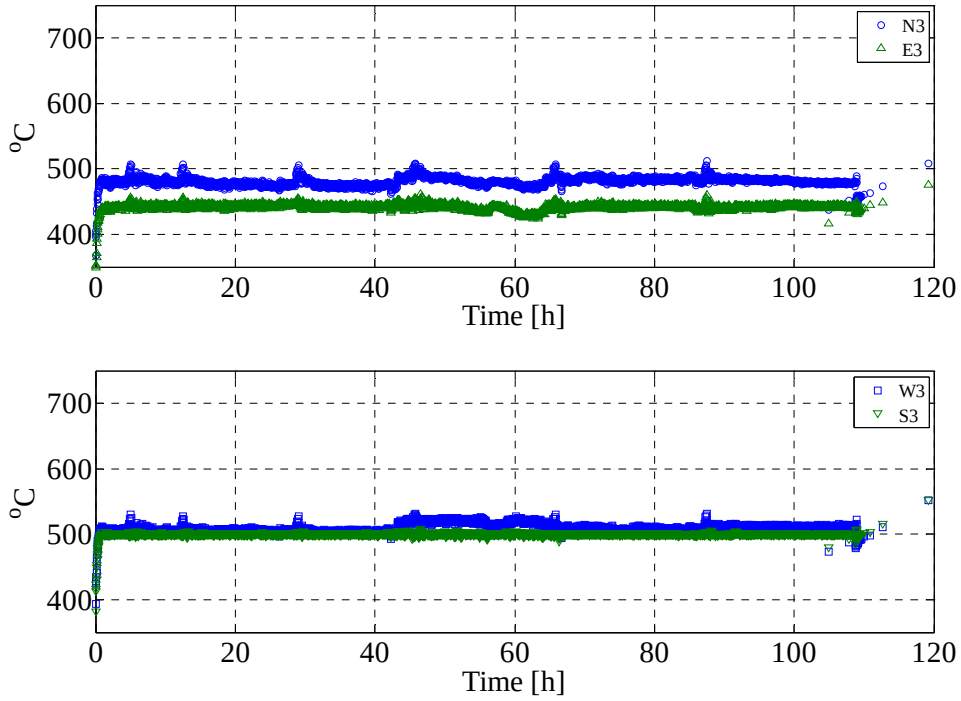

Figure B 21: Measured probe surface temperatures during test 4.

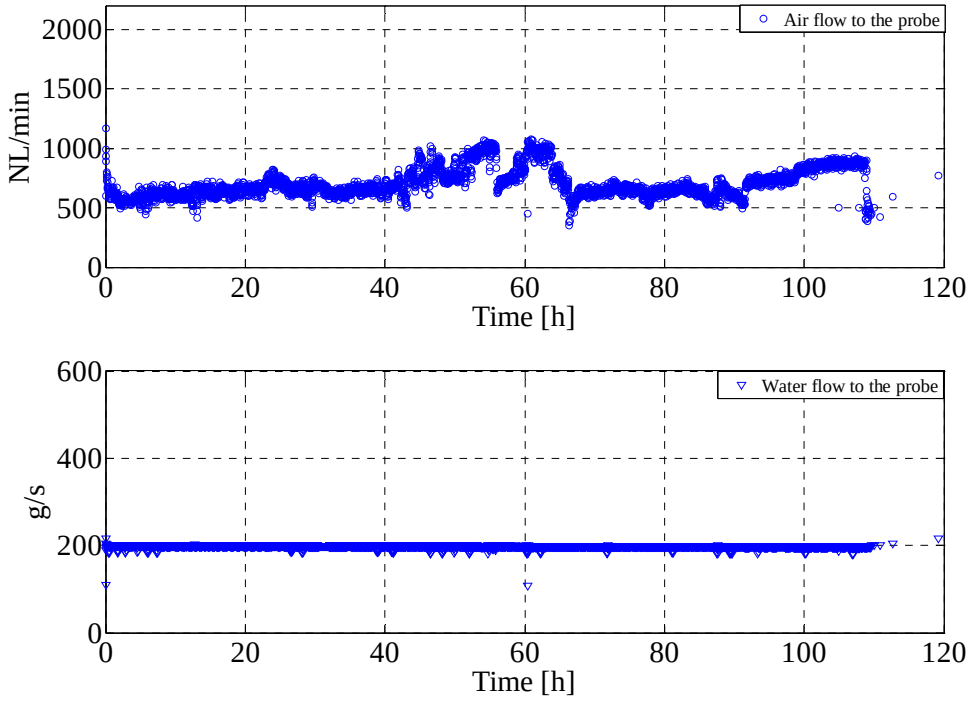

Figure B 22: Water and air flow to the probe measured during test 4.

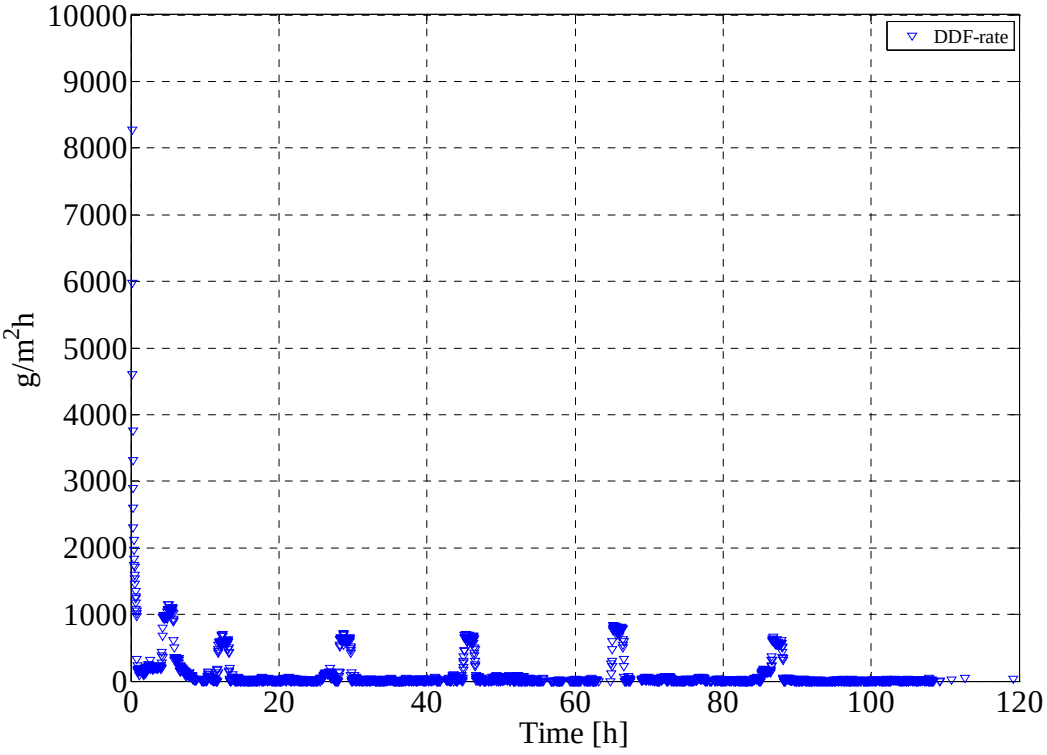

Figure B 23: Calculated Derivative-based Deposit Formation (DDF) rate during test 4.

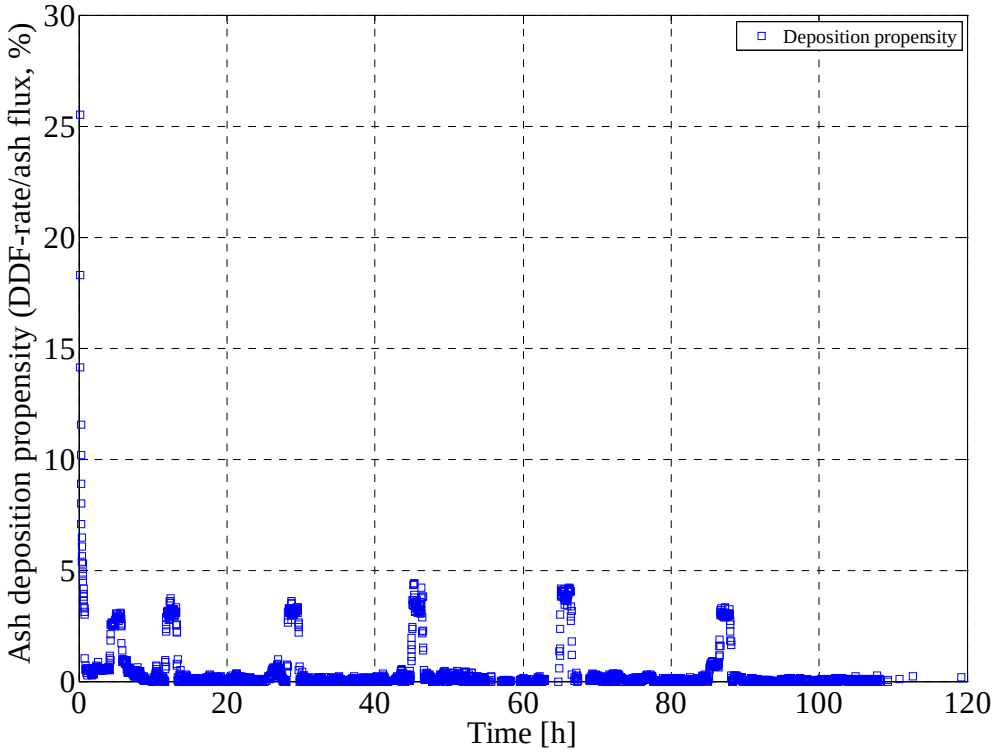

Figure B 24: Calculated ash deposition propensity during test 4.

Test 5

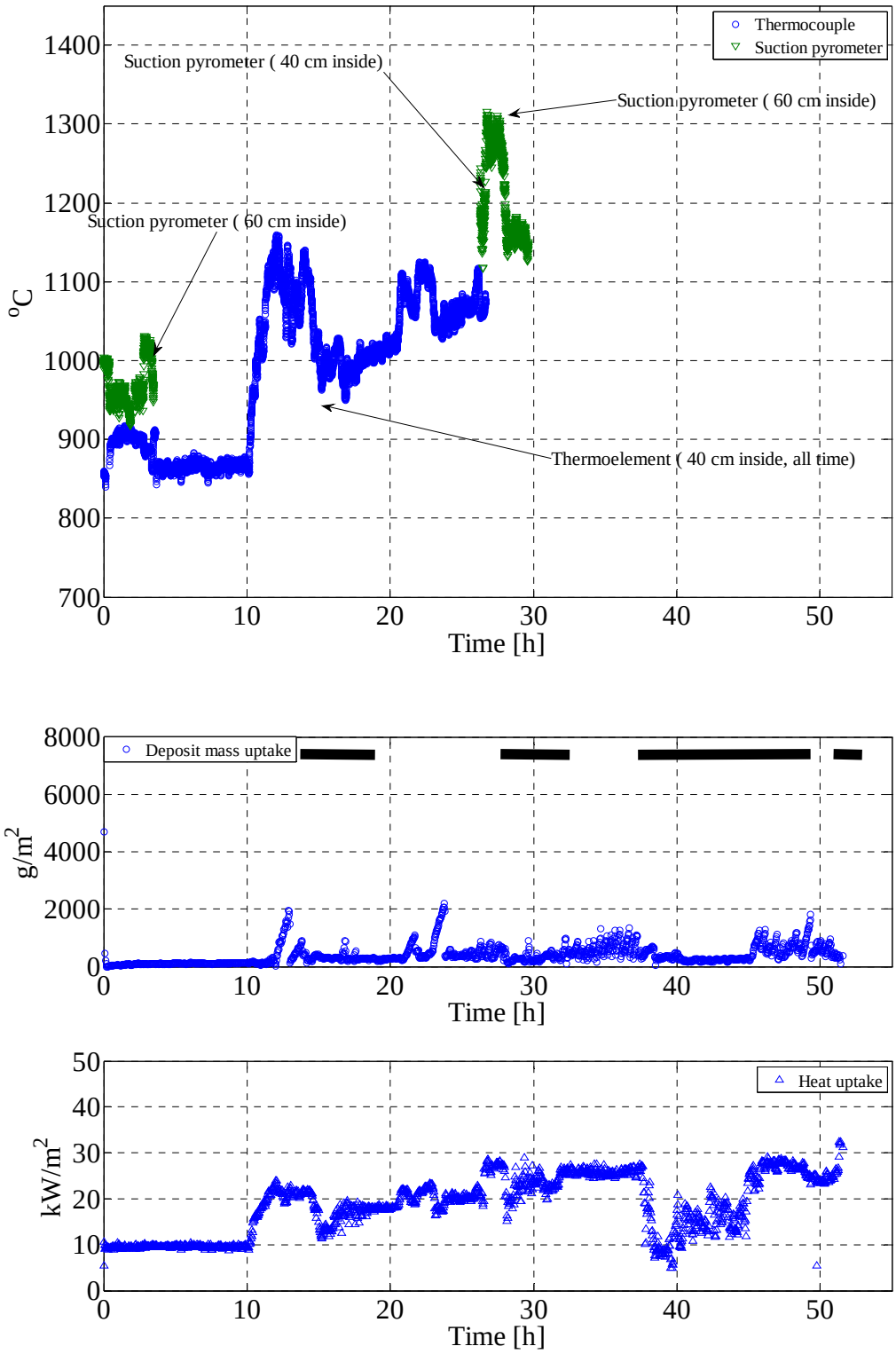

Figure B 25: Flue gas temperature, deposit mass uptake, sootblowing events and probe heat uptake during test 5. The black lines in the middle figure show the time when the surrounding sootblowers were in operation.

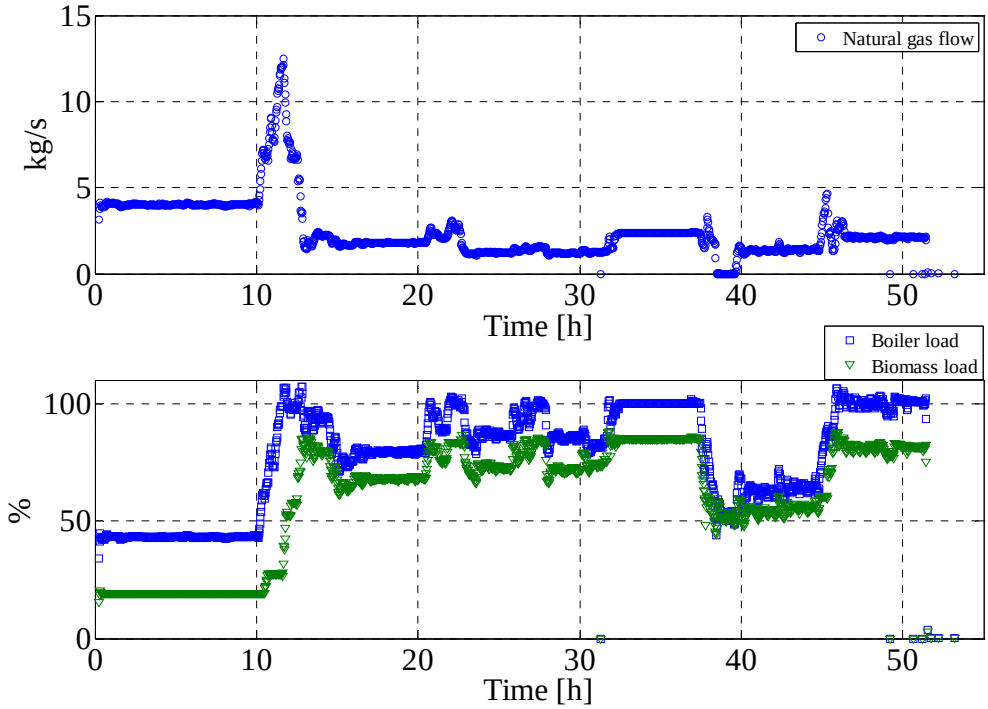

Figure B 26: Natural gas flow, overall boiler load and biomass load during test 5.

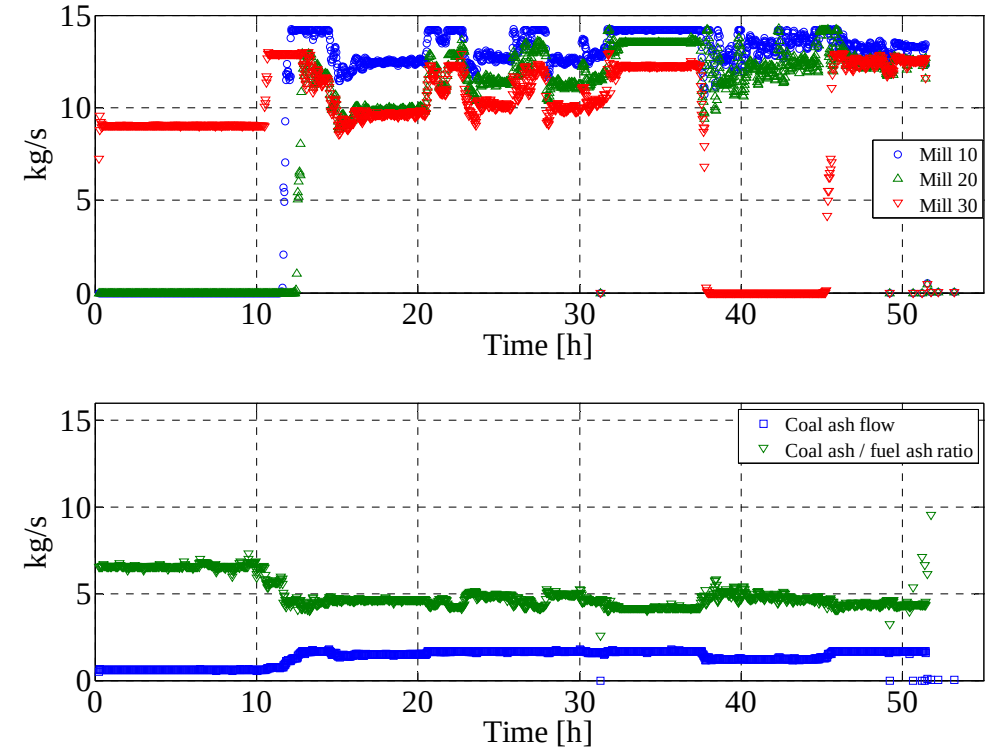

Figure B 27: Fuel flow (wood) through each mill, coal ash flow (kg/s) and ratio between coal ash and wood ash during test 5.

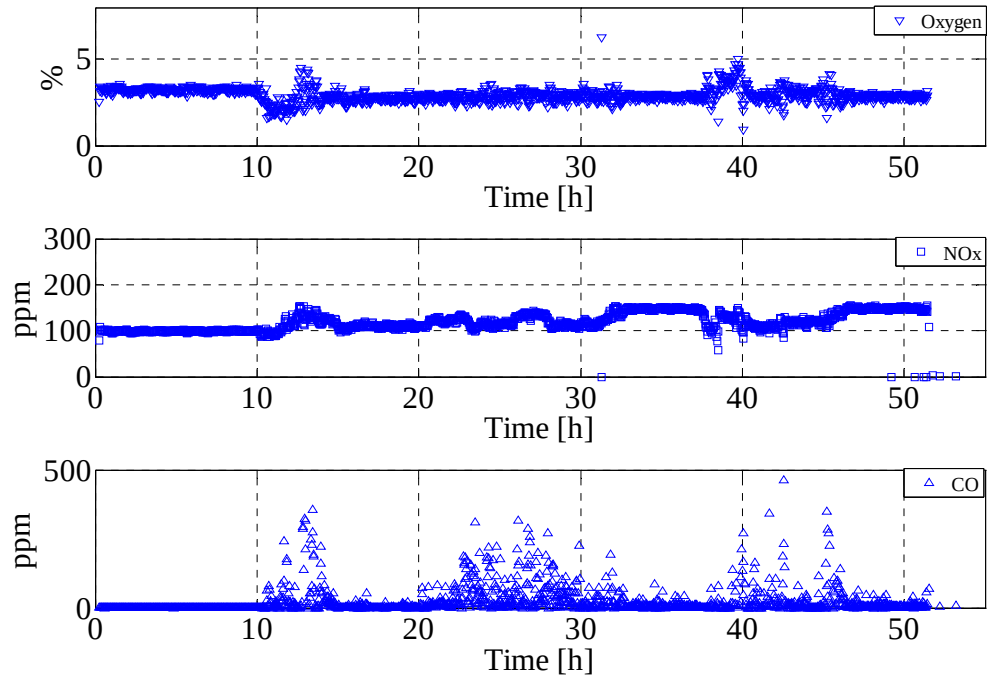

Figure B 28: Oxygen level, NOx level before DeNOx and CO level during test 5.

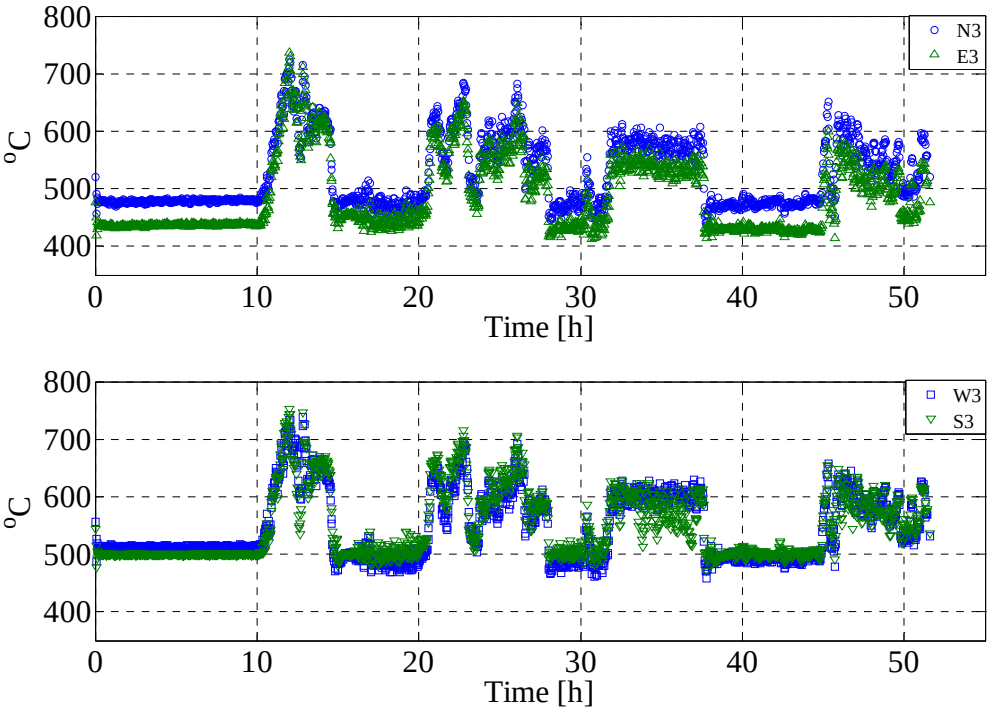

Figure B 29: Measured probe surface temperatures during test 5.

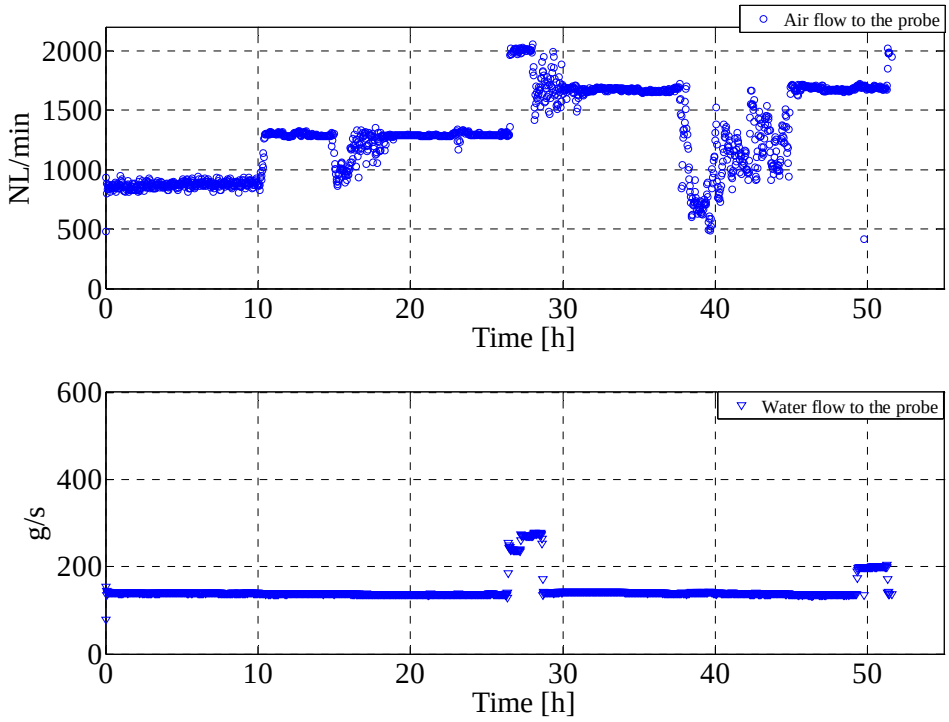

Figure B 30: Water and air flow to the probe measured during test 5.

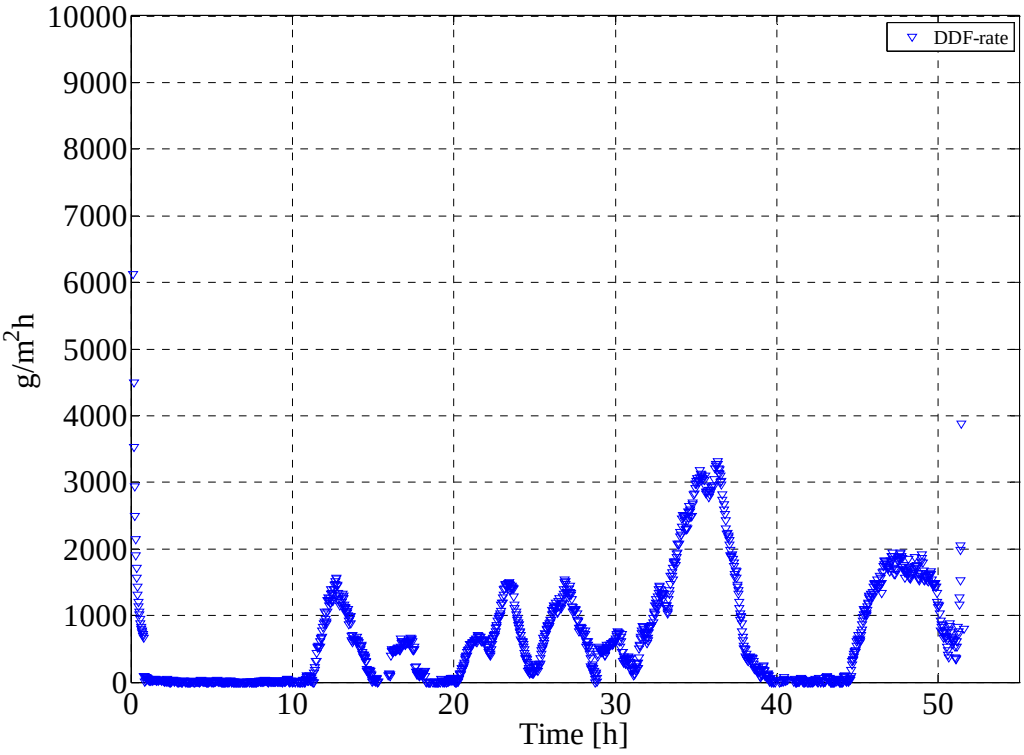

Figure B 31: Calculated Derivative-based Deposit Formation (DDF) rate during test 5.

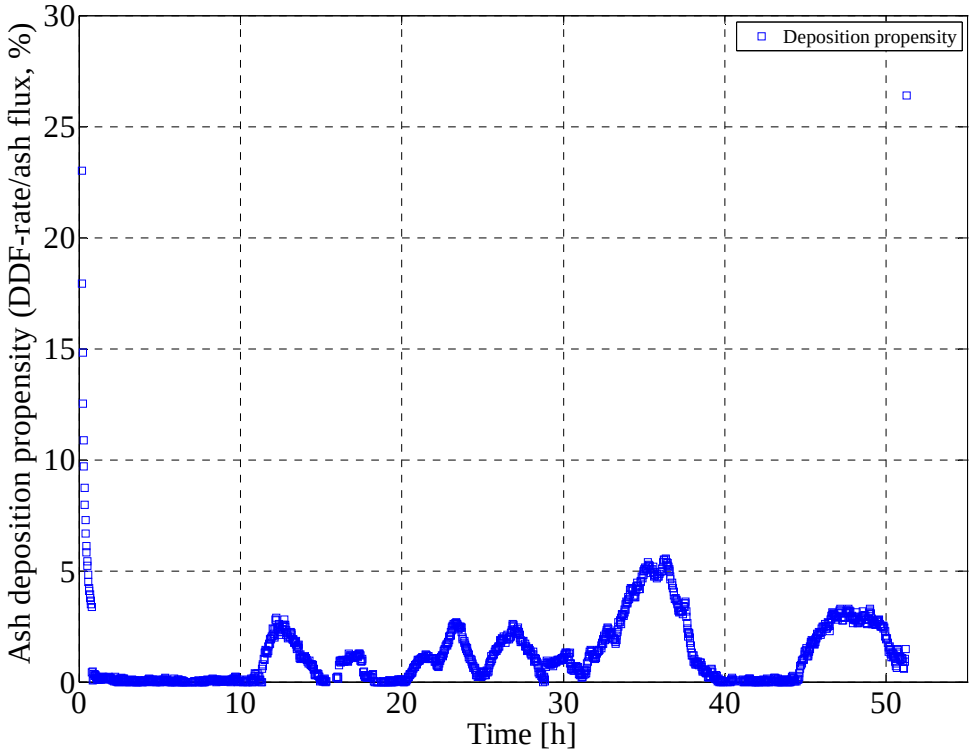

Figure B 32: Calculated ash deposition propensity during test 5.

Appendix C

Method to determine Derivative-based Deposit Formation rate (DDF-rate) (Bashir et al. [18])

The amount of deposit collected on the probe is a function of both the deposit formation process and shedding events. The true deposit formation rate ($g/m^2/h$) cannot be accurately determined, but based on the measured deposit mass increase divided by a given time, the integral deposit formation rate (IDF-rate) or the derivate-based deposit formation rate (DDF-rate), calculated by taking the time derivative of the deposit mass uptake in-between two macro shedding events. However, the DDF-rate should represent a fairly characteristic net-deposition rate for any plant, allowing general features of deposition and its dependence on operating conditions.

The deposit mass uptake signal is influenced by several processes: large shedding events, smaller shedding events (observed as a sudden deposit mass loss on the curve), a relatively slow deposit build-up process and some noise mainly caused by boiler fluctuations. Boiler fluctuations could be mechanical vibrations or large changes in boiler flow dynamics. Some fluctuations are observed when the boiler plant sootblowers were used. Even though the plant sootblowers very near to the probe were shutdown, the rest of the sootblowers to some extent were effective in causing both minor and larger shedding events.

In order to analyze data systematically under these conditions where noise, small and large shedding events are present, a deposit mass uptake signal treatment method is developed. The method allows us to identify shedding events and can quantify the deposit formation rate between major shedding events. The idea is to average out the noise in the deposit mass uptake signals and to identify the larger shedding events.

The steps involved in the deposit mass signal treatment are based on Matlab procedures and are:

Step A: The deposit mass uptake signals are filtered using a 10 point resampling method implemented in Matlab. This effectively smoothes the data over 10 points, returning one resampled data point for further use.

Step B: Slope calculations are done using a moderately low order polynomial (3^{rd} order, current case) that is fitted to the data in a sliding window (5 data points) and finally differentiation of the model is performed.

Step C: Cut off of negative slope values is made to remove major shedding events. The cut off level is adjusted to determine the number of major shedding events accurately while still giving a satisfactory prediction of apparent deposit formation rates. A high cut off level e.g. -200 $g/m^2/h$ may count some noise as shedding events which results in higher deposit formation rate values. A low cut off e.g. -6,000 $g/m^2/h$ will include some shedding in the DDF-rate calculation and results in lower deposit formation rate values. The selected cut off level was -3,800 $g/m^2/h$ for all the tests. This represents a subjective judgment that strikes a balance between determining the most shedding events (a high cut off level is

needed) and not removing selectively a negative noise contribution to the DDF-rate determination (a low cut off level is needed).

Step D: Smoothing of the raw slope calculations is made using a moving average filter over 51 points. Based on the data used in the present study, our choice of 25 data points on each side of the *i*th data point represents a subjective judgment that balances effective smoothing against undesired removal of minor, but significant variations in the deposit formation rate. The result of the smoothed data is the DDF-rate.

This complete procedure was validated. It should be kept in mind that our aim is to treat all data systematically once the subjective judgments of steps C and D have been made, thus avoiding the pitfall of seeing or not seeing trends from case to case based on incomparable criteria. A comparison the approximate manually calculated slopes of the 0-8 h interval during test 1 of these slopes and the calculated DDF-rates using the procedure described above is shown in Figure C 1. It is clear that the DDF-rates calculated by steps A through D are in good agreement with manually calculated average deposition rates.

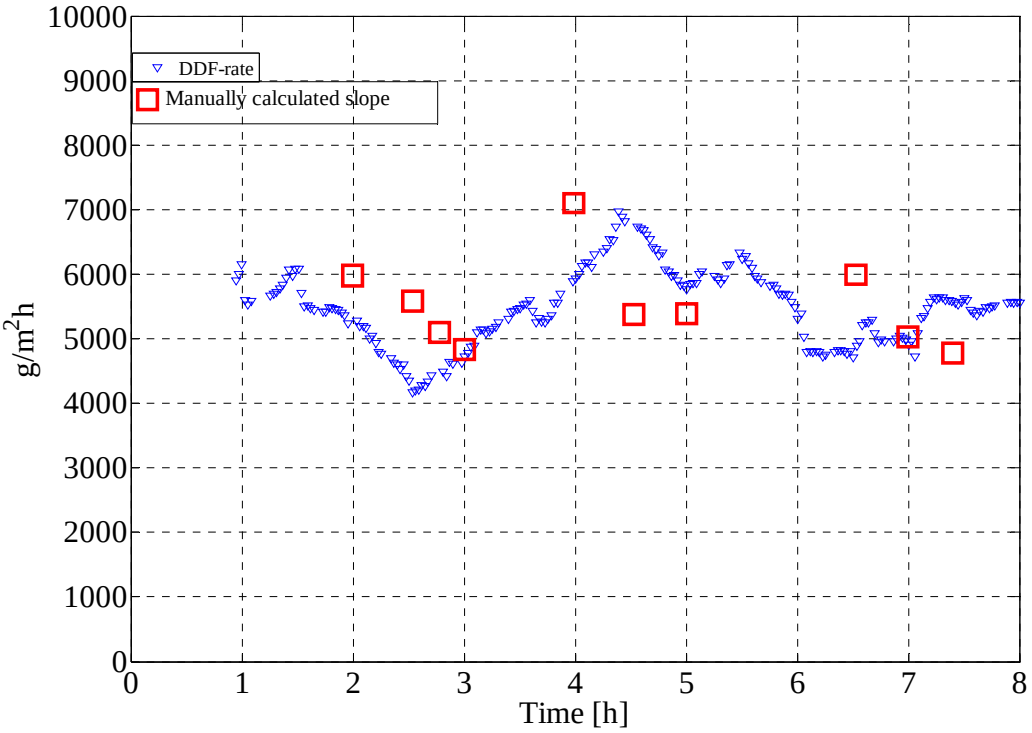

Figure C 1: Comparison of manually calculated slopes and slopes calculated by the mathematical procedure (DDF-rate) for the initial 8 hours of test 1.

June. 2012, DTU no. 50530

Appendix A7

Mechanistic modeling of deposit formation

Energinet.dk project no. 7217

Characterization and quantification of deposits build up and removal in straw suspension fired boilers

Muhammad Shafique Bashir, Peter Arendt Jensen, Flemming Frandsen, Stig Wedel, Kim Dam-Johansen.

Department of Chemical and Biochemical Engineering

Technical University of Denmark

Søltofts Plads, Building 229, DK-2800 Lyngby, Denmark

CHEC no. R1301

Due to project resources constrains it was decided to limit the modeling to the deposit formation process and leaves out the shedding process. The model used is a modified version of the model developed by Zhou et al. [1]

At the beginning of the deposit formation process, when the probe is perfect clean, only vapors and fine and intermediate-sized particles (for examples, deposition by condensation and by thermophoresis) which arrive at the surface in a sticky condition contribute to the initial deposit formation. Inertial impaction contributes to the ash deposit build-up after the initial deposition forms. The deposit surface temperature increases with the increase of the thickness of the deposit which results in the deposit becomes a much more efficient collector [1].

A schematic of the deposit layers on the horizontal ash deposition probe is shown in Figure 7.1. The model developed by Zhou et al. [1], is a dynamic mechanistic model accounting for ash deposition and shedding by surface melting in a straw grate-fired boiler. The necessary modifications in the model were made to apply the model for suspension firing conditions, without any deposit shedding considerations. For more details about the model, please refer to Zhou et al. [1].

Principal assumptions in the model are [1]:

- The incoming fly ash is uniform; and gas-particle interaction is a one-way coupling i.e. the presence of particles in the flue gas has no influence on the gas flow field.
- Particles motion and temperature follow the local gas velocity and temperature.
- The effect of ash build-up on the flow field around the probe is negligible.
- A linear temperature profile is assumed across the deposit.
- The heat transfer occurs only along the radial direction of the deposit, and the energy change caused by the phase change of the deposit is negligible.
- Heterogeneous reactions and sintering in the deposit are neglected i.e. chemical compositions of the deposits and the fly ash are the same.
- Deposit shedding is not taken into account.
- The chemical compositions and particle size of the fly ash obtained from experiments are used as input parameter in the model due to the lack of an ash transformation model.

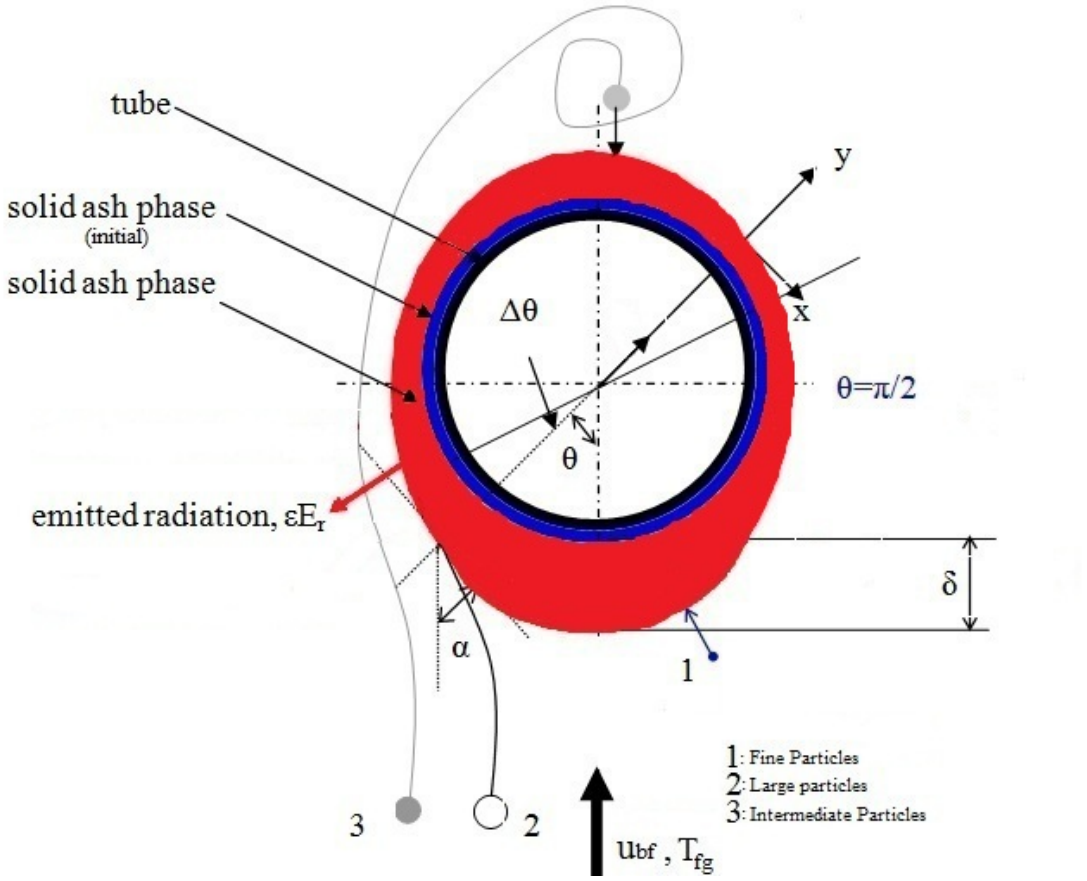

Figure 7. 1: A schematic of the deposit layers on the horizontal ash deposition probe [1].

The principal mechanisms by which deposits formed are; thermophoresis and diffusion and/or diffusion followed by condensation, inertial impaction on the upstream side, and eddy impaction on the downstream side. The overall deposit build-up rate can be written as,

$$\frac{d_m(t,\theta)}{dt} = C(t,\theta) + TH(t,\theta) + I(t,\theta) \qquad (7.1)$$

In the above equation, C counts for condensation, TH for thermophoresis and I for inertial impaction, while t is the time and θ is the angular position.

Thermophoresis

Thermophoresis is a process of particle transport in a gas due to local temperature gradients [2]. Vapors may homogeneously nucleate to form a fume and subsequently deposit by thermophoresis on the surface and vapors may heterogeneously condense on other particles in the boundary layer and arrive the surface through thermophoresis [3]. The thermophoretic flux

of submicron particles to the tube surface can be calculated based on the thermophoretic velocity.

$$TH(t,\theta) = \sum u_T \cdot C_{ash,i} \qquad (7.2)$$

where u_T is the thermophoretic velocity and $C_{ash,i}$ is approximated based on the aerosol concentration ($C_{ash,1}$) and concentration of the intermediate sized particles ($C_{ash,3}$). It was assumed that all fine particles reach the probe may stick. The mass loading of aerosol particles in the flue gas was approximated based on the correlation proposed by Zhou et al. [1]. The correlation is, $\frac{0.00026}{\left(\frac{T_{fg}}{293.15}\right)}$. The concentration of the intermediate sized particles ($C_{ash,3}$) was estimated from the calculated concentration of large sized particles ($C_{ash,2}$), which was approximated as,

$$C_{ash,2} = \frac{\dot{m}_{fuel} \cdot ash\% \cdot f_{entrained}}{V_{fg}} \qquad (7.3)$$

In this equation $\dot{m}_{fuel}$ is the inlet fuel feeding mass flow rate, $f_{entrained}$ is fraction of residual entrained as residual fly ash, *ash*% is the percentage of ash in a dry fuel and V_{fg} is the volumetric flow rate of flue gas. The flue gas velocity (u_{bg}) can be estimated using,

$$u_{bg} = \frac{V_{fg}}{A_r} \qquad (7.4)$$

A_r is the cross-sectional area of the boiler at probe measuring area.

The thermophoretic velocity can be calculated based on various correlations proposed by different authors. The formula proposed by Brock [4] is,

$$u_T = -B \cdot v_g \cdot C_c \cdot \frac{\nabla T}{T_c} \qquad (7.5)$$

where, B is constant and can be estimated empirically, v_g is the kinematic gas viscosity, T_c is the temperature on the surface of the tube and ∇T (K/m) is the temperature gradient. C_c is called the Cunningham slip factor and can be calculated using the method proposed by Flagan et al. [5].

Diffusion followed by Condensation

Condensation is a mechanism by which vapors can be collected on surfaces cooler than the local gas. For the case of biomass firing, the initial deposition is governed by condensation because of the presence of alkali metals. For simplification, the overall condensation rate controlled by mass transfer was expressed at [10],

$$C(t,\theta) = \sum k_{C,i}\left(C_{i,b} - C_{i,s}\right) \qquad (7.6)$$

In this equation, $k_{C,i}$ is mass transfer coefficient, $C_{i,b}$ is the concentration of gas specie in the bulk gas and $C_{i,s}$ is the concentration of gas specie at the probe surface. *i* represents KCl(g) and K_2SO_4 (g) in the bulk flue gas. The mass transfer coefficient is determined by the Sherwood number (Sh),

$$Sh = \frac{k_{C,i} \cdot d}{D_i} \qquad (7.7)$$

In this equation, d is the diameter of the probe and D_i is the diffusion coefficient.

Inertial Impaction

Inertial impaction takes place when particles have too much inertial momentum to follow the gas streamlines around a heat transfer surface, and instead impacts on the surface. As mentioned by Zhou et al. [1], the influencing deposition mechanism for straw fired boilers is inertial mechanism during grate firing and will be even more important for the suspension firing of straw since the percentage of the entrained ash ranges from 80-90%. The deposition rate caused by the impaction of the particles can be written as,

$$I(t,\theta) = u_{bg} \cdot C_{ash,2} \cdot \eta_{imp} \cdot f_{stick} \cdot s_d \qquad (7.8)$$

In the above equation, u_{bg} is the bulk gas velocity, $C_{ash,2}$ is the concentration of large sized particles, η_{imp} is the impaction efficiency, f_{stick} is the sticking efficiency, and s_d is the deposit surface area. For eddy impaction on the rear side of the probe, please refer to [1].

Impaction Efficiency

Impaction efficiency of the fly ash particles hitting the probe is a function of the particles which impact on the probe, and the fraction of the particles captured once collision on the surface has occurred. The impact efficiency is dependent on the particle velocity, particle

density, particle diameter, bulk gas viscosity and the probe dimensions. A dimensionless number called the Stokes number represents of these parameters and is given as,

$$Stk = \frac{\rho_p \cdot d_p^{\,2} \cdot u_{bg}}{9 \cdot \mu_{fg} \cdot d} \qquad (7.9)$$

The impact efficiency can then be calculated based on the Stokes number. For more details, please refer to Zhou et al. [1].

Sticking Efficiency

The sticking efficiency of the particles depends upon the composition and viscosity of the particle and the deposit surface and the thermal and chemical compatibility between the particle and the deposit surface [6]. The combined stickiness of the deposit surface and the incoming ash particles was approximated using the following correlation [7],

$$f_{stick} = f(T_{fg}) + f_s(T_s) \cdot (1 - f(T_{fg})) \qquad (7.10)$$

In the above equation, $f(T_{fg})$ is the sticking probability for the incoming particles and $f_s(T_s)$ is the sticking probability for the particles exposed on the surface. A prediction of ash melt fraction as function of temperature based on the ash composition was made by using the model proposed by Zhou et al. [1].

Heat Transfer Modeling

The heat transfer between the deposit and the flue gas includes contributions from radiation and convection. The overall heat balance can be approximated using,

$$\varepsilon_r \sigma (T_{fg}^{\,4} - T_s^4) + Q_c = Q_{in} \qquad (7.11)$$

The convective heat transfer will be,

$$Q_c = h_f (T_{fg} - T_s) \qquad (7.12)$$

In the above equations, ε_r is the emissivity coefficient for deposit (ranging from 0.75-0.8 [1]), h_f is the convective heat transfer coefficient in the furnace region, T_s is the surface temperature, T_{fg} is the flue gas temperature and σ is the Stephen Boltzmann Constant.

Heat transfer through the deposit layer was estimated using,

$$Q_{in} = \frac{k_{eff}(T_d - T_t)}{\delta_e} \qquad (7.13)$$

In this equation, δ_e is the effective thickness of the solid deposit, T_t is the probe metal temperature, and k_{eff} is the effective thermal conductivity of the deposit.

Simulation Conditions

Two types of fuel input data and fly ash compositions data were used as input as shown in Table 7.1. For simplification and in order to compare the results with available experimental data, only two cases of the fuels were used as input: 1) fuel (fly ash) with straw share greater than 20 wt.%, and 2) fuel (fly ash) with straw share less than 20 wt.%. The detailed simulation conditions are shown in Table 7.2. Most of the input conditions are taken from the measurement data shown in appendix 4 and 5. The changed conditions were probe temperature (500 ^{o}C and 600 ^{o}C), flue gas temperature (770 ^{o}C, 820 ^{o}C and 900 ^{o}C) and applied fuel and fly ash inputs. Most of the values are kept the same as were used by Zhou et al. [1].

The deposit probe related parameters shown in Table 7.2 were approximately the same as were used by Zhou et al. [1]. The input value for the boiler cross-sectional area is different (72 m^2 instead of 24 m^2). The fuel related input data, for example, the inlet fuel rate, the entrained ash as fly ash, and the ultimate and proximate analysis of the ash was different from the ones used by Zhou et al. [1], but the percentages of released inorganic elements are kept the same. The selected values for flue gas temperature were 770 ^{o}C, 820 ^{o}C and 900 ^{o}C. The correlations for the approximation of thermal conductivity and viscosity of the flue gas are same as were used by Zhou et al. [1]. The particle size for the fine and medium particles was kept the same, while the size of the course particles is different. The reason is that as shown in appendix 4 and 5 that the particle size of the coarse particles generated during suspension firing is significantly larger than the coarse particles formed during grate firing. The deposit related properties were kept the same.

Table 7. 1: Composition of the fuel input data and fly ash input data.

Fuel	Case 1 (straw> 20 wt.%)	Case 2 (straw < 20 wt.%)
Moisture (wt. %, a.r.)	6.67	6.5
Ash (wt.%, d.b.)	5.63	1.0
Volatiles (wt.%, d.b.)	82.9	80.0
C	51.2	55.0
H	5.85	6.0
N	0.8	0.70
S	0.121	0.04
Cl	0.19	0.01
K	0.9	0.1
Ultimate Analysis of the fuel ash (wt.%, d.b.)		
Si	23.45	35.0
Al	0.35	0.50
Fe	0.20	0.20
Ca	5.78	14.0
Mg	1.31	1.0
Na	1.41	0.10
K	16.14	5.0
S	0.77	0.50
P	1.30	0.10
Cl	5.53	0.55

Table 7. 2: Simulation conditions

Parameter		Value
The probe	Total length, L (m)	3
	Effective deposition length, L_d (m)	1.5
	Effective heat transfer length, L_h (m)	2.0
	Probe diameter, d (mm)	40.5
	Temperature of the probe metal, T_s (^{o}C)	500/600
The boiler	The effective boiler cross-sectional area at probe measuring position (m^2)	72
The fuel	Inlet fuel flow rate, $\dot{m}_f$ (kg/s)	15.8
	The entrained ash, (ash%)	80
	Ultimate and proximate analysis	See Table 7.1
	Released inorganic elements (from the fuel to flue gas), %	S: 50 K: 20 Cl: 100
The gas	Excess air ratio, λ	1.25
	Temperature of the flue gas, T_{fg} (^{o}C)	770/820/900
	Thermal conductivity, k_{fg} (W/m/K)	$4.8\times10^{-4}\cdot T_f^{\,0.717}$
	Viscosity, μ_{fg} (Pa.s)	$1.98\times10^{-5}\cdot\left(\frac{T_f}{300}\right)^{2/3}$
	SO_2 concentraion (ppmv at STP)	60
Fly ash	Particle size, d_p (μm)	Fine particle (1): 0.27 Coarse particle (1): 110 Intermediate particle (1): 8
	Particle density, ρ_p (kg/m^3)	All particles: 2600
	Chemical composition	See Table 7.1

Deposit	Deposit bulk density, ρ_p (kg/m^3)	1500
	Emissivity coefficient, ε_r	0.8
	Conductivity of the solid phase,	6.7 (innermost)
	k_s (W/m/K)	5.5 (other layers)
	Initial deposit thickness, $\delta_{d,i}$ (m)	Half of the diameter of fine particles
Simulation time, hour		6
Number of computational cell (semi-cylinder)		40

Simulation Results

The simulation results of the deposit mass uptake and DDF-rate for the first six hours when straw share was more than 20 wt.% are shown in Figure 7.2 and Figure 7.3, respectively. It can be seen that there is an increase in the deposit mass uptake and DDF-rate with increase in flue gas temperature. The qualitative behavior of the results is in accordance with the experimental findings, presented in appendix 4. Increased flue gas temperatures probably increase the fraction of molten ash as well as provide an increased content of gas phase alkali species, and both will lead to higher amount of ash being deposited. The results of changed probe surface temperature show that the changed probe surface temperatures in the range from 500 to 600 ^{o}C do not seem to significantly influence the deposit formation rate.

The simulation results of the deposit mass uptake for the first six hours when straw share was less than 20 wt.%, are shown in Figure 7.4. The deposit mass uptake was low possibly due to the fact that the deposit formation caused by inertial impaction is minimal because of low sticking efficiency of the fly ash and deposit. The difference between deposit mass uptake at probe temperature of 500 ^{o}C and 600 ^{o}C is possibly due to a higher deposit formation caused by condensation at lower temperature.

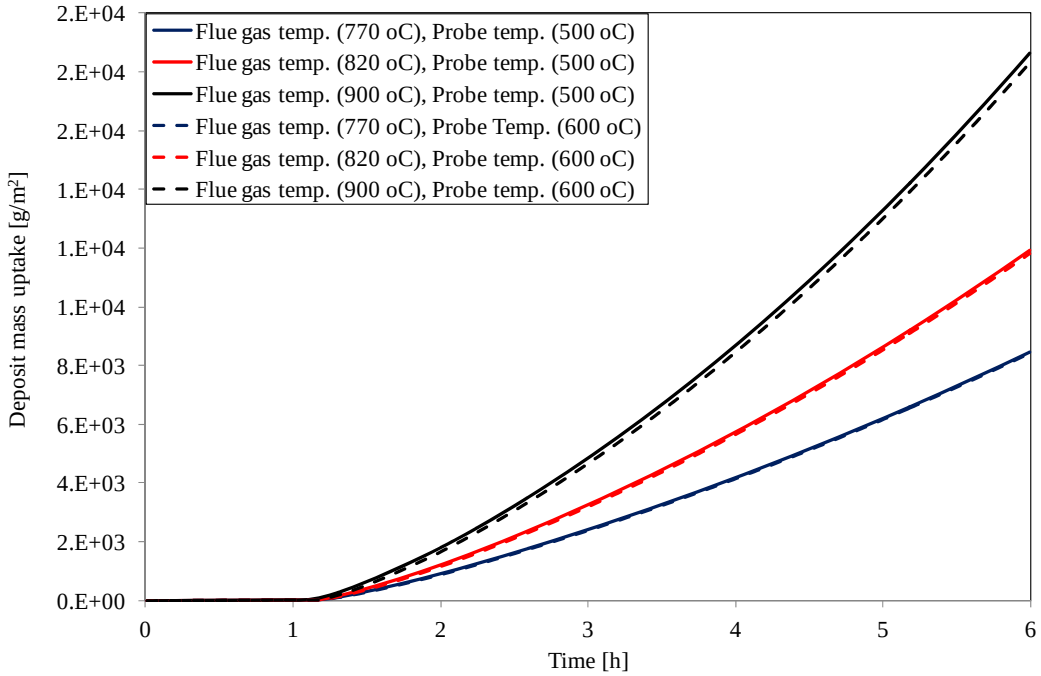

Figure 7. 2: Simulation results of deposit mass uptake for the first six hours for different sets of flue gas temperatures and probe surface temperatures. The fuel (fly ash) input is case 1 (straw > 20 wt.%) shown in Table 7.1.

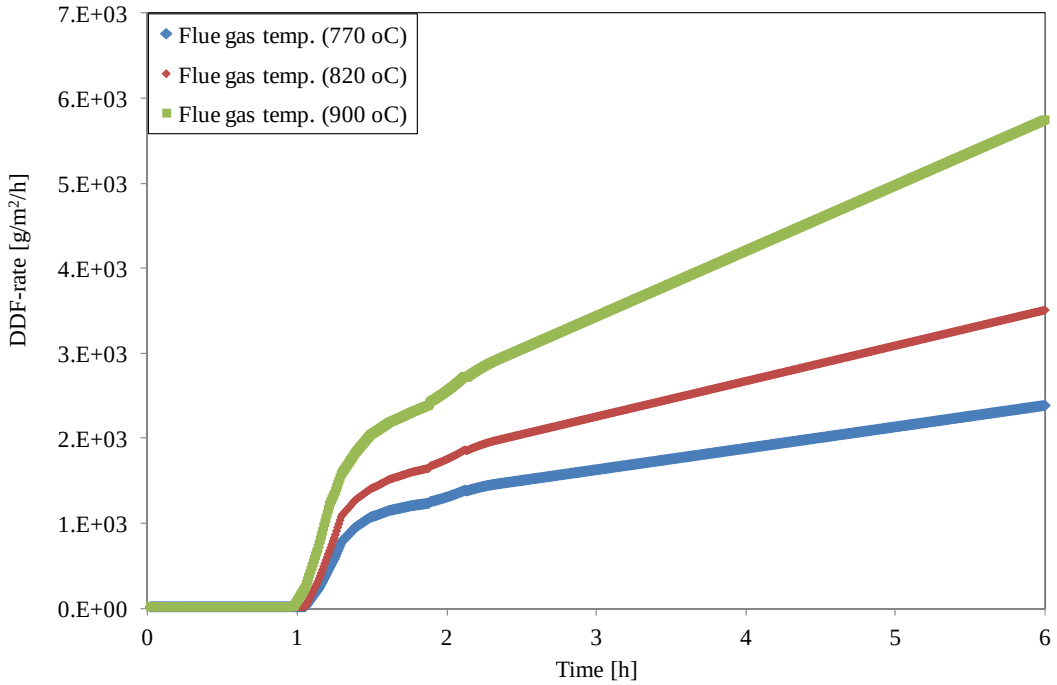

Figure 7. 3: Simulation results of DDF-rate ($\frac{dm_d}{dt}$) for the first six hours for different sets of flue gas temperatures and probe surface temperatures. The fuel (fly ash) input is case 1 (straw > 20 wt.%) shown in Table 7.1.

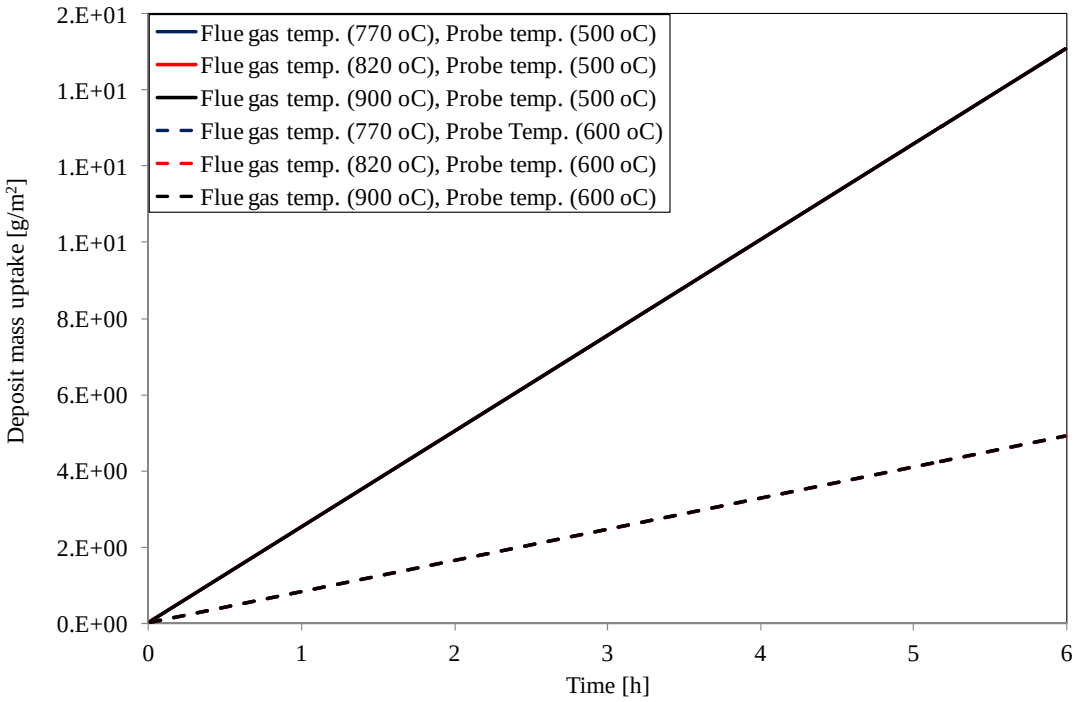

Figure 7. 4: Simulation results of deposit mass uptake for the first six hours for different sets of flue gas temperatures and probe surface temperatures. The fuel (fly ash) input is case 2 (straw < 20 wt.%) shown in Table 7.1.

A comparison of the measured DDF-rates and DDF-rates resulted from the simulation is shown in Table 7.3. High values of DDF-rates can be seen for both measured and simulated results for the case when the straw share was more than 20 wt.%. For ashes produced during straw combustion, due to the presence of liquid phase, the sticking probability of the ash increases and thereby higher DDF-rates are the result. The model overestimates the DDF-rate when the straw share was more than 20 wt.% possibly due to a higher sticking efficiency of the fly ash and deposit. The melt fraction was directly taken as the sticking probability, which is rough estimation. In addition, the model only accounts for deposit build-up, and no deposit shedding mechanisms are taken into account. Experimental observations have shown that the amount of deposits on the probe can affect the rate of

deposit formation rate, and for lower deposit mass loads, the DDF-rates are normally lower. The model predicted low DDF-rate for case 2 (straw < 20 wt.%) due to a lower sticking probability of the fly ash used as input. However, as shown in Table 7.3 and Figure 7.2, there is a clear relationship between measured and calculated ash deposit formation rates. Most of the data points show that even though the model does not quantitatively agree with the measured results, a qualitative agreement is seen. The results seem to be reasonable, taking into account the simplicity of the model.

Table 7. 3: Comparison of measured data and simulated data (initial 6 h).

		Flue gas temp. (^oC)	Probe temp. (^oC)	DDF-rate ($g/m^2/h$)	Heat Uptake (kW/m^2)
Straw > 20 wt. %	Measured	909	491	457	49.7
	Simulation	900	500	3109	36.3
Straw > 20 wt. %	Measured	821	590	519	25.2
	Simulation	820	600	1975	20.2
Straw < 20 wt. %	Measured	810	525	25	33.0
	Simulation	820	500	3	32.8

The complete measured data of ash deposit formation rate (DDF-rate) are divided into groups and shown in Table 7.4 in order to make it possible to analyze the influence of changed conditions in flue gas temperature (above or below 850 ^oC), probe surface temperature (500 ^oC or 600 ^oC), straw fuel share (weight fraction of straw in the fuel above or below 20 %) and deposit mass load (above or below 5,000 g/m^2). The details of the selection criteria have been explained in appendix 5. The idea here is to compare the simulation results with the complete measured data to analyze the qualitative behavior of measured data and simulation data. It can be seen that simulated DDF-rate follow the measured results based on the changed conditions in flue gas temperature, probe surface temperature, straw fuel share and deposit mass load. The measured and simulated DDF-rate

are low when straw share is low (below 20 wt.%), deposit mass load is low (below 5,000 g/m^2) and flue gas temperature is low (below 850 ^oC), while change in probe surface temperature does not affect the measured and simulation results. However, in addition to the deposit build-up model, incorporation of a deposit shedding model can potentially result in quantitatively more realistic deposit formation rates.

The predicted heat uptake by the model is shown in Figure 7.5 as a function of different deposit mass loads on the probe. It can be seen that the model generally predicts the probe heat uptake within the range of the experimental results. The differences between the measured and simulated heat uptake can be attributed to the assumed effective thermal conductivity, which may be lower for porous deposits.

Unfortunately, because of lack of time, the shedding model was not implemented and was considered as a part of a new Ph.D. project.

Table 7. 4: Measured DDF-rates and DDF-rates resulted from the simulation for two different sets of flue gas temperatures, probe surface temperatures, straw shares and deposit mass loads. [a] mean value of flue gas temperature. [b] the actual value of deposit mass uptake on the probe (simulated).

		Flue gas temperature	< 850 °C		> 850 °C	
Fuel straw share	Probe deposit mass load	Probe surface temperature (°C) Simulation flue gas temperature (°C)	500 °C 820 °C	600 °C 820 °C	500 °C 900 °C	600 °C 900 °C
Straw > 20 wt. %	> 5000 g/m^2 (⊔ 11,000 g/m^2) [b]	Mean flue gas temperature (measured, °C)	--	--	(909) [a]	(902) [a]
		Mean DDF-rate (g/m^2/h) (measured)			2691	1934
		Mean DDF-rate (g/m^2/h) (simulation)			4614	4594
		Mean heat uptake (kW/m^2) (measured)			34.0	18.8
		Mean heat uptake (kW/m^2) (simulation)			32.2	26.4
	< 5000 g/m^2 (⊔ 1,500 g/m^2) [b]	Mean flue gas temperature (measured, °C)	(823) [a]	(823) [a]	(906) [a]	
		Mean DDF-rate (g/m^2/h) (measured)	234	313	1245	
		Mean DDF-rate (g/m^2/h) (simulation)	1347	1336	1648	
		Mean heat uptake (kW/m^2) (measured)	30.6	22.3	41.6	
		Mean heat uptake (kW/m^2) (simulation)	28.6	21.8	40.4	
Straw < 20 wt. %	> 5000 g/m^2	Mean DDF-rate (g/m^2/h) (measured)				
		Mean DDF-rate (g/m^2/h) (simulation)				
		Mean heat uptake (kW/m^2) (measured)				
		Mean heat uptake (kW/m^2) (simulation)				
	< 5000 g/m^2 (⊔ 8 g/m^2) [b]	Mean flue gas temperature (measured, °C)	(773) [a]			
		Mean DDF-rate (g/m^2/h) (measured)	221			
		Mean DDF-rate (g/m^2/h) (simulation)	2.5			
		Mean heat uptake (kW/m^2) (measured)	34.3			
		Mean heat uptake (kW/m^2) (simulation)	32.8			

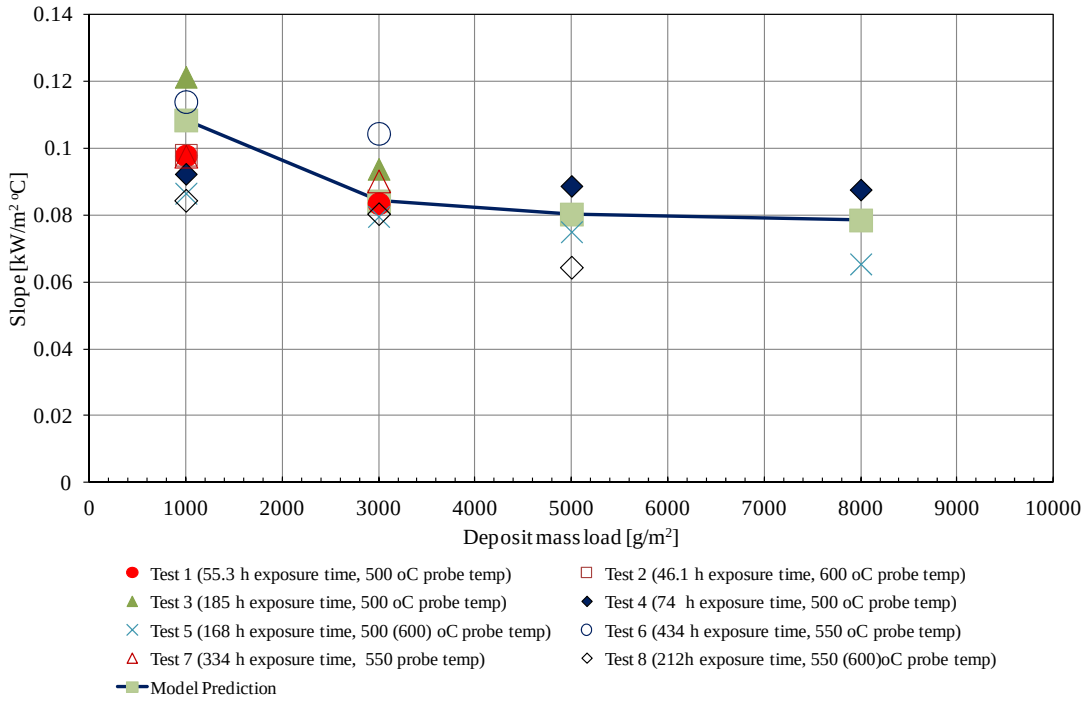

Figure 7. 5: Prediction of heat uptake for different deposit mass loads on the probe.

1.1 Conclusions

Modeling of the ash deposition process and heat uptake in a suspension fired biomass boiler was done to get better understandings of the key processes responsible for ash deposition. The model describes the deposit related processes as a function of the local parameters as flue gas velocity, flue gas temperature, probe surface temperature and fly ash properties. Simulation results showed that when the straw share was high, there is an increase in the deposit mass uptake and DDF-rate with an increase in flue gas temperature. Increased flue gas temperatures increase the fraction of molten ash and that will lead to higher amount of the fly ash being deposited. The results of changed probe surface temperature showed that the changed probe surface temperatures in the range from 500 to 600 ^{o}C do not seem to significantly influence the deposit formation rate. The model over predicts the ash deposition rate quantitatively but the qualitative behavior was in accordance with the experimental findings. The heat uptake model predictions were comparable with experimental findings both quantitatively and qualitatively. From a practical point of view, it was seen that the flue gas temperature and share of straw in wood are the two parameters responsible for an increased deposit formation on the superheater tubes.

References

1. H. Zhou, P. A. Jensen, F. J. Frandsen, Fuel, 86 (2007), 1519-1533.

2. B. M. Jenkins, L. L. Baxter, T. R. Miles (Jr.), T. R. Miles, Fuel Processing Technology, 54 (1998), 17-46.

3. L. L. Baxter, Biomass and Bioenergy, 4 (1993), 85-102.

4. J. R. Brock, J. Col. Sci., 17 (1962), 768.

5. R. C. Flagan, J. H. Seinfeld, Fundamentals of air pollution engineering, Prentice-Hall Inc., New Jersey, (1988).

6. K. H. Andersen, Deposition formation during coal straw co-combustion in a utility pf-boiler, PhD Thesis, 1998, Technical University of Denmark, ISBN 87-90142-47-0.

7. P. M. Walsh, A. N. Sayre, D. O. Loehden, L. S. Monroe, J. M. Beer, A. F. Saro_m, Prog Energy Combust Sci, 4 (1990), 327-346.

June. 2012, DTU no. 50530

Appendix A8

Innovative ideas for deposit shedding

Energinet.dk project no. 7217

Characterization and quantification of deposits build up and removal in straw suspension fired boilers

Muhammad Shafique Bashir, Peter Arendt Jensen, Flemming Frandsen, Stig Wedel, Johan Wadenbäck, Søren Thaaning Pedersen, Kim Dam-Johansen.

Department of Chemical and Biochemical Engineering

Technical University of Denmark

Søltofts Plads, Building 229, DK-2800 Lyngby, Denmark

CHEC no. R1301

1.1 Introduction

At some brainstorming meetings during the project novel ideas for deposit removal were discussed. Considerations regarding deposit removal techniques, optimal plant sootblowing and ash mixing to minimize deposit problems are discussed in this appendix.

1.2 Proposed Ideas for Deposit Shedding in Biomass Suspension-Fired Boilers

Deposit Removal Using Ring (DRUR)

Experimental findings presented documented in appendix 3 to 5 have showed that short exposure time (< 2-10 h) deposits formed on the superheater tubes of biomass suspension-fired boilers are easy to remove. In addition, deposits removal mechanism during straw and wood suspension firing is primarily debonding. It may therefore be possible to use deposit removing metal rings on the superheater tubes to remove the short exposure deposits effectively with increased deposit removal frequency compared to the natural deposit shedding. A schematic of a possible deposit removal ring system is shown in Figure 8.1 and Figure 8.2. Deposit ring movement can be based on a force control set-up attached with a thin wire that can withstand the higher temperatures. An advantage of the system is that there probably will be consumed a very low amount of energy compared to soot blowing systems. The concept may be tested on the horizontal probe for small exposure time deposits. The limitations of the concept are the high number of rings needed on a superheater, that it only can be used in areas with free hanging tubes and that it presently is not know if the rings sometimes may be stuck on the tubes. However, such a ring system could probably keep the deposit on a low level and both erosion and operational costs imposed by the plant sootblowers can be avoided by using the rings.

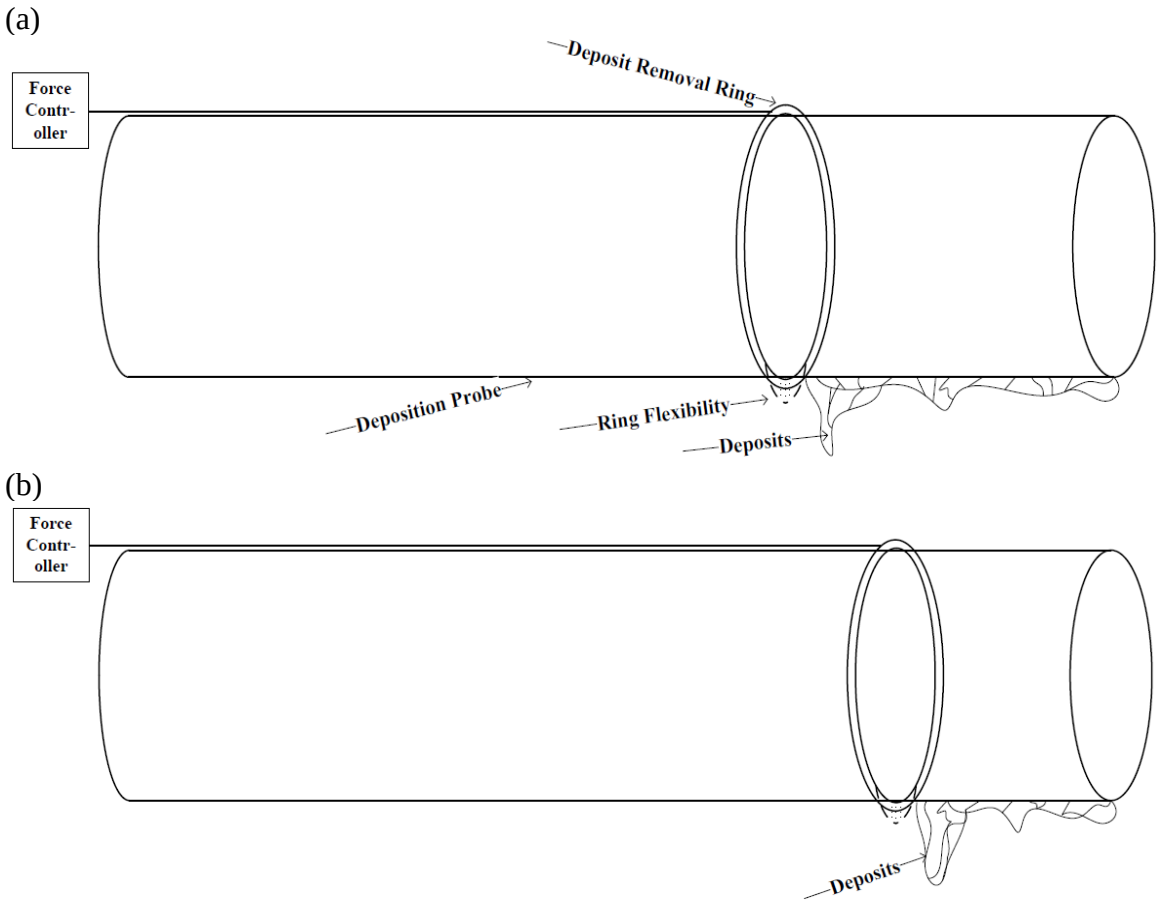

Figure 8. 1: A schematic of deposit removal using a ring.

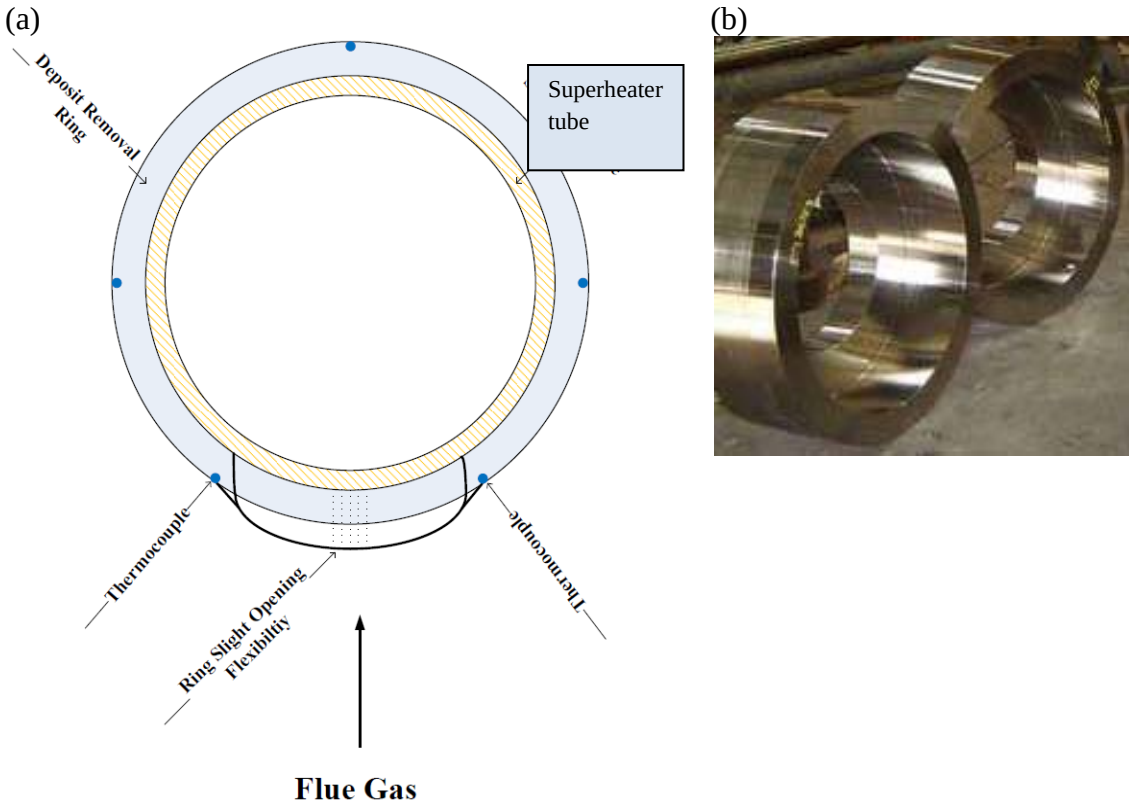

Figure 8. 2: a) A schematic layout of the ring for deposit removal on a superheater tube, b) a potential ring that can be used with modifications.

Deposit Removal using Mechanical Hitting

Deposits that are not strongly bonded with the boiler tube can be removed using mechanical hitting (vibrations), as is done in some waste incinerators. Thus, the short exposure (< 2-10 h) deposits formed in biomass suspension-fired boilers can be effectively removed. The main limitation of such mechanical systems is that they have not been developed to function at the high temperatures prevailing in biomass boilers. However, they may have the potential to function well in the lower flue gas temperature part of the super heaters where the most severe problems with deposits often appear.

Steam Sootblower Optimization

Optimization of a plant sootblower can be made in terms of the frequency of the sootblowing and by controlling it dependent on the local boiler conditions with respect to steam and flue gas temperatures. Experimental results presented in appendix 5 have shown that at lower probe surface temperatures (500 ^{o}C), the deposits formed at an exposure time of less than 91 h could be removed with a PIP of less than 55 kPa. At higher probe surface temperature (> 550 ^{o}C), the PIP needed to remove the probe deposits significantly increases. Based on local steam temperature, the sootblowers can be optimized by reducing their excessive use, and by reducing the amount of steam used. At lower superheater temperatures (< 500 ^{o}C), the sootblower operation frequency should be lower compared to areas with high steam temperatures (> 550 ^{o}C). In addition, for the shorter exposure time (< 2-10 h) deposits formed at lower superheater temperatures, the applied steam pressure to the sootblowers could maybe be reduced considerably compared to that needed in the case of mature deposits and/or deposits formed at higher superheater surface temperatures. So by an adaption of soot blower use to local boiler conditions, based on the knowledge obtained in this project, the amount of steam used for soot blowing can probably be reduced.

Fuel/Ash Mixing

The results presented in appendix 6 indicate that the addition of coal fly ash can significantly affect the ash deposition behaviors and the deposit properties during wood suspension combustion. The effect was evident in two measurement locations. At the location with flue gas temperature of 1250-1300 ^{o}C, although the addition of coal fly ash increases the DDF-rate and the ash deposition propensity, the deposits formed during coal ash addition seem to shed frequently, suggesting that they are easily removable. On the other hand, the amount of K_2SO_4 in the deposits is significantly reduced when coal ash is added, which is favorable from a corrosion point of view. At the location with a flue gas temperature of 750-800 ^{o}C, the

addition of coal fly ash reduces the ash deposition propensity and causes the formed deposits to becoming easily removable. Moreover, the Cl present in the deposits without coal ash addition disappears when coal ash is added, which is also favorable from a corrosion point of view.

Effective fuel mixing by minimizing the K/Si molar ratio in the fuel (ash) can possibly result in reducing the concentration of K and Cl in the fly ash produced as discussed in Chapter 5. During the process of pelletizing of straw, certain amount of Si and Al can be added to the straw pellets, and this will potentially reduce the concentration of Cl in the fly ash. A reduced percentage of Cl in the fly ash can thereby reduce the sticking efficiency of the produced fly ash.